Also available as e Book

ROBOTICS AND CONTROL

R K Mittal
I J Nagrath

Mc Graw Hill Education

1

Introduction to Robotics

Mankind has always strived to give life-like qualities to its artifacts in an attempt to find substitutes for himself to carry out his orders and also to work in a hostile environment. The popular concept of a robot is of a machine that looks and works like a human being. This humanoid concept has been inspired by science fiction stories and films in the twentieth century. The industrial robots of today may not look the least bit like a human being although all the research is directed to provide more and more anthropomorphic and human-like features and super-human capabilities in these.

To sum up, machines that can replace human beings as regards to physical work and decision making are categorized as *robots* and their study as *robotics*.

The robot technology is advancing rapidly. The industry is moving from the current state of automation to robotization, to increase productivity and to deliver uniform quality. Robots and robot-like manipulators are now commonly employed in hostile environment, such as at various places in an atomic plant for handling radioactive materials. Robots are being employed to construct and repair space stations and satellites. There are now increasing number of applications of robots such as in nursing and aiding a patient. Microrobots are being designed to do damage control inside human veins. Robot like systems are now employed in heavy earth-moving equipment. It is not possible to put up an exhaustive list of robot applications. One type of robot commonly used in the industry is a robotic manipulator or simply a *manipulator* or a *robotic arm*. It is an open or closed kinematic chain of rigid links interconnected by movable joints. In some configurations, links can be considered to correspond to human anatomy as waist, upper arm, and forearm with joints at shoulder and elbow. At the end of the arm, a wrist joint connects an *end-effector* to the forearm. The end-effector may be a tool and its fixture or a *gripper* or any other device to do the work. The end-effector is similar to the human hand with or without fingers. A robotic arm, as described above, is shown in Fig. 1.1, where various joint movements are also indicated.

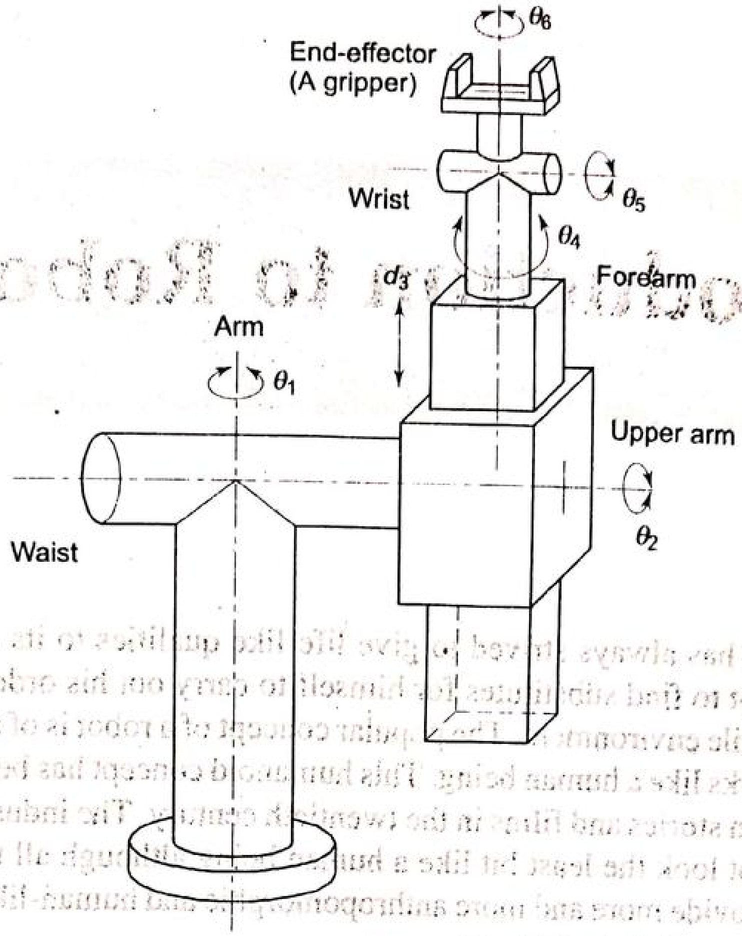

Fig. 1.1 *An industrial robot that least looks like a human*

1.1 EVOLUTION OF ROBOTS AND ROBOTICS

Czech writer, Karel Capek, in his drama, introduced the word robot to the world in 1921. It is derived from Czech word *robota* meaning "forced labourer". Isaac Asimov the well-known Russian science fiction writer, coined the word ***robotics*** in his story "Runaround", published in 1942, to denote the science devoted to study of robots.

The antecedents of the modern reprogrammable automation dates back to the eighteenth century. Perhaps, the best record is of Joseph Jacquard's use of punched cards in mechanical looms, which laid the foundations for NC, CNC, and automats, in addition to robotics.

Numerical control (NC) works on control actions based on stored information that may include start and stop operations, coordinate points, actions, logic for branching, and control sequences. A manufacturing system producing a variety of products in small batches, without requiring major hardware changes, with frequent changes in product models and production schedules, requires flexibility. In the transfer line approach, raw material is automatically transferred from one machine to another till it is converted to the final product. Such a transfer line approach, producing a large quantity of the same product for an extended period of time, may become useless when a major product change is required. It often ends up in abandoning the large capital investment. Contemporary industrial robots are reprogrammable machines that can perform different operations by simply modifying stored data, a feature that evolved from numerical control and is a solution for both of the above situations.

Need of systems to work in hostile environments that human workers cannot easily or safely access (for example radioactive material handling) led to the development of *teleoperated manipulator* in 1940s. The field of "telecherics" deals with the use of remote manipulators controlled by a human being in a "master-slave" configuration. Here, the actual machine (slave) is operated from a distance by a control "joystick" of a geometrically similar machine (master), as shown in Fig. 1.2.

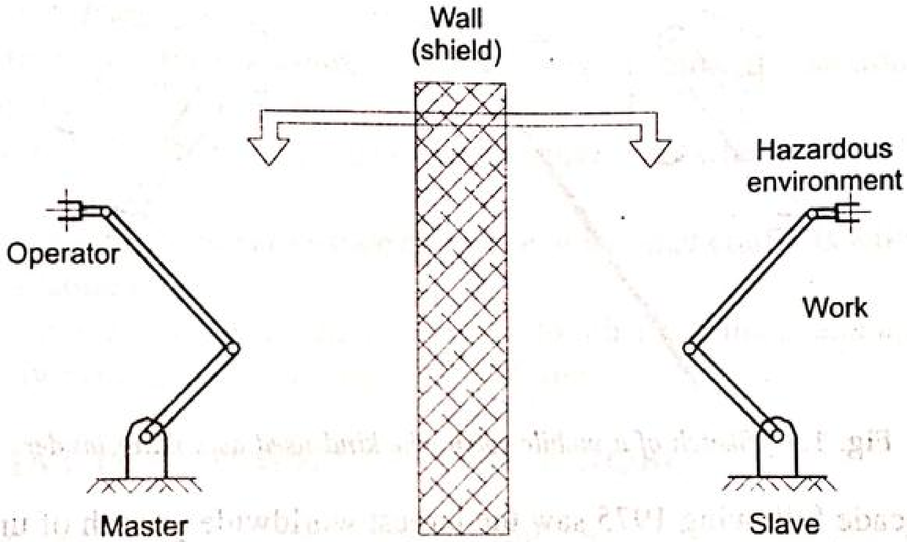

Fig. 1.2 *A master-slave manipulator*

The combination of numerical control and telecherics have evolved the basic concepts of modern industrial robots with human operator and master manipulator of Fig. 1.2 replaced by a programmable controller. This merging created a new field of engineering referred to as ***robotics***, and with it a number of engineering and scientific issues in design, control, and programming have emerged, which are substantially different from those of the existing techniques.

Some of the landmark developments in the field are now enunciated. In 1938–1939, a *jointed mechanical arm* was invented for use in spray painting. A process controller that could be used as a general-purpose playback device for operating machines, was developed in 1946, the year in which first large-scale electronic computer ENIAC was built. The first numerically controlled machine tool was developed in 1952. The patenting of the first manipulator, with the basic concept of teaching/playback, in 1954, set rolling the exponential growth in robotics.

The unmatched quality, reliability, and productivity offered by these robots, although in very limited applications, was recognized by the industry and sparked the formation of several world-wide centres of research in this area by the mid-1960s. The new field of robotics received support from simultaneously developing fields of *artificial intelligence* (AI), artificial vision, and developments in digital microcomputers. In 1967–1968, the first legged and wheeled walking machines using vision and other sensors, were reported. The servomotors were used in place of hydraulic devices in 1970 to power the robots. In 1974, the first servomotor actuated and microcomputer-controlled robots were commercially launched and in 1976, they were used by NASA *Viking* lander to collect samples from the surface of Mars. An elementary sketch of this lander is drawn in Fig. 1.3.

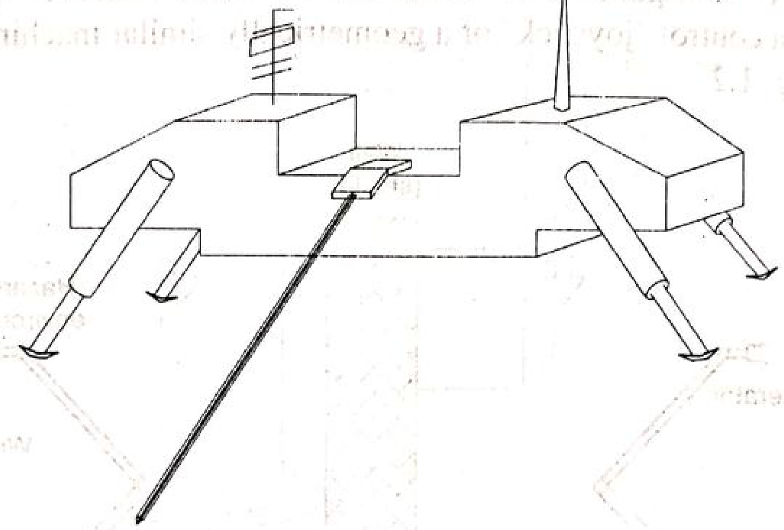

Fig. 1.3 *Sketch of a mobile robot, the kind used as Viking lander*

The decade following 1975 saw the largest worldwide growth of university-based laboratories, research centres, curricula, and publications in robotics. Mobile robotics also grew substantially during this period with designs of legged vehicles based on gait of both human beings and insects. The research activity in robotics started almost 40 years ago. The Robotic Institute of America (RIA), now called Robotic Industries Association (RIA), was formed only in 1975 as an organization of robot manufacturers and users.

The growth, thereafter, in robotics has been closely associated with developments in microcomputers, micro-controllers, sensor technology, vision technology, and artificial intelligence. The year 1997 saw the amalgamation of all these in the success of the Mars mission through "Pathfinder" and "Sojourner".

Recent Japanese exhibition *Robodex 2000* exhibited several varieties of entertainment robots; but there were no robots which could effectively do the onerous chores of house cleaning and dishwashing. Such robots are yet to be designed. None of the varieties exhibited attracted the industry.

Industrial robots are increasingly used in manufacturing plants, medical surgery, and rescue efforts. These require more difficult technology as much higher degree of accuracy, repeatability, flexibility, and reliability is needed for industrial robots.

Robotics today is dealing with research and development in a number of interdisciplinary areas, including kinematics, dynamics, control, motion planning, sensing, programming, and machine intelligence. These topics are introduced in the following sections and constitute the core of material in this book.

1.2 LAWS OF ROBOTICS

Issac Asimov conceived the robots as humanoids, devoid of feelings, and used them in a number of stories. His robots were well-designed, fail-safe machines, whose brains were programmed by human beings. Anticipating the dangers and havoc such a device could cause, he postulated rules for their ethical conduct. Robots were required to perform according to three principles known as "three laws of Robotics", which are as valid for real robots as they were for Asimov's robots, and they are:

1. A robot should not injure a human being or, through inaction, allow a human to be harmed.
2. A robot must obey orders given by humans except when that conflicts with the First Law.
3. A robot must protect its own existence unless that conflicts with the First or Second Law.

These are very general laws and apply even to other machines and appliances. They are always taken care of in any robot design.

1.3 WHAT IS AND WHAT IS NOT A ROBOT

Automation as a technology is concerned with the use of mechanical, electrical, electronic, and computer-based control systems to replace human beings with machines, not only for physical work but also for the intelligent information processing. Industrial automation, which started in the eighteenth century as fixed automation has transformed into flexible and programmable automation in the last 15 or 20 years. Computer Numerically Controlled (CNC) machine tools, transfer, and assembly lines are some examples in this category.

Common people are easily influenced by science fiction and thus, imagine a robot as a humanoid that can walk, see, hear, speak, and do the desired work. But the scientific interpretation of science fiction scenario propounds a robot as an automatic machine that is able to interact with and modify the environment in which it operates. Therefore, it is essential to define what constitutes a robot. Different definitions from diverse sources are available for a robot.

Japan is the world leader in robotics development and robot use. Japan Industrial Robot Association (JIRA) and the Japanese Industrial Standards Committee defines the industrial robot at various levels as:

"*Manipulator:* a machine that has functions similar to human upper limbs, and moves the objects spatially.

Playback robot: a manipulator that is able to perform an operation by reading off the memorized information for an operating sequence, which is learned beforehand.

Intelligent robot: a robot that can determine its own behaviour and conduct through its functions of sense and recognition.

The British Robot Association (BRA) has defined the industrial robot as:

"A reprogrammable device with minimum of four degrees of freedom designed to both manipulate and transport parts, tools, or specialized manufacturing implements through variable programmed motions for performance of specific manufacturing task."

The Robotics Industries Association (RIA) of USA defines the robot as:

"A reprogrammable, multifunctional manipulator designed to move material through variable programmed motions for the performance of a variety of tasks."

The definition adopted by International Standards Organization (ISO) and agreed upon by most of the users and manufacturers is:

"An industrial robot is an automatic, servo-controlled, freely programmable, multipurpose manipulator, with several areas, for the handling of work pieces, tools, or special devices. Variably programmed operations make the execution of a multiplicity of tasks possible."

Despite the fact that a wide spectrum of definitions exist, none covers the features of a robot exhaustively. The RIA definition lays emphasis on programmability, whereas while the BRA qualifies minimum degrees of freedom. The JIRA definition is fragmented. Because of all this, there is still confusion in distinguishing a robot from automation and in describing functions of a robot. To distinguish between a robot and automation, following guidelines can be used.

For a machine to be called a robot, it must be able to respond to stimuli based on the information received from the environment. The robot must interpret the stimuli either passively or through active sensing to bring about the changes required in its environment. The decision-making, performance of tasks and so on, all are done as defined in the programs taught to the robot. The functions of a robot can be classified into three areas:

"Sensing" the environment by external sensors, for example, vision, voice, touch, proximity and so on, "decision-making" based on the information received from the sensors, and "performing" the task decided.

1.4 PROGRESSIVE ADVANCEMENT IN ROBOTS

The growth in the capabilities of robots has been taking rapid strides since the introduction of robots in the industry in early 1960s, but there is still a long way to go to obtain the super-humanoid anthropomorphic robot depicted in fiction. The growth of robots can be grouped into *robot generations*, based on characteristic breakthroughs in robot's capabilities. These generations are overlapping and include futuristic projections.

1.4.1 First Generation

The first generation robots are repeating, nonservo, pick-and-place, or point-to-point kind. The technology for these is fully developed and at present about 80% robots in use in the industry are of this kind. It is predicted that these will continue to be in use for a long time.

1.4.2 Second Generation

The addition of sensing devices and enabling the robot to alter its movements in response to sensuary feedback marked the beginning of second generation. These robots exhibit path-control capabilities. This technological breakthrough came around 1980s and is yet not mature.

1.4.3 Third Generation

The third generation is marked with robots having human-like intelligence. The growth in computers led to high-speed processing of information and, thus, robots also acquired artificial intelligence, self-learning, and conclusion-drawing capabilities by past experiences. On-line computations and control, artificial vision, and active force/torque interaction with the environment are the significant characteristics of these robots. The technology is still in infancy and has to go a long way.

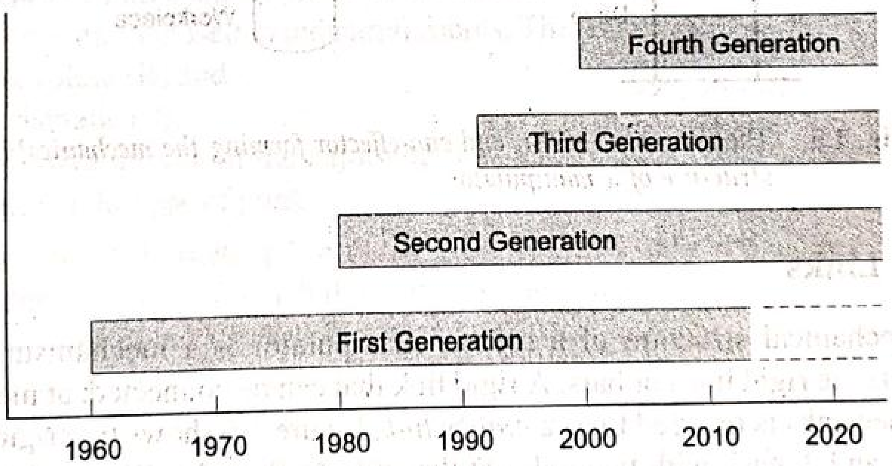

Fig. 1.4 *The four generations of robots*

1.4.4 Fourth Generation

This is futuristic and may be a reality only during this millennium. Prediction about its features is difficult, if not impossible. It may be a true android or an artificial biological robot or a super humanoid capable of producing its own clones. This might provide for fifth and higher generation robots.

A pictorial visualization of these overlapping generations of robots is given in Fig. 1.4.

1.5 ROBOT ANATOMY

As mentioned in the introduction to the chapter, the manipulator or robotic arm has many similarities to the human body. The mechanical structure of a robot is like the skeleton in the human body. The robot anatomy is, therefore, the study of skeleton of robot, that is, the physical construction of the manipulator structure.

The mechanical structure of a manipulator that consists of rigid bodies (links) connected by means of articulations (joints), is segmented into an *arm* that ensures mobility and reachability, a *wrist* that confers orientation, and an end-effector that performs the required task. Most manipulators are mounted on a base fastened to the floor or on the mobile platform of an autonomous guided vehicle (AGV). The arrangement of base, arm, wrist, and end-effector is shown in Fig. 1.5.

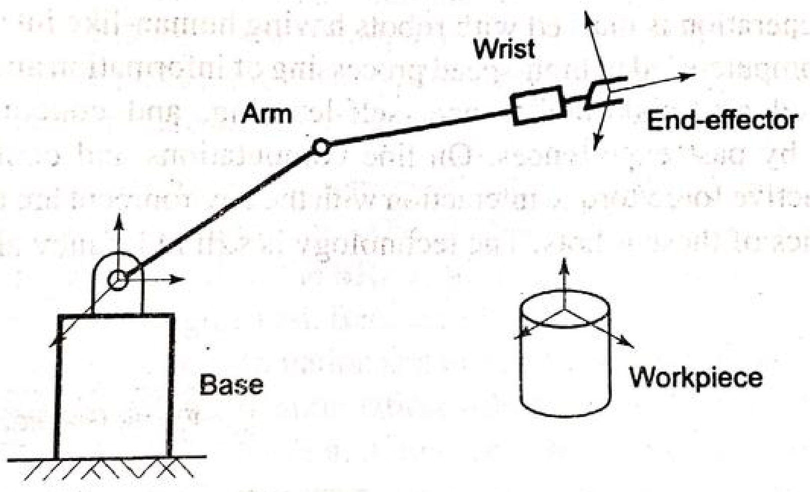

Fig. 1.5 *The base, arm, wrist, and end-effector forming the mechanical structure of a manipulator*

1.5.1 Links

The mechanical structure of a robotic manipulator is a mechanism, whose members are rigid links or bars. A rigid link that can be connected, at most, with two other links is referred to as a *binary link.* Figure 1.6 shows two rigid binary links, 1 and 2, each with two holes at the ends A, B, and C, D, respectively to connect with each other or to other links.

Two links are connected together by a joint. By putting a pin through holes B and C of links 1 and 2, an *open kinematic chain* is formed as shown in Fig. 1.7. The joint formed is called a *pin joint* also known as a *revolute* or *rotary joint.* Relative rotary motion between the links is possible and the two links are said to

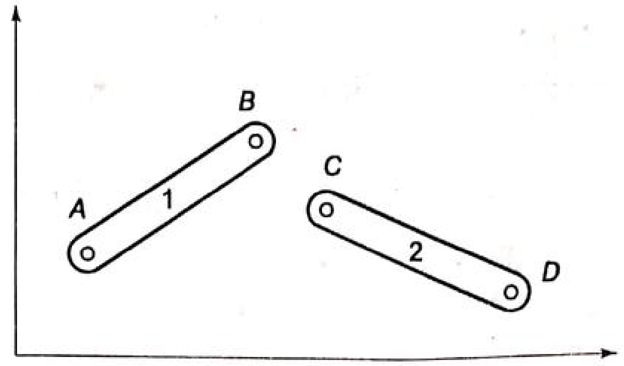

Fig. 1.6 *Two rigid binary links in free space*

be paired. In Fig. 1.7 links are represented by straight lines and rotary joint by a small circle.

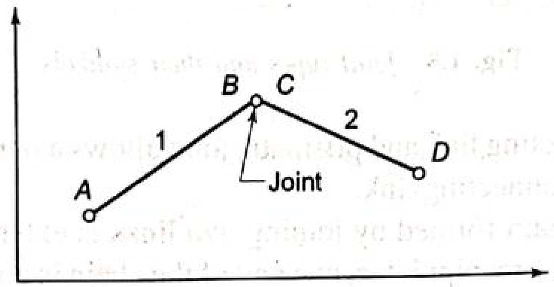

Fig. 1.7 *An open kinematic chain formed by joining two links*

1.5.2 Joints and Joint Notation Scheme

Many types of joints can be made between two links. However, only two basic types are commonly used in industrial robots. These are

- Revolute (R) and
- Prismatic (P).

The relative motion of the adjoining links of a joint is either rotary or linear depending on the type of joint.

Revolute joint: It is sketched in Fig. 1.8(a). The two links are jointed by a pin (pivot) about the axis of which the links can rotate with respect to each other.

Prismatic joint: It is sketched in Fig. 1.8(b). The two links are so jointed that these can slide (linearly move) with respect to each other. Screw and nut (slow linear motion of the nut), rack and pinon are ways to implement prismatic joints.

Other types of possible joints used are: planar (one surface sliding over another surface); cylindrical (one link rotates about the other at 90° angle, Fig. 1.8(c)); and spherical (one link can move with respect to the other in three dimensions). Yet another variant of rotary joint is the 'twist' joint, where two links remain aligned along a straight line but one turns (twists) about the other around the link axis, Fig. 1.8(d).

At a joint, links are connected such that they can be made to move relative to each other by the actuators. A rotary joint allows a pure rotation of one link

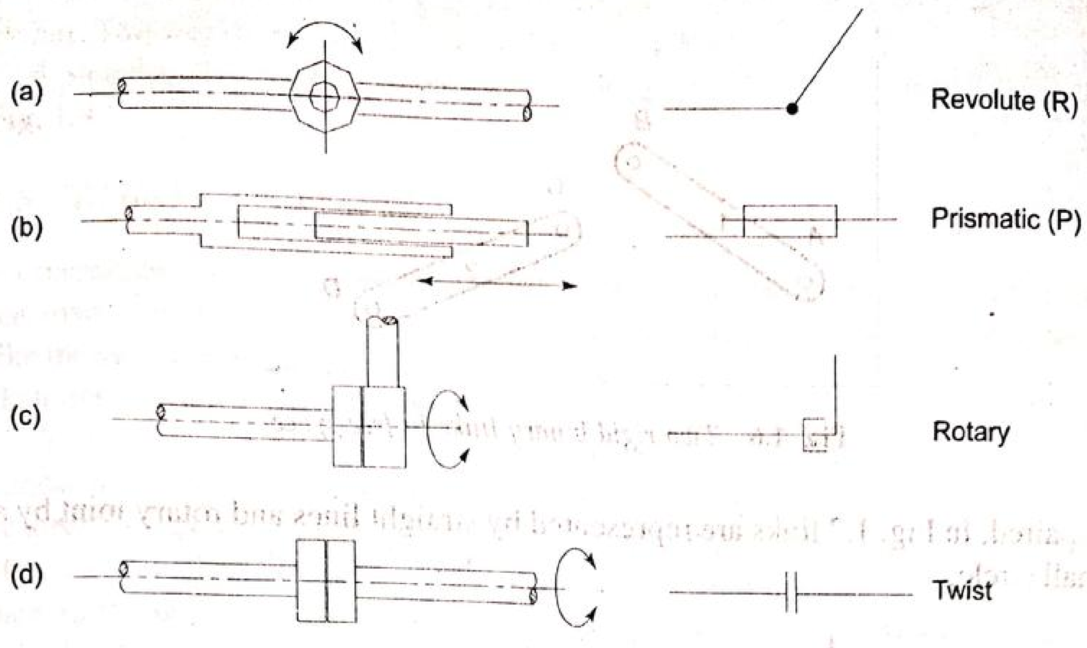

Fig. 1.8 *Joint types and their symbols*

relative to the connecting link and prismatic joint allows a pure translation of one link relative to the connecting link.

The kinematic chain formed by joining two links is extended by connecting more links. To form a manipulator, one end of the chain is connected to the base or ground with a joint. Such a manipulator is an open kinematic chain. The end-effector is connected to the free end of the last link, as illustrated in Fig. 1.5. Closed kinematic chains are used in special purpose manipulators, such as parallel manipulators, to create certain kind of motion of the end-effector.

The kinematic chain of the manipulator is characterized by the degrees of freedom it has, and the space its end-effector can sweep. These parameters are discussed in next sections.

1.5.3 Degrees of Freedom (DOF)

The number of independent movements that an object can perform in a 3-D space is called the number of *degrees of freedom* (DOF). Thus, a rigid body free in space has six degrees of freedom—three for position and three for orientation. These six independent movements pictured in Fig. 1.9 are:

(i) three translations (T_1, T_2, T_3), representing linear motions along three perpendicular axes, specify the position of the body in space.

(ii) three rotations (R_1, R_2, R_3), which represent angular motions about the three axes, specify the orientation of the body in space.

Note from the above that six independent variables are required to specify the location (position and orientation) of an object in 3-D space, that is, $2 \times 3 = 6$. Nevertheless, in a 2-D space (a plane), an object has 3-DOF—two translatory and one rotational. For instance, link 1 and link 2 in Fig. 1.6 have 3-DOF each.

Consider an open kinematic chain of two links with revolute joints at A and B (or C), as shown in Fig. 1.10. Here, the first link is connected to the ground by a

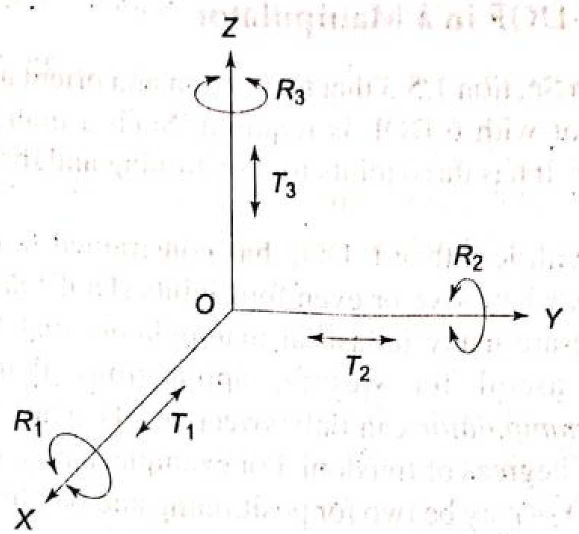

Fig. 1.9 *Representation of six degrees of freedom with respect to a coordinate frame*

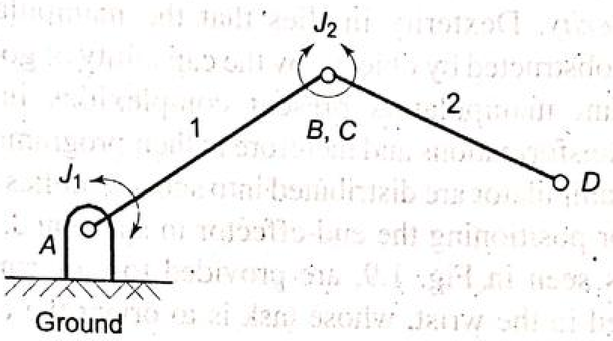

Fig. 1.10 *A two-DOF planar manipulator–two links, two joints*

joint at A. Therefore, link 1 can only rotate about joint 1 (J_1) with respect to ground and contributes one independent variable (an angle), or in other words, it contributes one degree of freedom. Link 2 can rotate about joint 2 (J_2) with respect to link 1, contributing another independent variable and so another DOF. Thus, by induction, conclude that an open kinematic chain with one end connected to the ground by a joint and the farther end of the last link free, has as many degrees of freedom as the number of joints in the chain. It is assumed that each joint has only one DOF.

The DOF is also equal to the number of links in the open kinematic chain. For example, in Fig. 1.10, the open kinematic chain manipulator with two DOF has two links and two joints.

The variable defining the motion of a link at a joint is called a *joint-link variable*. Thus, for an ***n***-DOF manipulator ***n*** independent joint-link variables are required to completely specify the location (position and orientation) of each link (and joint), specifying the location of the end-effector in space. Thus, for the two-link, in turn 2-DOF manipulator, in Fig. 1.10, two variables are required to define location of end-point, point D.

1.5.4 Required DOF in a Manipulator

It is concluded from Section 1.5.3 that to position and orient a body freely in 3-D space, a manipulator with 6-DOF is required. Such a manipulator is called a *spatial manipulator*. It has three joints for positioning and three for orienting the end-effector.

A manipulator with less than 6-DOF has constrained motion in 3-D space. There are situations where five or even four joints (DOF) are enough to do the required job. There are many industrial manipulators that have five or fewer DOF. These are useful for specific applications that do not require 6-DOF. A *planar manipulator* can only sweep a 2-D space or a plane and can have any number of degrees of freedom. For example, a planar manipulator with three joints (3-DOF)— may be two for positioning and one for orientation —can only sweep a plane.

Spatial manipulators with more than 6-DOF have surplus joints and are known as *redundant manipulators*. The extra DOF may enhance the performance by adding to its *dexterity*. Dexterity implies that the manipulator can reach a subspace, which is obstructed by objects, by the capability of going around these. However, redundant manipulators present complexities in modelling and coordinate frame transformations and therefore in their programming and control.

The DOF of a manipulator are distributed into subassemblies of *arm* and *wrist*. The arm is used for positioning the end-effector in space and, hence, the three positional DOF, as seen in Fig. 1.9, are provided to the arm. The remaining 3-DOF are provided in the wrist, whose task is to orient the end-effector. The type and arrangement of joints in the arm and wrist can vary considerably. These are discussed in the next section.

1.5.5 Arm Configuration

The mechanics of the arm with 3-DOF depends on the type of three joints employed and their arrangement. The purpose of the arm is to position the wrist in the 3-D space and the arm has following characteristic requirements.

- Links are long enough to provide for maximum reach in the space.
- The design is mechanically robust because the arm has to bear not only the load of workpiece but also has to carry the wrist and the end-effector.

According to joint movements and arrangement of links, four well-distinguished basic structural configurations are possible for the arm. These are characterized by the distribution of three arm joints among prismatic and rotary joints, and are named according to the coordinate system employed or the shape of the space they sweep. The four basic configurations are:

(i) Cartesian (rectangular) configuration – all three *P* joints.
(ii) Cylindrical configuration – one *R* and two *P* joints.
(iii) Polar (spherical) configuration – two *R* and one *P* joint.
(iv) Articulated (Revolute or Jointed-arm) Configuration – all three *R* joints.

Each of these arm configurations is now discussed briefly.

(i) Cartesian (Rectangular) Configuration This is the simplest configuration with all three prismatic joints, as shown in Fig. 1.11. It is constructed by three perpendicular slides, giving only linear motions along the three principal axes. There is an upper and lower limit for movement of each link. Consequently, the *endpoint* of the arm is capable of operating in a cuboidal space, called *workspace*.

The workspace represents the portion of space around the base of the manipulator that can be accessed by the arm endpoint. The shape and size of the workspace depends on the arm configuration, structure, degrees of freedom, size of links, and design of joints. The physical space that can be swept by a manipulator (with wrist and end-effector) may be more or less than the arm endpoint workspace. The volume of the space swept is called *work volume*; the surface of the workspace describes the *work envelope*.

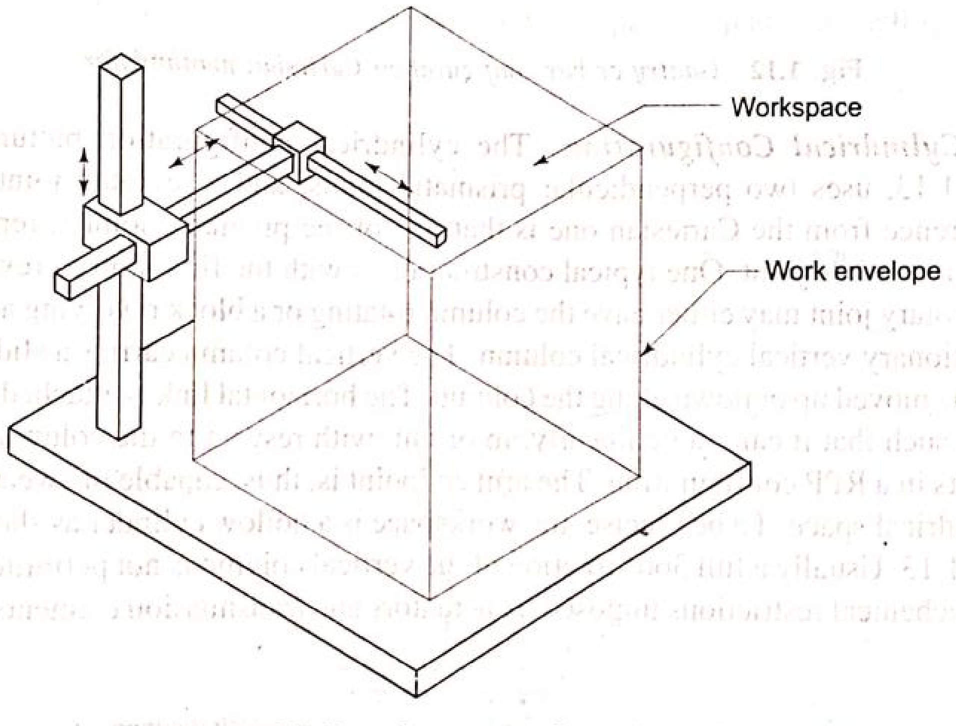

Fig. 1.11 *A 3-DOF Cartesian arm configuration and its workspace*

The workspace of Cartesian configuration is cuboidal and is shown in Fig. 1.11. Two types of constructions are possible for Cartesian arm: a *Cantilevered Cartesian*, as in Fig. 1.11, and a *Gantry* or *box Cartesian.* The latter one has the appearance of a gantry-type crane and is shown in Fig. 1.12. Despite the fact that Cartesian arm gives high precision and is easy to program, it is not preferred for many applications due to limited manipulatability. Gantry configuration is used when heavy loads must be precisely moved. The Cartesian configuration gives large work volume but has a low dexterity.

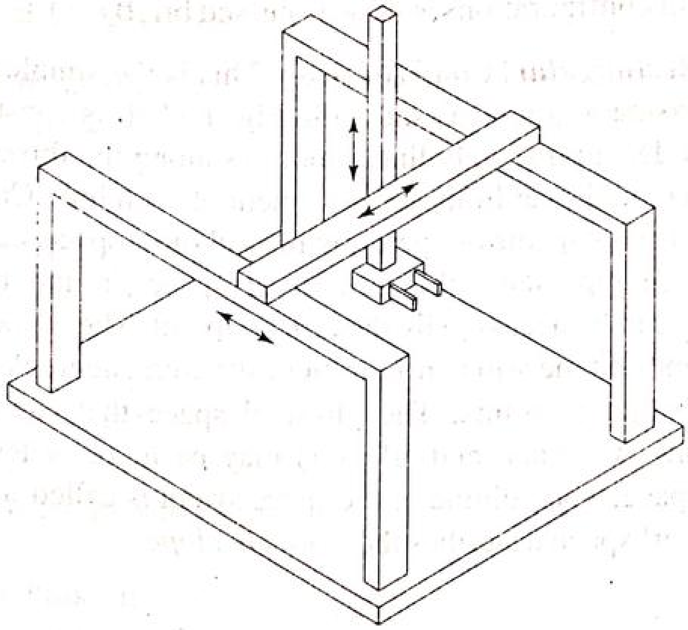

Fig. 1.12 *Gantry or box configuration Cartesian manipulator*

(ii) Cylindrical Configuration The cylindrical configuration pictured in Fig. 1.13, uses two perpendicular prismatic joints, and a revolute joint. The difference from the Cartesian one is that one of the prismatic joint is replaced with a revolute joint. One typical construction is with the first joint as revolute. The rotary joint may either have the column rotating or a block revolving around a stationary vertical cylindrical column. The vertical column carries a slide that can be moved up or down along the column. The horizontal link is attached to the slide such that it can move linearly, in or out, with respect to the column. This results in a RPP configuration. The arm endpoint is, thus, capable of sweeping a cylindrical space. To be precise, the workspace is a hollow cylinder as shown in Fig. 1.13. Usually a full 360° rotation of the vertical column is not permitted due to mechanical restrictions imposed by actuators and transmission elements.

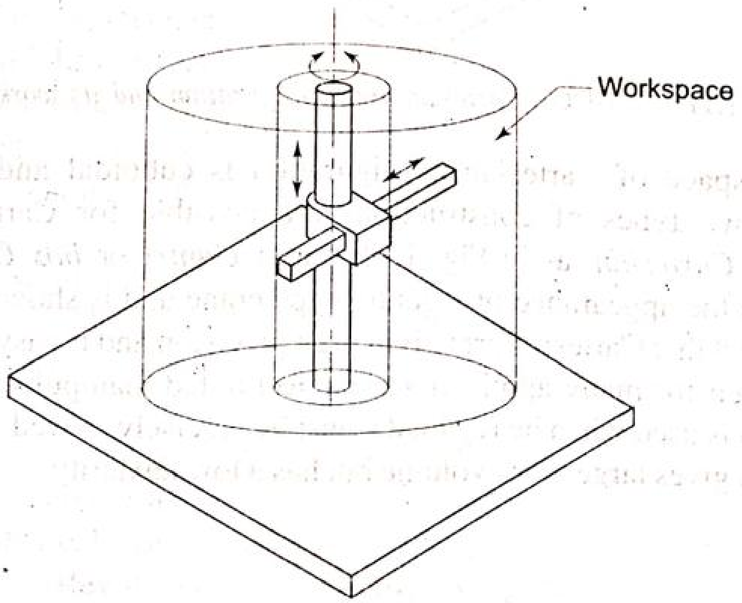

Fig. 1.13 *A 3-DOF cylindrical arm configuration and its workspace*

Many other joint arrangements with two prismatic and one rotary joint are possible for cylindrical configuration, for example, a PRP configuration. Note that all combinations of 1R and 2P are not useful configurations as they may not give suitable workspace and some may only sweep a plane. Such configurations are called *nonrobotic configurations*. It is left for the reader to visualize as to which joint combinations are robotic arm configurations.

The cylindrical configuration offers good mechanical stiffness and the wrist positioning accuracy decreases as the horizontal stroke increases. It is suitable to access narrow horizontal cavities and, hence, is useful for machine-loading operations.

(iii) Polar (Spherical) Configuration The polar configuration is illustrated in Fig. 1.14. It consists of a telescopic link (prismatic joint) that can be raised or lowered about a horizontal revolute joint. These two links are mounted on a rotating base. This arrangement of joints, known as RRP configuration, gives the capability of moving the arm end-point within a partial spherical shell space as work volume, as shown in Fig. 1.14.

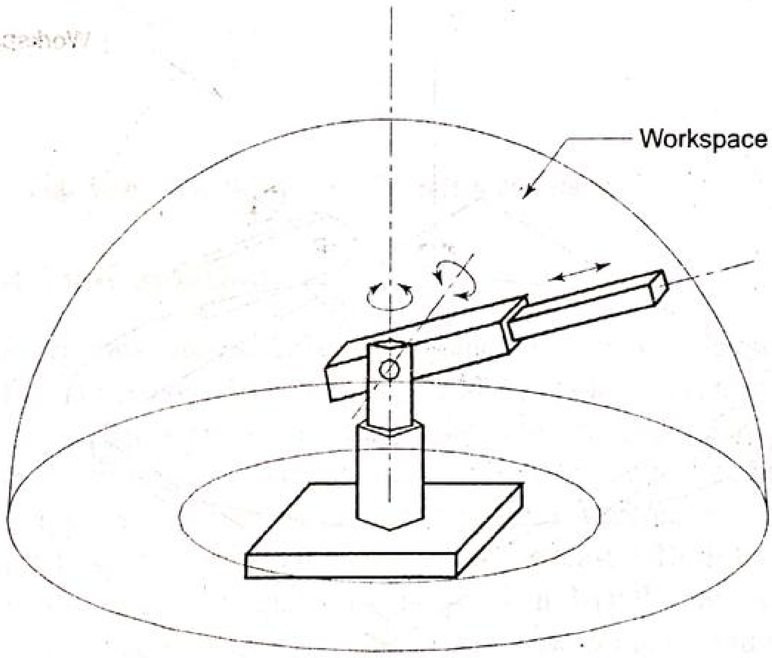

Fig. 1.14 *A 3-DOF polar arm configuration and its workspace*

This configuration allows manipulation of objects on the floor because its shoulder joint allows its end-effector to go below the base. Its mechanical stiffness is lower than Cartesian and cylindrical configurations and the wrist positioning accuracy decreases with the increasing radial stroke. The construction is more complex. Polar arms are mainly employed for industrial applications such as machining, spray painting and so on. Alternate polar configuration can be obtained with other joint arrangements such as RPR, but PRR will not give a spherical work volume.

(iv) Articulated (Revolute or Jointed-arm) Configuration The articulated arm is the type that best simulates a human arm and a manipulator with this type of an arm is often referred as an *anthropomorphic manipulator*. It consists of two straight links, corresponding to the human "forearm" and "upper arm" with two rotary joints corresponding to the "elbow" and "shoulder" joints. These two links are mounted on a vertical rotary table corresponding to the human waist joint. Figure 1.15 illustrates the joint-link arrangement for the *articulated arm*.

This configuration (RRR) is also called revolute because three revolute joints are employed. The work volume of this configuration is spherical shaped, and with proper sizing of links and design of joints, the arm endpoint can sweep a full spherical space. The arm endpoint can reach the base point and below the base, as shown in Fig. 1.15. This anthropomorphic structure is the most dexterous one, because all the joints are revolute, and the positioning accuracy varies with arm endpoint location in the workspace. The range of industrial applications of this arm is wide.

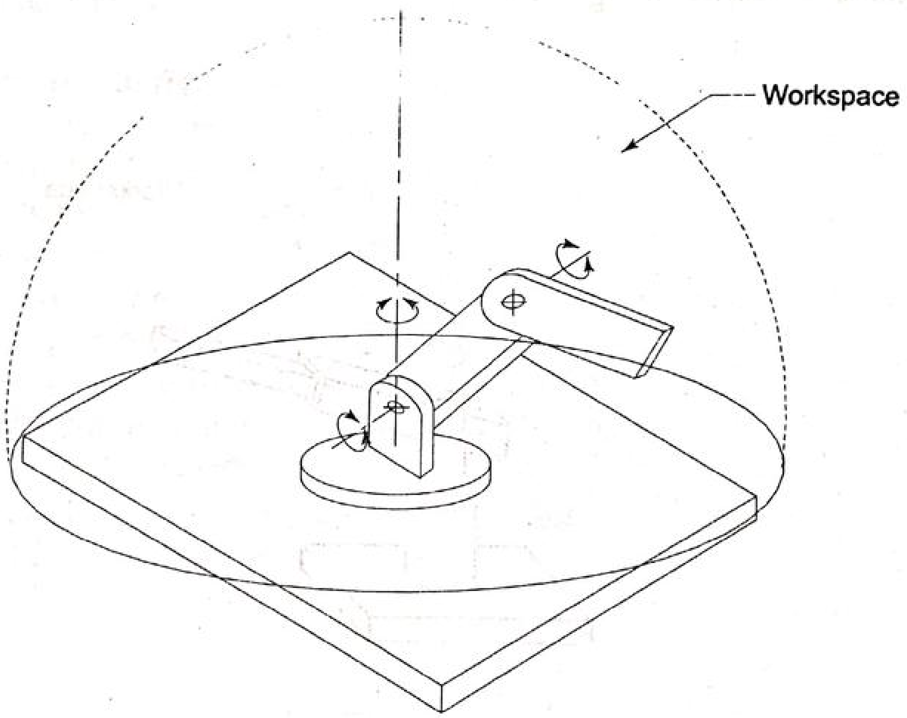

Fig. 1.15 *A 3-DOF articulated arm configuration and its workspace*

(v) Other Configurations New arm configurations can be obtained by assembling the links and joints differently, resulting in properties different from those of basic arm configurations outlined above. For instance, if the characteristics of articulated and cylindrical configurations are combined, the result will be another type of manipulator with revolute motions, confined to the horizontal plane. Such a configuration is called SCARA, which stands for Selective Compliance Assembly Robot Arm.

The SCARA configuration has vertical major axis rotations such that gravitational load, Coriolis, and centrifugal forces do not stress the structure as much as they would if the axes were horizontal. This advantage is very important at high speeds and high precision. This configuration provides high stiffness to the arm in the vertical direction, and high compliance in the horizontal plane, thus making SCARA congenial for many assembly tasks. The SCARA configuration and its workspace are presented pictorially in Fig. 1.16.

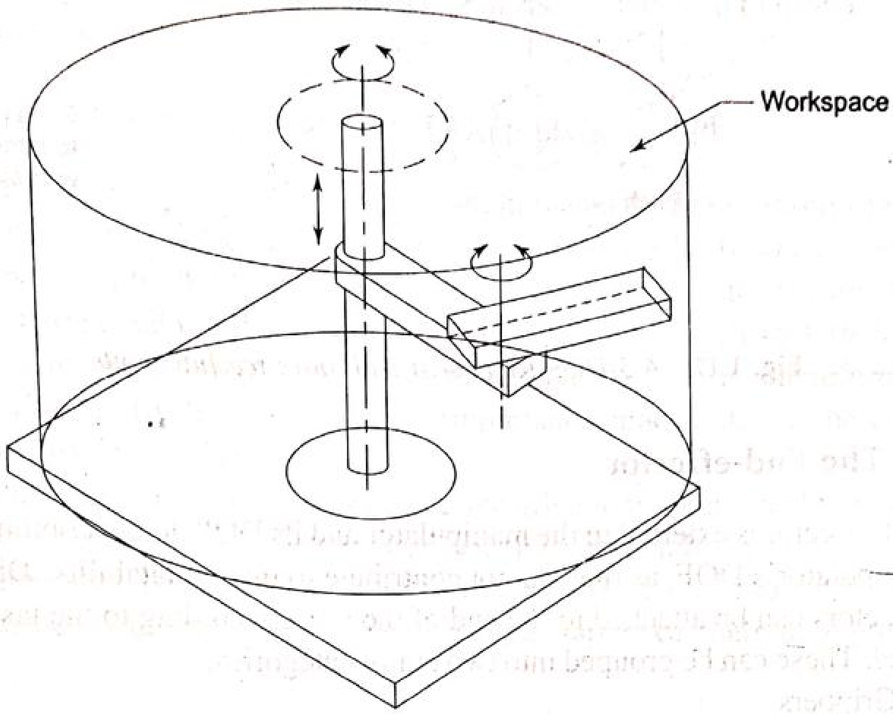

Fig. 1.16 *The SCARA configuration and its workspace*

1.5.6 Wrist Configuration

The arm configurations discussed above carry and position the wrist, which is the second part of a manipulator that is attached to the endpoint of the arm. The wrist subassembly movements enable the manipulator to orient the end-effector to perform the task properly, for example, the gripper (an end-effector) must be oriented at an appropriate angle to pick and grasp a workpiece. For arbitrary orientation in 3-D space, the wrist must possess at least 3-DOF to give three rotations about the three principal axes. Fewer than 3-DOF may be used in a wrist, depending on requirements. The wrist has to be compact and it must not diminish the performance of the arm.

The wrist requires only rotary joints because its sole purpose is to orient the end-effector. A 3-DOF wrist permitting rotation about three perpendicular axes provides for *roll* (motion in a plane perpendicular to the end of the arm), *pitch* (motion in vertical plane passing through the arm), and *yaw* (motion in a horizontal plane that also passes through the arm) motions. This type of wrist is called *roll-pitch-yaw* or *RPY* wrist and is illustrated in Fig. 1.17. A wrist with the highest dexterity is one where three rotary joint axes intersect at a point. This complicates the mechanical design.

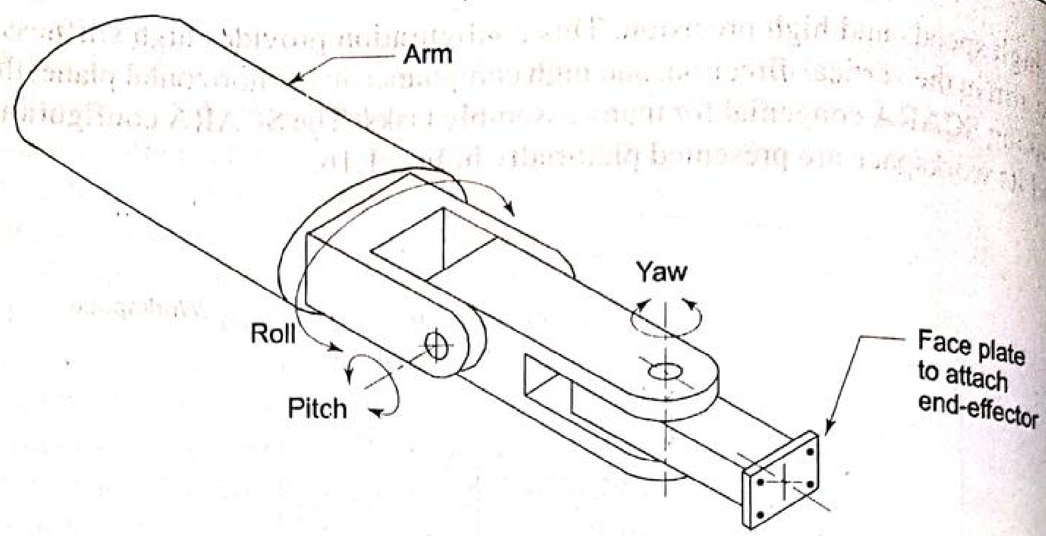

Fig. 1.17 *A 3-DOF RPY wrist with three revolute joints*

1.5.7 The End-effector

The end-effector is external to the manipulator and its DOF do not combine with the manipulator's DOF, as they do not contribute to manipulatability. Different end-effectors can be attached to the end of the wrist according to the task to be executed. These can be grouped into two major categories:

1. Grippers
2. Tools

Grippers are end-effectors to grasp or hold the workpiece during the work cycle. The applications include material handling, machine loading-unloading, palletizing, and other similar operations. Grippers employ mechanical grasping or other alternative ways such as magnetic, vacuum, bellows, or others for holding objects. The proper shape and size of the gripper and the method of holding are determined by the object to be grasped and the task to be performed. Some typical mechanical grippers are shown in Fig. 1.18.

For many tasks to be performed by the manipulator, the end-effector is a *tool* rather than a gripper. For example, a cutting tool, a drill, a welding torch, a spray

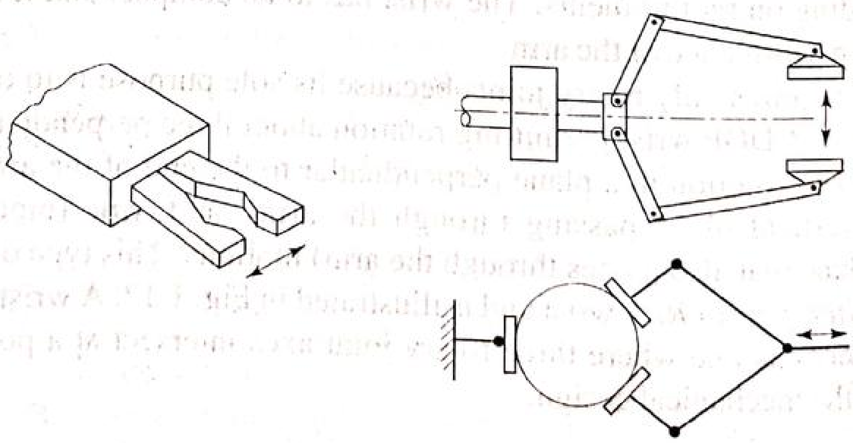

Fig. 1.18 *Some fingered grippers for holding different types of jobs*

gun, or a screwdriver is the end-effector for machining, welding, painting, or assembly task, mounted at the wrist endpoint. The tool is usually directly attached to the end of the wrist. Sometimes, a gripper may be used to hold the tool instead of the workpiece. *Tool changer* devices can also be attached to the wrist end for multi-tool operations in a work cycle.

1.6 HUMAN ARM CHARACTERISTICS

The industrial robot, though not similar to human arm, draws inspiration for its capabilities from the latter. The human arm and its capabilities make the human race class apart from other animals. The design of the human arm structure is a unique marvel and is still a challenge to replicate. Certain characteristics of the human arm are a far cry for today's manipulators. It is, therefore, worth considering briefly, human arm's most important characteristics as these serve as a benchmark for the manipulators.

The human arm's basic performance specifications are defined from the *zero reference position*, which is the stretched right arm and hand straight out and horizontal with the palm in downward direction. The three motions to orient the hand, which is the first part of human arm, are approximately in the following range.

$$-180° \leq \text{Roll} \leq +90°$$
$$-90° \leq \text{Pitch} \leq +50°$$
$$-45° \leq \text{Yaw} \leq +15°$$

Note that to provide the roll motion to the hand, forearm, and the upper-arm, both undergo a twist, while pitch and yaw are provided by the wrist joint. The second part of the human arm consists of upper arm and forearm with shoulder and elbow joints. It has 2-DOF in the shoulder with a ball and socket joint, 1-DOF in the elbow between forearm and upper-arm, with two bones in the forearm and one in upper arm. The 2-DOF shoulder joint provides an approximately hemispherical sweep to the elbow joint. The elbow joint moves the forearm by approximately 170° (from –5° to 165°) in different planes, depending on the orientation of two forearm bones and the elbow joint. For the zero reference position defined above, the forearm and the wrist can only sweep an arc in the horizontal plane.

Another important feature of the human arm is the ratio of the length of the upper arm to that of the forearm, which is around 1.2. Any ratio other than this results in performance impairment. A mechanical structure identical to the human arm, with 2-DOF shoulder joint, three-bones elbow joint, eight-bones wrist joint with complicated geometry of each bone and joint, is yet to be designed and constructed. The technology has to go a long way to replicate human arm's bone shapes, joint mechanisms, mechanism to power and move joints, motion control, safety, and above all, self repair.

The human hand, at the end of arm, with four fingers and a thumb, each with 4-DOF, is another marvel with no parallel. The finger and thumb joints can act independently or get locked, depending on the task involved, offering a very high dexterity to zero dexterity. This, coupled with the joint actuation and control mechanism and tactile sensing provided by the skin makes the human hand a marvel. In contrast, the robot gripper with two or three fingers has almost no dexterity. The human arm's articulation, and to the same extent, the human leg's locomotion are challenges yet to be met.

1.7 DESIGN AND CONTROL ISSUES

Robots are driven to perform more and more variety of highly skilled jobs with minimum human assistance or intervention. This requires them to have much higher mobility, manipulatability, and dexterity than conventional machine tools. The mechanical structure of a robot, which consists of rigid cantilever beams connected by hinged joints forming spatial mechanism, is inherently poor in stiffness, accuracy, and load carrying capacity. The errors accumulate because joints are in a serial sequence. These difficulties are overcome by advanced design and control techniques.

The serial-spatial linkage geometry of a manipulator is described by complex nonlinear transcendental equations. The position and motion of each joint is affected by the position and motion of all other joints. Further, each joint has to be powered independently, rendering modeling, analysis, and design to be quite an involved issue.

The weight and inertial load of each link is carried by the previous link. The links undergo rotary motion about the joints, making centrifugal and Coriolis effects significant. All these make the dynamic behaviour of the robot manipulator complex, highly coupled, and nonlinear. The kinematic and dynamic complexities create unique control problems that make control of a robot a very challenging task and effective control system design a critical issue. The robot control problem has added a new dimension in control research.

The environment in which robots are used poses numerous other complexities as compared to conventional machine tools. The work environment of the latter is well-defined and structured and the machine tools are essentially self-contained to handle workpieces and tools in well-defined locations. The work environment of the robot is often poorly structured, uncertain, and requires effective means to identify locations, workpieces and tools, and obstacles. The robot is also required to interact and coordinate with peripheral devices.

Robots being autonomous systems, require to perform additional tasks of planning and generating their own control commands. The detailed procedure, control strategy, and algorithm must be taught in advance and coded in an appropriate form so that the robot can interpret these and execute these accurately. Effective means to store the data, commands, and manage memory are also needed. Thus, programming and command generation become critical issues in robotics. To monitor it's own motions and to adapt to disturbances and unpredictable environments, robot requires interfacing with internal and external sensors. To utilize the sensory information, effective sensor-based algorithms and advanced control systems are required, in addition to a thorough understanding of the task.

1.8 MANIPULATION AND CONTROL

This section briefly describes the topics, which will be covered in this text, and introduces some terminology in the robotics field.

In the analysis of spatial mechanisms (manipulators), the location of links, joints, and end-effector in 3-D space is continuosly required. Mathematical description of the position and orientation of links in space and manipulation of these is, naturally, one topic of immediate importance.

To describe position and orientation of a body in space, a frame is attached to the body. The position and orientation of this frame with respect to some reference coordinate frame, called *base frame*, mathematically describes the location of the body. Frames are attached to joints, links, end-effector, and workpieces in the environment of the robot to mathematically describe them, as illustrated in Fig. 1.19.

Often, the description of a body in one frame is known, while requirement is the description of the body with respect to another frame. This requires *mapping* or *transforming* or changing the description of its attributes from one frame to another. Conventions and methodologies for description of position and orientation, and the mathematics of transforming these quantities are first discussed in this text.

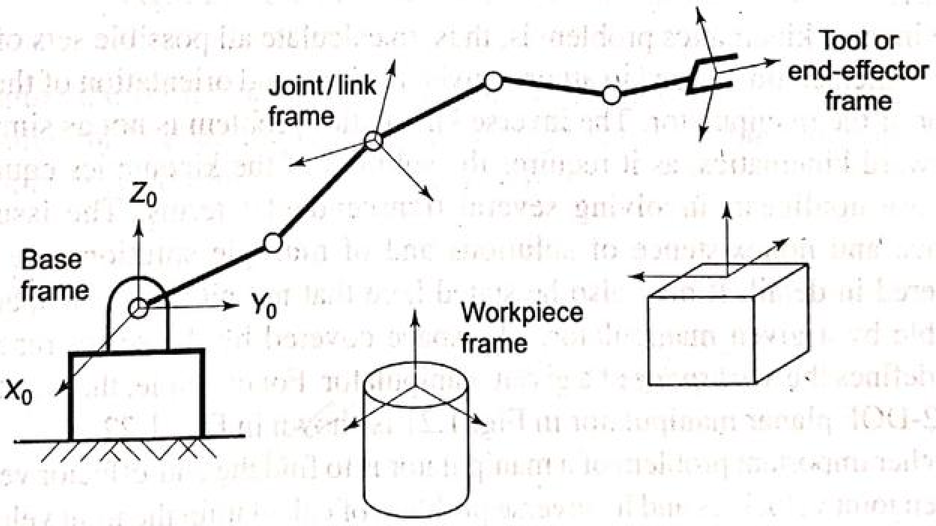

Fig. 1.19 *Attachment of frames for manipulator modelling*

Consider the simplest nontrivial two-link planar manipulator of Fig. 1.20 with link lengths (L_1, L_2) and assume that the joint angles are (θ_1, θ_2) and the coordinates of end-effector point P are (x, y). From simple geometrical analysis for this manipulator, it is possible to compute coordinates (x, y) from the given joint angles (θ_1, θ_2) and for a given location of point P (x, y), joint angles (θ_1, θ_2) can be computed.

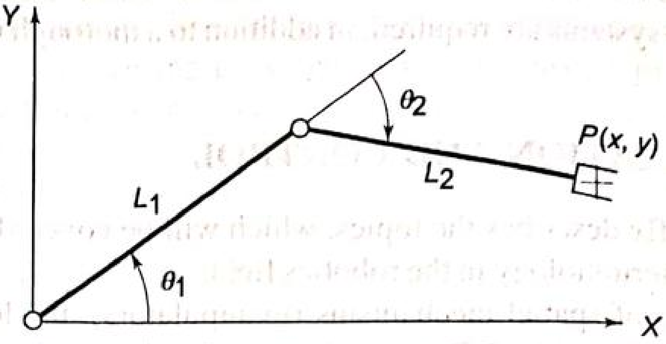

Fig. 1.20 *The 2-DOF two-link planar manipulator*

The basic problem in the study of mechanical manipulation is of computing the position and orientation of end-effector of the manipulator when the joint angles are known. This is referred to as *forward kinematics* problem. The *inverse kinematics* problem is to determine the joint angles, given the position and orientation of the end-effector.

A problem that can be faced in inverse kinematics is that the solution for joint angles may not be unique; there may be multiple solutions. This is illustrated for the simple planar 2-DOF manipulator in Fig. 1.20.

If the 2-DOF manipulator in Fig. 1.20 is used to position some object held in its end-effector to a specified position P_1 (x_1, y_1), the joint angles θ_1 and θ_2 that make the end point coincide with desired location must be found. This is the *inverse kinematics* problem. For the manipulator in Fig. 1.20, there are two sets of joint angles θ_1 and θ_2 that lead to the same endpoint position, as illustrated in Fig. 1.21.

The inverse kinematics problem is, thus, to calculate all possible sets of joint angles, which could be used to attain a given position and orientation of the end-effector of the manipulator. The inverse kinematics problem is not as simple as the forward kinematics, as it requires the solution of the kinematics equations which are nonlinear, involving several transcendental terms. The issues of existence and nonexistence of solutions and of multiple solutions are to be considered in detail. It may also be stated here that not all points in space are reachable by a given manipulator. The space covered by the set of reachable points defines the *workspace* of a given manipulator. For example, the workspace of the 2-DOF planar manipulator in Fig. 1.21 is shown in Fig. 1.22.

Another important problem of a manipulator is to find the end-effector velocity for given joint velocities and its inverse problem of calculating the joint velocities for specified end-effector velocity. These two problems, direct and inverse need the manipulator Jacobian (matrix), which is obtained from the kinematic parameters.

An identical problem of the static force analysis can also be solved through the Jacobian. This problem is stated as: given a desired contact force and moment,

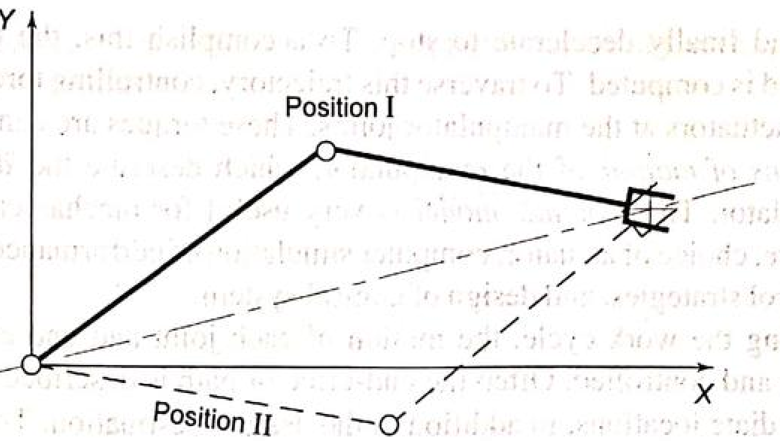

Fig. 1.21 *Two possible joint positions for a given end point position*

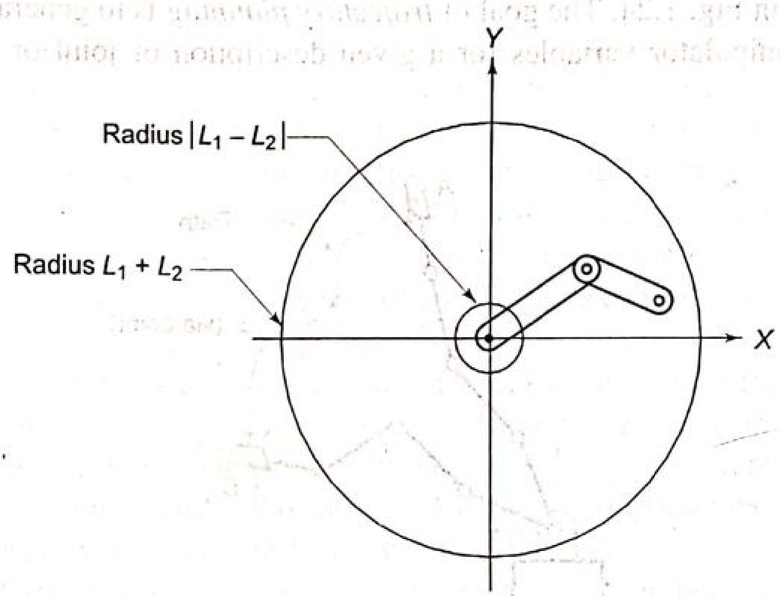

Fig. 1.22 *The workspace of a 2-DOF planar manipulator*

determine the set of joint torques to generate them or vice-versa. Figure 1.23 illustrates the interaction of a manipulator at rest with the environment; the manipulator is exerting a force $\boldsymbol{F}$ on the body.

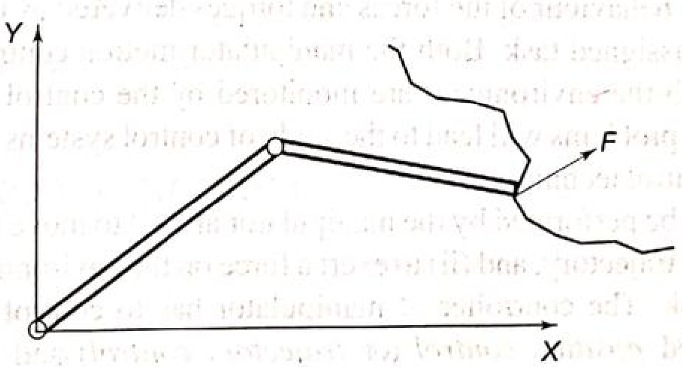

Fig. 1.23 *Manipulator exerting a force on the environment*

To perform an assigned task or to attain a desired position, a manipulator is required to accelerate from rest, travel at specified velocity, traverse a specified path, and finally decelerate to stop. To accomplish this, the trajectory to be followed is computed. To traverse this trajectory, controlling torques are applied by the actuators at the manipulator joints. These torques are computed from the *equations of motion* of the manipulator, which describe the *dynamics* of the manipulator. The *dynamic model* is very useful for mechanical design of the structure, choice of actuator, computer simulation of performance, determination of control strategies, and design of control system.

During the work cycle, the motion of each joint and end-effector must be smooth and controlled. Often the end-effector path is described by a number of intermediate locations, in addition to the desired destination. The term *spline* is used to refer to a smooth function, which passes through a set of specified points. The motion of end-effector through space from point A to point C via point B is illustrated in Fig. 1.24. The goal of *trajectory planning* is to generate time laws for the manipulator variables for a given description of joint or end-effector motion.

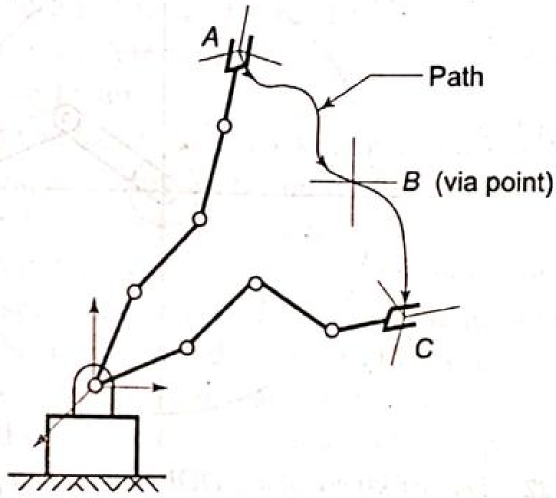

Fig. 1.24 *Trajectory generation for motion from A to C via B*

The dynamic model and the generated trajectory constitute the inputs to the motion-control system of the manipulator. The problem of manipulator control is to find the time behaviour of the forces and torques delivered by the actuators for executing the assigned task. Both the manipulator motion control and its force interaction with the environment are monitored by the control algorithm. The above exposed problems will lead to the study of control systems for manipulator and several control techniques.

The tasks to be performed by the manipulator are: (i) to move the end-effector along a desired trajectory, and (ii) to exert a force on the environment to carry out the desired task. The controller of manipulator has to control both tasks, the former is called *position control* (or *trajectory control*) and the latter *force control*. A schematic sketch of a typical controller is given in Fig. 1.25. The positions, velocities, forces, and torques are measured by *sensors* and based on these measurements and the desired behaviour, the controller determines the inputs to the actuators on the robot so that the end-effector carries out the desired task as closely as possible.

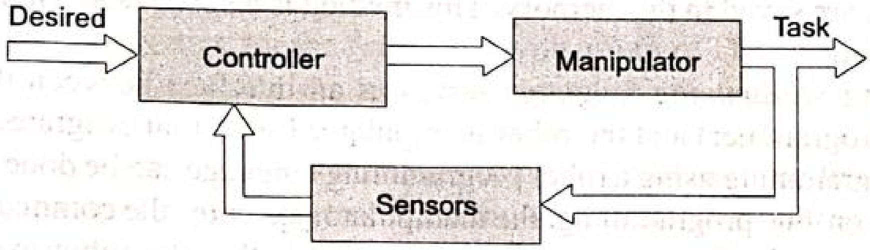

Fig. 1.25 *A schematic sketch of a manipulator control system*

1.9 SENSORS AND VISION

The control of the manipulator demands exact determination of parameters of interest so that the controller can compare them with desired values and accordingly command the actuators of the manipulator. Sensors play the most important role in the determination of actual values of the parameters of interest. For manipulator motion control, joint-link positions, velocities, torques, or forces are required to be sensed and the end-effector position and orientation is required for determining actual trajectory being tracked. The force control requires sensing of joint force/torque and end-effector force/torque.

Sensors used in robotics include simple devices such as a potentiometer as well as sophisticated ones such as a *robotic vision system*. Sensors can be an integral part of the manipulator (*internal sensors*) or they may be placed in the robot's environment or workcell (*external sensors*) to permit the robot to interact with the other activities and objects in the workcell.

The task performance capability of a robot is greatly dependent on the sensors used and their capabilities. Sensors provide intelligence to the manipulator. Sensors used in robotics are *tactile sensors* or *nontactile sensors*; *proximity or range sensors*; *contact* or *noncontact sensors*, or a vision system.

A robotic vision system imparts enormous capabilities to a robot. The robotic vision or vision sensing provides the capability of viewing the workspace and interpreting what is seen. Vision-equipped robots are used for inspection, part recognition, and identification, sorting, obstacle avoidance, and other similar tasks.

1.10 PROGRAMMING ROBOTS

Robots have no intelligence to learn by themselves. They need to be "taught" what they are expected to do and "how" they should do it. The teaching of the workcycle to a robot is known as *robot programming*. Robots can be programmed in different ways. One is "teach-by-showing" and the other is using textual commands with a suitable interface.

The manipulator is required to execute a specified workcycle and, therefore, must know where to move, how to move, what work to do, where and so on. In teach-by-showing method of programming, the manipulator is made to move through the desired motion path of the entire workcycle and the path and other parameters are saved in the memory. This method is also known as *lead through programming*.

A *robot programming language* serves as an interface between the human user (the programmer) and the robot manipulator for textual programming. The textual programming using a robot programming language can be done on-line or off-line. In on-line programming, the manipulator executes the command as soon as it is entered and the programmer can verify whether the robot executes the desired task. Any discrepancy is, therefore, corrected immediately.

In off-line programming, the robot is not tied-up and can continue doing its task, that is, there is no loss of production. The programmer develops the program and tests it in a simulated graphical environment without the access to the manipulator. After the programmer is satisfied with the correctness of the program, it is uploaded to the manipulator. In off-line and on-line programming, after the program is complete, it is saved and the robot executes it in the 'run' mode relentlessly.

The robot programming languages are built on the lines of conventional computer programming languages and have their own 'vocabulary', 'grammar', and 'syntaxes'. A typical vocabulary includes command verbs for (i) definition of points, paths, frames and so on, (ii) motion of joints-links and end-effector, (iii) control of end-effector, say grippers to open, close and so on; and (iv) interaction with sensors, environment, and other devices.

Each robot-programming language will also require traditional commands and functions for: arithmetic, logical, trigonometric operations; condition testing and looping operations; input-output operations; storage, retrieval, update, and debugging and so on.

The robot programming encompasses all the issues of traditional computer programming or software development and computer programming languages. This is an extensive subject itself and is not included in this book.

1.11 THE FUTURE PROSPECTS

The use of robots in industries has been increasing at the rate of about 25% annually. This growth rate is expected to increase rapidly in the years to come with more capable robots being available to the industry at lesser costs. The favourable factors for this prediction are:

(i) More people in the industry are becoming aware of robot technology and its potential benefits.
(ii) The robotics technology will develop rapidly in the next few years and more user-friendly robots will be available.
(iii) The hardware, software interfacing, and installations will become easier.
(iv) The production of industrial robots will increase and will bring down the unit cost, making deployment of robots justifiable.

(v) The medium and small-scale industries will be able to beneficially utilize the new technology.

All these will increase the customer base and, therefore, demand for the industrial robots and manpower geared with robot technology.

Robot is the technology for the future and with a future. The current research goals and trends indicate that the industrial robots of the future will be more robust, more accurate, more flexible, with more than one arm, more mobile, and will have many more capabilities. The robots will be human friendly and intelligent, capable of responding to voice commands and will be easy to program.

1.11.1 Biorobotics and Humanoid Robotics

A new research field in robotics inspired by biological systems has arisen. The technological developments have made it possible for engineers and robot designers to look for solutions in nature and look forward to achieving one of their most attractive goals to develop a humanoid robot.

Conventional viewpoint in robot design is dominated by its industrial applications, where emphasis is on mechanical properties that go beyond human performance, such as doing stereotype work tirelessly, carrying heavy loads, working in hostile environment, or giving high precision and consistent performance.

The biorobotics is historically connected to service robotics. These robots are conceptualized in a different manner than industrial robots. Their task is usually to help humans in diverse activities from house cleaning to carrying out a surgery, or playing the piano to assisting the disabled and the elderly.

The motion abilities of biological systems, their intelligence, and sensing are far ahead of all the achievements in manmade things till date. Progress in robot technology, rapid technological developments through the remarkable achievements in computer-aided technology in recent years have opened an entirely new research area, where the objective is to analyze and model biological systems behaviour, intelligence, sensing, and motions in order to incorporate properties of biological systems in robots. The ultimate objective is to produce a humanoid robot. The aspirations are not to limit these to service robots but these are to be extended to the industrial robots. It is expected that humanoid robots will be able to communicate with humans and other robots; facilitate robot programming; increase their flexibility and adaptability for executing different tasks; learn from experience; and adapt to different tasks and environments or change of place.

In the implementation of biological behavioural systems, the replication of anthropomorphic characteristics is possibly the answer in every context of development in robotics. The research in anthropomorphic robotics has advanced to development of anthropomorphic components for humanoid robots like anthropomorphic visual and tactile sensors, anthropomorphic actuators and anthropomorphic computing techniques. Replicating the functionality of the human brain is one of the hardest challenges in the biorobotics and in general still one of the most difficult objectives.

1.12 NOTATIONS

In a subject of interdisciplinary nature like robotics encompassing mechanical, electrical and many other disciplines, use of clear and consistent notations is always an issue. In this text we have used the following notations and conventions:

1. Vectors and matrices are written in upper case-bold-italic. Unit vectors are lower case-bold-italic, as an exception. Lower case italic is used for scalars. Vectors are taken as column vectors. Components of a vector or matrix are scalars with single subscript for vector components and double subscripts for matrix components. For example, components of a vector are a_i or b_z and elements of a matrix are a_{ij}.
2. Coordinate frames are enclosed in curved parenthesis { }, for example coordinate frame with axes XYZ is $\{x\ y\ z\}$ or coordinate frame 1 is {1} and square parenthesis [ ] are used for elements of vectors and matrices.
3. The association of a vector to a coordinate frame is indicated by a leading superscript. For example, $^0\boldsymbol{P}$ is a position vector $\boldsymbol{P}$ in frame {0}.
4. A trailing subscript on a vector is used, wherever necessary to indicate what the vector represents. For example, $\boldsymbol{P}_{tool}$, represents the tool position vector and $\boldsymbol{v}_i$ represents velocity vector for link i.
5. Matrices used for transformation from one coordinate frame to another, have a leading superscript and a trailing subscript. For example, $^0\boldsymbol{T}_1$ denotes the coordinate transformation matrix, which transforms coordinates from frame {1} to frame {0}.
6. Trailing superscripts on matrices are used for inverse or transpose of a matrix, for example, $\boldsymbol{R}^{-1}$ or $\boldsymbol{R}^T$ and on vectors for transpose of a vector, for example, if $\boldsymbol{P}$ is a column vector $\boldsymbol{P}^T$ is a row vector.
7. Many trigonometric functions are required in mathematical models. The sines and cosines of an angle θ_i can take any of the forms: $\cos\theta_i = C\theta_i = C_i$ and $\sin\theta_i = S\theta_i = S_i$. Some more shortened forms are $V\theta_i$ for $(1 - \cos\theta_i)$ and S_{ij} for $\sin(\theta_i + \theta_j)$.

A complete list of symbols used in the text is available in Appendix E.

1.13 BIBLIOGRAPHICAL REFERENCE TEXTS

Literature production in the nascent field of robotics has been conspicuous in the last twenty years, both in terms of research monographs and textbooks. The number of scientific and technical journals dedicated to robotics are also few, though the robotics field has simulated an ever-increasing number of scholars and has established a truly respectable international research community.

This chapter, therefore, includes a selection of journals, reference texts and monographs related to the field. The bibliography references cited here are representative of publications dealing with topics of interest in robotics and related fields.

General and Specialized Texts

The following texts include general and specialized books on robotics and allied subjects. The texts on robotics share an affinity of contents with this text and may provide the complimentary reading for the material in this text. Other books and monographs render supplementary material for those readers who wish to make a thorough study in the robotics.

1. Issac Asimov, *The Complete Robot*, Doubleday & Company, Garden City, New York, 1982.
2. Amitabh Bhattacharya, *Robotics and their Applications in India: A State of the Art Report*, Department of Science and Technology, New Delhi, 1987.
3. J.J. Craig, *Introduction to Robotics, Mechanics and Control*, 2nd edition, Addison-Wesley, 1989.
4. R.C. Dorf and S. Nof, Editors, *The International Encyclopedia of Robotics*, John C. Wiley and Sons, 1988.
5. D.M. Etter, *Engineering Problem Solving with MATLAB*, Prentice-Hall Englewood Cliffs, 1993.
6. Daniel T. Finkbeiner, II, *Introduction of Matrices and Linear Transformation*, D.B. Taraporevala Sons & Co. Pvt. Ltd., Mumbai, 1968.
7. K.S. Fu, R.C. Gonzalez and C.S.G. Lee, *Robotics: Control, Sensing, Vision, and Intelligence*, McGraw-Hill, 1987.
8. M.P. Groover, M.Weiss, R.N.Nagel and N.G.Odrey, *Industrial Robotics—Technology, Programming and Applications*, McGraw-Hill, 1986.
9. R.S. Hartenberg and J. Denavit, *Kinematic Synthesis of Linkages*, McGraw-Hill, 1964.
10. P.A. Janakiraman, *Robotics and Image Processing*, Tata McGraw-Hill Co. Ltd., New Delhi, 1995.
11. R.D. Klafter, Thomas A. Chmielewski and Michael Negin, *Robotic Engineering: An Integrated Approach*, Prentice-Hall, 1994.
12. J.C. Latombe, *Robot Motion Planning*, Kluwer Academic Publishers, 1991.
13. N.E. Leonard and W.S. Levone, *Using MATLAB to Analysis and Design Control Systems*, Addison-Wesley, 1995.
14. Fairhurst C. Micheal, *Computer Vision for Robotic Systems*, Prentice-Hall International (UK), 1988.
15. I.J. Nagrath and M. Gopal, *Control Systems Engineering*, New Age International Ltd., 3rd ed., 1999.
16. R.P. Paul, *Robot Manipulators: Mathematics, Programming, and Control*, MIT Press, Cambridge, Mass, 1981.
17. E. I. Rivin, *Mechanical Design of Robots*, McGraw-Hill, 1988.

18. R.J. Schilling, *Fundamentals of Robotics: Analysis and Control*, Prentice-Hall of India, New Delhi, 1996.
19. L. Sciavicco and B. Siciliano, *Modeling and Control of Robot Manipulators*, The McGraw-Hill Companies Inc., New York, 1996.
20. J.E. Shigley and Jr.J.J. Uicker, *Theory of Machines and Mechanisms*, 2nd edition, McGraw-Hill, 1995.
21. M.W. Spong, F.L. Lewis and C. Abdallah, *Robot Control: Dynamics, Motion Planning, and Analysis*, IEEE Press, New York, 1993.
22. W. Stadler, *Analytical Robotics and Mechatronics*, McGraw-Hill Inc., New York, 1995.
23. T. Yoshikawa, *Foundations of Robotics: Analysis and Control*, Prentice-Hall of India, 1998. (MIT Press, Cambridge, Mass., 1990).

Dedicated and Related Journals

Some of the following journals and magazines are dedicated to robotics while other prestigious journals give substantial space to robotics and occasionally or routinely publish papers in the robotics field, on allied topics or contain articles on various aspects of robots and robotics.

1. *Advanced Robotics*, Published (8 issues) by Robotics Society of Japan.
2. American Society of Mechanical Engineers (ASME), New York Publications:
   - *Journal of Mechanical Design*, Quarterly.
   - *Mechanical Engineering Magazine*, Monthly.
   - *Journal of Applied Mechanics*, Bimonthly.
   - *Journal of Dynamics Systems, Measurement and Control*, Quarterly.
   - *Journal of Mechanisms, Transmission and Automaton in Design*.
3. *Artificial Intelligence*, Published monthly by Elsevier Science.
4. *Computers Graphics, Vision & Image Processing*, Published monthly by Academic Press.
5. *Institute of Electrical and Electronic Engineering* (IEEE) Inc., New York Publications:
   - *IEEE Computer Magazine*, Monthly.
   - *IEEE Control Systems Magazine*, Bimonthly.
   - *IEEE/ASME Journal of Microelectromechanical Systems*, Bimonthly.
   - *IEEE Robotics and Automation Magazine*, Quarterly.
   - *IEEE Sensors Journal*, Bimonthly.
   - *IEEE Transactions on Biomedical Engineering*, Monthly.
   - *IEEE Transactions on Control Systems Technology*, Quarterly.
   - *IEEE Transactions on Pattern Analysis and Machine Intelligence*, Monthly.
   - *IEEE Transactions on Robotics and Automation*, Bimonthly.
   - *IEEE Transactions on System, Man and Cybernetics*, Bimonthly.
   - *Proceedings of IEEE*.

6. *The Industrial Robots*, Published monthly by Society of Manufacturing Engineers.
7. *International Journal of Robotics Research*, Published Monthly by Sage Science Press, USA.
8. *International Journal of Robotics & Automation*, Published quarterly by ACTA Press (IASTED).
9. *Journal of Manufacturing Technology*, Published by Indian Institute of Production Engineers.
10. *International Journals of Robotics,* Published bimonthly by Robotics Society of Japan.
11. *Journal of Robotic Systems*, Published monthly by Wiley InterScience, John Wiley & Sons Inc., New York.
12. *Journal of Robotics and Computer Integrated Manufacturing*, Published by monthly by Elsevier Science Ltd.
13. *Journal of Intelligent and Robotic Systems—Theory and Applications* (*incorporating Mechatronics Systems Engineering*), Published monthly by Kluwer Press.
14. *Robotica*, (International Journal of Information, Educational Research in Robotics and Artificial Intelligence), Published monthly by Cambridge University Press, UK.
15. *Robotics and Autonomous Systems,* Published quarterly by Elsevier Science, North Holland.

Selected References

The technical articles cited below are on topics introduced in this chapter and other topics of interest in robotics and related fields. The references at the end of later chapters are specific to the topics discussed in the chapter.

1. C. Buhler, "Robotics for rehabilitation—a European (?) Perspective," *Robotica*, ***16***, 487–489, 1998.
2. R.A. Brooks, "Solving the Path Finding Problem, by Good Representation of Free Space," *IEEE Tr on Systems, Man, and Cybernetics*, ***13***, 190–197, 1983.
3. Susan Bonner and Kang G. Shin, "A Comparative Study of Robot Languages," *IEEE Computer Magazine*, ***15***(12), 82–96, Dec. 1982.
4. K.D. Chaney and J.K. Davidson, "A Synthesis Method for Placing Workpieces in RPR Planar Robotic Workcells", *ASME Journal of Mechanical Design*, ***120***, 262–268, 1998.
5. P. Dario, E. Guglielmelli and C. Laschi, "Humanoids and Personal Robots: Design and Experiments," *J. of Robotic Systems*, ***18***(12), 673–690, 2001.
6. Y. Eiichi, "Local Communication of Multiple Mobile Robots," *Journal of Robotic Systems*, ***15***(7), 407–409, 1998.
7. C. Gosselin, "Determination of the Workspace of 6-DoF Parallel Manipulators," *J of Mechanical Design*, ***114***, 331–335, Sep 1992.

8. W. Hsu, C.S.G. Lee and A. Lim, "A Computer-aided Product Redesign System for Robotic Assembly," *Robotica*, ***16***, 239–249, 1998.
9. A. Kumar and K.J. Waldron, "The Workspaces of Mechanical Manipulators," *J of Mechanical Design*, ***103***, 665–672, Jul 1981.
10. K.B. Kim, "Introduction to the Special Issue on Design and Applications in Robotics," *Robotica*, ***17***(1), 1–2, 1999.
11. M.H. Lee, "Tactile sensing: New Direction, New Challenges," *Int. J. of Robotic Research*, ***19***(7), 636–343, 2001.
12. J.Y.S. Luh, "Conventional Controller Design for Industrial Robots—A Tutorial," *IEEE Tr on Systems, Man, and Cybernetics*, ***13***(3), 298–316, 1983.
13. F.C. Park and R.W. Brockett, "Kinematic Dexterity of Robotic Mechanisms," *The International Journal of Robotics Research*, ***13***(1), 1–15, Feb 1994.
14. R.P. Paul, B.E. Shimano and G. Mayer, "Kinematic Control Equations for Simple Manipulators," *IEEE Tr on Systems, Man, and Cybernetics*, ***11***(6), 449–455, 1981.
15. B.K. Rout and R.K. Mittal, A Review on Minimizing variability in product performance with the help of computational tools by controlling active and noise factor for Robust design, *Proc. of National Seminar on Current Applications of Computers in Design Engineering*, Jodhpur, India, 81–90, March 3–4, 2001.
16. B. Siciliano and J. Lenarcic, "Biorobotics and Human Robotics," editorial for special issue of *J. of Robotic Systems*, ***18***(12), 671–672, 2001.
17. C. Schafer and R Dillmann, "Kinematic Design of a Humanoid Robot Wrist," *J. of Robotic Systems*, ***18***(12), 747–754, 2001.
18. N.N. Sharma and R.K. Mittal, "Examination of Design Model's Influences on Control Performance of Robotic Manipulator", *Proc. of 9th IASTED International Conference: Applied Informatics (AI2001)*, Innsbruck, Austria, 131–136, Feb. 19–23, 2001.
19. Ken Taylor, Barney Dalton and James Trevelyan, "Web-based Telerobotics," *Robotica*, ***17***(1), 49–57, 1999.
20. T. Yoshikawa, "Manipulability of Robotic Mechanisms," *The International Journal of Robotics Research*, ***4***(2), 3–9, 1985.

EXERCISES

1.1 Name the four basic components of a robot system.

1.2 Describe the functions of four basic components of a robot.

1.3 Define the degree of freedom.

1.4 Name the four basic arm configurations that are used in robotic manipulators.

1.5 Where is the end-effector connected to the manipulator?

1.6 Give all possible classifications of robots.

1.7 Describe the role of arm and wrist of a robotic manipulator.
1.8 Define the term work envelope.
1.9 Draw the side view of the workspace of a typical
(a) Cylindrical configuration arm.
(b) Polar configuration arm.
(c) Articulated configuration arm.
1.10 Briefly describe the four basic configurations of arm in robotic manipulators.
1.11 Define the following
(a) Load carrying capacity
(b) Work volume
(c) End-effector.
1.12 What is the range of number of axes that may be found in industrial manipulators?
1.13 How many degrees of freedom are normally provided in the arm of a manipulator?
1.14 How many degrees of freedom can a wrist have? What is the purpose of these degrees of freedom?
1.15 Discuss the differences between polar arm and articulated arm configurations.
1.16 What are the advantages and disadvantages of cylindrical arm configuration over a polar arm configuration?
1.17 For each of the following tasks, state whether a gripper or an end-of-arm tooling is appropriate:
(a) Welding.
(b) Scraping paint from a glass pane.
(c) Assembling two parts.
(d) Drilling a hole.
(e) Tightening a nut of automobile engine.
1.18 An end-effector attached to a robot makes the robot "specialized" for a particular task. Explain the statement.
1.19 Make a chart showing the major industrial applications of robots.
1.20 Make a chronological chart showing the major developments in the field of robotics.
1.21 Prepare a state of art report on robotics in India.
1.22 Who are the users of robots in India? Prepare a status report on industrial applications of robots in India and project the demand for the future.
1.23 Find out the applications of robots in space exploration.
1.24 Discuss reasons for using a robot instead of human being to perform a specific task.
1.25 Discuss the possible applications of robots other than industrial applications. Prepare a report and indicate the weakest areas.
1.26 What are the socioeconomic issues in using robots to replace human workers from the workplace? Explain.

1.27 What are the control issues in robotic control? Explain briefly.
1.28 Describe the methods of teaching robots.
1.29 How are robots different from conventional machine tools? Discuss the design and control issues involved in the two cases and compare.
1.30 Explore the anatomy of the human wrist joint and analyze it for type of motions provided, number of degrees of freedom, number of joints, type of joints, etc.
1.31 A robot is required to perform an assembly of a shaft into a bearing placed in an arbitrary position. How many degrees of freedom are required for a manipulator to perform this task? If the bearing is placed in a fixed plane, say a horizontal plane, what will be the required number of degrees of freedom? Explain.
1.32 Study the human arm anatomy and describe the features a humanoid robot should have.

2

Coordinate Frames, Mapping, and Transforms

The robot (manipulator or arm) consists of several rigid links, connected together by joints, to achieve the required motion in space and perform the desired task. The modeling of robot comprises of establishing a special relationship between the manipulator and the manipulated object. The position of links in space and their motion are described by spatial geometry.

A systematic and generalized approach for mathematical modeling of position and orientation of links in space with respect to a reference frame is carried out with the help of vector and matrix algebra. Because the motion of each link can be described with respect to a reference coordinate frame, it is convenient to have a coordinate frame attached to the body of each link.

2.1 COORDINATE FRAMES

In a 3-D space, a coordinate frame is a set of three orthogonal right-handed axes X, Y, Z, called *principal axes*. Such a frame is shown in Fig. 2.1 with the origin of the principal axes at 'O' along with three unit vectors $\hat{x}, \hat{y}, \hat{z}$ along these axes. This frame is labelled as $\{x\,y\,z\}$ or by a number as $\{1\}$ using a numbering scheme. Other frames in the space are similarly labelled.

Any point P in a 3-D space can be defined with respect to this coordinate frame by a vector $\overrightarrow{OP}$ (a directed line from origin O to point P pointing towards P). In vector notation

$$\vec{P} = \overrightarrow{OP} = p_x\hat{x} + p_y\hat{y} + p_z\hat{z} \tag{2.1}$$

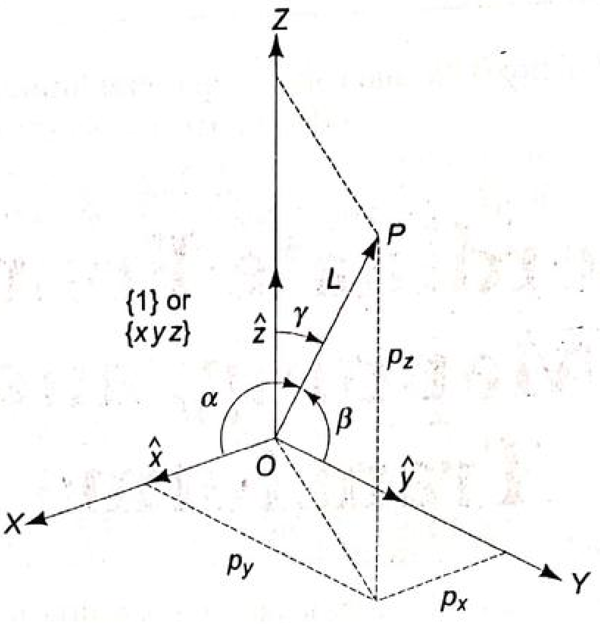

Fig. 2.1 *Position and orientation of a point P in a coordinate frame*

where p_x, p_y, p_z are the components of the vector $\overrightarrow{OP}$ along the three coordinate axes or the projections of the vector $\overrightarrow{OP}$ on the axes X, Y, Z, respectively. A *frame-space* notation is introduced as ${}^1\boldsymbol{P}$ to refer to the point P (or vector $\overrightarrow{OP}$) with respect to frame {1} with its components in the frame as ${}^1p_x$, ${}^1p_y$, and ${}^1p_z$, that is,

$$ {}^1\boldsymbol{P} = {}^1p_x\hat{x} + {}^1p_y\hat{y} + {}^1p_z\hat{z} \tag{2.2}$$

In vector-matrix notation, this equation can be written in terms of the vector components only as:

$$ {}^1\boldsymbol{P} = \begin{bmatrix} {}^1p_x \\ {}^1p_y \\ {}^1p_z \end{bmatrix} = \begin{bmatrix} {}^1p_x & {}^1p_y & {}^1p_z \end{bmatrix}^T \tag{2.3}$$

Observe that the leading superscript refers to the coordinate frame number (frame {1} in this case) and $[A]^T$ indicates the transpose of matrix $\boldsymbol{A}$. In addition, the direction of the position vector $\overrightarrow{OP}$ can be expressed by the direction cosines:

$$\cos\alpha = \frac{{}^1p_x}{L}, \ \cos\beta = \frac{{}^1p_y}{L}, \ \cos\gamma = \frac{{}^1p_z}{L}$$

with
$$L = |\vec{P}| = |\overrightarrow{OP}| = \sqrt{({}^1p_x)^2 + ({}^1p_y)^2 + ({}^1p_z)^2} \tag{2.4}$$

where α, β, and γ are, respectively, the right handed angles measured from the coordinate axes to the vector $\overrightarrow{OP}$, which has a length L.

2.1.1 Mapping

Mappings refer to changing the description of a point (or vector) in space from one frame to another frame. The second frame has three possibilities in relation to the first frame:

(a) Second frame is rotated with respect to the first; the origin of both the frames is same. In robotics, this is referred as changing the orientation.
(b) Second frame is moved away from the first, the axes of both frames remain parallel, respectively. This is a translation of the origin of the second frame from the first frame in space.
(c) Second frame is rotated with respect to the first and moved away from it, that is, the second frame is translated and its orientation is also changed.

These situations are modelled in the following sections. It is important to note that mapping changes the description of the point and not the point itself.

2.1.2 Mapping between Rotated Frames

Consider two frames, frame {1} with axes *X, Y, Z*, and frame {2} with axes *U, V, W* with a common origin, as shown in Fig. 2.2. A point *P* in space can be described by the two frames and can be expressed as vectors $^1\boldsymbol{P}$ and $^2\boldsymbol{P}$,

$$^1\boldsymbol{P} = {^1p_x}\hat{x} + {^1p_y}\hat{y} + {^1p_z}\hat{z} \tag{2.5}$$

$$^2\boldsymbol{P} = {^2p_u}\hat{u} + {^2p_v}\hat{v} + {^2p_w}\hat{w} \tag{2.6}$$

where ^2p_u, ^2p_v, ^2p_w are projections of point *P* on frame {2} or {*u v w*} (the *U, V, W* coordinates). Because the point *P* is same, its two descriptions given by Eqs. (2.5) and (2.6) are related.

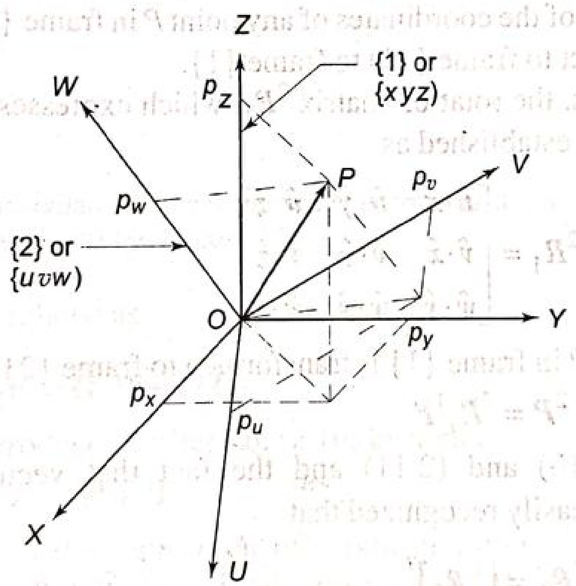

Fig. 2.2 *Representation of a point P in two frames {x y z} and {u v w} rotated with respect to each other*

Now, let the problem be posed as, "The description of point *P* in frame {2} is known and its description in frame {1} is to be found (or vice-versa)." This is accomplished by projecting the vector $^2\boldsymbol{P}$ on to the coordinates of frame {1}. Projections of $^2\boldsymbol{P}$ on frame {1} are obtained by taking the dot product of $^2\boldsymbol{P}$ with the unit vectors of frame {1}. Thus, substituting for $^2\boldsymbol{P}$ from Eq. (2.6) gives

$$
\begin{aligned}
{}^1p_x &= \hat{x}\cdot{}^2\boldsymbol{P} = \hat{x}\cdot{}^2p_u\hat{u} + \hat{x}\cdot{}^2p_v\hat{v} + \hat{x}\cdot{}^2p_w\hat{w} \\
{}^1p_y &= \hat{y}\cdot{}^2\boldsymbol{P} = \hat{y}\cdot{}^2p_u\hat{u} + \hat{y}\cdot{}^2p_v\hat{v} + \hat{y}\cdot{}^2p_w\hat{w} \\
{}^1p_z &= \hat{z}\cdot{}^2\boldsymbol{P} = \hat{z}\cdot{}^2p_u\hat{u} + \hat{z}\cdot{}^2p_v\hat{v} + \hat{z}\cdot{}^2p_w\hat{w}
\end{aligned} \tag{2.7}
$$

This can be written in matrix form as

$$
\begin{bmatrix} {}^1p_x \\ {}^1p_y \\ {}^1p_z \end{bmatrix} = \begin{bmatrix} \hat{x}\cdot\hat{u} & \hat{x}\cdot\hat{v} & \hat{x}\cdot\hat{w} \\ \hat{y}\cdot\hat{u} & \hat{y}\cdot\hat{v} & \hat{y}\cdot\hat{w} \\ \hat{z}\cdot\hat{u} & \hat{z}\cdot\hat{v} & \hat{z}\cdot\hat{w} \end{bmatrix} \begin{bmatrix} {}^2p_x \\ {}^2p_y \\ {}^2p_z \end{bmatrix} \tag{2.8}
$$

In compressed vector-matrix notation Eq. (2.8) is written as

$$
{}^1\boldsymbol{P} = {}^1\boldsymbol{R}_2\,{}^2\boldsymbol{P} \tag{2.9}
$$

where

$$
{}^1\boldsymbol{R}_2 = \begin{bmatrix} \hat{x}\cdot\hat{u} & \hat{x}\cdot\hat{v} & \hat{x}\cdot\hat{w} \\ \hat{y}\cdot\hat{u} & \hat{y}\cdot\hat{v} & \hat{y}\cdot\hat{w} \\ \hat{z}\cdot\hat{u} & \hat{z}\cdot\hat{v} & \hat{z}\cdot\hat{w} \end{bmatrix} \tag{2.10}
$$

Because frames {1} and {2} have the same origin, they can only be rotated with respect to each other, therefore, $\boldsymbol{R}$ is called a *rotation matrix* or *rotational transformation matrix*. It contains only the dot products of unit vectors of the two frames and is independent of the point P. Thus, rotation matrix ${}^1\boldsymbol{R}_2$ can be used for transformation of the coordinates of any point P in frame {2} (which has been rotated with respect to frame {1}) to frame {1}.

On similar lines, the rotation matrix ${}^2\boldsymbol{R}_1$, which expresses frame {1} as seen from frame {2}, is established as

$$
{}^2\boldsymbol{R}_1 = \begin{bmatrix} \hat{u}\cdot\hat{x} & \hat{u}\cdot\hat{y} & \hat{u}\cdot\hat{z} \\ \hat{v}\cdot\hat{x} & \hat{v}\cdot\hat{y} & \hat{v}\cdot\hat{z} \\ \hat{w}\cdot\hat{y} & \hat{w}\cdot\hat{y} & \hat{w}\cdot\hat{z} \end{bmatrix} \tag{2.11}
$$

Hence, a point P in frame {1} is transformed to frame {2} using

$$
{}^2\boldsymbol{P} = {}^2\boldsymbol{R}_1\,{}^1\boldsymbol{P} \tag{2.12}
$$

From Eqs. (2.10) and (2.11) and the fact that vector dot product is commutative, it is easily recognized that

$$
{}^2\boldsymbol{R}_1 = [{}^1\boldsymbol{R}_2]^T \tag{2.13}
$$

From Eqs. (2.9), (2.12), and (2.13), ${}^2\boldsymbol{P}$ is expressed as

$$
{}^2\boldsymbol{P} = [{}^1\boldsymbol{R}_2]^{-1}\,{}^1\boldsymbol{P} = {}^2\boldsymbol{R}_1{}^1\boldsymbol{P} = [{}^1\boldsymbol{R}_2]^T\,{}^1\boldsymbol{P} \tag{2.14}
$$

Therefore, it is concluded that

$$
{}^2\boldsymbol{R}_1 = [{}^1\boldsymbol{R}_2]^{-1} = [{}^1\boldsymbol{R}_2]^T
$$

or, in general, for any rotational transformation matrix $\boldsymbol{R}$

$$R^{-1} = R^T \quad \text{and} \quad RR^T = I \tag{2.15}$$

where I is the 3×3 identity matrix.

2.1.3 Mapping between Translated Frames

Consider two frames, frame {1} and frame {2}, with origins O_1 and O_2 such that the axes of frame {1} are parallel to axes of frame {2}, as shown in Fig. 2.3. A point P in space can be expressed as vectors $\overrightarrow{O_1P}$ and $\overrightarrow{O_2P}$ with respect to the frames {1} and {2}, respectively.

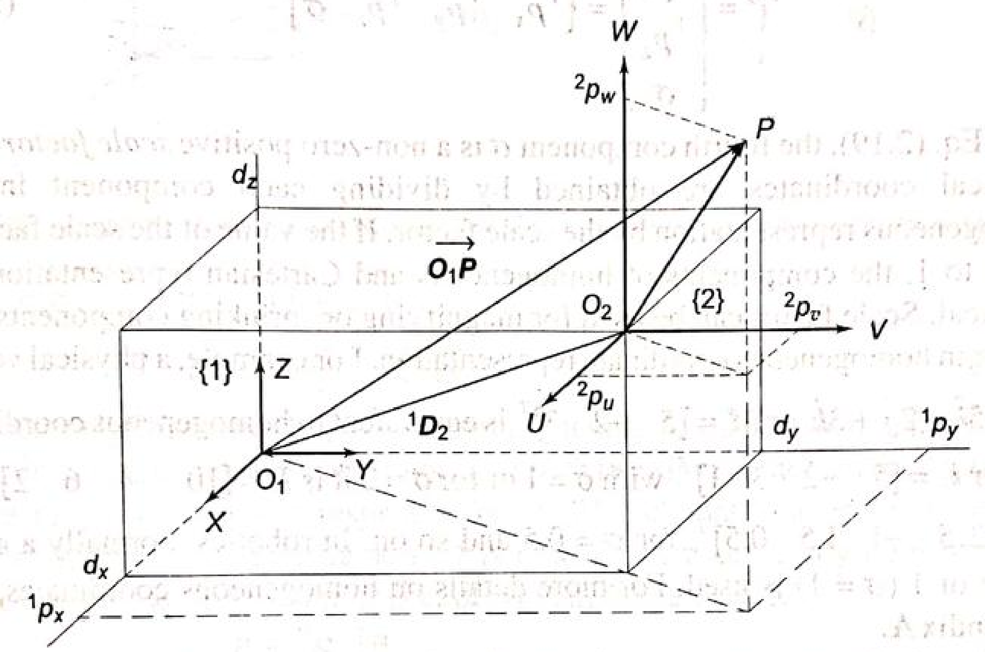

Fig. 2.3 *Translation of frames: frame {2} is translated with respect to frame {1} by distance $^1D_2$*

The two vectors are related as

$$\overrightarrow{O_1P} = \overrightarrow{O_2P} + \overrightarrow{O_1O_2} \tag{2.16}$$

or in the notation introduced earlier Eq. (2.16) becomes

$$^1P = {}^2P + {}^1D_2 \tag{2.17}$$

where $^1D_2 = \overrightarrow{O_1O_2}$ is the translation of origin of frame {2} with respect to frame {1}. Because $^2P = [^2p_u \ ^2p_v \ ^2p_w]^T$, substituting ^2P and $^1D_2$ in Eq. (2.17) gives

$$^1P = (^2p_u + d_x)\hat{x} + (^2p_v + d_y)\hat{y} + (^2p_w + d_z)\hat{z} \tag{2.18}$$

As $\quad {}^1P = {}^1p_x\hat{x} + {}^1p_y\hat{y} + {}^1p_z\hat{z}$, this gives

$$^1p_x = {}^2p_u + d_x; \quad ^1p_y = {}^2p_v + d_y; \quad ^1p_z = {}^2p_z + d_z$$

which is verified from Fig. 2.3.

Translation is qualitatively different from rotation in one important respect. In rotation, the origin of two coordinate frames is same. This invariance of the origin characteristic allows the representation of rotations in 3-D space as a 3×3 rotation matrix $\boldsymbol{R}$. However, in translation, the origins of translated frame and original frame are not coincident and translation is represented by a 3×1 vector, ${}^1\boldsymbol{D}_2$.

A powerful representation of translation is in a 4-D space of *homogeneous coordinates*. In these coordinates, point P in space with respect to frame $\{1\}$ is denoted as [refer to Fig. 2.1 and Eq. (2.3)]:

$$ {}^1\boldsymbol{P} = \begin{bmatrix} {}^1p_x \\ {}^1p_y \\ {}^1p_z \\ \sigma \end{bmatrix} = [{}^1p_x \quad {}^1p_y \quad {}^1p_z \quad \sigma]^T \tag{2.19} $$

In Eq. (2.19), the fourth component σ is a non-zero positive *scale factor*. The physical coordinates are obtained by dividing each component in the homogeneous representation by the scale factor. If the value of the scale factor σ is set to 1, the components of homogeneous and Cartesian representation are identical. Scale factor can be used for magnifying or shrinking components of a vector in homogeneous coordinate representation. For example, a physical vector $\vec{\boldsymbol{M}} = 5\hat{i} - 2\hat{j} + 3\hat{k}$ or $\boldsymbol{M} = [5 \quad -2 \quad 3]^T$ is equivalent to homogeneous coordinate vector $\boldsymbol{L} = [5 \quad -2 \quad 3 \quad 1]^T$ with $\sigma = 1$ or for $\sigma = 2$ it is $\boldsymbol{L} = [10 \quad -4 \quad 6 \quad 2]^T$ or $\boldsymbol{L} = [2.5 \quad -1 \quad 1.5 \quad 0.5]^T$ for $\sigma = 0.5$ and so on. In robotics, normally a scale factor of 1 ($\sigma = 1$) is used. For more details on homogeneous coordinates, see Appendix **A**.

Using the homogeneous coordinates, Eq. (2.17) is written in the vector-matrix form as:

$$ {}^1\boldsymbol{P} = \begin{bmatrix} 1 & 0 & 0 & d_x \\ 0 & 1 & 0 & d_y \\ 0 & 0 & 1 & d_z \\ 0 & 0 & 0 & 1 \end{bmatrix} \begin{bmatrix} {}^2p_u \\ {}^2p_v \\ {}^2p_w \\ 1 \end{bmatrix} $$

or

$$ {}^1\boldsymbol{P} = {}^1\boldsymbol{T}_2 \, {}^2\boldsymbol{P} \tag{2.20} $$

Here, ${}^1\boldsymbol{T}_2$ is a 4×4 homogeneous *transformation matrix* for translation of origin by ${}^1\boldsymbol{D}_2 = \overrightarrow{\boldsymbol{O}_1\boldsymbol{O}_2} = [d_x \quad d_y \quad d_z \quad 1]^T$. It is easily seen that Eq. (2.20) is same as Eq. (2.18). The 4×4 transformation matrix in Eq. (2.20) is called the *basic homogeneous translation matrix*.

2.1.4 Mapping between Rotated and Translated Frames

Consider now, the general case of two frames, frame $\{1\}$ and frame $\{2\}$. Frame $\{2\}$ is rotated and translated with respect to frame $\{1\}$ as shown in Fig. 2.4. The distance between the two origins is vector $\overrightarrow{\boldsymbol{O}_1\boldsymbol{O}_2}$ or ${}^1\boldsymbol{D}_2$. Assume a point P described with respect to frame {2} as $^2\boldsymbol{P}$, it is required to refer it to frame {1}, that is, to find $^1\boldsymbol{P}$.

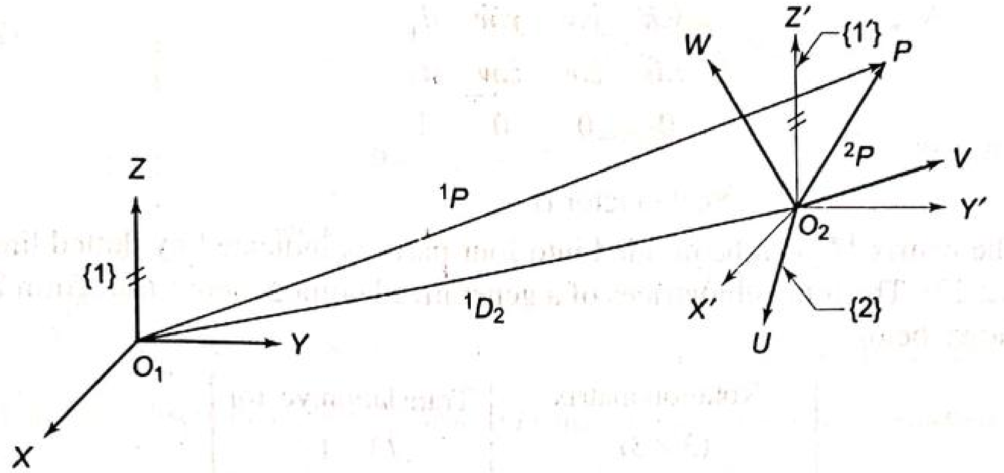

Fig. 2.4 *Mapping between two frames–translated and rotated with respect to each other*

In terms of vectors in Fig. 2.4,

$$\overrightarrow{O_1P} = \overrightarrow{O_2P} + \overrightarrow{O_1O_2} \tag{2.21}$$

Vector $\overrightarrow{O_2P}$ in frame {2} is $^2\boldsymbol{P}$; therefore, it must be transformed to frame {1}. First, consider an intermediate frame {1′} with its origin coincident with O_2. The frame {1′} is rotated with respect to frame {2} such that its axes are parallel to axes of frame {1}. Thus, frame {1′} is related to frame {2} by pure rotation. Hence, using Eq. (2.9), point P is expressed in frame {1′} as

$$^{1'}\boldsymbol{P} = {}^{1'}\boldsymbol{R}_2\,{}^2\boldsymbol{P} \tag{2.22}$$

Because frame {1′} is aligned with frame {1}, $^{1'}\boldsymbol{R}_2 = {}^1\boldsymbol{R}_2$. Hence

$$\overrightarrow{O_2P} = {}^{1'}\boldsymbol{P} = {}^1\boldsymbol{R}_2\,{}^2\boldsymbol{P} \tag{2.23}$$

Substituting this in Eq. (2.21) and converting to vector-matrix notation,

$$^1\boldsymbol{P} = {}^1\boldsymbol{R}_2\,{}^2\boldsymbol{P} + {}^1\boldsymbol{D}_2 \tag{2.24}$$

The vector $\overrightarrow{O_1O_2}$ or $^1\boldsymbol{D}_2$ has components $(d_x\ d_y\ d_z)$ in frame {1} as

$$\overrightarrow{O_1O_2} = {}^1\boldsymbol{D}_2 = [d_x \quad d_y \quad d_z]^T \tag{2.25}$$

Using the homogeneous coordinates, from Eqs. (2.10) and (2.20), the two terms on the right-hand side of Eq. (2.24) can be combined into a single 4×4 matrix, which is then written as

$$^1\boldsymbol{P} = {}^1\boldsymbol{T}_2\,{}^2\boldsymbol{P} \tag{2.26}$$

Here, $^1\boldsymbol{P}$ and $^2\boldsymbol{P}$ are 4×1 vectors as in Eq. (2.19) with a scale factor of 1 and $\boldsymbol{T}$ is 4×4 matrix referred to as the *homogeneous transformation matrix* (or *homogeneous transform*). It describes both the position and orientation of frame {2} with respect to frame {1} or any frame with respect to any other frame. The components of $^1\boldsymbol{T}_2$ matrix are as under

$${}^1\boldsymbol{R}_2 \qquad\qquad {}^1\boldsymbol{D}_2$$

$$
{}^1\boldsymbol{T}_2 = \begin{array}{ccc:c}
\hat{x}.\hat{u} & \hat{x}.\hat{v} & \hat{x}.\hat{w} & d_x \\
\hat{y}.\hat{u} & \hat{y}.\hat{v} & \hat{y}.\hat{w} & d_y \\
\hat{z}.\hat{u} & \hat{z}.\hat{v} & \hat{z}.\hat{w} & d_z \\
\hdashline
0 & 0 & 0 & 1
\end{array} \tag{2.27}
$$

Scale factor σ

The matrix ${}^1\boldsymbol{T}_2$ can be divided into four parts as indicated by dotted lines in Eq. (2.27). The four submatrices of a generalized homogeneous transform $\boldsymbol{T}$ are as shown below:

$$
\boldsymbol{T} = \left[\begin{array}{c:c}
\begin{array}{c}\text{Rotation matrix}\\(3\times 3)\end{array} & \begin{array}{c}\text{Translation vector}\\(3\times 1)\end{array} \\
\hdashline
\begin{array}{c}\text{Perspective}\\\text{transformation matrix}\\(1\times 3)\end{array} & \begin{array}{c}\text{Scale factor}\\(1\times 1)\end{array}
\end{array}\right] \tag{2.28}
$$

Perspective transformation matrix is useful in vision systems and is set to zero vector wherever no perspective views are involved. The scale factor σ has non-zero positive ($\sigma > 0$) values and is called *global scaling* parameter. $\sigma > 1$ is useful for reducing and $0 < \sigma < 1$ is useful for enlarging. For robotic study presented here $\sigma = 1$ is used. For describing the position and orientation of frame {2} with respect to frame {1}, $\boldsymbol{T}$ takes the form

$$
{}^1\boldsymbol{T}_2 = \left[\begin{array}{ccc:c}
 & {}^1\boldsymbol{R}_2 & & {}^1\boldsymbol{D}_2 \\
\hdashline
0 & 0 & 0 & 1
\end{array}\right] \tag{2.29}
$$

In the reverse problem when ${}^1\boldsymbol{P}$ is known and ${}^2\boldsymbol{P}$ is to be found, Eq. (2.26), takes the form

$$
{}^2\boldsymbol{P} = {}^2\boldsymbol{T}_1\,{}^1\boldsymbol{P} \tag{2.30}
$$

where ${}^2\boldsymbol{T}_1 = \left[{}^1\boldsymbol{T}_2\right]^{-1}$.

2.2 DESCRIPTION OF OBJECTS IN SPACE

The location of an object is completely specified in 3-D space by describing both its position and its orientation. Consider a body B in space whose location is to be specified with respect to a known reference frame {0}. Let a frame with origin O_1, frame {1}, be attached to the body B, as shown in Fig. 2.5. The homogeneous transform ${}^0\boldsymbol{T}_1$ completely describes the location (position and orientation) of the body B, that is, the position vector component ${}^0\boldsymbol{D}_1$ of ${}^0\boldsymbol{T}_1$ describes its position, while the rotation matrix component ${}^0\boldsymbol{R}_1$ describes the orientation of the body with respect to frame {0}.

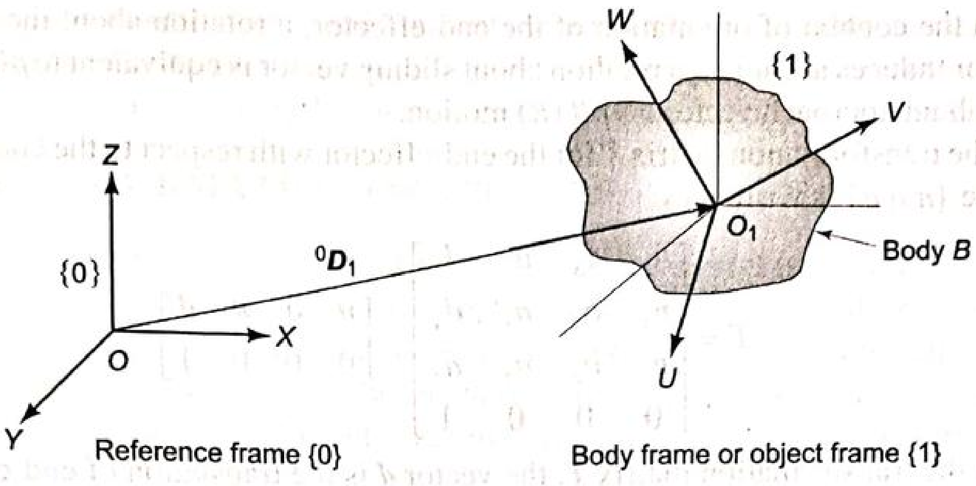

Fig. 2.5 *Description of a body (object) in space using homogeneous transform*

In a robotic arm, the location of links is specified by assigning frames to each link, starting from the base to the tool or end-effector. While the convention for assigning frames to links will be discussed in the next chapter, here, the convention for assigning frames to the end-effector using *normal*, *sliding*, and *approach* vectors, which are yaw, pitch, and roll vectors, respectively, is explained.

The end-effector coordinate frame is shown in Fig. 2.6. The axes of the frame are defined as: (i) z-axis is the approach vector $\hat{\boldsymbol{a}}$, that is, the direction in which the end-effector approaches towards the target, (ii) y-axis is the direction of the sliding vector, that is, the direction of opening and closing of the end-effector as it manipulates objects. It is also called *orientation* vector $\hat{\boldsymbol{o}}$, and (iii) x-axis is the normal vector $\hat{\boldsymbol{n}}$, which is orthogonal to the approach and sliding vectors in right-handed manner, that is, $\hat{\boldsymbol{o}} \times \hat{\boldsymbol{a}}$.

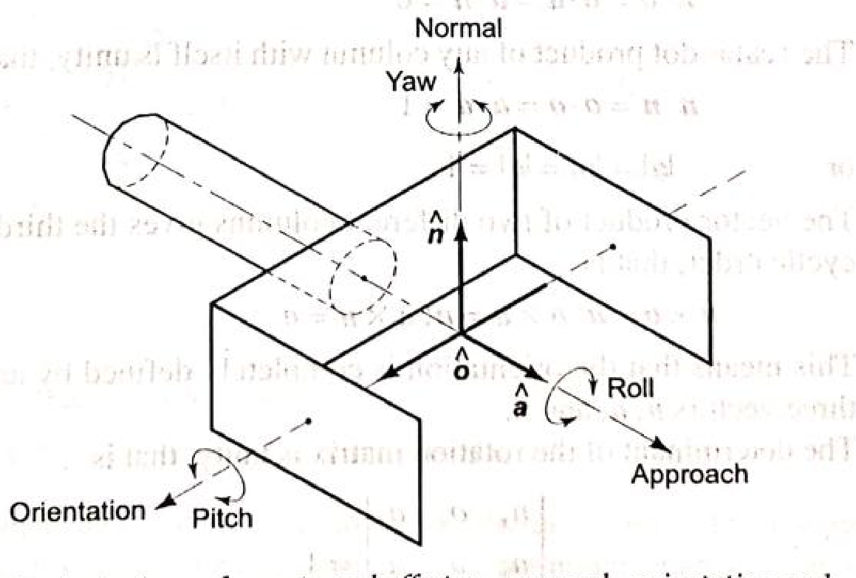

Fig. 2.6 *Assigning a frame to end-effector—approach, orientation and normal directions; and roll, pitch, and yaw motions*

In the context of orientation of the end-effector, a rotation about the normal vector induces a *yaw* (Y), a rotation about sliding vector is equivalent to *pitch* (P), and about approach vector is *roll* (R) motion.

The transformation matrix $\boldsymbol{T}$ for the end-effector with respect to the coordinate frame $\{n\ o\ a\}$ is written as

$$\boldsymbol{T} = \begin{bmatrix} n_x & o_x & a_x & d_x \\ n_y & o_y & a_y & d_y \\ n_z & o_z & a_z & d_z \\ 0 & 0 & 0 & 1 \end{bmatrix} = \begin{bmatrix} \boldsymbol{n} & \boldsymbol{o} & \boldsymbol{a} & \boldsymbol{d} \\ 0 & 0 & 0 & 1 \end{bmatrix} \tag{2.31}$$

In the transformation matrix $\boldsymbol{T}$, the vector $\boldsymbol{d}$ is the translation of end-effector frame from the reference frame and vectors ($\boldsymbol{n}, \boldsymbol{o}, \boldsymbol{a}$) describe the orientation of end-effector. The vectors $\boldsymbol{n}$, $\boldsymbol{o}$, and $\boldsymbol{a}$ represent the X, Y, Z axes of the end-effector frame. The matrix $\boldsymbol{T}$ in Eq. (2.31) is same as in Eq. (2.27) and would apply for any coordinate frame and, hence, to any joint of the manipulator.

The orientation of the end-effector is specified by the 3×3 rotation submatrix $\boldsymbol{R}$. From Eqs. (2.27) and (2.31), the end-effector rotation matrix is

$$\boldsymbol{R} = \begin{bmatrix} \hat{x}\cdot\hat{u} & \hat{x}\cdot\hat{v} & \hat{x}\cdot\hat{w} \\ \hat{y}\cdot\hat{u} & \hat{y}\cdot\hat{v} & \hat{y}\cdot\hat{w} \\ \hat{z}\cdot\hat{u} & \hat{z}\cdot\hat{v} & \hat{z}\cdot\hat{w} \end{bmatrix} = \begin{bmatrix} n_x & o_x & a_x \\ n_y & o_y & a_y \\ n_z & o_z & a_z \end{bmatrix} \tag{2.32}$$

This is the general rotation matrix. Its properties are enumerated below:

- The vectors $\boldsymbol{n}$, $\boldsymbol{o}$, and $\boldsymbol{a}$ are in three mutually perpendicular directions and hence the rotation matrix $\boldsymbol{R}$ is an *orthogonal transformation*. Because the vectors in the dot products are all unit vectors, it is also called *orthonormal transformation*.
- The scalar dot product of two different columns is zero, that is,
$$\boldsymbol{n}\cdot\boldsymbol{o} = \boldsymbol{o}\cdot\boldsymbol{a} = \boldsymbol{a}\cdot\boldsymbol{n} = 0 \tag{2.33}$$
- The scalar dot product of any column with itself is unity, that is,
$$\boldsymbol{n}\cdot\boldsymbol{n} = \boldsymbol{o}\cdot\boldsymbol{o} = \boldsymbol{a}\cdot\boldsymbol{a} = 1$$
or
$$|\boldsymbol{n}| = |\boldsymbol{o}| = |\boldsymbol{a}| = 1 \tag{2.34}$$
- The vector product of two different columns gives the third column in a cyclic order, that is
$$\boldsymbol{n}\times\boldsymbol{o} = \boldsymbol{a};\ \boldsymbol{o}\times\boldsymbol{a} = \boldsymbol{n};\ \boldsymbol{a}\times\boldsymbol{n} = \boldsymbol{o} \tag{2.35}$$
This means that the orientation is completely defined by any two of the three vectors $\boldsymbol{n}$, $\boldsymbol{o}$, and $\boldsymbol{a}$.
- The determinant of the rotation matrix is unity, that is
$$\begin{vmatrix} n_x & o_x & a_x \\ n_y & o_y & a_y \\ n_z & o_z & a_z \end{vmatrix} = 1 \tag{2.36}$$
- The inverse and transpose relationships are as in Eq. (2.15).

The rotation matrix $\boldsymbol{R}$ has nine elements in total, which are subjected to the orthogonality constraints [Eqs. (2.33)–(2.35)]. Thus, only three of the nine elements are independent or, the rotation matrix representation has redundancy.

2.3 TRANSFORMATION OF VECTORS

In the previous section, concepts of mapping and the spatial transformation of frames were developed. These concepts will now be applied to vector transformations. Transformation of vectors, rotation and/or translation is distinctly different from mapping, where the description of a point from one frame to another is changed. Different situations of transformation of vectors are discussed now.

2.3.1 Rotation of Vectors

Let us consider a vector ${}^1\boldsymbol{P}$, which is rotated by an angle θ to give new vector ${}^1\boldsymbol{Q}$. If $\boldsymbol{R}(\theta)$ is the rotation that describes the rotation θ about k-axis (which can be x- y-or z-axis), then

$$ {}^1\boldsymbol{Q} = \boldsymbol{R}(\theta)\, {}^1\boldsymbol{P} \tag{2.37} $$

For the rotation matrix $\boldsymbol{R}(\theta)$ no super- or subscripts are used because both ${}^1\boldsymbol{P}$ and ${}^1\boldsymbol{Q}$ are in the same frame $\{1\}$.

Equation (2.37) is similar to Eq. (2.12) in mathematical form but both have different interpretation. The distinction is that when vector ${}^1\boldsymbol{P}$ is rotated with reference to frame $\{1\}$, it may be considered either as the vector rotation, as shown in Fig. 2.7(a), to give ${}^1\boldsymbol{Q}$ or as the rotation of the frame in "opposite" direction to give rotated frame $\{u\, v\, w\}$, as shown in Fig. 2.7(b), for rotation about x-axis.

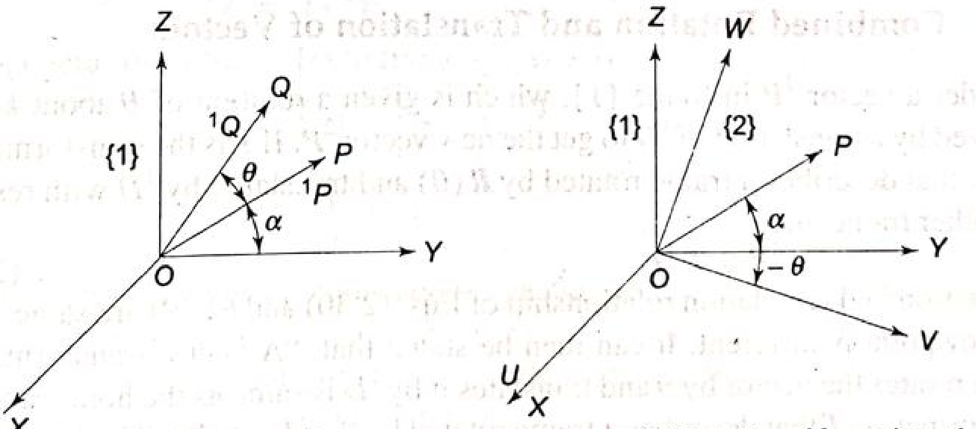

(a) Rotation of vector by θ (b) Rotation of frame by $-\theta$

Fig. 2.7 *The equivalence of rotation of a vector and a frame*

The operations involved in two cases are identical, only the viewpoint is different. This allows using the rotational transformation matrices for vector rotations. It is also noted that, "The rotation matrix $\boldsymbol{R}(\theta)$ which rotates a vector through some angle θ about k-axis, is the same as the rotational transformation matrix, which describes a frame rotated by θ relative to the reference frame."

2.3.2 Translation of Vectors

Suppose, a vector ${}^1\boldsymbol{P}$ is translated by a vector ${}^1\boldsymbol{D}$ to get ${}^1\boldsymbol{Q}$, as shown in Fig. 2.8(a), then the vector ${}^1\boldsymbol{Q}$ is given by

$$ {}^1\boldsymbol{Q} = {}^1\boldsymbol{P} + {}^1\boldsymbol{D} \tag{2.38}$$

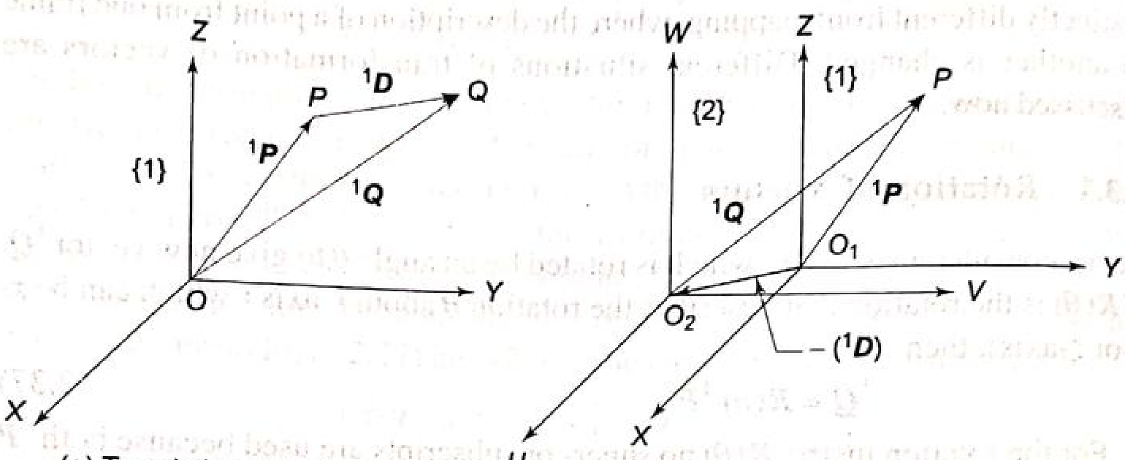

(a) Translation of vector by ${}^1\boldsymbol{D}$ (b) Translation of frame by – (${}^1\boldsymbol{D}$)

Fig. 2.8 *Translation of vector ${}^1\boldsymbol{P}$ by distance ${}^1\boldsymbol{D}$*

Here, as in case of rotations, instead of moving the vector "forward" by ${}^1\boldsymbol{D}$, the frame can be moved in the opposite sense, as shown in Fig. 2.8(b), which is equivalent to the problem of mapping. This explains why Eq. (2.38) is similar to Eq. (2.17) obtained by mapping between translated frames.

2.3.3 Combined Rotation and Translation of Vectors

Consider a vector ${}^1\boldsymbol{P}$ in frame {1}, which is given a rotation of θ about k-axis followed by a translation of ${}^1\boldsymbol{D}$ to get the new vector ${}^2\boldsymbol{P}$. If $\boldsymbol{T}$ is the transformation matrix that describes a frame rotated by $\boldsymbol{R}(\theta)$ and translated by ${}^1\boldsymbol{D}$ with respect to another frame, then

$$ {}^2\boldsymbol{P} = \boldsymbol{T}\,{}^1\boldsymbol{P} \tag{2.39}$$

Rotation and translation relationship of Eqs. (2.30) and (2.39) are same, only the viewpoint is different. It can then be stated that, "A vector transformation which rotates the vector by θ and translates it by ${}^1\boldsymbol{D}$ is same as the homogeneous transformation $\boldsymbol{T}$ that describes a frame rotated by θ and translated by ${}^1\boldsymbol{D}$ relative to the reference frame."

2.3.4 Composite Transformation

Three frames, with each frame rotated and translated from its preceding frame, are depicted in Fig. 2.9. It is proposed to find the transform, which relates ${}^3\boldsymbol{P}$ in frame {3} to ${}^1\boldsymbol{P}$, as it is seen from frame {1}.

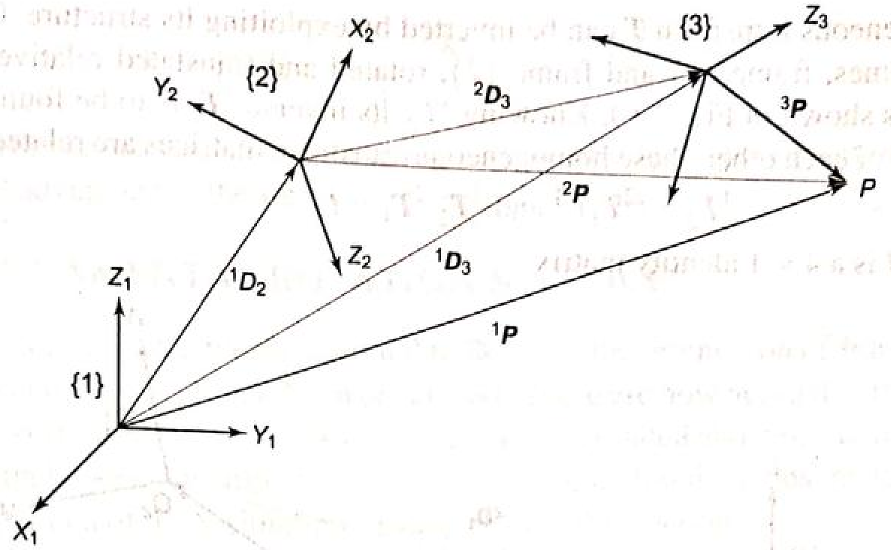

Fig. 2.9 *Composite transformation of three frames*

The transformation matrix $\boldsymbol{T}$ can be used to progressively map $^3\boldsymbol{P}$, the point P in frame {3}, to frame {2}, and then to frame {1} as

$$^2\boldsymbol{P} = {}^2\boldsymbol{T}_3\ {}^3\boldsymbol{P} \tag{2.40}$$

and

$$^1\boldsymbol{P} = {}^1\boldsymbol{T}_2\ {}^2\boldsymbol{P} \tag{2.41}$$

These lead to the overall transformation as

$$^1\boldsymbol{P} = {}^1\boldsymbol{T}_2\ {}^2\boldsymbol{T}_3\ {}^3\boldsymbol{P} \tag{2.42}$$

or

$$^1\boldsymbol{P} = {}^1\boldsymbol{T}_3\ {}^3\boldsymbol{P} \tag{2.43}$$

The overall transformation between frame {3} and frame {1} is obtained from Eqs. (2.42) and (2.43) as

$$^1\boldsymbol{T}_3 = {}^1\boldsymbol{T}_2\ {}^2\boldsymbol{T}_3 \tag{2.44}$$

It easily follows that the transformation from frame {i} to frame {1} is

$$^1\boldsymbol{T}_i = {}^1\boldsymbol{T}_2\ {}^2\boldsymbol{T}_3 \dots {}^j\boldsymbol{T}_{j+1} \dots {}^{i-1}\boldsymbol{T}_i \tag{2.45}$$

or in general from frame {i} to frame {j}, ($i > j$)

$$^j\boldsymbol{T}_i = {}^j\boldsymbol{T}_{j+1}\ {}^{j+1}\boldsymbol{T}_{j+2} \dots {}^{i-1}\boldsymbol{T}_i$$

or

$$^j\boldsymbol{T}_i = \prod_{k=j}^{i-1} {}^k\boldsymbol{T}_{k+1} \tag{2.46}$$

That is, the individual homogeneous transformation matrices can be multiplied together to obtain composite homogeneous transformation matrix. Matrix multiplication being not commutative, the order of multiplication, in above equations is fixed and cannot be altered.

2.4 INVERTING A HOMOGENEOUS TRANSFORM

In robotic analysis, often $^i\boldsymbol{T}_j$ is required, while $^j\boldsymbol{T}_i$ is known. This is found by computing the inverse of $^j\boldsymbol{T}_i$. The inverse of the 4 × 4 transformation matrix can be computed using the conventional methods of matrix inversion. However, the homogeneous transform T can be inverted by exploiting its structure. Consider two frames, frame {1} and frame {2}, rotated and translated relative to each other as shown in Fig. 2.10. Knowing ${}^1T_2$, its inverse ${}^2T_1$ is to be found. Being inverse of each other, these homogeneous transform matrices are related as

$$ {}^1T_2 = ({}^2T_1)^{-1} \text{ and } {}^1T_2\,{}^2T_1 = I $$

where I is a 4 × 4 identity matrix.

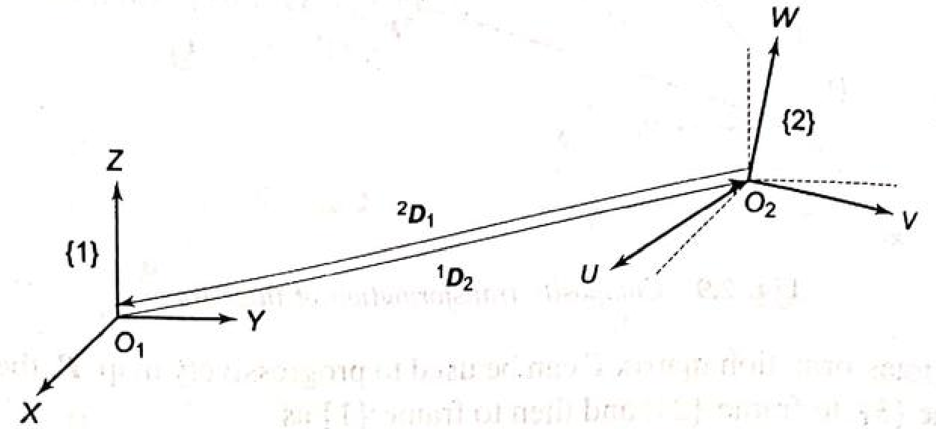

Fig. 2.10 *Inverting a homogeneous transform*

Homogenous transforms ${}^1T_2$ and ${}^2T_1$ can be written in partitioned form from Eq. (2.29) as

$$ {}^1T_2 = \left[\begin{array}{ccc|c} & {}^1R_2 & & {}^1D_2 \\ \hline 0 & 0 & 0 & 1 \end{array}\right] \tag{2.47} $$

and

$$ {}^2T_1 = \left[\begin{array}{ccc|c} & {}^2R_1 & & {}^2D_1 \\ \hline 0 & 0 & 0 & 1 \end{array}\right] \tag{2.48} $$

The rotation sub-matrix R has the property ${}^2R_1 = {}^1R_2^T$ (Eq. 2.13). Therefore, the mapping of a point P from frame {2} to frame {1}, is

$$ {}^1P = {}^1D_2 + {}^1R_2\,{}^2P \tag{2.49} $$

Premultiplying both sides by ${}^2R_1$ gives

$$ {}^2R_1\,{}^1P = {}^2R_1\,{}^1D_2 + {}^2R_1\,{}^1R_2\,{}^2P $$

As ${}^2R_1\,{}^1R_2 = I$, it gives

$$ {}^2R_1\,{}^1P = {}^2R_1\,{}^1D_2 + {}^2P $$

or

$$ {}^2P = {}^2R_1\,{}^1P - {}^2R_1\,{}^1D_2 \tag{2.50} $$

The mapping of a point P from frame {1} to frame {2} is

$$ {}^2P = {}^2R_1\,{}^1P + {}^2D_1 \tag{2.51} $$

Comparing Eqs. (2.50) and (2.51), gives

$$ {}^2D_1 = -\,{}^2R_1\,{}^1D_2 $$

or

$$ {}^2D_1 = -\,{}^1R_2^T\,{}^1D_2 \tag{2.52} $$

Substituting Eq. (2.52) in Eq. (2.48), gives

$$ {}^2T_1 = \left[{}^1T_2\right]^{-1} = \left[\begin{array}{ccc|c} & {}^1R_2^T & & -{}^1R_2^T\,{}^1D_2 \\ \hline 0 & 0 & 0 & 1 \end{array}\right] \tag{2.53}$$

This gives an easy way of computing inverse of a homogeneous transform taking full advantage of the structure inherent in the transform.

2.5 FUNDAMENTAL ROTATION MATRICES

In the previous section, the background to describe the orientation of frame $\{2\}$ with respect to frame $\{1\}$ has been developed. These are now applied to rotation matrices in different situations. A frame $\{2\}$ may be rotated about one or more of the principal axes, an arbitrary axis, or by some fixed angles relative to frame $\{1\}$. Each of these situations is discussed in this section.

2.5.1 Principal Axes Rotation

To determine the orientation of frame $\{2\}$, which is rotated about one of the three principal axes of frame $\{1\}$, consider, for example, the rotation of frame $\{2\}$ with respect to frame $\{1\}$ by angle θ about the z-axis of frame $\{1\}$, as shown in a 3-D view in Fig. 2.11 (a) and on xy-plane in Fig. 2.11 (b). The corresponding rotation matrix ${}^1\boldsymbol{R}_2$, known as the *fundamental rotation matrix*, is denoted by the symbol $\boldsymbol{R}_z(\theta)$ or $\boldsymbol{R}(z, \theta)$ or $\boldsymbol{R}_{z,\theta}$.

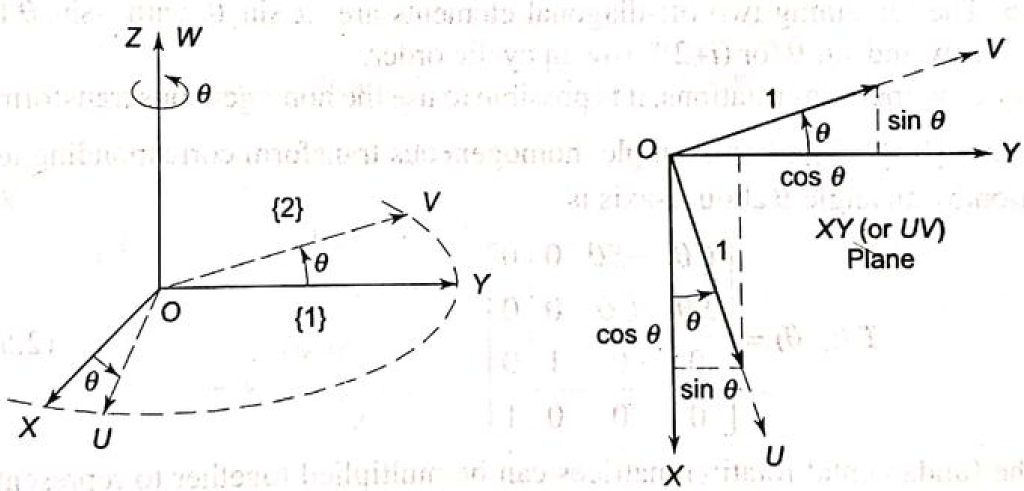

(a) Rotation of frame {1} by θ (b) xy-plane showing the rotation

Fig. 2.11 *Fundamental rotation by an angle θ about z-axis*

From Eq. (2.10), $\boldsymbol{R}_z(\theta)$ is computed from the dot product of unit vectors along the principal axes. The dot product of two unit vectors is the cosine of the angle between them, for example, $\hat{x}\cdot\hat{u} = \cos\theta$. Thus,

$$\boldsymbol{R}_z(\theta) = \begin{bmatrix} \cos\theta & \cos(90^\circ+\theta) & \cos 90^\circ \\ \cos(90^\circ-\theta) & \cos\theta & \cos 90^\circ \\ \cos 90^\circ & \cos 90^\circ & \cos 0^\circ \end{bmatrix}$$

or
$$R_z(\theta) = \begin{bmatrix} C\theta & -S\theta & 0 \\ S\theta & C\theta & 0 \\ 0 & 0 & 1 \end{bmatrix} \tag{2.54}$$

where $S\theta = \sin\theta$ and $C\theta = \cos\theta$.

Equation (2.54) is the fundamental rotation matrix for a rotation of angle θ about z-axis of the frame. Similarly, fundamental rotation matrices for rotation about x-axis and y-axis can be obtained and these are:

$$R_x(\theta) = \begin{bmatrix} 1 & 0 & 0 \\ 0 & C\theta & -S\theta \\ 0 & S\theta & C\theta \end{bmatrix} \tag{2.55}$$

and
$$R_y(\theta) = \begin{bmatrix} C\theta & 0 & S\theta \\ 0 & 1 & 0 \\ -S\theta & 0 & C\theta \end{bmatrix} \tag{2.56}$$

The rotation matrices R_x, R_y, and R_z exhibit a pattern and using this pattern these matrices can be easily written. The rotation matrix for rotation about k^{th} principal axis $R_k(\theta)$ can be obtained as follows: The elements of ith row and i^{th} column for $i = 1, 2,$ or 3 for $k = x, y,$ or z respectively, of 3×3 matrix $R_k(\theta)$ are zero except the element (i, i), which is 1. The other two diagonal elements are $\cos\ \theta$. The remaining two off-diagonal elements are $\pm \sin\ \theta$, with $-\sin\ \theta$ for $(i+1)^{th}$ row and $\sin\ \theta$ for $(i+2)^{th}$ row in cyclic order.

For principal axes rotations, it is possible to use the homogeneous transform T with $D = [0\ \ 0\ \ 0]^T$. For example, homogeneous transform corresponding to a rotation by an angle θ about z-axis is

$$T(z, \theta) = \left[\begin{array}{ccc:c} C\theta & -S\theta & 0 & 0 \\ S\theta & C\theta & 0 & 0 \\ 0 & 0 & 1 & 0 \\ \hdashline 0 & 0 & 0 & 1 \end{array}\right] \tag{2.57}$$

The fundamental rotation matrices can be multiplied together to represent a sequence of finite rotations. For example, the overall rotation matrix representing a rotation of angle θ_1 about x-axis followed by a rotation of angle θ_2 about y-axis can be obtained by multiplying Eq. (2.55) and Eq. (2.56). That is,

$$R = R_y(\theta_2)\, R_x(\theta_1)$$

or
$$R = \begin{bmatrix} C\theta_2 & 0 & S\theta_2 \\ 0 & 1 & 0 \\ -S\theta_2 & 0 & C\theta_2 \end{bmatrix} \begin{bmatrix} 1 & 0 & 0 \\ 0 & C\theta_1 & -S\theta_1 \\ 0 & S\theta_1 & C\theta_1 \end{bmatrix}$$

or
$$R = \begin{bmatrix} C_2 & S_1S_2 & C_1S_2 \\ 0 & C_1 & -S_1 \\ -S_2 & S_1C_2 & C_1C_2 \end{bmatrix} \tag{2.58}$$

where $C_i = C\theta_i = \cos\,\theta_i$ and $S_i = S\theta_i = \sin\,\theta_i$.

It is important to note the sequence of multiplication of R matrices. A different sequence may not give the same result and obviously will not correspond to same orientation of the rotated frame. This is because the matrix product is not commutative. In view of this, it can be concluded that two rotations in general do not result in same orientation and the resultant rotation matrix depends on the order of rotations.

Another significant variable is how the rotations are performed. There are two alternatives:

(i) to perform successive rotations about the principal axes of the fixed frame.

(ii) to perform successive rotations about the current principal axes of a moving frame.

The successive rotations in either case, in general, do not produce identical results.

Figure 2.12 shows the effect of two successive rotations of 90° to an object about the principal axes of the fixed frame. It is observed that the final orientation of the object is different when same two rotations are made but the order of rotations is changed.

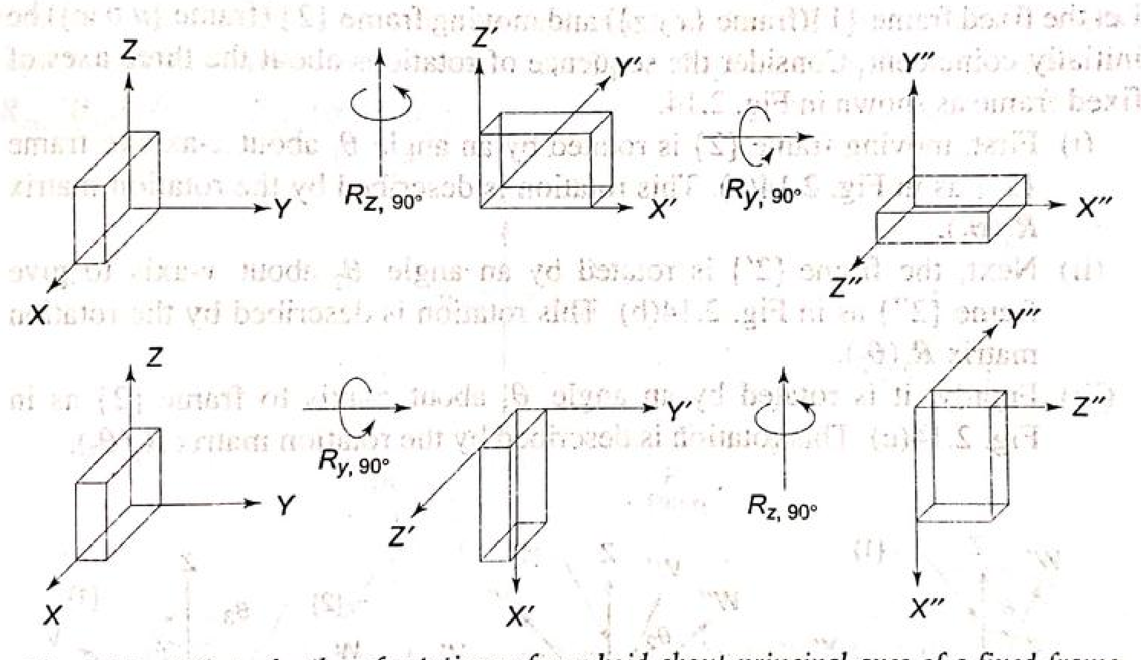

Fig. 2.12 *Effect of order of rotations of a cuboid about principal axes of a fixed frame*

Similarly, the order of rotations about the principal axes of the moving frame also produces different final orientation of the object. This is illustrated in Fig. 2.13.

The representation of orientation of rotated frames for different types of rotations is discussed next.

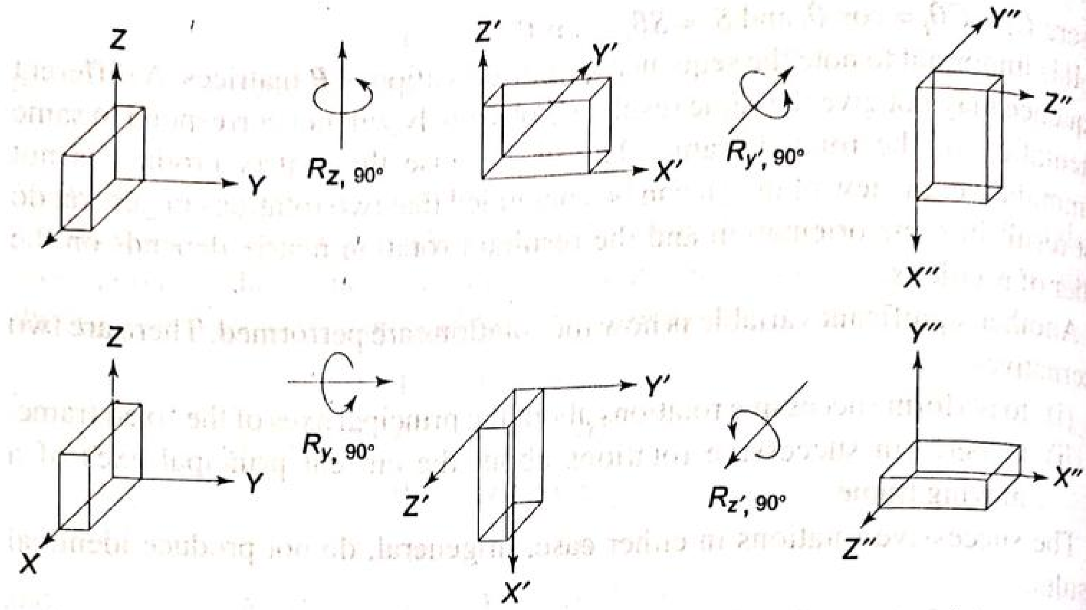

Fig. 2.13 *Effect of order of rotations of a cuboid about axes of the moving frame*

2.5.2 Fixed Angle Representation

Let the fixed frame {1}(frame {$x\,y\,z$}) and moving frame {2} (frame {$u\,v\,w$}) be initially coincident. Consider the sequence of rotations about the three axes of fixed frame as shown in Fig. 2.14.

(i) First, moving frame {2} is rotated by an angle θ_1 about x-axis to frame {2′} as in Fig. 2.14(a). This rotation is described by the rotation matrix $\boldsymbol{R}_x(\theta_1)$.

(ii) Next, the frame {2′} is rotated by an angle θ_2 about y-axis to give frame {2″} as in Fig. 2.14(b). This rotation is described by the rotation matrix $\boldsymbol{R}_y(\theta_2)$.

(iii) Finally, it is rotated by an angle θ_3 about z-axis to frame {2} as in Fig. 2.14(c). This rotation is described by the rotation matrix $\boldsymbol{R}_z(\theta_3)$.

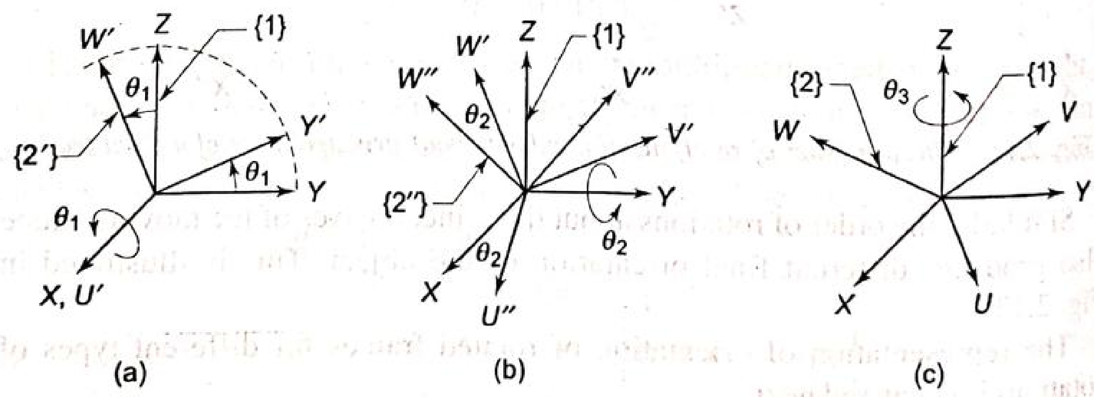

Fig. 2.14 *Three rotations of θ_1, θ_2, and θ_3 about fixed axes*

This convention for specifying orientation is known as *fixed angle representation* because each rotation is specified about an axis of fixed reference frame. The above three rotations are referred as *XYZ-fixed angle* rotations.

The final frame orientation is obtained by composition of rotations with respect to the fixed frame and the overall rotation matrix ${}^1\boldsymbol{R}_2$ is computed by pre-multiplication of the matrices of elementary rotations, that is,

$$\boldsymbol{R}_{xyz}(\theta_3\,\theta_2\,\theta_1) = {}^1\boldsymbol{R}_2 = \boldsymbol{R}_z(\theta_3)\boldsymbol{R}_y(\theta_2)\boldsymbol{R}_x(\theta_1) \tag{2.59}$$

(rotation ordering right to left)

Substituting the results of Eqs. (2.54)–(2.56) in Eq. (2.59) for fixed angle rotations, the final rotation matrix is

$$\boldsymbol{R}_{xyz}(\theta_3\,\theta_2\,\theta_1) = \begin{bmatrix} C_3 & -S_3 & 0 \\ S_3 & C_3 & 0 \\ 0 & 0 & 1 \end{bmatrix} \begin{bmatrix} C_2 & 0 & S_2 \\ 0 & 1 & 0 \\ -S_2 & 0 & C_2 \end{bmatrix} \begin{bmatrix} 1 & 0 & 0 \\ 0 & C_1 & -S_1 \\ 0 & S_1 & C_1 \end{bmatrix}$$

or

$$\boldsymbol{R}_{xyz}(\theta_3\,\theta_2\,\theta_1) = \begin{bmatrix} C_2C_3 & S_1S_2C_3 - C_1S_3 & C_1S_2C_3 + S_1S_3 \\ C_2S_3 & S_1S_2S_3 + C_1C_3 & C_1S_2S_3 - S_1C_3 \\ -S_2 & S_1C_2 & C_1C_2 \end{bmatrix} \tag{2.60}$$

The final frame orientation for any set of rotations performed about the axes of the fixed frame (e.g. ZYX, ZXZ etc.) can be obtained by multiplying the rotation matrices in a consistent order as indicated in Eq. (2.59). In fixed angle representation, order of rotations XYZ or ZYX are equivalent, that is, $\boldsymbol{R}_{xyz}(\theta_1\,\theta_2\,\theta_3) = \boldsymbol{R}_{zyx}(\theta_1\,\theta_2\,\theta_3)$.

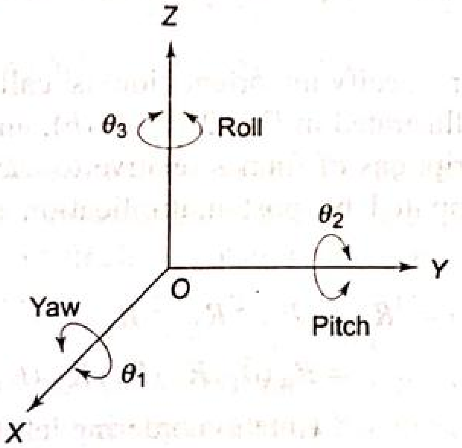

Fig. 2.15 *Representation of roll, pitch, and yaw (RPY) rotations*

The three rotations about the three fixed principal axes in fixed angle rotation produce the motions, which are also known as *roll*, *pitch*, and *yaw* motions, as shown in Fig. 2.15. The XYZ-fixed angle transformation in Eq. (2.60) is equivalent to *roll-pitch-yaw* (RPY) transformation.

2.5.3 Euler Angle Representations

The moving frame, instead of rotating about the principal axes of the fixed frame, can rotate about its own principal axes. Consider alternate rotations of frame {2} with respect to frame $\{1\}$, as shown in Fig. 2.16, starting from the position when the two frames are coincident.

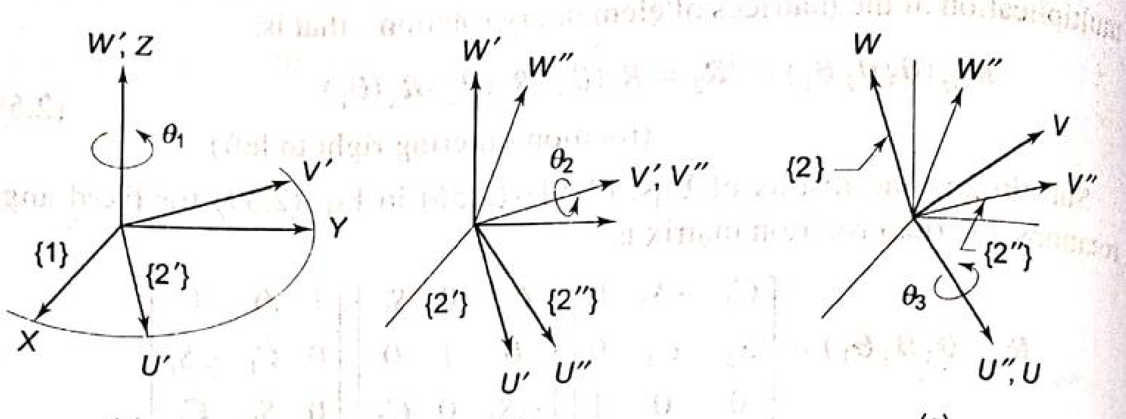

Fig. 2.16 *Euler angle representation for three rotations of θ_1, θ_2, and θ_3*

(i) To begin with, frame $\{2\}$ is rotated by an angle θ_1 about its w-axis coincident with z-axis of frame $\{1\}$. The rotated frame is now $\{2'\}$ and the rotation is described by the rotation matrix $\boldsymbol{R}_w(\theta_1)$.

(ii) Next, moving frame $\{2'\}$ is rotated by an angle θ_2 about v'-axis, the rotated v-axis to frame $\{2''\}$. This rotation is described by the rotation matrix $\boldsymbol{R}_{v'}(\theta_2)$.

(iii) Finally, frame $\{2''\}$ is rotated by an angle θ_3 about its u''-axis, the rotated u-axis to give frame $\{2\}$. This rotation is described by the rotation $\boldsymbol{R}_{u''}(\theta_3)$.

This convention for specifying orientation is called *WVU-Euler angle representation* and is illustrated in Fig. 2.16(a), (b), and (c). Viewing each of these rotations as descriptions of frames relative to each other, the equivalent rotation matrix is computed by post multiplication of the matrices of the elementary rotations as

$$\begin{aligned}\boldsymbol{R}_{wvu}(\theta_1\theta_2\theta_3) = {}^1\boldsymbol{R}_2 &= {}^1\boldsymbol{R}_{2'}\ {}^{2'}\boldsymbol{R}_{2''}\ {}^{2''}\boldsymbol{R}_2 \\ &= \boldsymbol{R}_w(\theta_1)\boldsymbol{R}_{v'}(\theta_2)\boldsymbol{R}_{u''}(\theta_3) \qquad (2.61)\end{aligned}$$

(rotation ordering left to right)

The rotations are performed about the current axes of the moving frame $\{uvw\}$. Using the results of Eqs. (2.54)–(2.56), the resulting frame orientation or the rotation matrix is

$$\boldsymbol{R}_{wvu}(\theta_1\theta_2\theta_3) = \begin{bmatrix} C_1 & -S_1 & 0 \\ S_1 & C_1 & 0 \\ 0 & 0 & 1 \end{bmatrix}\begin{bmatrix} C_2 & 0 & S_2 \\ 0 & 1 & 0 \\ -S_2 & 0 & C_2 \end{bmatrix}\begin{bmatrix} 1 & 0 & 0 \\ 0 & C_3 & -S_3 \\ 0 & S_3 & C_3 \end{bmatrix}$$

or

$$\boldsymbol{R}_{wvu}(\theta_1\theta_2\theta_3) = \begin{bmatrix} C_2C_3 & S_1S_2C_3 - C_1S_3 & C_1S_2C_3 + S_1S_3 \\ C_2S_3 & S_1S_2S_3 + C_1C_3 & C_1S_2S_3 - S_1C_3 \\ -S_2 & S_1C_2 & C_1C_2 \end{bmatrix} \qquad (2.62)$$

It is observed that this result is exactly same as that obtained for fixed angle representation, Eq. (2.60), but the rotations about the fixed axes were performed in opposite order. In general, three rotations performed about fixed axes give the same final orientation as obtained by the same three rotations performed in the opposite order about the moving axes. Hence,

$$\boldsymbol{R}_{xyz}(\theta_3\,\theta_2\,\theta_1) = \boldsymbol{R}_{wvu}(\theta_1\theta_2\theta_3) = \boldsymbol{R}_{zyx}(\theta_1\,\theta_2\,\theta_3) \tag{2.63}$$

Another most widely used Euler angle representation consists of the so called *ZYZ* representation for rotations about the axes of the current frame. The sequences of elementary rotations corresponding to this representation are:

(i) A rotation by angle θ_1 about the w-axis (or z-axis of the fixed frame), that is, $\boldsymbol{R}_w(\theta_1)$.

(ii) The second rotation by angle θ_2 about the rotated v-axis, that is $\boldsymbol{R}_{v'}(\theta_2)$. These two rotations are same as the previous case in Fig. 2.13.

(iii) Finally, a rotation of angle θ_3 about the rotated w-axis, that is $\boldsymbol{R}_{w''}(\theta_3)$.

The resulting rotation matrix is

$$\boldsymbol{R}_{wvw}(\theta_1\theta_2\theta_3) = {}^1\boldsymbol{R}_2 = \boldsymbol{R}_w(\theta_1)\boldsymbol{R}_{v'}(\theta_2)\boldsymbol{R}_{w''}(\theta_3)$$

$$= \begin{bmatrix} C_1 & -S_1 & 0 \\ S_1 & C_1 & 0 \\ 0 & 0 & 1 \end{bmatrix} \begin{bmatrix} C_2 & 0 & S_2 \\ 0 & 1 & 0 \\ -S_2 & 0 & C_2 \end{bmatrix} \begin{bmatrix} C_3 & -S_3 & 0 \\ S_3 & C_3 & 0 \\ 0 & 0 & 1 \end{bmatrix} \tag{2.64}$$

$$= \begin{bmatrix} C_1C_2C_3 - S_1S_3 & -C_1C_2S_3 - S_1C_3 & C_1S_2 \\ S_1C_2C_3 + C_1S_3 & -S_1C_2S_3 + C_1C_3 & S_1S_2 \\ -S_2C_3 & S_2S_3 & C_2 \end{bmatrix}$$

The above Euler angle rotation matrix can also be obtained by rotations about the fixed frame as: a rotation by angle θ_3 about z-axis followed by a rotation by angle θ_2 about y-axis and finally a rotation angle θ_1 again about z-axis. The reader should verify this.

In all, twelve distinct sets of Euler angles and twelve sets of fixed angles are possible, with regard to sequence of elementary rotations. Other alternative Euler angle representations are also in vogue. For each of these, the rotation matrix can be found on similar lines.

2.5.4 Equivalent Angle Axis Representation

A third representation of orientation is by a single rotation about an arbitrary axis. A coordinate frame can be rotated about an arbitrary axis k passing through the origin of fixed reference frame {1}. The rotation matrix for this case is obtained by viewing the rotation as a sequence of rotations of frame {2} (along with k-axis) about the principal axes of frame {1}.

Consider frame {2}, initially coincident with frame {1}. Frame {2} is rotated by an angle θ about k-axis, in frame {1}, as shown in Fig. 2.17. The rotation of frame {2} is decomposed into rotations about the principal axes of frame {1}.

First, suitable rotations are made about the principal axes of frame {1} so as to align the axis k with x-axis. Next, the rotation of angle θ is made about the k-axis (which is coincident with x-axis). Then, by reverse rotations about the axes of frame {1}, k-axis is returned to its original location.

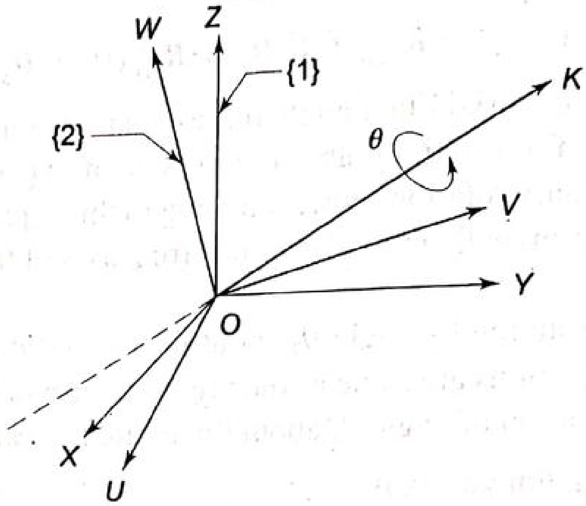

Fig. 2.17 *Equivalent angle axis representation*

These rotations are illustrated with the help of a vector $\boldsymbol{P}$, initially in the direction of k-axis, in Fig. 2.18.

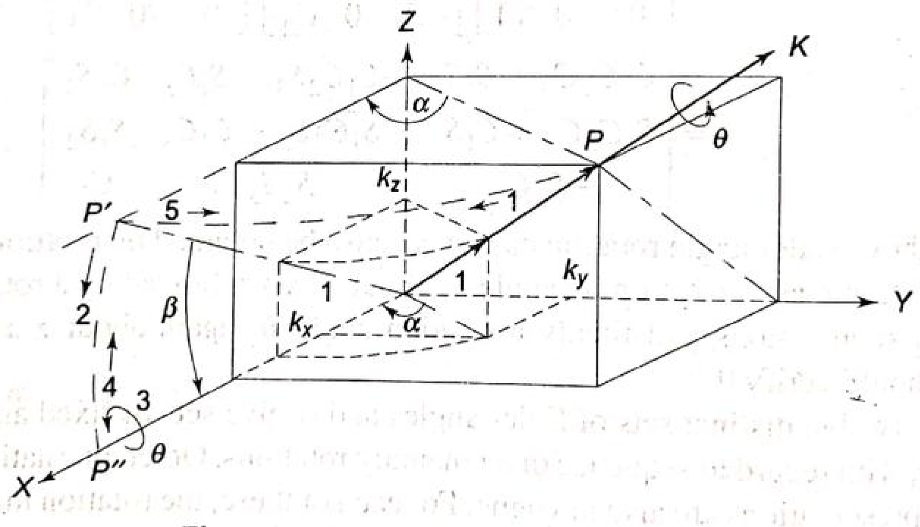

Fig. 2.18 *Rotations of frame about k-axis*

First, rotate the vector $\boldsymbol{P}$ (along with axis k and frame {2} of Fig. 2.17) by an angle $-\alpha$ about z-axis such that this rotation causes the axis k to lie in xz-plane of frame {1}. This rotation, marked as "1" in Fig. 2.18 and is written as

$$^{1}\boldsymbol{R}_2 = \boldsymbol{R}_z(-\alpha) \tag{2.65}$$

Next, vector $\boldsymbol{P}$ (along with rotated axis k) is rotated about y-axis by an angle β so that axis k aligns with x-axis, rotation "2". At the end of this rotation,

$$^{1}\boldsymbol{R}_2 = \boldsymbol{R}_y(\beta)\,\boldsymbol{R}_z(-\alpha) \tag{2.66}$$

Now a rotation "3" of angle θ about the rotated axis k, which is rotation about x-axis, is made. The resulting rotation matrix is then

$$^1R_2 = R_x(\theta)\, R_y(\beta)\, R_x(-\alpha) \tag{2.67}$$

Finally, the rotations "4" and "5" of $-\beta$ and α are made about y- and z-axes, respectively, in the opposite sense and reverse order so as to restore the k-axis to its original position leaving frame {2} in the rotated position. This gives

$$^1R_2 = R_k(\theta) = R_z(\alpha)\, R_y(-\beta)\, R_x(\theta)\, R_y(\beta)\, R_z(-\alpha) \tag{2.68}$$

Substituting the values for the fundamental rotation matrices from Eqs. (2.54)–(2.56) gives,

$$^1R_2 = \begin{bmatrix} C\alpha & -S\alpha & 0 \\ S\alpha & C\alpha & 0 \\ 0 & 0 & 1 \end{bmatrix} \begin{bmatrix} C\beta & 0 & -S\beta \\ 0 & 1 & 0 \\ S\beta & 0 & C\beta \end{bmatrix} \begin{bmatrix} 1 & 0 & 0 \\ 0 & C\theta & -S\theta \\ 0 & S\theta & C\theta \end{bmatrix} \begin{bmatrix} C\beta & 0 & S\beta \\ 0 & 1 & 0 \\ -S\beta & 0 & C\beta \end{bmatrix} \begin{bmatrix} C\alpha & S\alpha & 0 \\ -S\alpha & C\alpha & 0 \\ 0 & 0 & 1 \end{bmatrix} \tag{2.69}$$

The angles α and β can be eliminated from Eq. (2.69) using the geometry. From Fig. 2.18, following are easily observed for the unit vector $\hat{k} = [k_x \quad k_y \quad k_z]^T$

$$\sin\alpha = \frac{k_y}{\sqrt{k_x^2 + k_y^2}}, \cos\alpha = \frac{k_x}{\sqrt{k_x^2 + k_y^2}}$$

$$\sin\beta = k_z, \cos\beta = \sqrt{k_x^2 + k_y^2} \tag{2.70}$$

Substituting these in Eq. (2.69) and simplifying gives

$$^1R_2 = R_k(\theta) = \begin{bmatrix} k_x^2 V\theta + C\theta & k_x k_y V\theta - k_z S\theta & k_x k_z V\theta + k_y S\theta \\ k_x k_y V\theta + k_z S\theta & k_y^2 V\theta + C\theta & k_y k_z V\theta - k_x S\theta \\ k_x k_z V\theta - k_y S\theta & k_y k_z V\theta + k_x S\theta & k_z^2 V\theta + C\theta \end{bmatrix} \tag{2.71}$$

where k_x, k_y, k_z are the projections of a unit vector $\hat{k}$ on frame $\{xyz\}$, and $V\theta = 1 - \cos\theta$.

This is an important rotation matrix and must be thoroughly understood. The principal axes fundamental rotations can be obtained from Eq. (2.71). For example, if k-axis is aligned with z-axis, $R_k(\theta)$ becomes $R_z(\theta)$ with $k_x = k_y = 0$ and $k_z = 1$. Substituting these k_x, k_y, k_z in Eq. (2.71) gives

$$R_k(\theta) = R_z(\theta) = \begin{bmatrix} C\theta & -S\theta & 0 \\ S\theta & C\theta & 0 \\ 0 & 0 & 1 \end{bmatrix} \tag{2.72}$$

which is same as Eq. (2.54) derived before.

Note that any combination of rotations about the principal axes of a coordinate frame is always equivalent to a single rotation by some angle θ about some arbitrary axis k. To find the direction K, consider the general rotational transformation matrix R of Eq. (2.32). It is required to determine θ and $\hat{k}$. Equating Eqs. (2.32) and (2.71), one gets nine equations in four unknowns k_x, k_y, k_z, and θ, which can be easily computed (see Review Question 2.21).

The concepts of transformation developed in this chapter will be required for analysis of manipulators for various aspects of robotics covered in rest of the chapters. To enhance the understanding, several examples are worked out involving different concepts of transformations.

SOLVED EXAMPLES

Example 2.1 *Use of Transformations*

The coordinates of point P in frame {1} are $[3.0 \quad 2.0 \quad 1.0]^T$. The position vector P is rotated about the z-axis by 45°. Find the coordinates of point Q, the new position of point P.

Solution The 45° rotation of P about the z-axis of frame {1} from Eq. (2.54) is

$$\boldsymbol{R}_z(45°) = \begin{bmatrix} \cos 45° & -\sin 45° & 0 \\ \sin 45° & \cos 45° & 0 \\ 0 & 0 & 1 \end{bmatrix} = \begin{bmatrix} 0.707 & -0.707 & 0 \\ 0.707 & 0.707 & 0 \\ 0 & 0 & 1 \end{bmatrix} \tag{2.73}$$

For the rotation of vectors, Eq. (2.37) gives

$$^1\boldsymbol{Q} = \boldsymbol{R}_z(45°)\ ^1\boldsymbol{P}$$

Substituting values of $\boldsymbol{R}_z$ and $^1\boldsymbol{P}$,

$$^1\boldsymbol{Q} = \begin{bmatrix} 0.707 & -0.707 & 0 \\ 0.707 & 0.707 & 0 \\ 0 & 0 & 1 \end{bmatrix} \begin{bmatrix} 3.0 \\ 2.0 \\ 1.0 \end{bmatrix} = \begin{bmatrix} 0.707 \\ 3.535 \\ 1 \end{bmatrix} \tag{2.74}$$

Thus, the coordinates of the new point Q relative to frame {1} are $[0.707 \quad 3.535 \quad 1.0]^T$ or the new position vector is

$$\boldsymbol{Q} = [0.707 \quad 3.535 \quad 1.0]^T \tag{2.75}$$

Example 2.2 *Homogeneous Transformation*

Frame {2} is rotated with respect to frame {1} about the x-axis by an angle of 60°. The position of the origin of frame {2} as seen from frame {1} is $^1\boldsymbol{D}_2 = [7.0 \quad 5.0 \quad 7.0]^T$. Obtain the transformation matrix $^1\boldsymbol{T}_2$, which describes frame {2} relative to frame {1}. Also, find the description of point P in frame {1} if $^2\boldsymbol{P} = [2.0 \quad 4.0 \quad 6.0]^T$.

Solution The homogeneous transform matrix describing frame {2} with respect to frame {1}, Eq. (2.29), is

$$ {}^1\boldsymbol{T}_2 = \left[\begin{array}{ccc:c} & {}^1\boldsymbol{R}_2 & & {}^1\boldsymbol{D}_2 \\ \hdashline 0 & 0 & 0 & 1 \end{array}\right] $$

Because frame {2} is rotated relative to frame {1} about x-axis by 60°, Eq. (2.55) gives

$$ {}^1\boldsymbol{R}_2 = \begin{bmatrix} 1 & 0 & 0 \\ 0 & \cos 60^\circ & -\sin 60^\circ \\ 0 & \sin 60^\circ & \cos 60^\circ \end{bmatrix} = \begin{bmatrix} 1 & 0 & 0 \\ 0 & 0.500 & -0.866 \\ 0 & 0.866 & 0.500 \end{bmatrix} \tag{2.76} $$

Substituting ${}^1\boldsymbol{R}_2$ and ${}^1\boldsymbol{D}_2$ in the above equation

$$ {}^1\boldsymbol{T}_2 = \left[\begin{array}{ccc:c} 1 & 0 & 0 & 7.000 \\ 0 & 0.500 & -0.866 & 5.000 \\ 0 & 0.866 & 0.500 & 7.000 \\ \hdashline 0 & 0 & 0 & 1 \end{array}\right] \tag{2.77} $$

Given: ${}^2\boldsymbol{P} = [2.0 \;\; 2.0 \;\; 6.0]^T$, point P in frame {1} is given by

$$ {}^1\boldsymbol{P} = {}^1\boldsymbol{T}_2 \, {}^2\boldsymbol{P} $$

Substituting values

$$ {}^1\boldsymbol{P} = \begin{bmatrix} 1 & 0 & 0 & 7.000 \\ 0 & 0.500 & -0.866 & 5.000 \\ 0 & 0.866 & 0.500 & 7.000 \\ 0 & 0 & 0 & 1 \end{bmatrix} \begin{bmatrix} 2.0 \\ 4.0 \\ 6.0 \\ 1 \end{bmatrix} = \begin{bmatrix} 9.000 \\ 1.804 \\ 13.464 \\ 1 \end{bmatrix} \tag{2.78} $$

or
$$ {}^1\boldsymbol{P} = [9.000 \;\; 1.804 \;\; 13.464 \;\; 1]^T \tag{2.79} $$

The 3×1 position vector of point P in frame {1} in physical coordinates is then

$$ {}^1\boldsymbol{P} = [9.000 \;\; 1.804 \;\; 13.464]^T \tag{2.80} $$

Example 2.3 ***Transformation of Vector and Frames***

Consider a point P in space. Determine the new location of this point after rotating it by an angle of 45° about z-axis and then translating it by –1 unit along x-axis and –2 units along z-axis. Pictorially show the transformation of the vector. What will be the equivalent frame transformation for this vector transformation? Show the transformation of frames.

Solution Figure 2.19 shows a point P and a vector from origin as ${}^1\boldsymbol{P}$ in frame {1} and its new location after the rotational and transnational transformation as ${}^1\boldsymbol{Q}$. The relation between ${}^1\boldsymbol{Q}$ and ${}^1\boldsymbol{P}$ is described by Eq. (2.26) as

$$ {}^1\boldsymbol{Q} = \boldsymbol{T} \, {}^1\boldsymbol{P} $$

where
$$ \boldsymbol{T} = \left[\begin{array}{ccc:c} & \boldsymbol{R}(\theta) & & \boldsymbol{D} \\ \hdashline 0 & 0 & 0 & 1 \end{array}\right] $$

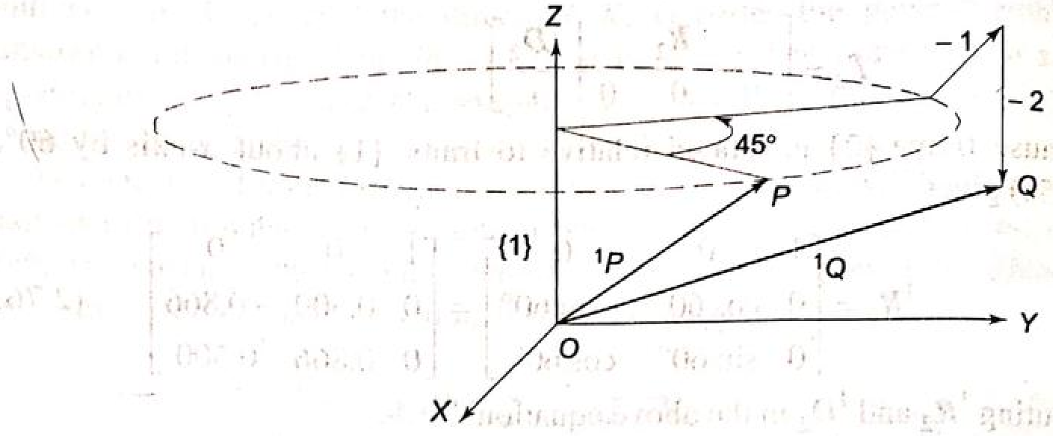

Fig. 2.19 *Transformation of point P in space*

Substituting values gives

$$^{1}\boldsymbol{Q} = \begin{bmatrix} \cos 45^\circ & -\sin 45^\circ & 0 & -1 \\ \sin 45^\circ & \cos 45^\circ & 0 & 0 \\ 0 & 0 & 1 & -2 \\ 0 & 0 & 0 & 1 \end{bmatrix} {}^{1}\boldsymbol{P} = \begin{bmatrix} 0.707 & -0.707 & 0 & -1 \\ 0.707 & 0.707 & 0 & 0 \\ 0 & 0 & 1 & -2 \\ 0 & 0 & 0 & 1 \end{bmatrix} {}^{1}\boldsymbol{P} \quad (2.81)$$

The transformation in Eq. (2.81) can be regarded as transformation of two frames {1} and {2}. Assuming frame {1} and frame {2} to be initially coincident, the final position of frame {2} is obtained by translating it by +2 units along z_1-axis (motion 1), and +1 unit along x_1-axis (motion 2) and then rotating it by an angle of –45° about z_1-axis (motion 3). The two frames are shown in Fig. 2.20.

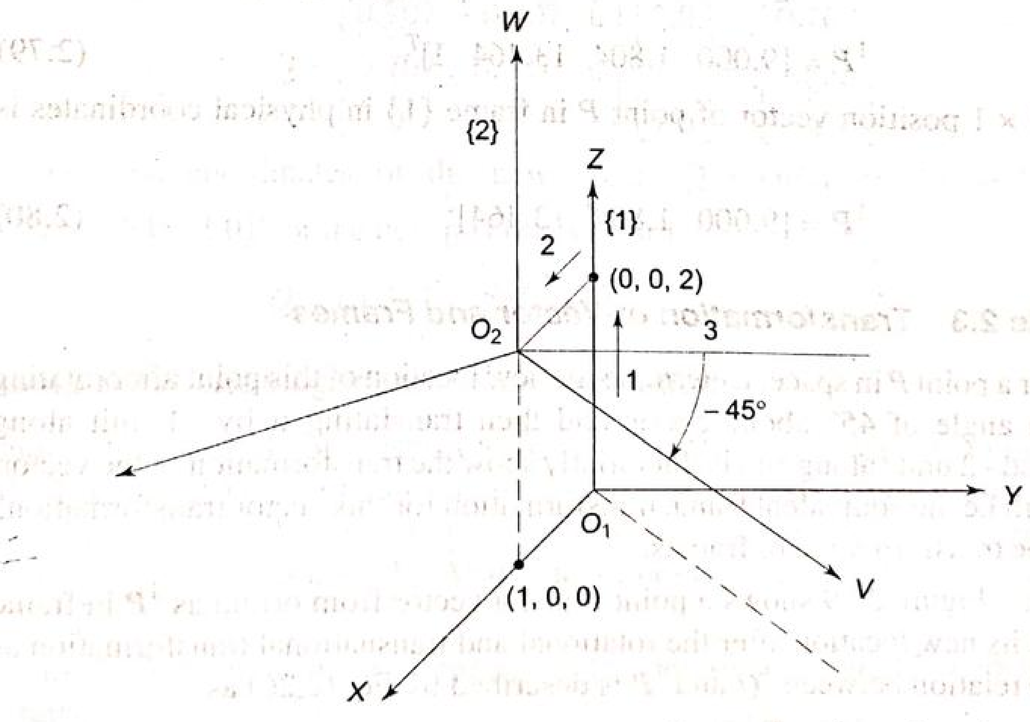

Fig. 2.20 *Transformation of frames corresponding to transformation of vectors*

Example 2.4 ***Description of Frames***

In Example 2.2, the transformation matrix ${}^1\boldsymbol{T}_2$ was obtained, which describes the position and orientation of frame {2} relative to frame {1}. Using this matrix, determine the description of frame {1} relative to frame {2}.

Solution The homogeneous transformation for describing frame {1} relative to frame {2}, ${}^2\boldsymbol{T}_1$ is given by

$$ {}^2\boldsymbol{T}_1 = \left[\begin{array}{ccc|c} & {}^2\boldsymbol{R}_1 & & {}^2\boldsymbol{D}_1 \\ \hline 0 & 0 & 0 & 1 \end{array}\right] = [{}^1\boldsymbol{T}_2]^{-1} \tag{2.82} $$

The inverse of ${}^1\boldsymbol{T}_2$ is given by Eq. (2.53), that is,

$$ {}^2\boldsymbol{T}_1 = \left[\begin{array}{ccc|c} & {}^1\boldsymbol{R}_2^{\,T} & & -{}^1\boldsymbol{R}_2^{\,T}\,{}^1\boldsymbol{D}_2 \\ \hline 0 & 0 & 0 & 1 \end{array}\right] $$

From ${}^1\boldsymbol{T}_2$ in Example 2.2, Eq. (2.77),

$$ {}^1\boldsymbol{R}_2 = \begin{bmatrix} 1 & 0 & 0 \\ 0 & 0.500 & -0.866 \\ 0 & 0.866 & 0.500 \end{bmatrix} $$

and $$ {}^1\boldsymbol{D}_2 = [7.0 \;\; 5.0 \;\; 7.0]^T $$

Hence, $$ {}^2\boldsymbol{R}_1 = {}^1\boldsymbol{R}_2^T = \begin{bmatrix} 1 & 0 & 0 \\ 0 & 0.500 & 0.866 \\ 0 & -0.866 & 0.500 \end{bmatrix} \tag{2.83} $$

and the position of the origin of frame {1} with respect to frame {2} is given by

$$ {}^2\boldsymbol{D}_1 = -{}^1\boldsymbol{R}_2^T\,{}^1\boldsymbol{D}_2 $$

Substituting values

$$ {}^2\boldsymbol{D}_1 = -\begin{bmatrix} 1 & 0 & 0 \\ 0 & 0.500 & 0.866 \\ 0 & -0.866 & 0.500 \end{bmatrix} \begin{bmatrix} 7.0 \\ 5.0 \\ 7.0 \end{bmatrix} = \begin{bmatrix} -7.000 \\ -8.562 \\ 0.830 \end{bmatrix} \tag{2.84} $$

Therefore,

$$ {}^2\boldsymbol{T}_1 = \begin{bmatrix} 1 & 0 & 0 & -7.000 \\ 0 & 0.500 & 0.866 & -8.562 \\ 0 & -0.866 & 0.500 & 0.830 \\ 0 & 0 & 0 & 1 \end{bmatrix} \tag{2.85} $$

Example 2.5 ***Euler Angle Rotations***

In Euler angle representation, the equivalent rotation matrix relating the two frames is specified by a set of *ZYX*-Euler angle rotations. Consider now the inverse of this problem: Given the rotation matrix ${}^1\boldsymbol{R}_2$, relating the orientation of frame {2} with respect to frame {1}. Determine the corresponding set of *ZYX*-Euler angle rotations.

Solution Let the given rotation matrix which specifies the orientation of frame {2} with respect to frame {1} be

$$^1\boldsymbol{R}_2 = \begin{bmatrix} r_{11} & r_{12} & r_{13} \\ r_{21} & r_{22} & r_{23} \\ r_{31} & r_{32} & r_{33} \end{bmatrix} \tag{2.86}$$

The equivalent rotation matrix for a set of *ZYX*-Euler angle rotation ($\theta_1\ \theta_2\ \theta_3$) is given by Eq. (2.62),

$$^1\boldsymbol{R}_2 = \begin{bmatrix} C_2C_3 & S_1S_2C_3 - C_1S_3 & S_1S_3 + C_1S_2C_3 \\ C_2S_3 & S_1S_2S_3 + C_1C_3 & -S_1C_3 + C_1S_2S_3 \\ -S_2 & S_1C_2 & C_1C_2 \end{bmatrix} \tag{2.87}$$

Equating the corresponding elements of these matrices gives nine equations in three independent variables, θ_1, θ_2, θ_3. Apart from the redundancy in equations, additional complication is that these are transcendental in nature.

Equating elements (1,1) and (2,1) in Eq (2.86) with corresponding elements in Eq. (2.87) gives,

$$C_2C_3 = r_{11} \text{ and } C_2S_3 = r_{21}$$

Squaring and adding gives

$$C_2 = \cos\theta_2 = \pm\sqrt{r_{11}^2 + r_{21}^2} \tag{2.88}$$

Combining with the element (3,1), ($-S_2 = r_{31}$), the angle θ_2 is computed as

$$\tan\theta_2 = \frac{S_2}{C_2}$$

which gives

$$\theta_2 = A\tan2(-r_{31}, \pm\sqrt{r_{11}^2 + r_{21}^2}) \tag{2.89}$$

where $A\tan2(a, b)$ is a two-argument *arc tangent* function (see Appendix **A**).

The solution for θ_1 and θ_3 depends on value of θ_2. Here, two cases arise which are worked out as follows:

Case 1 $\theta_2 \neq 90°$

From the elements (1,1) and (2,1) in Eqs. (2.86) and (2.87), θ_3 is obtained as

$$\theta_3 = A\tan2\left(\frac{r_{21}}{C_2}, \frac{r_{11}}{C_2}\right) \tag{2.90}$$

and from elements (3,2) and (3,3), θ_1 is

$$\theta_1 = A\tan2\left(\frac{r_{32}}{C_2}, \frac{r_{33}}{C_2}\right) \tag{2.91}$$

Note that there is one set of solution corresponding to each value of θ_2.

Case 2 $\theta_2 = \pm 90°$

For $\theta_2 = \pm 90°$, the solution obtained in Case 1 degenerates. However, it is possible to find only the sum or difference of θ_3 and θ_1. Comparing elements (1, 2) and (2, 2)

$$r_{12} = S_1S_2C_3 - C_1S_3$$

and
$$r_{22} = S_1S_2S_3 + C_1C_3 \tag{2.92}$$

If $\theta_2 = +90°$, these equations reduce to

$$r_{12} = \sin(\theta_1 - \theta_3)$$
$$r_{22} = \cos(\theta_1 - \theta_3)$$

and
$$\theta_1 - \theta_3 = \text{Atan2}(r_{12}, r_{22}) \tag{2.93}$$

Choosing $\theta_3 = 0°$ gives the particular solution

$$\theta_2 = 90°;\ \theta_3 = 0° \text{ and } \theta_1 = \text{Atan2}(r_{12}, r_{22}) \tag{2.94}$$

With $\theta_2 = -90°$, the solution is

$$r_{12} = -\sin(\theta_1 + \theta_2)$$
$$r_{22} = \cos(\theta_1 + \theta_2)$$

and
$$\theta_1 + \theta_2 = \text{Atan2}(-r_{12}, r_{22}) \tag{2.95}$$

Choosing $\theta_2 = 0°$ gives the particular solution

$$\theta_2 = -90°;\ \theta_3 = 0° \text{ and } \theta_1 = \text{Atan2}(-r_{12}, r_{22}) \tag{2.96}$$

Example 2.6 ***Multiple Rotations of a Frame***

Frame {1} and {2} have coincident origins and differ only in orientation. Frame {2} is initially coincident with frame {1}. Certain rotations are carried out about the axis of the fixed frame {1}: first rotation about x-axis by 45° then about y-axis by 30° and finally about x-axis by 60°. Obtain the equivalent rotation matrix ${}^1\boldsymbol{R}_2$.

Solution Rotations are in order X-Y-X about the fixed axes; hence, it is a case of fixed angle representation. Therefore,

$${}^1\boldsymbol{R}_2 = \boldsymbol{R}_x(60°)\,\boldsymbol{R}_y(30°)\,\boldsymbol{R}_x(45°) \tag{2.97}$$

or

$${}^1\boldsymbol{R}_2 = \begin{bmatrix} 1 & 0 & 0 \\ 0 & \cos 60° & -\sin 60° \\ 0 & \sin 60° & \cos 60° \end{bmatrix} \begin{bmatrix} \cos 30° & 0 & \sin 30° \\ 0 & 1 & 0 \\ -\sin 30° & 0 & \cos 30° \end{bmatrix} \begin{bmatrix} 1 & 0 & 0 \\ 0 & \cos 45° & -\sin 45° \\ 0 & \sin 45° & \cos 45° \end{bmatrix}$$

On multiplication,

$${}^1\boldsymbol{R}_2 = \begin{bmatrix} 0.866 & 0.354 & 0.354 \\ 0.433 & -0.177 & -0.884 \\ -0.25 & 0.919 & 0.306 \end{bmatrix} \tag{2.98}$$

The reader must verify that the same orientation could have been obtained by performing the same rotations about the moved xyx-axes of the moving frame but in the opposite order. This convention is also referred as *XYX*-Euler angle representation.

Example 2.7 ***Equivalent Axis Representation***

Two coordinate frames {1} and {2} are initially coincident. Frame {2} is rotated by 45° about a vector $\hat{k} = [0.5\ 0.866\ 0.707]^T$ passing through the origin. Determine the new description of frame {2}.

Solution Substituting $\hat{k}$ and $\theta = 45°$ in Eq. (2.71) yields the rotation matrix ${}^1\boldsymbol{R}_2$ for rotation about k-axis as

$$\boldsymbol{R}_k(45°) = {}^1\boldsymbol{R}_2 = \begin{bmatrix} 0.780 & -0.373 & 0.716 \\ 0.627 & 0.927 & -0.174 \\ -0.509 & 0.533 & 0.854 \end{bmatrix} \tag{2.99}$$

Since there is no translation of frame {2}, the position vector is $\boldsymbol{D} = [0\,0\,0\,1]^T$ and the description of frame {2} with respect to frame {1} is:

$${}^1\boldsymbol{T}_2 = \begin{bmatrix} 0.780 & -0.373 & 0.716 & 0 \\ 0.627 & 0.927 & -0.174 & 0 \\ -0.509 & 0.533 & 0.854 & 0 \\ 0 & 0 & 0 & 1 \end{bmatrix} \tag{2.100}$$

Example 2.8 ***Screw Transformation***

The moving coordinate frame $\{u\ v\ w\}$ undergoes a "screw transformation", that is, it is translated by 4 units along z-axis and rotated by an angle of 180° about same axis of stationary reference coordinate frame $\{x\ y\ z\}$. Coordinates *XYZ* and *UVW* are initially coincident.

(a) Obtain the homogeneous transformation matrix for the screw transformation.

(b) Show the coordinate frames before and after the transformation.

(c) If the order of transformations is reversed, will the homogeneous screw transformation matrix change?

Solution (a) In screw transformation the moving frame is translated and rotated about same axis. The overall transformation matrix for the given situation is

$$\boldsymbol{T} = \boldsymbol{T}(z, \pi)\ \boldsymbol{T}\ (0, 0, 4)$$

or

$$\boldsymbol{T} = \begin{bmatrix} -1 & 0 & 0 & 0 \\ 0 & -1 & 0 & 0 \\ 0 & 0 & 1 & 0 \\ 0 & 0 & 0 & 1 \end{bmatrix} \begin{bmatrix} 1 & 0 & 0 & 0 \\ 0 & 1 & 0 & 0 \\ 0 & 0 & 1 & 4 \\ 0 & 0 & 0 & 1 \end{bmatrix} = \begin{bmatrix} -1 & 0 & 0 & 0 \\ 0 & -1 & 0 & 0 \\ 0 & 0 & 1 & 4 \\ 0 & 0 & 0 & 1 \end{bmatrix} \tag{2.101}$$

Assume a unit vector along y-axis. This is given by $\hat{p} = [0\ 1\ 0]^T$. This vector moves with the moving frame and undergoes the two transformations specified. Its position after given translation and rotation will be

$$P' = TP = \begin{bmatrix} -1 & 0 & 0 & 0 \\ 0 & -1 & 0 & 0 \\ 0 & 0 & 1 & 4 \\ 0 & 0 & 0 & 1 \end{bmatrix} \begin{bmatrix} 0 \\ 1 \\ 0 \\ 1 \end{bmatrix} = \begin{bmatrix} 0 \\ -1 \\ 4 \\ 1 \end{bmatrix} \tag{2.102}$$

(b) The initial and final positions of two frames and point P are is shown in Fig. 2.21.

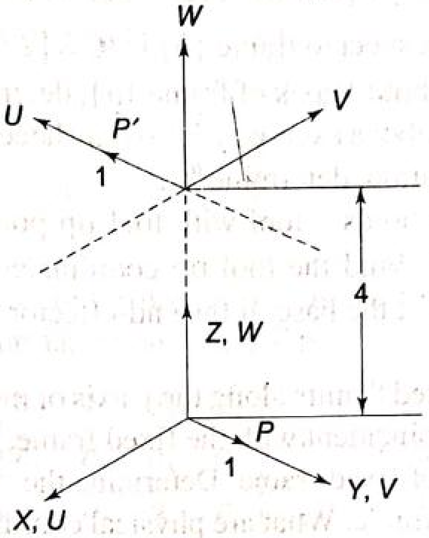

Fig. 2.21 *Screw transformation of point P.*

(c) If the order of transformations is reversed, that is, rotation followed by translation, the overall transformation matrix will not change. This can be easily verified by the reader and is the property of screw transformation.

EXERCISES

2.1 The coordinates of point P with respect to a moving coordinate frame are given as $\boldsymbol{P} = [0.5 \quad 0.8 \quad 1.3 \quad 1]^T$. What are the coordinates of P with respect to fixed coordinate frame, if the moving frame is rotated by 90° about z-axis of the fixed frame?

2.2 Determine the rotation matrix for a rotation of 45° about y-axis, followed by a rotation of 120° about z-axis, and a final rotation of 90° about x-axis.

2.3 A vector $\boldsymbol{P} = 3\hat{i} - 2\hat{j} + 5\hat{k}$ is first rotated by 90° about x-axis, then by 90° about z-axis. Finally, it is translated by $-3\hat{i} + 2\hat{j} - 5\hat{k}$. Determine the new position of vector $\boldsymbol{P}$.

2.4 Find the new location of point G, initially at $\boldsymbol{G} = [3 \quad 0 \quad -1 \quad 1]^T$, if (i) it is rotated by π about z-axis and then translated by 3 units along y-axis, and (ii) it is first translated by 3 units along y-axis and then rotated by π about z-axis. Are the two locations same? Explain why the final position in two cases is same or different.

2.5 A moving frame is rotated about x-axis of the fixed coordinate frame by $\pi/6$ radians. The coordinates of a point Q in fixed coordinate frame are given by $\boldsymbol{Q} = [2 \;\; 0 \;\; 3]^T$. What will be the coordinates of a point Q with respect to the moving frame?

2.6 Show that determinant of the rotation matrix $\boldsymbol{R}$, is +1 for a right-hand coordinate system and –1 for a left-hand coordinate system.

2.7 The end-effector of a robot is rotated about fixed axes starting with a yaw of $-\pi/2$, followed by a pitch of $-\pi/2$. What is the resulting rotation matrix?

2.8 A vector $\boldsymbol{C}$ with respect to frame $\{b\}$ is ${}^b\boldsymbol{C} = [2 \;\; 4 \;\; -5]^T$. If frame $\{b\}$ is rotated by $-\pi/4$ about x-axis of frame $\{a\}$, determine ${}^a\boldsymbol{C}$.

2.9 If vector $\boldsymbol{C}$ in the above exercise is also translated by 4 units in $-y$ direction in addition to rotation, determine ${}^a\boldsymbol{C}$.

2.10 The end-effector holds a tool with tool tip point P having coordinates $\boldsymbol{P} = [0 \;\; 0 \;\; 1.2]^T$. Find the tool tip coordinates with respect to a fixed coordinate frame at the base, if the end-effector coordinates are given by Eq. (2.31).

2.11 A point Q is located 8 units along the y-axis of moving frame. The mobile frame, initially coincident with the fixed frame, is rotated by $\pi/3$ radians about the z-axis of fixed frame. Determine the coordinates of point Q in fixed coordinate frame. What are physical coordinates of point Q in fixed coordinate frame?

2.12 The end-effector of a manipulator is a gripper. The gripper is relocated from initial point $[2 \;\; 0 \;\; 4 \;\; 1]^T$ to $[4 \;\; 0 \;\; 0 \;\; 1]^T$. Determine the direction of axis k and the angle of rotation about this k-axis.

2.13 Show that a rotation by θ about axis k (Eq. (2.71)) can be used to get the fundamental rotation by choosing axis k to be axis x- or y- or z-axis, respectively.

2.14 An end-effector is rotated by 60° about an axis whose unit vector is $\hat{\boldsymbol{k}} = \left[1/\sqrt{2} \;\; 1/\sqrt{2} \;\; 1 \;\; 1\right]^T$. Find the homogeneous transformation matrix representing this rotation.

2.15 The end-point of a link of a manipulator is at $\boldsymbol{P} = [2 \;\; 2 \;\; 6 \;\; 1]^T$. The link is rotated by 90° about x-axis, then by –180° about its own w-axis, and finally by –90° about its own v-axis. Find the resulting homogeneous transformation matrix and the final location of end-point.

2.16 For a rotation of 90° about z-axis followed by a rotation of 90° about y-axis followed by a rotation of 90° about x-axis, determine an equivalent k-axis of rotation and rotation angle θ about this axis.

2.17 Determine the transformation matrix $\boldsymbol{T}$ that represents a translation of a unit along x-axis, followed by a rotation of angle α about x-axis followed by a rotation of θ about the rotated z-axis.

2.18 Two frames, $\{A\}$ and $\{B\}$, are initially coincident. Frame $\{B\}$ undergoes the following four motions in sequence with respect to axes of frame $\{A\}$:

(i) A rotation of θ about z-axis,

(ii) A translation of d along z-axis,

(iii) A translation of a along x-axis, and finally

(iv) A rotation of α about x-axis.

Determine the final homogeneous transformation matrix to describe frame $\{B\}$, after the transformations, with respect to the frame $\{A\}$.

2.19 The homogeneous transformation matrices between frames $\{i\}$–$\{j\}$ and $\{i\}$–$\{k\}$ are:

$$
{}^{j}\boldsymbol{T}_i = \begin{bmatrix} 0.866 & -0.500 & 0 & 11 \\ 0.500 & 0.866 & 0 & -1 \\ 0 & 0 & 1 & 8 \\ 0 & 0 & 0 & 1 \end{bmatrix};\ {}^{k}\boldsymbol{T}_i = \begin{bmatrix} 1 & 0 & 0 & 0 \\ 0 & 0.866 & -0.500 & 10 \\ 0 & 0.500 & 0.866 & -20 \\ 0 & 0 & 0 & 1 \end{bmatrix} \tag{2.103}
$$

Determine ${}^{j}\boldsymbol{T}_k$.

2.20 Show that the inverse of the homogeneous transformation matrix with no perspective transformation, that is, if $\boldsymbol{T}$ is

$$
\boldsymbol{T} = \begin{bmatrix} n_x & o_x & a_x & d_x \\ n_y & o_y & a_y & d_y \\ n_z & o_z & a_z & d_z \\ 0 & 0 & 0 & 1 \end{bmatrix} = \begin{bmatrix} \boldsymbol{n} & \boldsymbol{o} & \boldsymbol{a} & \boldsymbol{d} \\ 0 & 0 & 0 & 1 \end{bmatrix} \tag{2.104}
$$

$\boldsymbol{T}^{-1}$ is given by

$$
\boldsymbol{T}^{-1} = \begin{bmatrix} n_x & n_y & n_z & -\boldsymbol{d}\cdot\boldsymbol{n} \\ o_x & o_y & o_z & -\boldsymbol{d}\cdot\boldsymbol{o} \\ a_x & a_y & a_z & -\boldsymbol{d}\cdot\boldsymbol{a} \\ 0 & 0 & 0 & 1 \end{bmatrix} \tag{2.105}
$$

2.21 For a given equivalent rotation matrix $\boldsymbol{R}$, show that the equivalent angle of rotation θ about k-axis and the direction of axis k are given by

$$
\theta = \cos^{-1}\left[\frac{(r_{11} + r_{22} + r_{33}) - 1}{2}\right]
$$

$$
\begin{bmatrix} k_x \\ k_y \\ k_z \end{bmatrix} = \frac{1}{2\sin\theta}\begin{bmatrix} r_{32} - r_{23} \\ r_{13} - r_{31} \\ r_{21} - r_{12} \end{bmatrix} \tag{2.106}
$$

where r_{ij} are the elements of the known 3×3 orientation matrix $\boldsymbol{R}$,

$$
\boldsymbol{R} = \begin{bmatrix} r_{11} & r_{12} & r_{13} \\ r_{21} & r_{22} & r_{23} \\ r_{31} & r_{32} & r_{33} \end{bmatrix} \tag{2.107}
$$

Assume that $\sin\theta \neq 0$

2.22 The rotation matrix ${}^1\boldsymbol{R}_2$, relating the orientation of frame {2} with respect to frame {1} is given by

$$ {}^1\boldsymbol{R}_2 = \begin{bmatrix} 0.87 & -0.43 & 0.25 \\ 0.50 & 0.75 & -0.43 \\ 0 & 0.50 & 0.87 \end{bmatrix} \tag{2.108} $$

Determine the corresponding set of ZYX-Euler angles

2.23 If the rotation matrix ${}^1\boldsymbol{R}_2$ in Exercise 2.22 corresponds to the fixed angle rotations, determine the corresponding set of roll, pitch, and yaw angles.

2.24 In a roll-pitch-roll convention, roll stands for rotation (δ) about z-axis, pitch for rotation (λ) about new y-axis, and roll again (α) about new z-axis. The roll-pitch-roll geometry can be represented by Euler angles. Show that the overall rotation matrix $\boldsymbol{R}_{RPR}$ (δ, λ, α) is given by

$$ \boldsymbol{R}_{RPR}(\delta, \lambda, \alpha) = \begin{bmatrix} C\delta\, C\lambda\, C\alpha - S\delta\, S\alpha & -C\delta\, C\lambda\, S\alpha - S\delta\, C\alpha & C\delta\, S\lambda \\ S\delta\, C\lambda\, C\alpha + C\delta\, S\alpha & -S\delta\, C\lambda\, S\alpha + C\delta\, C\alpha & S\delta\, S\lambda \\ -S\lambda\, C\alpha & S\lambda\, S\alpha & C\lambda \end{bmatrix} \tag{2.109} $$

where $C\delta = \cos\delta$, $C\lambda = \cos\lambda$, $C\alpha = \cos\alpha$, $S\delta = \sin\delta$, $S\lambda = \sin\lambda$, and $S\alpha = \sin\alpha$.

2.25 A frame is given two rotations, one about x-axis by 60° and one about y-axis by 45°. Show that $\boldsymbol{R}_x \boldsymbol{R}_y \neq \boldsymbol{R}_y \boldsymbol{R}_x$. Explain why.

2.26 Determine the orientation matrix for

(a) ZXZ fixed angle rotations.

(b) ZXZ Euler angle rotations.

2.27 For the rotations about an arbitrary axis k, show that

$$ \boldsymbol{R}_{-k}(-\theta) = \boldsymbol{R}_k(\theta) \tag{2.110} $$

that is, the rotation by angle $-\theta$ about $-k$-axis produces the same effect as those of a rotation by angle θ about k-axis.

2.28 Show that the Euler angles θ_1, θ_2, and θ_3 in Eq. (2.64) can be computed for a known rotation matrix

$$ \boldsymbol{R} = \begin{bmatrix} r_{11} & r_{12} & r_{13} \\ r_{21} & r_{22} & r_{23} \\ r_{31} & r_{32} & r_{33} \end{bmatrix} \tag{2.111} $$

as

$$ \begin{aligned} \theta_1 &= A\tan 2(r_{23}, r_{13}) \\ \theta_2 &= A\tan 2\left(\sqrt{r_{13}^2 + r_{23}^2}, r_{33}\right) \\ \theta_3 &= A\tan 2(r_{32}, -r_{31}) \end{aligned} \tag{2.112} $$

in the range $0 \le \theta_2 \le \pi$.

2.29 A point P is moving with a uniform velocity ${}^2\boldsymbol{v} = [12 \quad 5 \quad 25]^T$ relative to frame{2}. If the transformation of frame {2} to frame {1} is given by

$$ {}^1\boldsymbol{T}_2 = \begin{bmatrix} 1 & 0 & 0 & 6 \\ 0 & 0.866 & -0.500 & 10 \\ 0 & 0.500 & 0.866 & -20 \\ 0 & 0 & 0 & 1 \end{bmatrix} \tag{2.113} $$

compute ${}^1\boldsymbol{v}$.

2.30 Explain why homogeneous coordinates are required in modeling of robotic manipulators.

2.31 Explain why homogeneous transformations are required in modeling of robotic manipulators.

2.32 What are global and local scale factors? When these are useful? Give one situation each where global scale factor is less than one and more than one.

2.33 What do you understand by screw transformations? Where these transformations can be useful?

2.34 What are fundamental rotation matrices? Obtain the three fundamental rotations matrices for rotations about axes x, y and z from the rotation matrix for rotation about an arbitrary axis k.

BIBLIOGRAPHY

1. J. Denavit and R.S. Hartenberg, "A Kinematic Notation for Lower-Pair Mechanisms Based on Matrices," *ASME J. of Applied Mechanics*, 215–221, Jun 1955.
2. A.J. Laub and G.R. Shiflett, "A linear algebra approach to the analysis of rigid body displacement from initial and final position data," *J. Appl. Mech.*, *49*, 213–216, 1982.
3. R.J. Schilling and H. Lee, *Engineering Analysis: A Vector Space Approach*, Wiley, New York, 1988.
4. D. VanArsdale, "Homogeneous Transformation Matrices for Computer Graphics," *Computers & Graphics*, *18*(2), 177–191, 1994.
5. D.E. Whitney, "The Mathematics of Coordinated Control of Prosthetic Arms and Manipulators, "*ASME J. of Dynamic Systems, Measurement and Control*, *94*, 303–309, 1972.

3

Symbolic Modeling of Robots—Direct Kinematic Model

A robotic manipulator is designed to perform a task in the 3-D space. The tool or end-effector is required to follow a planned trajectory to manipulate objects or carry out the task in the workspace. This requires control of position of each link and joint of the manipulator to control both the position and orientation of the tool. To program the tool motion and joint-link motions, a mathematical model of the manipulator is required to refer to all geometrical and/or time-based properties of the motion. Kinematic model describes the spatial position of joints and links, and position and orientation of the end-effector. The derivatives of kinematics deal with the mechanics of motion without considering the forces that cause it. The relationships between the motions and the forces and/or torques that cause them is the dynamics problem.

In designing a robot manipulator, kinematics and dynamics play a vital role. The mathematical tools of spatial descriptions developed in the previous chapter are used in the modeling of robotic manipulators. The *kinematic model* gives relations between the position and orientation of the end-effector and spatial positions of joint-links. The *differential kinematics* of manipulators refers to differential motion, that is, velocity, acceleration, and all higher order derivatives of position variables. The problem of completely describing the position and orientation of a manipulator, the kinematic model, is considered in this and the next chapter. The velocities and accelerations associated with motion would be discussed in Chapter 5 and the forces/torques which cause the motion in Chapter 6.

3.1 MECHANICAL STRUCTURE AND NOTATIONS

The anatomy of the manipulator was discussed in Chapter 1. A manipulator consists of a chain of rigid bodies, called *links*, connected to each other by joints, which allow linear or revolute motion between connected links each of which exhibits just one degree of freedom (DOF). Joints with more than one DOF are not common. A joint with m degrees of freedom can be modeled as m joints with one degree of freedom each connected with $(m–1)$ links of zero length. Most industrial robotic manipulators are open serial kinematic chains, that is, each link is connected to two other links, at the most, without the formation of closed loops. In open chain robots, all joints are motorized (active). Some robots may have closed kinematic chains such as parallelogram linkages and require different considerations to model them.

The number of degrees of freedom a manipulator possesses is the number of independent parameters required to completely specify its position and orientation in space. Because each joint has only one degree of freedom, the degrees of freedom of a manipulator are equal to number of joints.

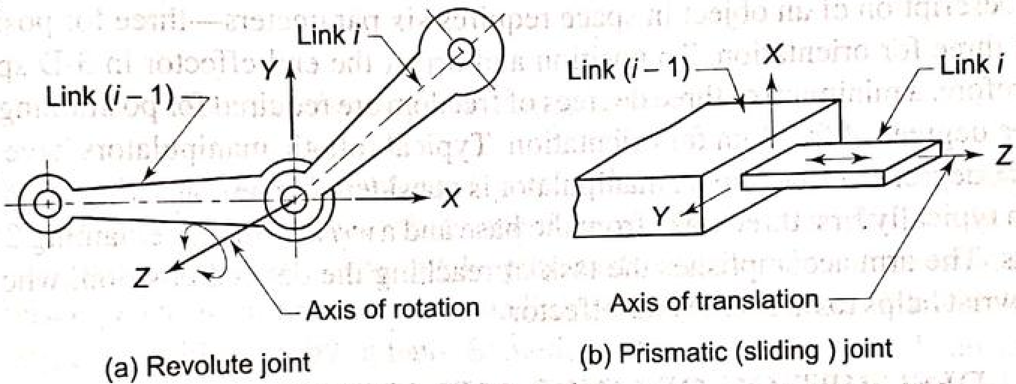

Fig. 3.1 *Two common types of joints and axis of motion (joint axis)*

Single DOF joints between links of a manipulator can be classified as revolute or prismatic. A *revolute joint*, denoted as R-joint, allows rotational motion between connected links. A *prismatic joint*, denoted as P-joint, also known as sliding or rectilinear joint, permits translational motion between the connected links. Each joint has a *joint axis* with respect to which, the motion of joint is described, as shown in Fig. 3.1. In the case of revolute joints, the axis of relative rotation is the joint axis. For the prismatic joint, the axis of relative translational motion is the joint axis. By convention, the z-axis of a coordinate frame is aligned with the joint axis.

The links of a manipulator are numbered outwardly starting from the immobile base as link 0, first moving body as link 1, to the last link out to the free end as link n. Link n is the "*tool*" or "*end-effector*". The joints are numbered, similarly, with joint 1 between link 0 and link 1 and so on, out to the joint n between link $(n–1)$ and link n. The numbering scheme for labelling links and joints is shown in Fig. 3.2 for a 3-DOF manipulator arm which is an open serial kinematic chain of rigid bodies having three revolute joints. Thus, an n-DOF manipulator arm consists of $(n+1)$ links (including link 0) connected by n joints.

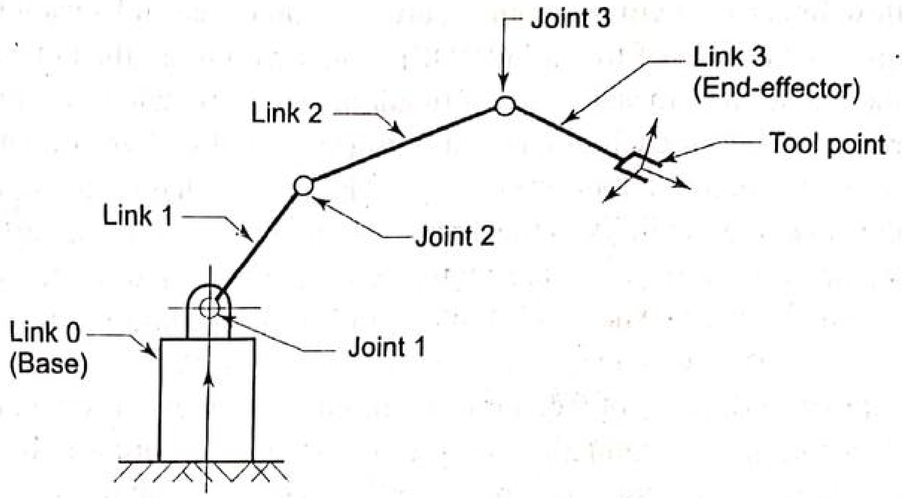

Fig. 3.2 *A 3-DOF manipulator arm—numbering of links and joints*

Description of an object in space requires six parameters—three for position and three for orientation. To position and orient the end-effector in 3-D space, therefore, a minimum of three degrees of freedom are required for positioning and three degrees of freedom for orientation. Typical robotic manipulators have five or six degrees of freedom. A manipulator is considered to be consisting of an *arm* with typically first three links from the base and a *wrist* with the remaining 2 or 3 links. The arm accomplishes the task of reaching the desired position, whereas the wrist helps to orient the end-effector.

3.2 DESCRIPTION OF LINKS AND JOINTS

The n-DOF robotic manipulator is modelled as a chain of rigid links inter-connected by revolute and/or prismatic joints. To describe the position and orientation of a link in space, a coordinate frame is attached to each link, namely, frame $\{i\}$ to link i. The position and orientation of frame $\{i\}$, relative to previous frame $\{i-1\}$, can be described by a homogeneous transformation matrix as discussed in the previous chapter.

In this section, the parameters required to completely specify the position and orientation of links and joints of a manipulator are discussed. Every link of the manipulator is connected to two other links with joints at either end, with the exception of the base and the end-effector, the first and the last link (recall that immobile base is link 0), which have only one joint. Figure 3.3 shows link i of a manipulator with associated joint axes $(i-1)$ and i.

From a geometric viewpoint, the link defines the relative position and orientation of joint axes at its two ends. For the two axes $(i-1)$ and i, there exist a mutual perpendicular, which gives the shortest distance between the two axes. This shortest distance along the common normal is defined as the *link length* and is denoted as a_i. The angle between the projection of axis $(i-1)$ and axis i, on a plane perpendicular to the common normal AB, is known as the *link twist* and is denoted by α_i. The link twist α_i is measured from axis $(i-1)$ to axis i in the right-hand sense about AB, as shown in Fig. 3.3.

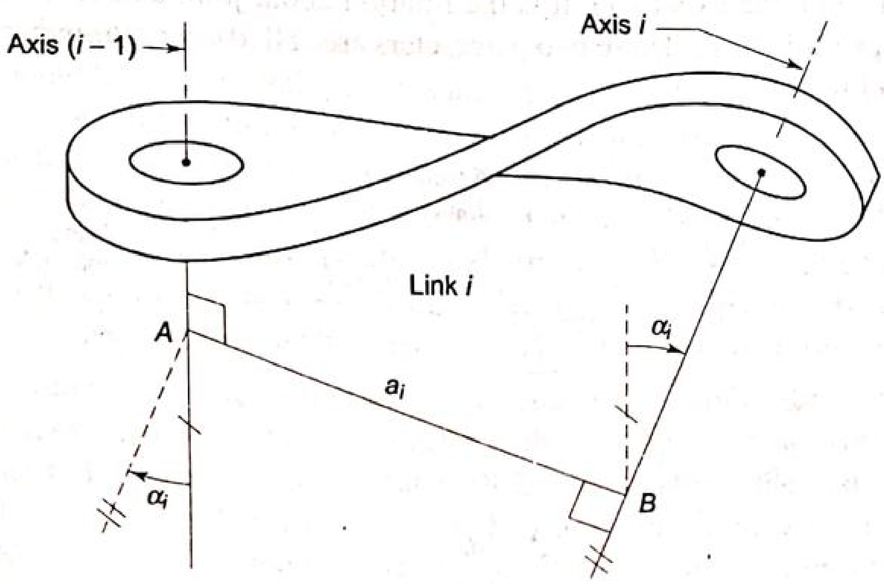

Fig. 3.3 *Description of link parameters a_i and α_i*

These two parameters, a_i and α_i are known as *link parameters* and are constant for a given link. For industrial robots, the links are usually straight, that is, the two joint axes are parallel, giving link length equal to physical link dimension and link twist equal to zero. Another common link geometry is straight link with link twist angle as multiple of $\pi/2$ radians. Sometimes, the link may have a bend such that the axis of joint $(i-1)$ and joint i intersect and in this case the link length of link i is zero although physical link dimension is not zero. Figure 3.4 shows a straight link with link twist of $\pi/2$ radians.

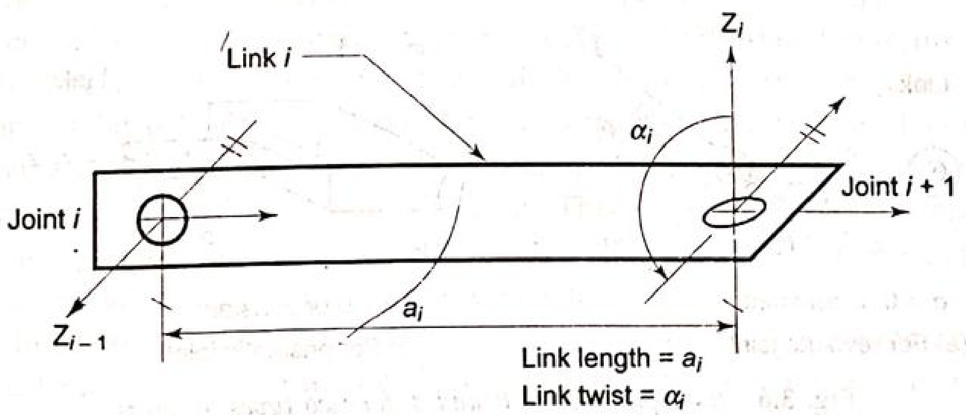

Fig. 3.4 *Link parameters for a straight link with a twist of 90°*

For two links connected by either a revolute or a prismatic joint, the relative position of these links is measured by the displacement at the joint, which is either *joint distance* or *joint angle*, depending on the type of joint. Joint distance (d_i) is the perpendicular distance between the two adjacent common normals a_{i-1} and a_i measured along axis (i–1). In other words, joint distance is the translation needed along joint axis (i–1) to make a_{i-1} intersect with a_i. Joint angle (θ_i) is the angle between the two adjacent common normals a_{i-1} and a_i, measured in right-handed direction about the axis (i–1). It is the rotation about joint axis (i–1) needed to make a_{i-1} parallel to a_i. These two parameters are called *joint parameters* and are shown in Fig. 3.5.

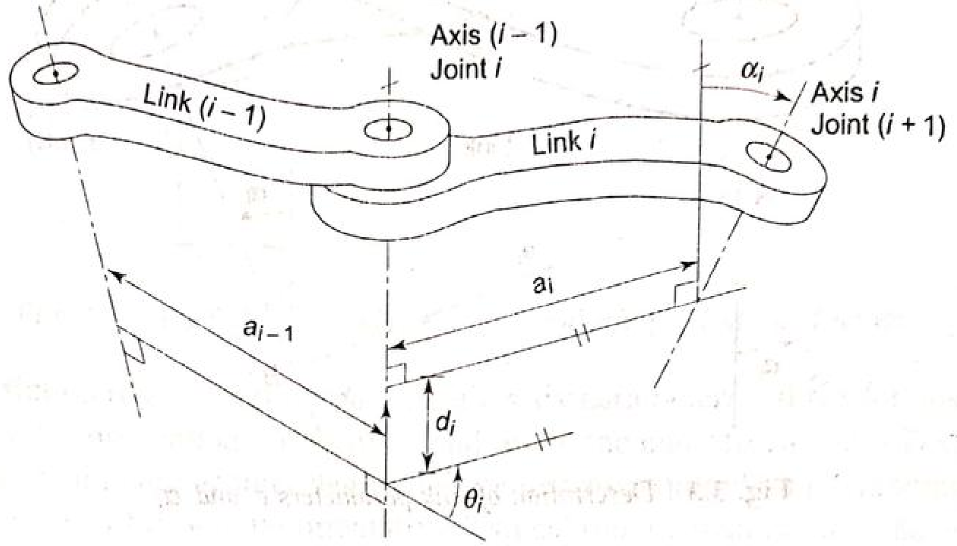

Fig. 3.5 *Description of joint-link parameters for joint i and link i*

A 1-DOF joint requires only one variable to describe its position. Thus, for every 1-DOF joint, it will always be the case that one of the two joint parameters (θ_i and d_i) is fixed and the other is a variable. The displacement of a joint is measured by either angle θ_i or distance d_i depending on the type of joint. The joint displacements for a revolute and prismatic joints are shown in Figs. 3.6(a) and (b), respectively.

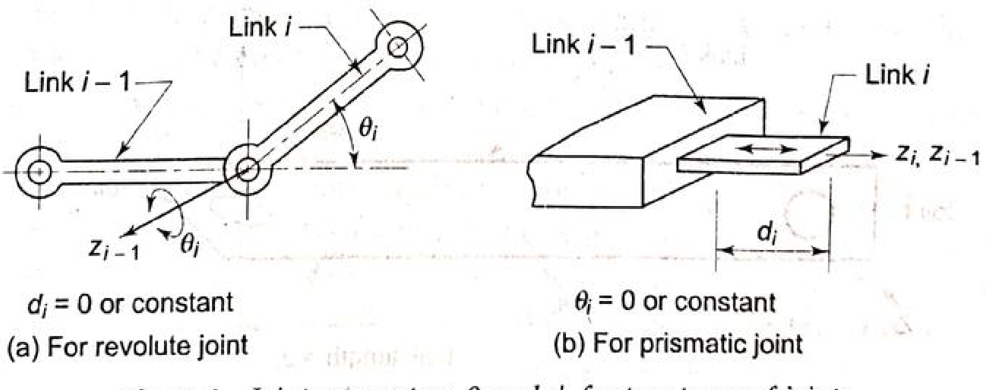

Fig. 3.6 *Joint parameters θ_i and d_i for two types of joints*

For a revolute joint, d_i is zero or constant and θ_i varies, while for a prismatic joint θ_i is zero or constant and d_i varies, describing the relative position of links. The varying parameter is known as *joint variable* and a generalized parameter q is used to denote the joint displacement (variable) of either type of joint. The generalized joint displacement variable is defined as

$$q_i = \begin{cases} \theta_i, & \text{if joint } i \text{ is revolute} \\ d_i, & \text{if joint } i \text{ is prismatic.} \end{cases} \tag{3.1}$$

3.3 KINEMATIC MODELING OF THE MANIPULATOR

With the definition of fixed and variable kinematic parameters for each link, kinematic models can be defined. This model is the analytical description of the spatial geometry of motion of the manipulator with respect to a fixed (inertial) reference frame, as a function of time. In particular, the relation between the joint-variables and the position and orientation of the end-effector is the kinematic model. It is required to control position and orientation of the end-effector, in 3-D space, so that it can follow a defined trajectory or manipulate objects in the workspace. The kinematic modeling problem is split into two problems as:

1. Given the set of joint-link parameters, the problem of finding the position and orientation of the end-effector with respect to a known (immobile or inertial) reference frame for an n-DOF manipulator is the first problem.
   This is referred to as *direct (or forward) kinematic model* or *direct kinematics*. This model gives the position and orientation of the end-effector as a function of the joint variables and other joint-link constant parameters.
2. For a given position and orientation of the end-effector (of the n-DOF manipulator), with respect to an immobile or inertial reference frame, it is required to find a set of joint variables that would bring the end-effector in the specified position and orientation.
   This is the second problem and is referred to as the *inverse kinematic model* or *inverse kinematics*.

The problem of manipulator control requires both the direct and inverse kinematic models of the manipulator. The block diagram for both the models is illustrated in Fig. 3.7, wherein the commonality is the joint-link fixed and variable parameters. The task to be performed by a manipulator is stated in terms of the end-effector location in space. The values of joint variables required to accomplish the task are computed using the inverse kinematic model. To find the location of end-effector in space, at any instant of time, the joint variable values are substituted in the direct kinematic model. This chapter addresses the problem of formulation of direct kinematic model. The inverse kinematic model formulation will be discussed in the next chapter.

For kinematic modeling, frames are assigned to each link of the manipulator starting from the base to the end-effector. The homogeneous transformation matrices relating the frames attached to successive links describe the spatial relationship between adjacent links. The composition of these individual transform matrices determines the overall transform matrix, describing tool frame with respect to base frame.

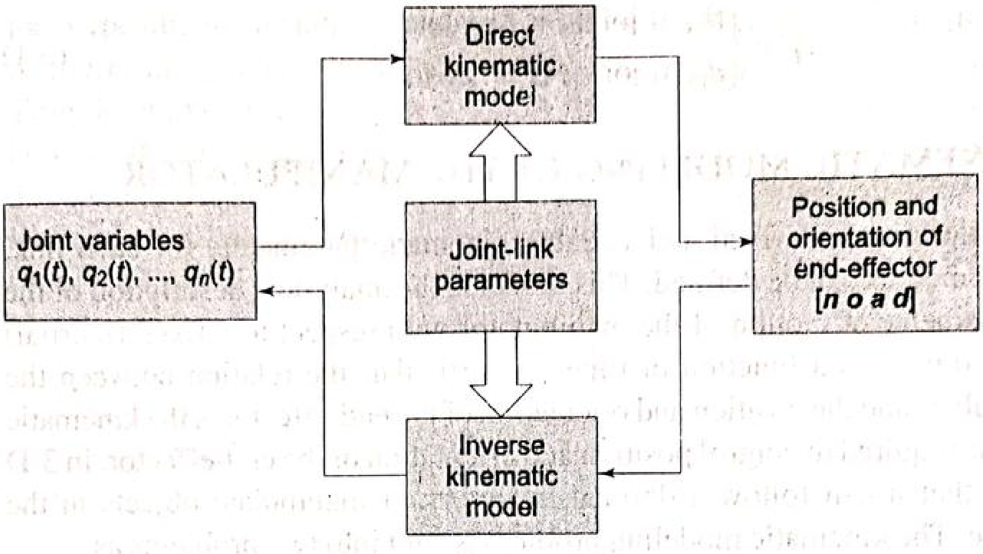

Fig. 3.7 *The direct and inverse kinematic models*

3.4 DENAVIT-HARTENBERG NOTATION

The definition of a manipulator with four joint-link parameters for each link and a systematic procedure for assigning right-handed orthonormal coordinate frames, one to each link in an open kinematic chain, was proposed by Denavit and Hartenberg (1955) and is known as *Denavit-Hartenberg (DH) notation*. This notation is presented in this section and followed throughout the text.

A frame $\{i\}$ is rigidly attached to distal end of link i and it moves with link i. An n-DOF manipulator will have $(n + 1)$ frames with the frame $\{0\}$ or base frame acting as the reference inertial frame and frame $\{n\}$ being the "*tool frame*".

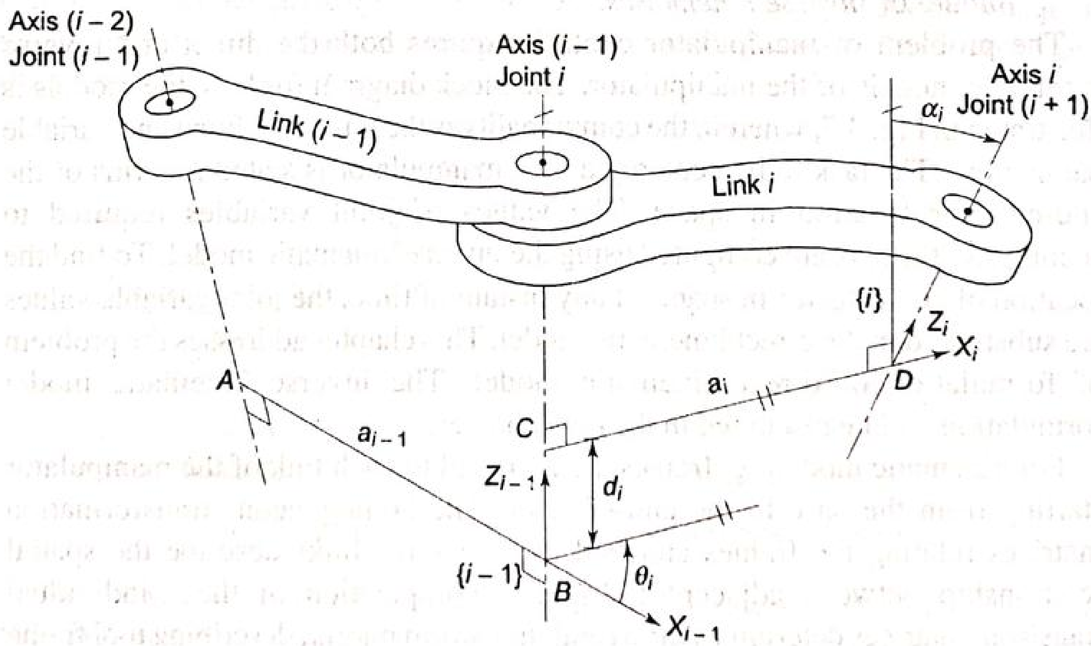

Fig. 3.8 *DH Convention for assigning frames to links and identifying joint-link parameters*

Figure 3.8 shows a pair of adjacent links, link $(i-1)$ and link i, their associated joints, joints $(i-1)$, i and $(i+1)$, and axes $(i-2)$, $(i-1)$, and i, respectively. Line AB, in the figure, is the common normal to $(i-2)$- and $(i-1)$-axes and line CD is the common normal to $(i-1)$- and i-axes. A frame $\{i\}$ is assigned to link i as follows:

(i) The z_i-axis is aligned with axis i, its direction being arbitrary. The choice of direction defines the positive sense of joint variable θ_i.

(ii) The x_i-axis is perpendicular to axis z_{i-1} and z_i and points away from axis z_{i-1}, that is, x_i-axis is directed along the common normal CD.

(iii) The origin of the i^{th} coordinate frame, frame $\{i\}$, is located at the intersection of axis of joint $(i+1)$, that is, axis i, and the common normal between axes $(i-1)$ and i (common normal is CD), as shown in the figure.

(iv) Finally, y_i-axis completes the right-hand orthonormal coordinate frame $\{i\}$.

Note that the frame $\{i\}$ for link i is at the distal end of link i and moves with the link.

With respect to frame $\{i-1\}$ and frame $\{i\}$, the four DH-parameters — two link parameters (a_i, α_i) and two joint parameters (d_i, θ_i) — are defined as:

(a) Link Length (a_i) — distance measured along x_i-axis from the point of intersection of x_i-axis with z_{i-1}-axis (point C) to the origin of frame $\{i\}$, that is, distance CD.

(b) Link twist (α_i) — angle between z_{i-1}- and z_i-axes measured about x_i-axis in the right-hand sense.

(c) Joint distance (d_i) — distance measured along z_{i-1}-axis from the origin of frame $\{i-1\}$ (point B) to the intersection of x_i- axis with z_{i-1}-axis (point C), that is, distance BC.

(d) Joint angle (θ_i) — angle between x_{i-1}- and x_i-axes measured about the z_{i-1}-axis in the right-hand sense.

The convention outlined above does not result in a unique attachment of frames to links because alternative choices are available. For example, joint axis i has two choices of direction to point z_i-axis, one pointing upward (as in Fig. 3.8) and other pointing downward. To minimize such options and get a consistent set of frames, an algorithm is presented below to assign frames to all links of a manipulator.

Algorithm 3.1 ➢ Link Frame Assignment

This algorithm assigns frames and determines the DH-parameters for each link of an n-DOF manipulator. Both, the first link 0 and the last link n, are connected to only one other link and, thus, have more arbitrariness in frame assignment. For this reason, the first (frame $\{0\}$) and the last (frame $\{n\}$) frames are assigned after assigning frames to intermediate links, link 1 to link $(n-1)$.

The displacement of each joint-link is measured with respect to a frame, therefore the *zero position* of each link needs to be clearly defined. The zero position for a revolute joint is when the joint angle θ is zero, while for a prismatic joint it is when the joint displacement is minimal; it may or may not be zero. When all the joints are in zero position, the manipulator is said to be in *home position.* Thus, the home position of an n-DOF manipulator is the position where the $n \times 1$ vector of joint variables is equal to the zero vector, that is, $q_i = 0$ for $i = 1, 2, \ldots, n$. Before assigning frames, the zero position of each joint, that is, the home position of the manipulator must be decided. The frames are then assigned imagining the manipulator in home position.

Because of mechanical constraints, the range of joint motion possible is restricted and, in some cases, this may result in a home position that is unreachable. In such cases, the home position is redefined by changing the initial manipulator joint positions and/or frame assignments. The new home position can be obtained by adding a constant value to the joint angle in case of revolute joint and to the joint displacement in case of prismatic joint. This shifting of the home position is illustrated in Example 3.3.

The algorithm is divided into four parts. The first segment gives steps for labelling scheme and the second one describes the steps for frame assignment to intermediate links 1 to (n–1). The third and fourth segments give steps for frame {0} and frame {n} assignment, respectively.

Step 0 Identify and number the joints starting with base and ending with end-effector. Number the links from 0 to n starting with immobile base as 0 and ending with last link as n.

Step 1 Align axis z_i with axis of joint (i+1) for $i = 0, 1, \ldots, n-1$.

Assigning frames to intermediate links – link 1 to link **(n–1)** For each link i repeat steps 2 and 3.

Step 2 The x_i-axis is fixed perpendicular to both z_{i-1}- and z_i-axes and points away from z_{i-1}. The origin of frame {i} is located at the intersection of z_i- and x_i-axes. Three situations are possible:

Case (i) If z_{i-1}- and z_i-axes intersect, choose the origin at the point of their intersection. The x_i-axis will be perpendicular to the plane containing z_{i-1}- and z_i-axes. This will give a_i to be zero.

Case (ii) If z_{i-1}- and z_i-axes are parallel or lie in parallel planes then their common normal is not uniquely defined. If joint i is revolute then x_i-axis is chosen along that common normal, which passes through origin of frame {i–1}. This will fix the origin and make d_i zero. If joint i is prismatic, x_i-axis is arbitrarily chosen as any convenient common normal and the origin is located at the distal end of the link i.

Case (iii) If z_{i-1}- and z_i-axes coincide, the origin lies on the common axis. If joint i is revolute, origin is located to coincide with origin of frame {i–1} and x_i-axis coincides with x_{i-1}-axis to cause d_i to be zero. If joint i is prismatic, x_i-axis is chosen parallel to x_{i-1}-axis to make a_i to be zero. The origin is located at distal end of link i.

Step 3 The y_i-axis has no choice and is fixed to complete the right-handed orthonormal coordinate frame {i}.

Assigning frame to link 0, the immobile base – frame {0}

Step 4 The frame {0} location is arbitrary. Its choice is made based on simplification of the model and some convenient reference in workspace. The x_0-axis, which is perpendicular to z_0-axis, is chosen to be parallel to x_1-axis in the home position to make $\theta_1 = 0$. The origin of frame {0} is located based on type of joint 1. If joint 1 is revolute, the origin of frame {0} can be chosen at a convenient reference such as, floor, work table, and so on, giving a constant value for parameter d_1 or at a suitable location along axis of joint 1 so as to make d_1 zero. If joint 1 is prismatic, parallel x_0- and x_1-axes will make θ_1 to be zero and origin of frame {0} is placed arbitrarily.

Step 5 The y_0-axis completes the right-handed orthonormal coordinate frame {0}.

Link n, the end-effector, frame assignment – frame {n}

Step 6 The origin of frame $\{n\}$ is chosen at the tip of the manipulator, that is, a convenient point on the last link (the end-effector). This point is called the "tool point" and the frame $\{n\}$ is the tool frame.

Step 7 The z_n-axis is fixed along the direction of z_{n-1}-axis and pointing away from the link n. It is the direction of "approach."

Step 8 If joint n is prismatic, take x_n parallel to x_{n-1}-axis. If joint n is revolute, the choice of x_n is similar to step 4, that is, x_n is perpendicular to both z_{n-1}- and z_n-axes. x_n direction is the "normal" direction. The y_n-axis is chosen to complete the right-handed orthonormal frame $\{n\}$. The y_n-axis is the "orientation" or "sliding" direction.

Once the frames are assigned to each link, the joint-link parameters (θ_i, d_i, α_i, a_i) can be easily identified for each link, using which the direct kinematic model is developed in the next section.

In fixing the frames, it is desirable to make as many of the joint-link parameters zero as possible because the amount of computations necessary in later analysis is dependent on these. Hence, whenever there is a choice in frame assignment, emphasis is on making a choice, which results in as many zero parameters as possible.

3.5 KINEMATIC RELATIONSHIP BETWEEN ADJACENT LINKS

To find the transformation matrix relating two frames attached to the adjacent links, consider frame $\{i-1\}$ and frame $\{i\}$ as shown in Fig. 3.9. These two frame are associated with link $(i-1)$ and i but for clarity the links are not shown in the figure. The kinematic joint-link parameters involved (θ_i, d_i, α_i, a_i) are shown therein. Points B, C, D and frame $\{i-1\}$ and $\{i\}$ are the same as in Fig. 3.8.

The transformation of frame $\{i-1\}$ to frame $\{i\}$ consists of four basic transformations as shown in Fig. 3.9.

(a) A rotation about z_{i-1}-axis by an angle θ_i;
(b) Translation along z_{i-1}-axis by distance d_i;
(c) Translation by distance α_i along x_i-axis, and
(d) Rotation by an angle α_i about x_i-axis.

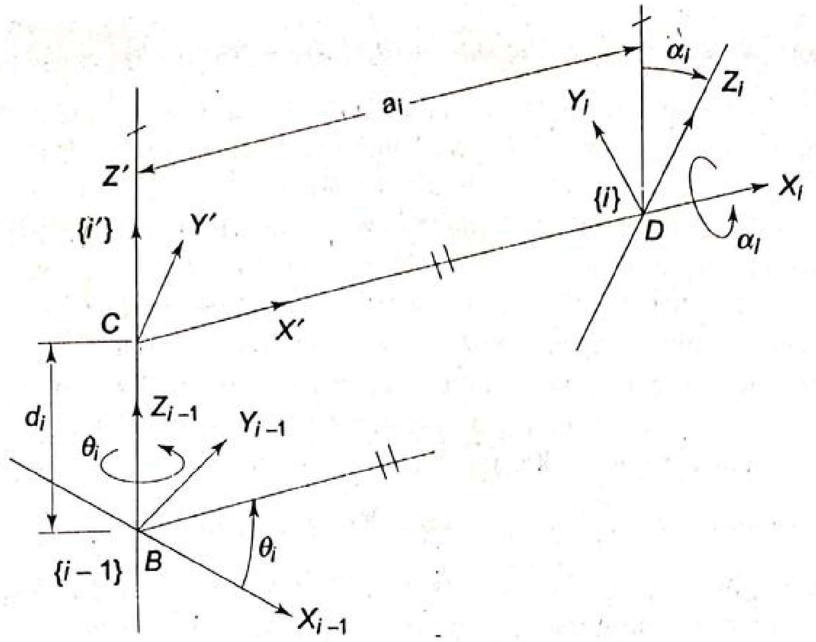

Fig. 3.9 *Geometric relationship between adjacent links*

Using the spatial coordinate transformations discussed in Chapter 2, the composite transformation matrix, which describes frame $\{i\}$ with respect to frame $\{i-1\}$, is obtained using Eq. (2.46) as

$$^{i-1}\boldsymbol{T}_i = \boldsymbol{T}_z(\theta_i)\boldsymbol{T}_z(d_i)\boldsymbol{T}_x(a_i)\boldsymbol{T}_x(\alpha_i) \tag{3.2}$$

From Eqs. (2.20), (2.54), and (2.55),

$$^{i-1}\boldsymbol{T}_i = \begin{bmatrix} C\theta_i & -S\theta_i & 0 & 0 \\ S\theta_i & C\theta_i & 0 & 0 \\ 0 & 0 & 1 & 0 \\ 0 & 0 & 0 & 1 \end{bmatrix} \begin{bmatrix} 1 & 0 & 0 & 0 \\ 0 & 1 & 0 & 0 \\ 0 & 0 & 1 & d_i \\ 0 & 0 & 0 & 1 \end{bmatrix} \begin{bmatrix} 1 & 0 & 0 & a_i \\ 0 & 1 & 0 & 0 \\ 0 & 0 & 1 & 0 \\ 0 & 0 & 0 & 1 \end{bmatrix} \begin{bmatrix} 1 & 0 & 0 & 0 \\ 0 & C\alpha_i & -S\alpha_i & 0 \\ 0 & S\alpha_i & C\alpha_i & 0 \\ 0 & 0 & 0 & 1 \end{bmatrix}$$

or

$$^{i-1}\boldsymbol{T}_i = \begin{bmatrix} C\theta_i & -S\theta_i C\alpha_i & S\theta_i S\alpha_i & a_i C\theta_i \\ S\theta_i & C\theta_i C\alpha_i & -C\theta_i S\alpha_i & a_i S\theta_i \\ 0 & S\alpha_i & C\alpha_i & d_i \\ 0 & 0 & 0 & 1 \end{bmatrix} \tag{3.3}$$

where $C\theta_i = \cos\theta_i$, $S\theta_i = \sin\theta_i$, $C\alpha_i = \cos\alpha_i$, and $S\alpha_i = \sin\alpha_i$.

The transformation from frame $\{i-1\}$ to frame $\{i\}$ can also be obtained by considering an intermediate coordinate frame $\{i'\}$ located at point C, as shown in Fig. 3.9. From the figure, the transformation from frame $\{i\}$ to frame $\{i'\}$ consists of a rotation and a translation about x_i-axis and the transformation from frame $\{i'\}$ to frame $\{i-1\}$ consists of a rotation and a translation about z_{i-1}-axis. The two homogeneous transformations are:

$$^{i'}\boldsymbol{T}_i = \begin{bmatrix} 1 & 0 & 0 & a_i \\ 0 & C\alpha_i & -S\alpha_i & 0 \\ 0 & S\alpha_i & C\alpha_i & 0 \\ 0 & 0 & 0 & 1 \end{bmatrix}$$

$$ {}^{i-1}\boldsymbol{T}_{i'} = \begin{bmatrix} C\theta_i & -S\theta_i & 0 & 0 \\ S\theta_i & C\theta_i & 0 & 0 \\ 0 & 0 & 1 & d_i \\ 0 & 0 & 0 & 1 \end{bmatrix} \tag{3.4} $$

The composite transformation from frame $\{i\}$ to frame $\{i-1\}$ is, thus, obtained as

$$ {}^{i-1}\boldsymbol{T}_i = {}^{i-1}\boldsymbol{T}_{i'}\,{}^{i'}\boldsymbol{T}_i $$

Substituting from Eq. (3.4) gives the basic link transformation matrix as:

$$ {}^{i-1}\boldsymbol{T}_i = \left[\begin{array}{ccc:c} C\theta_i & -S\theta_i C\alpha_i & S\theta_i S\alpha_i & a_i C\theta_i \\ S\theta_i & C\theta_i C\alpha_i & -C\theta_i S\alpha_i & a_i S\theta_i \\ 0 & S\alpha_i & C\alpha_i & d_i \\ \hdashline 0 & 0 & 0 & 1 \end{array}\right] \tag{3.5} $$

This is identical to Eq. (3.3) as it should be. This is an important result for modeling manipulators.

The homogeneous transformation matrix ${}^{i-1}\boldsymbol{T}_i$ describes the position and orientation of frame $\{i\}$ relative to frame $\{i-1\}$ and completely specifies the geometric relationship between these links in terms of four DH-parameters (θ_i, d_i α_i a_i). Of these four parameters, only one is a variable for link i, the displacement variable q_i (θ_i or d_i) and other three are constant. The matrix ${}^{i-1}\boldsymbol{T}_i(q_i)$ is known as link i transformation matrix. As shown before, the 3×3 upper left corner submatrix of Eq. (3.5) gives the orientation of coordinate axes of frame $\{i\}$, while the 3×1 upper right corner sub-matrix represents the position of the origin of frame $\{i\}$.

3.6 MANIPULATOR TRANSFORMATION MATRIX

In this section, the last step in formulating the forward kinematic model of a manipulator is discussed. This model describes position and orientation of the last link (tool frame) with reference to the base frame as a function of joint displacements q_1 through q_n. An n-DOF manipulator consists of $(n+1)$ links from base to tool point and a frame is assigned to each link. Figure 3.10 shows the $(n+1)$ frames, frame $\{0\}$ to frame $\{n\}$, attached to the links of the manipulator.

The position and orientation of the tool frame relative to the base frame can be found by considering the n consecutive link transformation matrices relating frames fixed to adjacent links. Thus,

$$ {}^{0}\boldsymbol{T}_n = {}^{0}\boldsymbol{T}_1(q_1)\,{}^{1}\boldsymbol{T}_2(q_2) \ldots {}^{n-1}\boldsymbol{T}_n(q_n) \tag{3.6} $$

where ${}^{i-1}\boldsymbol{T}_i(q_i)$ for $i = 1, 2, \ldots, n$ is the homogeneous link transformations matrix between frames $\{i-1\}$ and $\{i\}$ and is given by Eq. (3.5).

The tool frame, frame $\{n\}$, can also be considered as a translated and rotated frame with respect to base frame $\{0\}$. The transformation between these two frames is denoted by end-effector transformation matrix $\boldsymbol{T}$, Eq. (2.31), in terms of

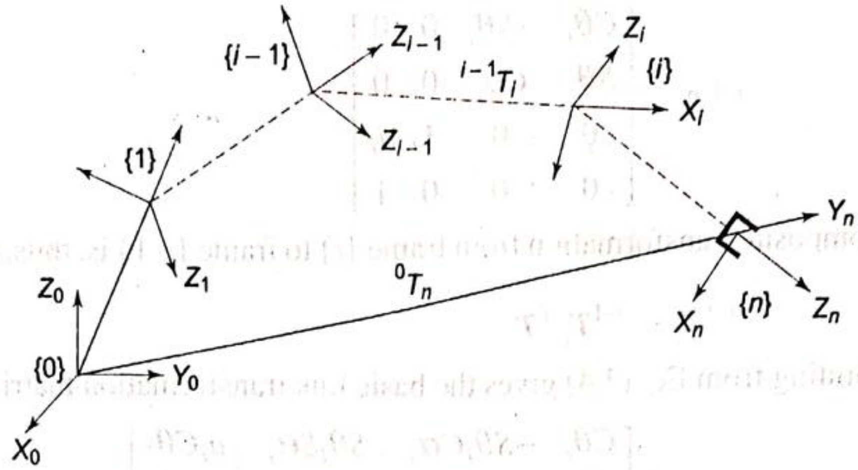

Fig 3.10 *Location of end-effector frame relative to base frame*

tool frame orientation ($\boldsymbol{n}, \boldsymbol{o}, \boldsymbol{a}$) and its displacement ($\boldsymbol{d}$) from the base frame $\{0\}$. In Fig. 3.10, frame $\{n\}$ is the tool frame, thus, $\boldsymbol{T}$ is equal to $^0\boldsymbol{T}_n$, or

$$\boldsymbol{T} = {}^0\boldsymbol{T}_n = {}^0\boldsymbol{T}_1\, {}^1\boldsymbol{T}_2 \ldots {}^{n-1}\boldsymbol{T}_n \tag{3.7}$$

Equation (3.7) is known as the kinematic model of the n-DOF manipulator. It provides the functional relationship between the tool frame (or end-effector) position and orientation and displacement of each link q_i, which may be angular or linear, depending on joint being revolute or prismatic. That is,

$$\boldsymbol{T} = f\,(q_i), \quad i = 1, 2, \ldots, n \tag{3.8}$$

or

$$\begin{bmatrix} n_x & o_x & a_x & d_x \\ n_y & o_y & a_y & d_y \\ n_z & o_z & a_z & d_z \\ 0 & 0 & 0 & 1 \end{bmatrix} = \begin{bmatrix} r_{11} & r_{12} & r_{13} & r_{14} \\ r_{21} & r_{22} & r_{23} & r_{24} \\ r_{31} & r_{32} & r_{33} & r_{34} \\ 0 & 0 & 0 & 1 \end{bmatrix} \tag{3.9}$$

where coefficient r_{ij} are functions of joint displacements q_i. For the known joint displacements q_i for $i = 1, 2, \ldots, n$, the end-effector orientation ($\boldsymbol{n\ o\ a}$) and position $\boldsymbol{d}$ can be computed from Eq. (3.8).

Several examples are now worked out to clarify the concepts of the direct kinematic modeling. The first example is a simple one, a 2-DOF manipulator, the others are of some common configurations of manipulator arm and wrist, and the last example illustrates the kinematic modeling of a 6-DOF industrial manipulator.

SOLVED EXAMPLES

Example 3.1 *A 2-DOF planar manipulator arm*

Obtain the position and orientation of the tool point P with respect to the base for the 2-DOF, RP planar manipulator shown in Fig. 3.11.

Solution The formulation of direct kinematic model of the manipulator begins with the study of its mechanical structure and identification of the links and joints. The frames are then assigned using Algorithm 3.1. This example is a simple one and illustrates the basic steps involved in formulation of kinematic model.

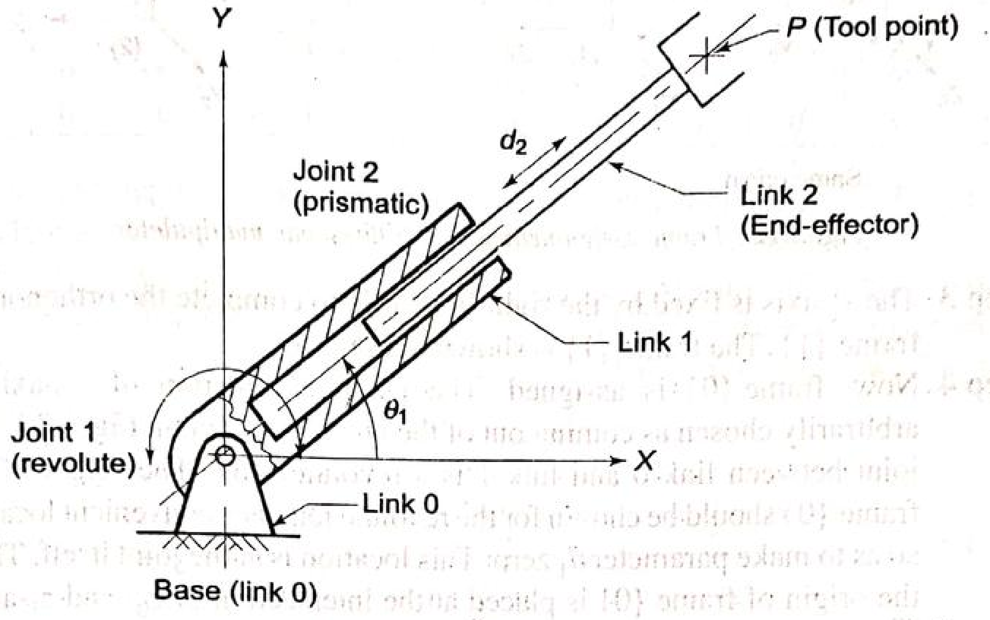

Fig. 3.11 *A 2-DOF planar manipulator arm with one rotary and one prismatic joint*

The planar configuration of this manipulator can be employed to manipulate objects within a plane, the *xy*-plane. The first joint is a revolute joint and the second one is prismatic. It is easy to see that it has a circular area as workspace. The size of the two links determines the radius of inner and outer circles of the workspace area. Point P may or may not traverse a full circle, depending on the mechanical design of joint and joint range available at joint 1.

The axis of joint 1 is perpendicular to the plane of workspace, while axis of joint 2 lies in the plane. The two joint axes intersect each other. The home position is considered as the horizontal position ($\theta_1 = 0$) and prismatic link completely retracted in, corresponding to radius of inner boundary of workspace. The step-by-step frame assignment is carried out, according to Algorithm 3.1, as explained below.

Step 0 The two joints are numbered as 1 and 2 and links as 0, 1, and 2 starting with the immobile base as 0.

Step 1 Joint axes z_0 and z_1 are aligned with the axes of joint 1 and 2, respectively.

The joint-link labelling and joint axes are shown in Figs. 3.11 and 3.12. Frames are assigned to intermediate links first, and then to the first and last links. In this example, there is only one intermediate link, link 1.

Step 2 For frame {1} of link 1, the z_1-axis is fixed in step 1 above. Because z_0- and z_1-axes intersect, the origin of frame {1} is fixed at the point of their intersection, according to Step 2 case (i) of the Algorithm 3.1. The x_1-axis is set in the direction of perpendicular to plane containing z_0- and

z_1-axes. Note that α_1, d_1, and a_1 will be defined after frame {0} is fixed. The variable parameter for this is θ_1.

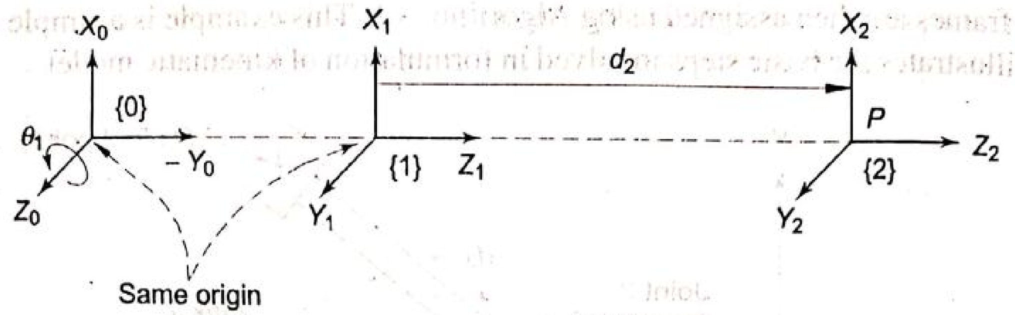

Fig. 3.12 *Frame assignment for 2-DOF planar manipulator*

Step 3 The y_1-axis is fixed by the right-hand rule to complete the orthonormal frame {1}. The frame {1} is shown in Fig. 3.12.

Step 4 Now, frame {0} is assigned. The positive direction of z_0-axis is arbitrarily chosen as coming out of the page, as shown in Fig. 3.12. The joint between link 0 and link 1 is a revolute joint. The origin of the frame {0} should be chosen for the revolute joint at a convenient location so as to make parameter d_1 zero. This location is at the joint itself. Thus, the origin of frame {0} is placed at the intersection of z_0- and z_1-axes. This is also situated the origin of frame {1} or two origins coincide giving $a_1 = 0$, and $d_1 = 0$. The x_0-axis is chosen parallel to x_1-axis, and it coincides with x_1-axis. The rotation of z_0-axis to z_1-axes about x_1-axis defines the twist angle α_1 as 90°. Thus, the choice of frame {0} and {1} defines parameters as $\alpha_1 = 90°$, $a_1 = 0$ and $d_1 = 0$.

Step 5 The y-axis is fixed to complete the orthonormal frame {0}.

Step 6 The origin frame {2}, the last frame, is fixed to the tool point P of the last link (the end-effector). The choice of this origin defines the joint variable d_2 as distance measured from origin of frame {1}.

Step 7 The direction of z_2-axis is chosen to be same as z_1-axis pointing away from link 2.

Step 8 Joint 2 is prismatic and, hence, x_2-axis is chosen to be parallel to x_1-axis. The y_2-axis is fixed to complete the frame {2}. Once the frame {2} is defined, the parameters get the values as: $a_2 = 0$, $\alpha_2 = 0$, and $\theta_2 = 0$.

The complete frame assignment is shown in Fig. 3.12. The coinciding frames, frame {0} and frame {1} are drawn away from each other for clarity but marked as "same origin" and there is zero distance between their origins.

The assigned frames define the four DH-parameters for each link so as to completely specify the geometric structure of the given manipulator. The joint-link parameters are tabulated in Table 3.1. For each link, the displacement variable q_i is identified and placed in the displacement variable column. It is important to note that each row of the joint-link parameter table has exactly one variable and there is no row without a variable. Any deviation from these conditions indicates an error in frame assignment and/or joint-link parameter identification. Note that out of six constant joint-link parameters, five are zero and the sixth is 90°. The two displacement variables are θ_1 and d_2.

Table 3.1 *Joint-link parameters for the RP manipulator arm*

Link i	a_i	α_i	d_i	θ_i	Displacement Variable q_i	$C\theta_i$	$S\theta_i$	$C\alpha_i$	$S\alpha_i$
1	0	90°	0	θ_1	θ_1	C_1	S_1	0	1
2	0	0	d_2	0	d_2	1	0	1	0

The next step is to obtain the individual transformation matrices ${}^0T_1$ and ${}^1T_2$ for relating successive links. These are obtained by substituting the values of the joint-link parameters in Eq. (3.5). To facilitate writing of transformation matrices, four columns defining cos θ_i, sin θ_i, cos α_i, and sin α_i are appended to the joint-link parameter table and values are filled in for each row. The two transformation matrices are, therefore,

$$ {}^0T_1(\theta_1) = \begin{bmatrix} C_1 & 0 & S_1 & 0 \\ S_1 & 0 & -C_1 & 0 \\ 0 & 1 & 0 & 0 \\ 0 & 0 & 0 & 1 \end{bmatrix} \tag{3.10} $$

$$ {}^1T_2(d_2) = \begin{bmatrix} 1 & 0 & 0 & 0 \\ 0 & 1 & 0 & 0 \\ 0 & 0 & 1 & d_2 \\ 0 & 0 & 0 & 1 \end{bmatrix} \tag{3.11} $$

Each of the above transformation matrices is a function of only one variable, the displacement variable for the link. Finally, The forward kinematic model is obtained by combining the individual transform matrices. Thus, ${}^0T_2$ the transformation of tool frame, frame {2}, with respect to base frame, frame {0} is obtained by substituting individual matrices, Eqs. (3.10) and (3.11) in Eq. (3.6). The final result after simplifying is:

$$ {}^0T_2 = {}^0T_1\,{}^1T_2 = \begin{bmatrix} C_1 & 0 & S_1 & d_2S_1 \\ S_1 & 0 & -C_1 & -d_2C_1 \\ 0 & 1 & 0 & 0 \\ 0 & 0 & 0 & 1 \end{bmatrix} \tag{3.12} $$

This overall transformation, Eq. (3.12), is equal to the end-effector transformation matrix, Eq. (2.31), and the direct kinematic model in matrix form is:

$$ \begin{bmatrix} n_x & o_x & a_x & d_x \\ n_y & o_y & a_y & d_y \\ n_z & o_z & a_z & d_z \\ 0 & 0 & 0 & 1 \end{bmatrix} = \begin{bmatrix} C_1 & 0 & S_1 & d_2S_1 \\ S_1 & 0 & -C_1 & -d_2C_1 \\ 0 & 1 & 0 & 0 \\ 0 & 0 & 0 & 1 \end{bmatrix} \tag{3.13} $$

This kinematic model can also be expressed by 12 equations as:

$$
\begin{aligned}
n_x &= C_1 \\
n_y &= S_1 \\
n_z &= 0 \\
o_x &= 0 \\
o_y &= 0 \\
o_z &= 1 \\
a_x &= S_1 \\
a_y &= -C_1 \\
a_z &= 0 \\
d_x &= d_2 S_1 \\
d_y &= -d_2 C_1 \\
d_z &= 0
\end{aligned} \tag{3.14}
$$

From Eq. (3.13) or Eq. (3.14), the orientation and position of the tool point P can be computed for given values of displacement variables θ_1 and d_2 at any instant of time. For example, for $\theta_1 = 120°$ and $d_2 = 200$ mm the end-effector transformation matrix will be

$$
T_E = \begin{bmatrix} -0.5 & 0 & 0.866 & 173.2 \\ 0.866 & 0 & 0.5 & 100.0 \\ 0 & 1 & 0 & 0 \\ 0 & 0 & 0 & 1 \end{bmatrix}
$$

It is assumed that θ_1 and d_2 chosen above are within the available range of joint motions.

Example 3.2 *Kinematic model of a cylindrical arm*

Formulate the forward kinematic model of the three-degree of freedom (RPP) manipulator arm shown in Fig. 3.13.

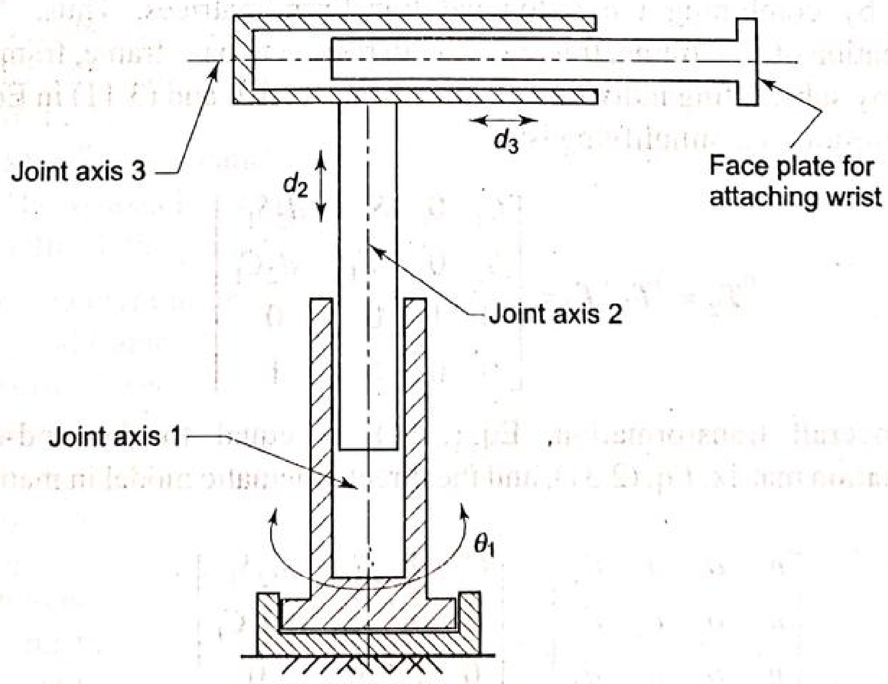

Fig. 3.13 *Mechanical structure of a 3-DOF cylindrical (RPP) manipulator arm*

Solution The cylindrical configuration manipulator arm has three joints—the first joint is revolute, while the next two are prismatic. The axes of the first two joints coincide. This configuration has a cylindrical workspace as discussed in Chapter 1.

As in the previous example, begin with fixing home position, labelling links, joints and assigning frames using Algorithm 3.1. The details of step-by-step frame assignment are left for the reader. The final frame assignment is shown in Fig. 3.14.

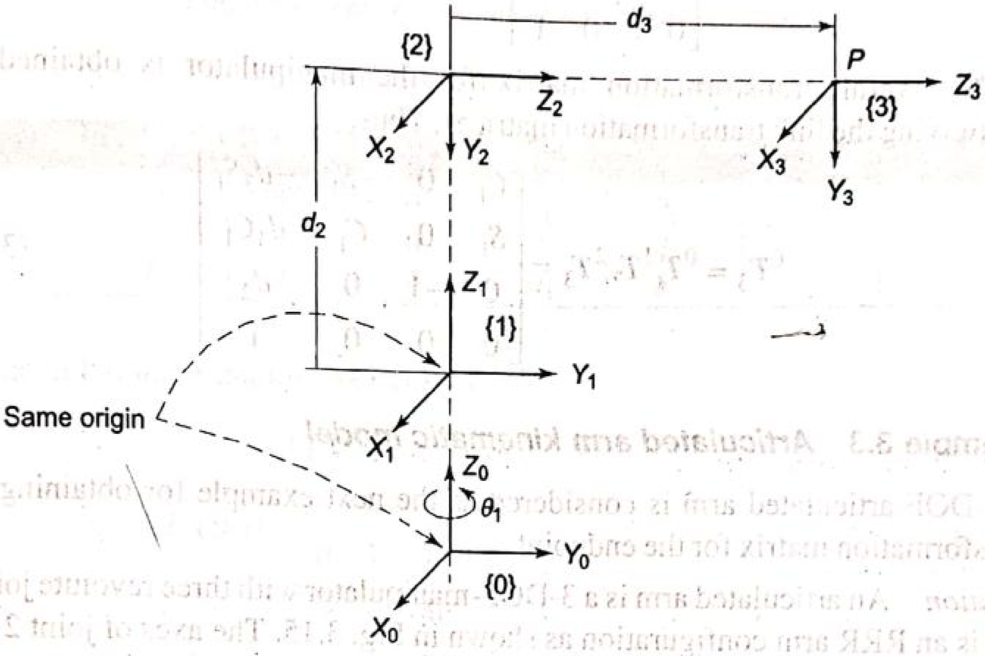

Fig. 3.14 *Frame assignment for the cylindrical manipulator arm*

Next, the joint-link parameters are identified and these are tabulated in Table 3.2.

Table 3.2 *Joint-link parameters for the RPP manipulator arm*

Link i	a_i	α_i	d_i	θ_i	q_i	$C\theta_i$	$S\theta_i$	$C\alpha_i$	$S\alpha_i$
1	0	0	0	θ_1	θ_1	C_1	S_1	1	0
2	0	–90°	d_2	0	d_2	1	0	0	–1
3	0	0	d_3	0	d_3	1	0	1	0

The transformation matrices for transformation of each link (frame) with respect to the previous one is obtained as:

$$ {}^0T_1(\theta_1) = \begin{bmatrix} C_1 & -S_1 & 0 & 0 \\ S_1 & C_1 & 0 & 0 \\ 0 & 0 & 1 & 0 \\ 0 & 0 & 0 & 1 \end{bmatrix} \tag{3.15} $$

$$ {}^1T_2(d_2) = \begin{bmatrix} 1 & 0 & 0 & 0 \\ 0 & 0 & 1 & 0 \\ 0 & -1 & 0 & d_2 \\ 0 & 0 & 0 & 1 \end{bmatrix} \tag{3.16} $$

$$ {}^2T_3(d_3) = \begin{bmatrix} 1 & 0 & 0 & 0 \\ 0 & 1 & 0 & 0 \\ 0 & 0 & 1 & d_3 \\ 0 & 0 & 0 & 1 \end{bmatrix} \tag{3.17} $$

The overall transformation matrix for the manipulator is obtained by multiplying the link transformation matrices. Thus,

$$ {}^0T_3 = {}^0T_1\,{}^1T_2\,{}^2T_3 = \begin{bmatrix} C_1 & 0 & -S_1 & -d_3S_1 \\ S_1 & 0 & C_1 & d_3C_1 \\ 0 & -1 & 0 & d_2 \\ 0 & 0 & 0 & 1 \end{bmatrix} \tag{3.18} $$

Example 3.3 *Articulated arm kinematic model*

A 3-DOF articulated arm is considered as the next example for obtaining the transformation matrix for the endpoint.

Solution An articulated arm is a 3-DOF-manipulator with three revolute joints, that is an RRR arm configuration as shown in Fig. 3.15. The axes of joint 2 and joint 3 are parallel and axis of joint 1 is perpendicular to these two. At the end of the arm, a faceplate is provided to attach the wrist.

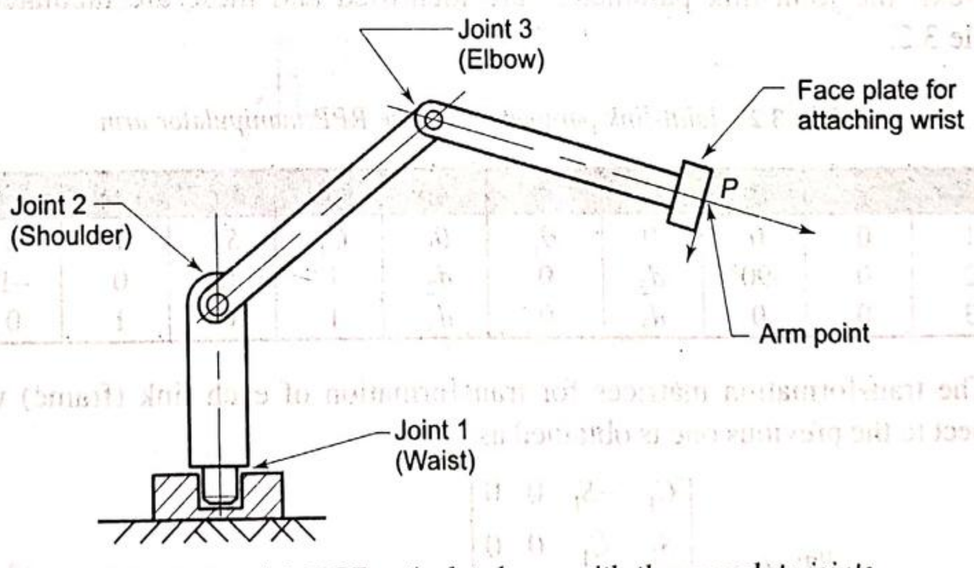

Fig. 3.15 *A 3-DOF articulated arm with three revolute joints*

To determine the "arm point" transformation matrix, the frames are assigned first as shown in Fig. 3.16. The resulting joint-link parameters are tabulated in Table 3.3. For all the three joints, joint-offsets are assumed to be zero.

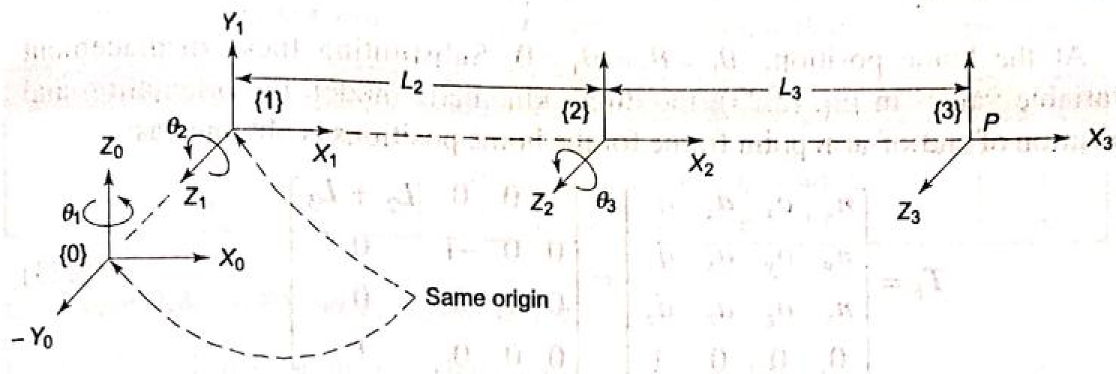

Fig. 3.16 *Frame assignment for articulated arm*

Table 3.3 *Joint-link parameters for articulated arm*

Link i	a_i	α_i	d_i	θ_i	q_i	$C\alpha_i$	$S\alpha_i$
1	0	90°	0	θ_1	θ_1	0	1
2	L_2	0	0	θ_2	θ_2	1	0
3	L_3	0	0	θ_3	θ_3	1	0

The link transformation matrices are

$$^0T_1(\theta_1) = \begin{bmatrix} C_1 & 0 & S_1 & 0 \\ S_1 & 0 & -C_1 & 0 \\ 0 & 1 & 0 & 0 \\ 0 & 0 & 0 & 1 \end{bmatrix} \tag{3.19}$$

$$^1T_2(\theta_2) = \begin{bmatrix} C_2 & -S_2 & 0 & L_2C_2 \\ S_2 & C_2 & 0 & L_2S_2 \\ 0 & 0 & 1 & 0 \\ 0 & 0 & 0 & 1 \end{bmatrix} \tag{3.20}$$

$$^2T_3(\theta_3) = \begin{bmatrix} C_3 & -S_3 & 0 & L_3C_3 \\ S_3 & C_3 & 0 & L_3S_3 \\ 0 & 0 & 1 & 0 \\ 0 & 0 & 0 & 1 \end{bmatrix} \tag{3.21}$$

The overall transformation matrix for the endpoint of the arm is, therefore,

$$^0T_1 = {^0T_1}\,{^1T_2}\,{^2T_3} = \begin{bmatrix} C_1C_{23} & -C_1S_{23} & S_1 & C_1(L_3C_{23} + L_2C_2) \\ S_1C_{23} & -S_1S_{23} & -C_1 & S_1(L_3C_{23} + L_2C_2) \\ S_{23} & C_{23} & 0 & L_3S_{23} + L_2S_2 \\ 0 & 0 & 0 & 1 \end{bmatrix} \tag{3.22}$$

where C_{23} and S_{23} refer to $\cos(\theta_2+\theta_3)$ and $\sin(\theta_2+\theta_3)$, respectively.

At the home position, $\theta_1 = \theta_2 = \theta_3 = 0$. Substituting these displacement variable values in Eq. (3.22), the direct kinematic model, the orientation and position of end-of-arm point frame for the home positions is obtained as:

$$T_E = \begin{bmatrix} n_x & o_x & a_x & d_x \\ n_y & o_y & a_y & d_y \\ n_z & o_z & a_z & d_z \\ 0 & 0 & 0 & 1 \end{bmatrix} = \begin{bmatrix} 1 & 0 & 0 & L_2 + L_3 \\ 0 & 0 & -1 & 0 \\ 0 & 1 & 0 & 0 \\ 0 & 0 & 0 & 1 \end{bmatrix} \quad (3.23)$$

From Eq. (3.23), it is observed that in the home position the arm point frame, frame {3}, has its x-axis (x_3-axis) in the same direction as x_0-axis, y_3-axis in the z_0-axis direction, and z_3-axis in the negative y_0-axis direction. The origin of frame {3} is translated by a distance of (L_2+L_3) in the x_0-axis direction. This means that if, initially frame {3} is coincident with frame {0}, its home position and orientation is obtained by translating the origin by (L_2+L_3) along x_0-axis and rotating it by +90° about x_0-axis. The position and orientation of frame {3} obtained from Eq. (3.23) matches with the coordinate system established in Fig. 3.16, verifying the correctness of the model obtained.

Home position of the articulated arm corresponding to the frame assigned in Fig. 3.16, that is, $\theta_1 = \theta_2 = \theta_3 = 0$, is drawn in Fig. 3.17(a). An alternate home position can be obtained by adding constant angles to θ_2 and θ_3. For example, if we added +90° to joint angle θ_2 and –90° to joint angle θ_3, the new home position is drawn in Fig. 3.17(b).

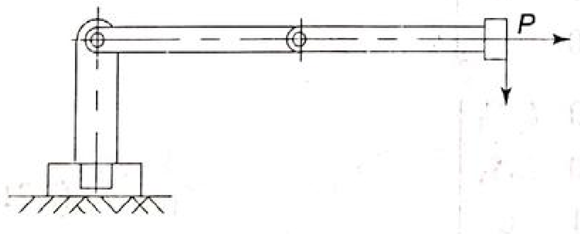

(a) Preferred home position

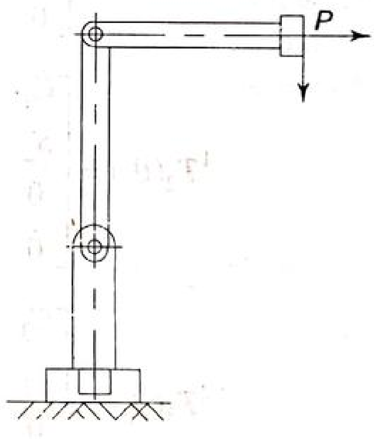

(b) Alternate home position

Fig. 3.17 *Two possible home positions for the articulated arm*

For this alternate home position of the manipulator the new joint displacements θ_2' and θ_3' are defined by adding +90° to joint angle θ_2 and –90° to joint angle θ_3, respectively.

Frame assignment and the kinematic model formulation for this new home position with displacement variables θ_1', θ_2', and θ_3' is left as an exercise for the reader. The joint-link parameters for this home position are tabulated in Table 3.4.

Table 3.4 *Joint-link parameters for the articulated arm with new home position*

[illegible]	[illegible]	[illegible]	[illegible]	[illegible]	[illegible]	[illegible]	[illegible]
1	0	90°	0	θ_1	$\theta'_1 = \theta_1$	0	1
2	L_2	0	0	θ'_2	$\theta'_2 = \theta_2 + 90°$	1	0
3	L_3	0	0	θ'_3	$\theta'_3 = \theta_3 - 90°$	1	0

Example 3.4 *RPY wrist kinematics*

For the 3-DOF roll-pitch-yaw (RPY) wrist shown in Fig. 3.18 obtain the direct kinematic model.

Solution The 3-DOF RPY wrist has three revolute (RRR) joints, which provide any arbitrary orientation to the end-effector in 3-D space.

To get the direct kinematic model, it is assumed that the arm end-point is stationary and can be considered as the stationary base frame, frame {0}, for the wrist.

The joints are labelled and joint axes are identified as shown in Fig. 3.18. Observe that for the "home position" shown in figure the axes of joint 1 and joint 2 are perpendicular to each other and intersect at joint 2. The axes of joint 2 and joint 3 are also mutually perpendicular but are in parallel planes. The three joint displacements θ_1, θ_2, and θ_3 are along three mutually perpendicular directions: roll, pitch, and yaw.

The frame assignment for the four frames, frames {0} to frame {3} is carried out next and is explained frame by frame in the paragraphs below.

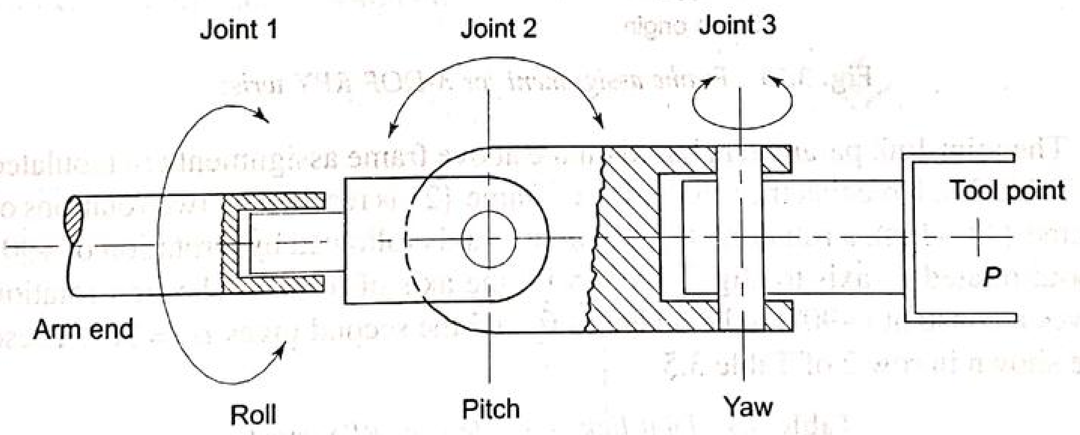

Fig. 3.18 *A 3-DOF freedom roll, pitch and yaw (RPY) wrist*

The frame {1} for link 1 is fixed with x_1-axis perpendicular to both z_0- and z_1-axes and its origin is fixed at joint 2, the point where axes z_0 and z_1 intersect, as per step 2(i) of Algorithm 3.1. For frame {3}, the axes z_1 and z_2 are perpendicular to each other but do not intersect as they lie in parallel planes. Because the joint is revolute, the common normal, which passes through origin of frame {1}, gives the direction of x_2-axis, as per step 2(ii) of Algorithm 3.1. The origin of frame {2} is fixed at the intersection of x_2- and z_2-axes and is located at origin of frame {1}, giving $a_2 = 0$ and $d_2 = 0$.

The base frame, frame {0} is fixed with its origin coinciding with origin of frame {1} and choosing x_0-axis parallel to x_1-axis to give $a_1 = 0$ and $d_1 = 0$. The physical distance between joint 1 and 2 can be accounted by increasing the size of last link of arm appropriately.

The origin of the last frame, frame {3}, is normally fixed to the tool point for convenience. If this is done, the distance between origins of frame {2} and frame {3}, corresponding to the size of the end-effector will be nonzero in the kinematic model. To simplify the kinematic model the origin of frame {3} can also be chosen to coincide with the origin of frame {2}, giving $a_3 = d_3 = 0$. The constant dimension of the end-effector can be accounted later by applying a constant translational transformation.

Now, the x_3- and z_3-axes of frame {3} are fixed to coincide with x_2- and z_3-axes. The complete frame assignment is shown in Fig. 3.19. Note that the origins of all four frames are coincident and that the orientation of frame{3}, the tool point frame is different from the conventional orientation where z-axis is taken in the approach direction.

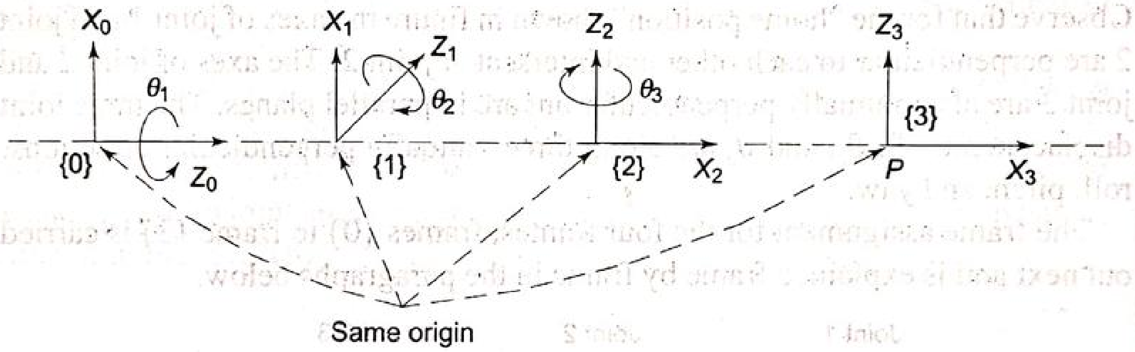

Fig. 3.19 *Frame assignment for 3-DOF RPY wrist*

The joint-link parameters based on the above frame assignment are tabulated in Table 3.5. Note that the orientation of frame {2} is reached by two rotations of frame {1} – first, a rotation of +90° about z_1-axis followed by a rotation of +90° about rotated x_1-axis to align z_2-axis with the axis of joint 3. The first rotation gives a constant (+90°) to be added to θ_2 and the second gives $\alpha_2 = 90°$. These are shown in row 2 of Table 3.5.

Table 3.5 *Joint-link parameters for RPY wrist*

Link i	a_i	α_i	d_i	θ_i	q_i	$C\theta_i$	$S\theta_i$	$C\alpha_i$	$S\alpha_i$
1	0	90°	0	θ_1	θ_1	C_1	S_1	0	1
2	0	90°	0	θ_2+ 90°	θ_2	$-S_2$	C_2	0	1
3	0	0	0	θ_3	θ_3	C_3	S_3	1	0

The transformation matrices are now obtained from Table 3.5 as

$$ {}^0T_1 = \begin{bmatrix} C_1 & 0 & S_1 & 0 \\ S_1 & 0 & -C_1 & 0 \\ 0 & 1 & 0 & 0 \\ 0 & 0 & 0 & 1 \end{bmatrix} \tag{3.24}$$

$$ {}^1T_2 = \begin{bmatrix} -S_2 & 0 & C_2 & 0 \\ C_2 & 0 & S_2 & 0 \\ 0 & 1 & 0 & 0 \\ 0 & 0 & 0 & 1 \end{bmatrix} \tag{3.25} $$

$$ {}^2T_3 = \begin{bmatrix} C_3 & -S_3 & 0 & 0 \\ S_3 & C_3 & 0 & 0 \\ 0 & 0 & 1 & 0 \\ 0 & 0 & 0 & 1 \end{bmatrix} \tag{3.26} $$

and the overall transformation matrix for the RPY wrist is

$$ {}^0T_3 = {}^0T_1\,{}^1T_2\,{}^2T_3 = \begin{bmatrix} -C_1S_2C_3 + S_1S_3 & C_1S_2S_3 + S_1C_3 & C_1C_2 & 0 \\ -S_1S_2C_3 - C_1S_3 & S_1S_2S_3 - C_1C_3 & S_1C_2 & 0 \\ C_2C_3 & -C_2S_3 & S_2 & 0 \\ 0 & 0 & 0 & 1 \end{bmatrix} \tag{3.27} $$

Checking the correctness of this model for the home position is left to the reader.

Example 3.5 *Kinematics of a 3-DOF Polar Arm*

For the 3-DOF (RRP) manipulator arm shown in Fig. 3.20, obtain the orientation and position of tool point P of the joint variable vector is $\boldsymbol{q} = [90° \; -45° \; 100 \text{ mm}]^T$ with $x_1 = 50$ mm and $x_2 = 40$ mm.

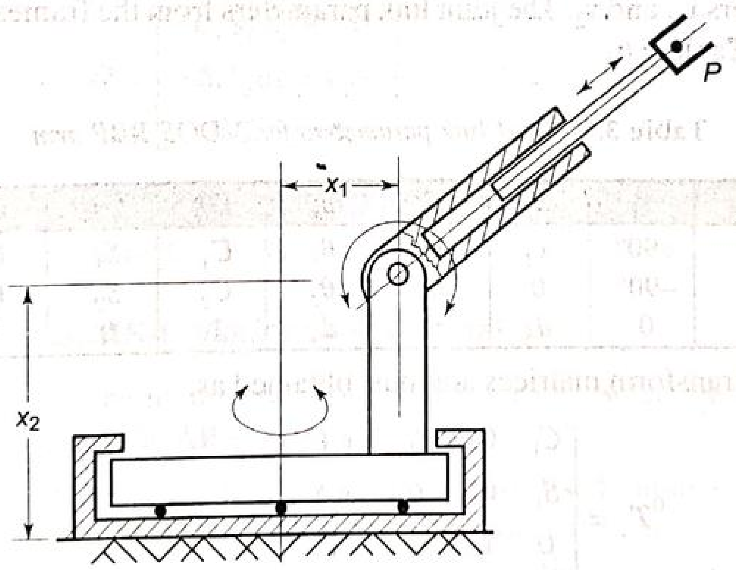

Fig. 3.20 *A 3-DOF (RRP) spherical configuration manipulator arm*

Solution The 3-DOF RRP manipulator is constructed by fixing the 2-DOF arm of Example 3.1, Fig. 3.11 on a rotary table.

Assume in home position of the arm, the last two links are vertical. For this home position, the frame assignment using Algorithm 3.1 will be as shown in Fig. 3.21.

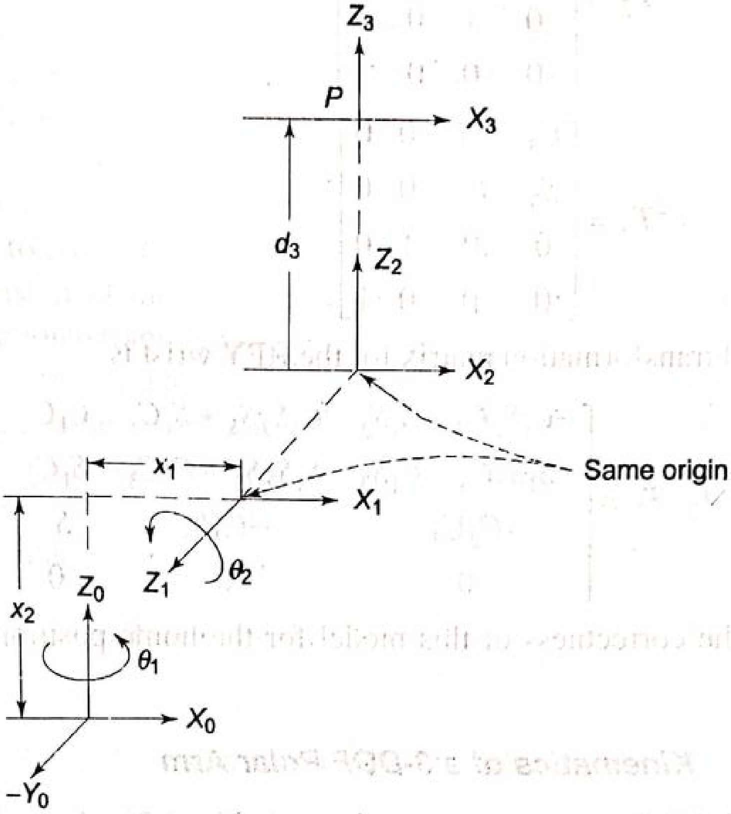

Fig. 3.21 *Frame assignment for home position of arm in Fig. 3.20*

Note the location of frame {1} with respect to frame {0} and the inclusion to two parameters x_1, and x_2. The joint link parameters from the frames assigned are tabulated in Table 3.6.

Table 3.6 *Joint link parameters for 3-DOF RRP arm*

i	a_i	α_i	d_i	θ_i	q_i	$C\theta_i$	$S\theta_i$	$C\alpha_i$	$S\alpha_i$
1	x_1	+90°	x_2	θ_1	θ_1	C_1	S_1	0	1
2	0	–90°	0	θ_2	θ_2	C_2	S_2	0	1
3	0	0	d_3	0	d_3	1	0	1	0

The three transform matrices are thus, obtained as:

$$
{}^0T_1 = \begin{bmatrix} C_1 & 0 & S_1 & x_1C_1 \\ S_1 & 0 & -C_1 & x_1S_1 \\ 0 & 1 & 0 & x_2 \\ 0 & 0 & 0 & 1 \end{bmatrix} \tag{3.28}
$$

$$
{}^1T_2 = \begin{bmatrix} C_2 & 0 & -S_2 & 0 \\ S_2 & 0 & C_2 & 0 \\ 0 & -1 & 0 & 0 \\ 0 & 0 & 0 & 1 \end{bmatrix} \tag{3.29}
$$

$$ {}^{2}\boldsymbol{T}_3 = \begin{bmatrix} 1 & 0 & 0 & 0 \\ 0 & 1 & 0 & 0 \\ 0 & 0 & 1 & d_3 \\ 0 & 0 & 0 & 1 \end{bmatrix} \tag{3.30} $$

and the overall transformation for the arm is

$$ \text{or} \quad \boldsymbol{T} = {}^{0}\boldsymbol{T}_1\, {}^{1}\boldsymbol{T}_2\, {}^{2}\boldsymbol{T}_3 = \begin{bmatrix} C_1C_2 & -S_1 & -C_1S_2 & -C_1S_2 / d_3 + x_1C_1 \\ S_1C_2 & C_1 & -S_1S_2 & -S_1S_2 / d_3 + x_1S_1 \\ S_2 & 0 & C_2 & C_2 / d_3 - x_2 \\ 0 & 0 & 0 & 1 \end{bmatrix} \tag{3.31} $$

The orientation of the end-effector (point P) is described in terms of joint variables by the rotation submatrix of $\boldsymbol{T}$, that is,

$$ \boldsymbol{R} = \begin{bmatrix} C_1C_2 & -S_1 & -C_1S_2 \\ S_1C_2 & C_1 & -S_1S_2 \\ S_2 & 0 & C_2 \end{bmatrix} \tag{3.32} $$

For $\theta_1 = 90°$ and $\theta_2 = -45°$, the orientation of P is

$$ \begin{bmatrix} n_x & o_x & a_x \\ n_y & o_y & a_y \\ n_z & o_z & a_z \end{bmatrix} = \begin{bmatrix} 0 & -1 & 0 \\ 0.707 & 0 & 0.707 \\ -0.707 & 0 & 0.707 \end{bmatrix} \tag{3.33} $$

and the position of end-effector is described by the translation vector $\boldsymbol{D}$ as

$$ \boldsymbol{D} = \begin{bmatrix} -C_1S_2d_3 + x_1C_1 \\ -S_1S_2d_3 + x_1S_1 \\ d_3C_2 - x_2 \end{bmatrix} \tag{3.34} $$

for given joint-link parameters and $\boldsymbol{q}$, the position of P is

$$ \boldsymbol{D} = [0 \quad 20.711 \quad 110.711]^T \tag{3.35} $$

Example 3.6 ***SCARA manipulator kinematics***

Obtain the direct kinematics equation of the 4-DOF Selective Compliance Assembly Robot Arm (SCARA) robots.

Solution The SCARA manipulator is a widely used industrial robot for assembly operations. Figure 3.22 shows the configuration of the SCARA manipulator, which is a four-axis horizontal-jointed articulated arm configuration as discussed in Chapter 1. The first two joints are revolute to establish the horizontal position of the tool. The third joint is prismatic which determines the vertical position of tool. Finally, the last joint is revolute which controls the tool orientation. Thus, SCARA has RRPR configuration and gives an upright cylindrical workspace. It may be useful to recall that the RPP manipulator discussed in Example 3.2 also has a cylindrical workspace, but the two are different (i) in the number of possible ways to reach a point within the work volume, and (ii) the orientation of tool point. In Example 3.2, the tool point orientation is radial, where as the tool point of the SCARA robot is always oriented in the vertical direction. The frame assignment for the SCARA manipulator is carried out as follows:

All the joints and links are identified and labeled from 1 to 4 and 0 to 4, respectively. The axis of each joint is vertical and frames are fixed next.

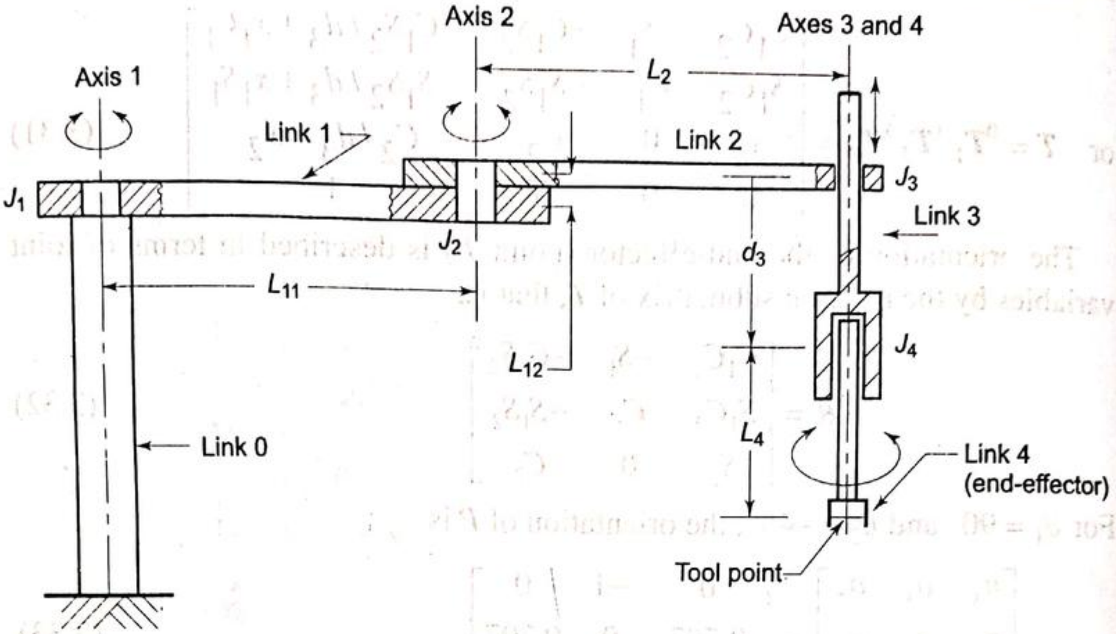

Fig 3.22 *A 4-DOF SCARA manipulator in home position*

Frame {1} Joints 1 and 2 axes are aligned with z_0- and z_1-axes, respectively. As z_0- and z_1-axes are parallel, choose x_1-axis as the common normal to z_0 and z_1 directed along the link 2. The origin of frame {1} is placed on z_1-axis at the joint as shown in Fig. 3.23. The y_1-axis completes right-handed orthonormal frame {1}. This gives $\alpha_1 = 0$.

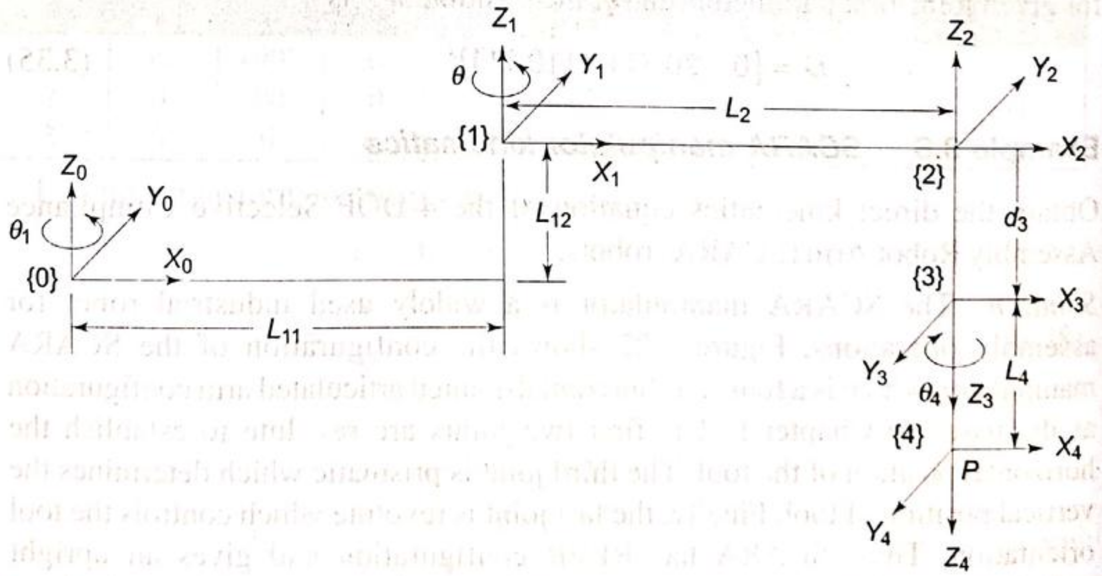

Fig. 3.23 *Frame assignment for SCARA robot*

Frame {2} Joint 3 axis is aligned with z_2-axis. Since z_1- and z_2-axes are parallel, set x_2-axis as the common normal which makes d_1 zero. This fixes the origin of frame {2} and results in $\alpha_2 = 0$, $d_2 = 0$ and $a_2 = L_2$.

Frame {3} Joint 3 is prismatic and z_3-axis coincides with z_2-axis, thus $\alpha_2 = 0$. Origin of frame {3} is placed at distal end of the prismatic link 3. Since the link displacement is downwards, it is convenient to point z_3-axis downward. This gives $\alpha_3 = 180°$. The x_3-axis is chosen parallel to x_2-axis making $\theta_3 = 0$.

Frame {0} z_0-axis has already been aligned along joint 1 axis. The x_0-axis is fixed along the link 1 axis such that x_0-axis remains parallel to x_1-axis. Since joint 1 is revolute, origin of frame {0} is placed at joint 1 at the intersection of axes z_0 and x_0 as shown in Fig. 3.23. The right-handed orthonormal coordinate frame {0} is computed with y_0-axis. The position of origin of frame {0} relative to frame {1} given by a translation by L_{11} in x_0 direction and L_{12} in z_0 direction, this frame assignment gives $a_1 = L_{11}$ and $d_1 = L_{12}$. Here L_{11} corresponds to the length of link 1 and the distance L_{12} is known as joint offset. Alternate locations of the origin of frame {0} are possible.

Frame {4} z_4-axis is chosen parallel to z_3-axis and origin of frame {4} is located at the tool tip. Joint 4 being revolute, x_4-axis is chosen to be parallel to x_3-axis giving $\alpha_4 = 0$, $a_4 = 0$ and $d_4 = L_4$.

The complete frame assignment is shown in Fig. 3.23 from which all the joint-link parameters are determined and tabulated in Table 3.7.

Table 3.7 *Joint-link parameters for SCARA robot*

Link i	a_i	α_i	d_i	θ_i	q_i	$C\theta_i$	$S\theta_i$	$C\alpha_i$	$S\alpha_i$
1	L_{11}	0	L_{12}	θ_1	θ_1	C_1	S_1	1	0
2	L_2	0	0	θ_2	θ_2	C_2	S_2	1	0
3	0	180°	d_3	0	d_3	1	0	−1	0
4	0	0	L_4	θ_4	θ_4	C_4	S_4	1	0

We now obtain the individual transformation matrices that specify the relationship between adjacent links as below:

$$^0T_1(\theta_1) = \begin{bmatrix} C_1 & -S_1 & 0 & L_{11}C_1 \\ S_1 & C_1 & 0 & L_{11}S_1 \\ 0 & 0 & 1 & L_{12} \\ 0 & 0 & 0 & 1 \end{bmatrix} \quad (3.36)$$

$$^1T_2(\theta_2) = \begin{bmatrix} C_2 & -S_2 & 0 & L_2C_2 \\ S_2 & C_2 & 0 & L_2S_2 \\ 0 & 0 & 1 & 0 \\ 0 & 0 & 0 & 1 \end{bmatrix} \quad (3.37)$$

$$
{}^2\boldsymbol{T}_3(d_3) = \begin{bmatrix} 1 & 0 & 0 & 0 \\ 0 & -1 & 0 & 0 \\ 0 & 0 & -1 & d_3 \\ 0 & 0 & 0 & 1 \end{bmatrix} \tag{3.38}
$$

$$
{}^3\boldsymbol{T}_4(\theta_4) = \begin{bmatrix} C_4 & -S_4 & 0 & 0 \\ S_4 & C_4 & 0 & 0 \\ 0 & 0 & 1 & L_4 \\ 0 & 0 & 0 & 1 \end{bmatrix} \tag{3.39}
$$

The manipulator transformation matrix obtained after multiplication of the above four matrices and simplification using trigonometric identities, is

$$
{}^0\boldsymbol{T}_4 = \begin{bmatrix} C_{124} & S_{124} & 0 & L_2C_{12} + L_{11}C_1 \\ S_{124} & -C_{124} & 0 & L_2S_{12} + L_{11}S_1 \\ 0 & 0 & -1 & L_{12} + d_3 - L_4 \\ 0 & 0 & 0 & 1 \end{bmatrix} \tag{3.40}
$$

Here, C_{124} denotes cos $(\theta_1 + \theta_2 - \theta_4)$, S_{124} denotes sin $(\theta_1 + \theta_2 - \theta_4)$, C_{12} denotes cos $(\theta_1 + \theta_2)$, and S_{12} denotes sin $(\theta_1 + \theta_2)$.

The fact that the third column of the matrix ${}^0\boldsymbol{T}_4$ is always $[0\ \ 0\ \ -1\ \ 0]^T$, means that at any instant the z-axis of the tool frame (approach vector) is in the direction of negative z-axis of the base frame. This is a characteristic of SCARA robots that are designed to manipulate objects from directly above. In addition, the SCARA wrist possesses only 1-DOF, the roll motion, to orient the tool.

Example 3.7 *Kinematics of a 5-DOF Industrial Manipulator*

In many industrial applications of robots five degrees of freedom are sufficient to carry out the industrial tasks effectively. Many common industrial manipulators are, therefore, constructed with a 3-DOF arm and a 2-DOF wrist with roll and pitch motions. One such manipulator with an articulated arm is shown in Fig. 3.24. All the five axes of the manipulator are revolute.

Obtain the kinematic model of the manipulator and test it for the home position. Determine the position and orientation of the end-effector (tool point P) if the joint variable vector is $\boldsymbol{q} = [\pi/4\ \ -3\pi/4\ \ \pi/2\ \ \pi/4\ \ \pi]^T$ and the link parameters are $L_1 = 50$, $L_2 = L_3 = 140$ and $L_5 = 20$.

Solution To determine the kinematic model of the manipulator, the home position of the manipulator is chosen such that link 2 of the arm is vertical and link 3 and the wrist are horizontal. For this home position the joint variable vector will be $\boldsymbol{q}_{\text{home}} = [0\ \ 0\ \ 0\ \ 0\ \ 0]^T$. For the home position, the frame assignment is carried out. Applying steps 0 to 8 of the Algorithm 3.1, the frames to all joints-links are assigned and are shown in Fig. 3.25.

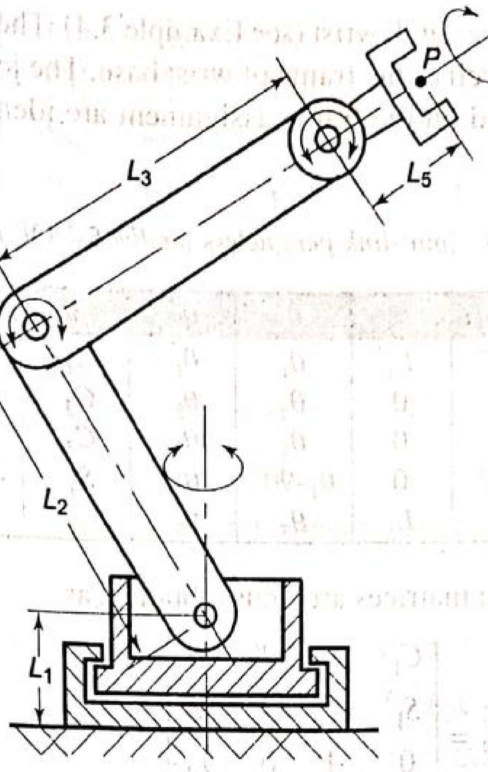

Fig. 3.24 *A five degree of freedom industrial manipulator*

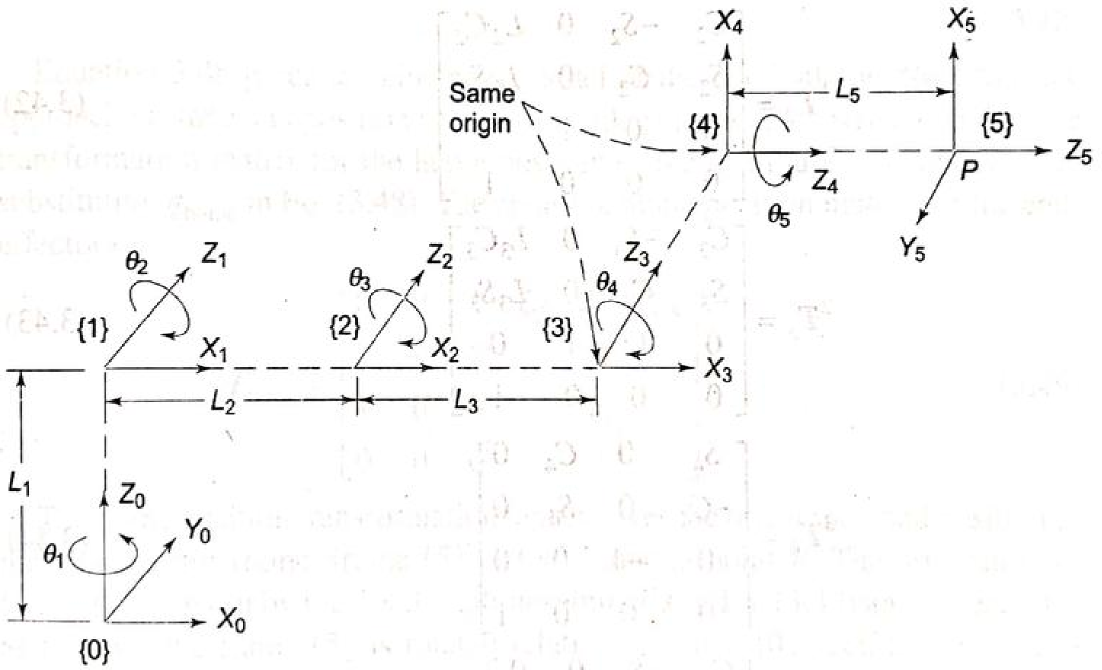

Fig. 3.25 *Frame assignment for 5-DOF industrial manipulator*

Note that the origins of frame {3} and frame {4} coincide but are shown separated to make the diagram clear. The orientation of frame {4} is obtained by two rotations of frame {3}, first by –90° about z_3-axis and, second by –90° about rotated x_3-axis. Recall that the frame assignment by Algorithm 3.1 is not unique, for example, a different frame assignment will be obtained by choosing the z-axis of any or all of the joins in the opposite direction. In Fig. 3.25 frames {0} to {3} correspond to the 3-DOF of articulated arm (see Example 3.3) and frame {3} to

{5} correspond to the 2-DOF wrist (see Example 3.4). The frame {3} is the frame of arm end-point as well as the frame of wrist base. The joint-link parameters for the manipulator based on the frame assignment are identified and tabulated in Table 3.8.

Table 3.8 *Joint-link parameters for the 5-DOF manipulator*

i	a_i	α_i	d_i	θ_i	q_i	$C\theta_i$	$S\theta_i$	$C\alpha_i$	$S\alpha_i$
1	0	–90°	L_1	θ_1	θ_1	C_1	S_1	0	–1
2	L_2	0	0	θ_2	θ_2	C_2	S_2	1	0
3	L_3	0	0	θ_3	θ_3	C_3	S_3	1	0
4	0	–90°	0	θ_4–90°	θ_4	S_4	$-C_4$	0	–1
5	0	0	L_5	θ_5	θ_5	C_5	S_5	1	0

The transformation matrices are, thus, obtained as

$$^{0}\boldsymbol{T}_1 = \begin{bmatrix} C_1 & 0 & -S_1 & 0 \\ S_1 & 0 & C_1 & 0 \\ 0 & -1 & 0 & L_1 \\ 0 & 0 & 0 & 1 \end{bmatrix} \tag{3.41}$$

$$^{1}\boldsymbol{T}_2 = \begin{bmatrix} C_2 & -S_2 & 0 & L_2C_2 \\ S_2 & C_2 & 0 & L_2S_2 \\ 0 & 0 & 1 & 0 \\ 0 & 0 & 0 & 1 \end{bmatrix} \tag{3.42}$$

$$^{2}\boldsymbol{T}_3 = \begin{bmatrix} C_3 & -S_3 & 0 & L_3C_3 \\ S_3 & C_3 & 0 & L_3S_3 \\ 0 & 0 & 1 & 0 \\ 0 & 0 & 0 & 1 \end{bmatrix} \tag{3.43}$$

$$^{3}\boldsymbol{T}_4 = \begin{bmatrix} S_4 & 0 & C_4 & 0 \\ -C_4 & 0 & S_4 & 0 \\ 0 & -1 & 0 & 0 \\ 0 & 0 & 0 & 1 \end{bmatrix} \tag{3.44}$$

$$^{4}\boldsymbol{T}_5 = \begin{bmatrix} C_5 & -S_5 & 0 & 0 \\ S_5 & C_5 & 0 & 0 \\ 0 & 0 & 1 & L_5 \\ 0 & 0 & 0 & 1 \end{bmatrix} \tag{3.45}$$

The transformation matrix for the arm is

$$ {}^{0}T_3 = {}^{0}T_1\,{}^{1}T_2\,{}^{2}T_3 = \begin{bmatrix} C_1C_{23} & -C_1S_{23} & -S_1 & C_1(L_2C_2 + L_3C_{23}) \\ S_1C_{23} & -S_1S_{23} & C_1 & S_1(L_2C_2 + L_3C_{23}) \\ -S_{23} & -C_{23} & 0 & L_1 - L_2S_2 - L_3S_{23} \\ 0 & 0 & 0 & 1 \end{bmatrix} \tag{3.46} $$

and the transformation matrix for the wrist is

$$ {}^{3}T_5 = {}^{3}T_4\,{}^{4}T_5 = \begin{bmatrix} S_4C_5 & -S_4S_5 & C_4 & L_5C_4 \\ -C_4C_5 & C_4S_5 & S_4 & L_5S_4 \\ -S_5 & -C_5 & 0 & 0 \\ 0 & 0 & 0 & 1 \end{bmatrix} \tag{3.47} $$

The overall transformation matrix for the manipulator is, therefore,

$$ {}^{0}T_5 = {}^{0}T_3\,{}^{3}T_5 $$

$$ = \begin{bmatrix} C_1S_{234}C_5 + S_1S_5 & -C_1S_{234}S_5 + S_1C_5 & C_1C_{234} & C_1(L_2C_2 + L_3C_{23} + L_5C_{234}) \\ S_1C_{234}C_5 - C_1S_5 & -S_1S_{234}S_5 - C_1C_5 & S_1C_{234} & S_1(L_2C_2 + L_3C_{23} + L_5C_{234}) \\ -C_{234}C_5 & C_{234}S_5 & -S_{234} & L_1 - L_2S_2 - L_3S_{23} - L_5S_{234} \\ 0 & 0 & 0 & 1 \end{bmatrix} \tag{3.48} $$

Equation 3.48 gives the kinematic model of the manipulator. Note that the approach vector $\boldsymbol{a}$ and position vector $\boldsymbol{p}$ are independent of the wrist roll (θ_5). The transformation matrix for the home position of the manipulator is obtained by substituting $\boldsymbol{q}_{\text{home}}$ in Eq. (3.48). The resulting home position matrix for the end-effector is

$$ T_{\text{home}} = \begin{bmatrix} 0 & 0 & 1 & L_2 + L_3 + L_5 \\ 0 & -1 & 0 & 0 \\ 1 & 0 & 0 & L_1 \\ 0 & 0 & 0 & 1 \end{bmatrix} \tag{3.49} $$

The home position transformation matrix gives the orientation and position of the end-effector frame, frame {5} or tool frame at point P. The orientation of frame {5} is given by the 3×3 rotation submatrix of Eq. (3.49) and is described as follows: the frame {5} is rotated relative to frame {0} such that x_5-axis is parallel and in same direction to z-axis of base frame, frame {0} or z_0-axis; y_5-axis is parallel to y_0-axis but in opposite direction; and z_5-axis is in x_0-axis direction. The position of point P or the origin of end-effector frame, frame {5}, is given by 3×1 displacement matrix of Eq. (3.49) and it is displaced by $[L_2 + L_3 + L_5 \quad 0 \quad L_1]^T$ from the base frame, frame {0}.

Finally, the position and orientation of the end-effector, point P, for the given joint variable vector $\boldsymbol{q} = [\pi/4 \quad -3\pi/4 \quad \pi/2 \quad \pi/4 \quad \pi]^T$ and link parameters $L_1 = 50$, $L_2 = L_3 = 140$ and $L_5 = 20$ is obtained by substituting these values of joint-variables in Eq. (3.48). This gives

$$T_E = \begin{bmatrix} 0 & -0.707 & 0.707 & 14.14 \\ 0 & 0.707 & 0.707 & 14.14 \\ -1 & 0 & 0 & 248 \\ 0 & 0 & 0 & 1 \end{bmatrix} \quad (3.50)$$

Example 3.8 ***Stanford manipulator kinematics***

The last example considered is of a 6-DOF industrial manipulator. Formulate the direct kinematic model of the six degrees of freedom Stanford manipulator shown in Fig. 3.26.

Solution The Stanford arm, shown in Fig. 3.26, is characterized by a three degree of freedom arm and three degree of freedom wrist. The first three joints, two revolute and one prismatic, constitute the arm of the spherical (RRP) configuration (see Section 1.6.5). The last three revolute joints constitute a wrist of RRR configuration. The first three links are larger in size and are used to position the wrist and the last three links for the wrist are small in size and are used to orient the end-effector. Joint 1 is a revolute joint, which rotates the whole body about the vertical axis (joint axis 1). Joint 2 is also revolute and moves about horizontal axis (joint axis 2) in a plane perpendicular to axis of joint 1.

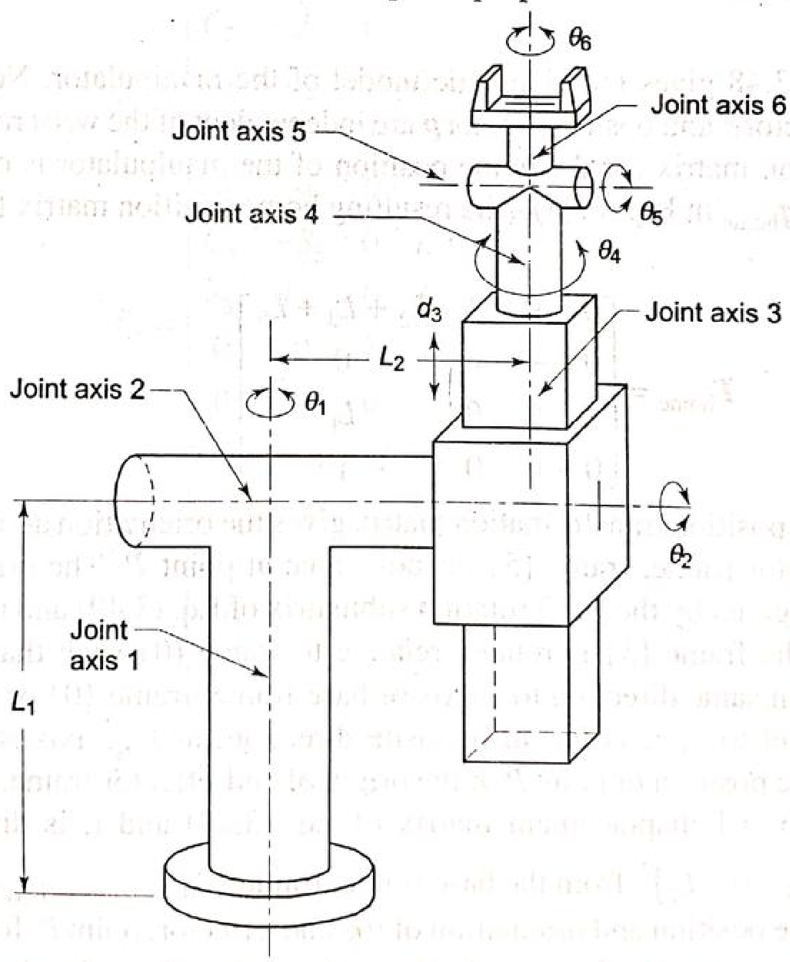

Fig. 3.26 *Six DOF (RRP : RRR) Stanford manipulator in home position*

Joint 3 is a prismatic joint that causes translational motion along joint axis 3 in a plane perpendicular to joint axis 2. The last three revolute joint motions are roll (joint 4), pitch (joint 5) and roll (joint 6) motions about joint axes 4, 5 and 6, respectively, which orient the end-effector. This wrist configuration is known as "Euler wrist", see Section 2.5.3. Observe that joint axes 4, 5 and 6 intersect at a point. Reader must note the differences between the RPY wrist discussed in Example 3.4 and the Euler wrist.

According to step 0, Algorithm 3.1, the six joints are numbered from 1 to 6 starting with joint 1 between link 0 (the immobile base) and link 1. The orientation of each joint axis and joint variables are identified and labeling corresponds to the home position as shown in Fig. 3.26. The reader must note that this is the home position of the manipulator in which all the joint variables are zero or at minimum.

The step-by-step frame assignment for each joint-link of the manipulator according to Algorithm 3.1 is explained below. Frames are first assigned to the intermediate links, links 1 to 5 and then to the link 0 and link 6. Refer Fig. 3.27 for the frame assignment.

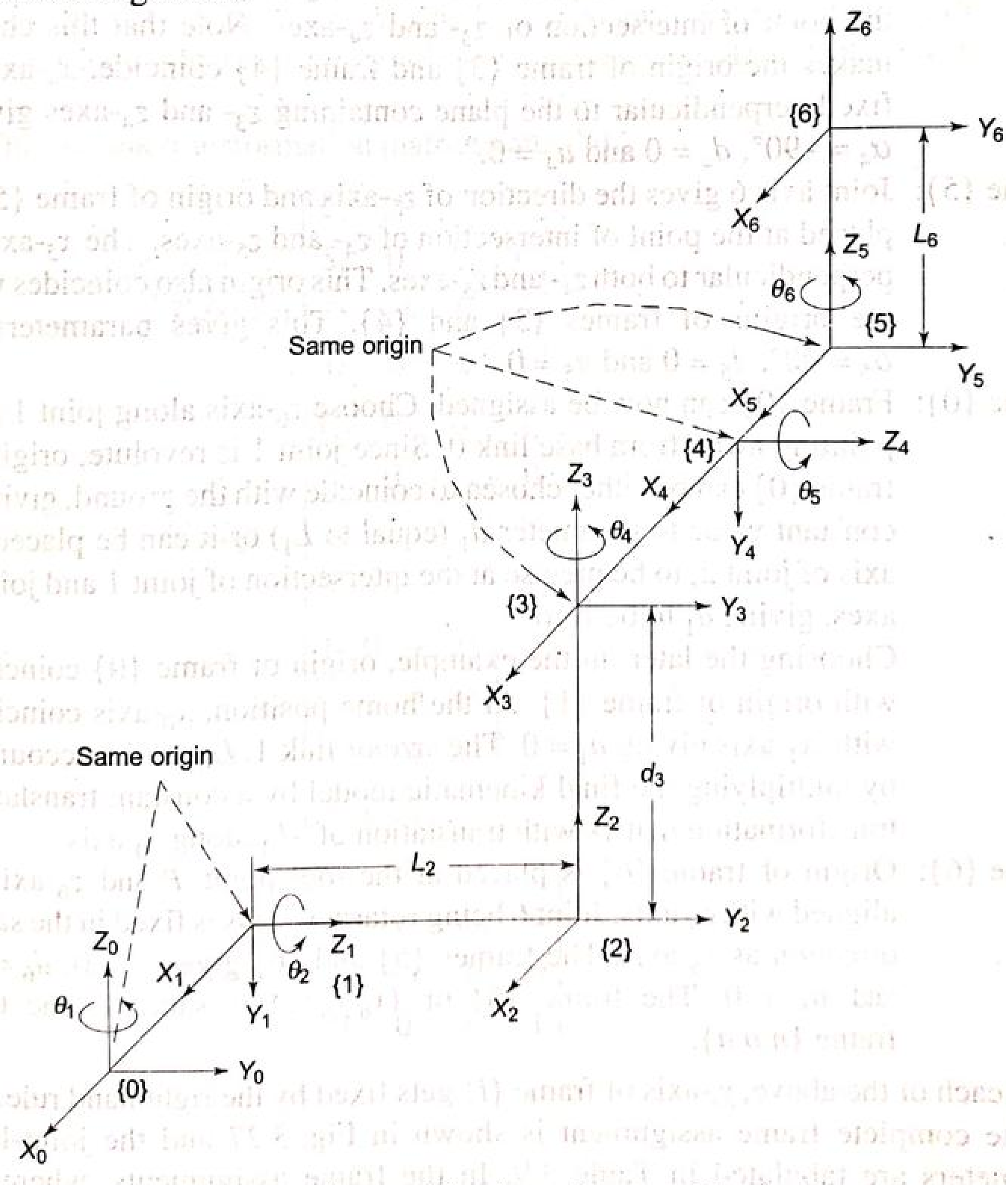

Fig. 3.27 *Frame assignment for chosen home position for Example 3.8*

Frame {1} Align z_0-axis with joint axis 1 and z_1-axis with joint axis 2. Because z_0- and z_1-axes intersect (step 2(i) Algorithm 3.1), fix origin of frame {1} at the point of their intersection and set x_1-axis perpendicular to the plane containing z_0- and z_1-axes.
The y_1-axis completes the right-hand orthonormal coordinate frame {1}. This frame assignment gives $\alpha_1 = -90°$.

Frame {2}: Align z_2-axis with joint axis 3. Fix origin of frame {2} at the intersection of z_1- and z_2-axes and set x_2-axis perpendicular to the plane containing z_1- and z_2-axes. Frames {1} and {2} give $\alpha_2 = 90°$, $d_2 = L_2$ and $a_2 = 0$.

Frame {3}: Align z_3-axis with axis 4. Since z_2- and z_3-axes coincide (step 2(iii)) and joint 3 being prismatic, choose x_3-axis in the same direction as x_2-axis making constant parameter α_3 to be zero. The origin is placed at the distal end of the link 3 to coincide with axis 4. From frames {2} and {3}, $\theta_3 = 0$, $\alpha_3 = 0$ and $a_3 = 0$. Note that for prismatic joint d_3 is the joint variable.

Frame {4}: z_4-axis is aligned with joint axis 5 and origin of frame {4} is fixed at the point of intersection of z_3- and z_4-axes. Note that this choice makes the origin of frame {3} and frame {4} coincide. x_4-axis is fixed perpendicular to the plane containing z_3- and z_4-axes giving $\alpha_4 = -90°$, $d_4 = 0$ and $a_4 = 0$.

Frame {5}: Joint axis 6 gives the direction of z_5-axis and origin of frame {5} is placed at the point of intersection of z_4- and z_5-axes. The x_5-axis is perpendicular to both z_4- and z_5-axes. This origin also coincides with the origins of frames {3} and {4}. This gives parameters as $\alpha_5 = 90°$, $d_5 = 0$ and $a_5 = 0$.

Frame {0}: Frame {0} can now be assigned. Choose z_0-axis along joint 1 axis pointing away from base link 0. Since joint 1 is revolute, origin of frame {0} can be either chosen to coincide with the ground, giving a constant value to parameter d_1 (equal to L_1) or it can be placed on axis of joint 2, to be precise at the intersection of joint 1 and joint 2 axes, giving d_1 to be zero.
Choosing the later, in the example, origin of frame {0} coincides with origin of frame {1}. At the home position, x_0-axis coincides with x_1-axis giving $a_1 = 0$. The size of link 1, L_1 can be accounted by multiplying the final kinematic model by a constant translation transformation matrix with translation of $-L_1$ along z_0-axis.

Frame {6}: Origin of frame {6} is placed at the tool point P and z_6-axis is aligned with z_5-axis. Joint 6 being rotary, x_6-axis is fixed in the same direction as x_5-axis. The frames {5} and {6} give $\alpha_6 = 0$, $d_6 = L_6$ and $a_6 = 0$. The frame {6} or $\{x_6\, y_6\, z_6\}$ is same as the tool frame $\{n\ o\ a\}$.

In each of the above, y_i-axis of frame $\{i\}$ gets fixed by the right hand rule.

The complete frame assignment is shown in Fig. 3.27 and the joint-link parameters are tabulated in Table 3.9. In the frame assignments, wherever alternatives exist, the choice has been made so that as many fixed parameters as possible are zeros. This results in the simplest possible direct kinematic model that has a small number of non-zero parameters. As in earlier example the displacement variable for each link is identified and tabulated in Table 3.9. It is noted that 12 out of 18 constants parameters are zero.

Table 3.9 *Joint-link parameters for Stanford manipulator*

Link i	a_i	α_i	d_i	θ_i	q_i	$C\theta_i$	$S\theta_i$	$C\alpha_i$	$S\alpha_i$
1	0	–90°	0	θ_1	θ_1	C_1	S_1	0	–1
2	0	90°	L_2	θ_2	θ_2	C_2	S_2	0	1
3	0	0	d_3	0	d_3	1	0	1	0
4	0	–90°	0	θ_4	θ_4	C_4	S_4	0	–1
5	0	90°	0	θ_5	θ_5	C_5	S_5	0	1
6	0	0	L_6	θ_6	θ_6	C_6	S_6	1	0

The next step is to find the individual transformation matrices ${}^{i-1}T_i(q_i)$ between successive links by substituting the joint-link parameter values in Eq. (3.5). As usual to facilitate writing these matrices, four columns defining $\cos\theta_i$, $\sin\theta_i$, $\cos\alpha_i$ and $\sin\alpha_i$ are appended to the joint-link parameters table, Table 3.9, for each link.

The six link transformation matrices are, thus,

$$
{}^0T_1(\theta_1) = \begin{bmatrix} C_1 & 0 & -S_1 & 0 \\ S_1 & 0 & C_1 & 0 \\ 0 & -1 & 0 & 0 \\ 0 & 0 & 0 & 1 \end{bmatrix} \tag{3.51}
$$

$$
{}^1T_2(\theta_2) = \begin{bmatrix} C_2 & 0 & S_2 & 0 \\ S_2 & 0 & -C_2 & 0 \\ 0 & 1 & 0 & L_2 \\ 0 & 0 & 0 & 1 \end{bmatrix} \tag{3.52}
$$

$$
{}^2T_3(d_3) = \begin{bmatrix} 1 & 0 & 0 & 0 \\ 0 & 1 & 0 & 0 \\ 0 & 0 & 1 & d_3 \\ 0 & 0 & 0 & 1 \end{bmatrix} \tag{3.53}
$$

$$
{}^3T_4(\theta_4) = \begin{bmatrix} C_4 & 0 & -S_4 & 0 \\ S_4 & 0 & C_4 & 0 \\ 0 & -1 & 0 & 0 \\ 0 & 0 & 0 & 1 \end{bmatrix} \tag{3.54}
$$

$$ {}^4T_5(\theta_5) = \begin{bmatrix} C_5 & 0 & S_5 & 0 \\ S_5 & 0 & -C_5 & 0 \\ 0 & 1 & 0 & 0 \\ 0 & 0 & 0 & 1 \end{bmatrix} \tag{3.55} $$

$$ {}^5T_6(\theta_6) = \begin{bmatrix} C_6 & -S_6 & 0 & 0 \\ S_6 & C_6 & 0 & 0 \\ 0 & 0 & 1 & L_6 \\ 0 & 0 & 0 & 1 \end{bmatrix} \tag{3.56} $$

Finally, obtain the transformation of the tool frame with respect to the base frame by substituting the individual transform matrices in Eq. (3.6) as

$$ {}^0T_6 = {}^0T_1\, {}^1T_2\, {}^2T_3\, {}^3T_4\, {}^4T_5\, {}^5T_6 \tag{3.57} $$

Substituting Eq. (3.51) to Eq. (3.56) in Eq. (3.57) and multiplying gives the final result for ${}^0T_6$ as in Eq. (3.58).

The manipulator (over all) transformation matrix ${}^0T_6$ represents the position and orientation of end-effector as a function of the six displacement variables θ_1, θ_2, d_3, θ_4, θ_5 and θ_6, other parameters are constant joint-link parameters.

Out of the 16 elements of the 4×4 homogeneous transformation matrix only 12 elements of upper 3×4 matrix are significant. Hence, only a maximum of 12 equations can be non-trivial. These equations give the forward kinematic model of the manipulator.

$$ {}^0T_6 = \left[\begin{array}{c:c:c:c} \begin{array}{l} C_1C_2C_4C_5C_6 \\ -S_1S_4C_5C_6 \\ -C_1S_2S_5C_6 \\ -C_1C_2S_4S_6 \\ -S_1C_4S_6 \end{array} & \begin{array}{l} C_1C_2C_4C_5S_6 \\ +S_1S_4C_5S_6 \\ +C_1S_2S_5S_6 \\ -C_1C_2S_4C_6 \\ -S_1C_4C_6 \end{array} & \begin{array}{l} C_1C_2C_4S_5 \\ -S_1S_4S_5 \\ +C_1S_2C_5 \end{array} & \begin{array}{l} C_1C_2C_4S_5L_6 \\ -S_1S_4S_5L_6 \\ +C_1S_2C_5L_6 \\ +C_1S_2d_3 - S_1L_2 \end{array} \\ \hdashline \begin{array}{l} S_1C_2C_4C_5C_6 \\ +C_1S_4C_5C_6 \\ -S_1S_2S_5C_6 \\ -S_1C_2S_4S_6 \\ +C_1C_4S_6 \end{array} & \begin{array}{l} -S_1C_2C_4C_5S_6 \\ -C_1S_4C_5S_6 \\ +S_1S_2S_5S_6 \\ -S_1C_2S_4C_6 \\ +C_1C_4C_6 \end{array} & \begin{array}{l} S_1C_2C_4S_5 \\ +C_1S_4S_5 \\ +S_1S_2C_5 \end{array} & \begin{array}{l} S_1C_2C_4S_5L_6 \\ +C_1S_4S_5L_6 \\ +S_1S_2C_5L_6 \\ +S_1S_2d_3 + C_1L_2 \end{array} \\ \hdashline \begin{array}{l} S_2C_4C_5C_6 \\ -C_2S_5C_6 \\ +S_2S_4S_6 \end{array} & \begin{array}{l} S_2C_4C_5S_6 \\ +C_2S_5S_6 \\ +S_2S_4C_6 \end{array} & \begin{array}{l} -S_2C_4S_5 \\ +C_2C_5 \end{array} & \begin{array}{l} -S_2C_4S_5L_6 \\ +C_2C_5L_6 + C_2d_3 \end{array} \\ \hdashline 0 & 0 & 0 & 1 \end{array}\right] \tag{3.58} $$

For given values of the joint displacements q_i and other constant joint-link parameters the end-effector position and orientation is obtained by equating ${}^0T_6$ to the end-effector orientation and position matrix T, Eq. (2.31), that is,

$$T = \begin{bmatrix} n_x & o_x & a_x & d_x \\ n_y & o_y & a_y & d_y \\ n_z & o_z & a_z & d_z \\ 0 & 0 & 0 & 1 \end{bmatrix} \tag{3.59}$$

Equating the elements of matrices in Eqs. (3.58) and (3.59), gives 12 equations as:

$$\begin{aligned}
n_x &= C_1C_2C_4C_5C_6 - S_1S_4C_5C_6 - C_1S_2S_5C_6 - C_1C_2S_4S_6 - S_1C_4S_6 \\
n_y &= S_1C_2C_4C_5C_6 + C_1S_4C_5C_6 - S_1S_2S_5C_6 - S_1C_2S_4S_6 + C_1C_4S_6 \\
n_z &= S_2C_4C_5C_6 - C_2S_5C_6 + S_2S_4S_6 \\
o_x &= C_1C_2C_4C_5S_6 + S_1S_4C_5S_6 + C_1S_2S_5S_6 - C_1C_2S_4C_6 - S_1C_4C_6 \\
o_y &= -S_1C_2C_4C_5S_6 - C_1S_4C_5S_6 + S_1S_2S_5S_6 - S_1C_2S_4C_6 + C_1C_4C_6 \\
o_z &= S_2C_4C_5S_6 + C_2S_5S_6 + S_2S_4C_6 \\
a_x &= C_1C_2C_4S_5 - S_1S_4S_5 + C_1S_2C_5 \\
a_y &= S_1C_2C_4S_5 + C_1S_4S_5 + S_1S_2C_5 \\
a_z &= -S_2C_4S_5 + C_2C_5 \\
d_x &= C_1C_2C_4S_5L_6 - S_1S_4S_5L_6 + C_1S_2C_5L_6 + C_1S_2d_3 - S_1L_2 \\
d_y &= S_1C_2C_4S_5L_6 + C_1S_4S_5L_6 + S_1S_2C_5L_6 + S_1S_2d_3 + C_1L_2 \\
d_z &= -S_2C_4S_5L_6 + C_2C_5L_6 + C_2d_3
\end{aligned} \tag{3.60}$$

Using this direct kinematic model for the home position ($\theta_1 = \theta_2 = \theta_4 = \theta_5 = \theta_6 = 0°$ and $d_3 = L_3$), assuming L_3 is minimum size of prismatic link, the end-effector position and orientation compute as

$$T = \left[\begin{array}{c:ccc} n_x & o_x & a_x & d_x \\ n_y & o_y & a_y & d_y \\ n_z & o_z & a_z & d_z \\ \hdashline 0 & 0 & 0 & 1 \end{array}\right] = \begin{bmatrix} 1 & 0 & 0 & 0 \\ 0 & 1 & 0 & L_2 \\ 0 & 0 & 1 & L_3 + L_6 \\ 0 & 0 & 0 & 1 \end{bmatrix} \tag{3.61}$$

This agrees with the coordinate system established in Fig. 3.27 and serves as a good check for the correctness of the model. It is important to note that the above 12 equations (Eq. (3.60)) require 10 transcendental function calls, 36 multiplications and 35 additions. Considerable computational saving can be obtained by calculating only 9 elements of the upper right 3×3 submatrix demarked by dotted lines in T above, Eq. (3.61). The first column of T can be obtained as a vector cross product of second and third columns. Further, if L_6 is made zero by shifting the end-effector frame origin (as was done in Example 3.4), this will reduce the computations for d_x, d_y and d_z significantly. This is left for the reader to verify.

EXERCISES

3.1 What are the parameters for a link for kinematic modeling? Which of these parameters are variable and which are constant for (a) a revolute joint, and (b) a prismatic joint?

3.2 Compute the manipulator transformation matrix for the 3-DOF manipulator arm with Cartesian (PPP) configuration. Three prismatic joints are perpendicular to each other and a possible frame assignment is given in Fig. E3.2.

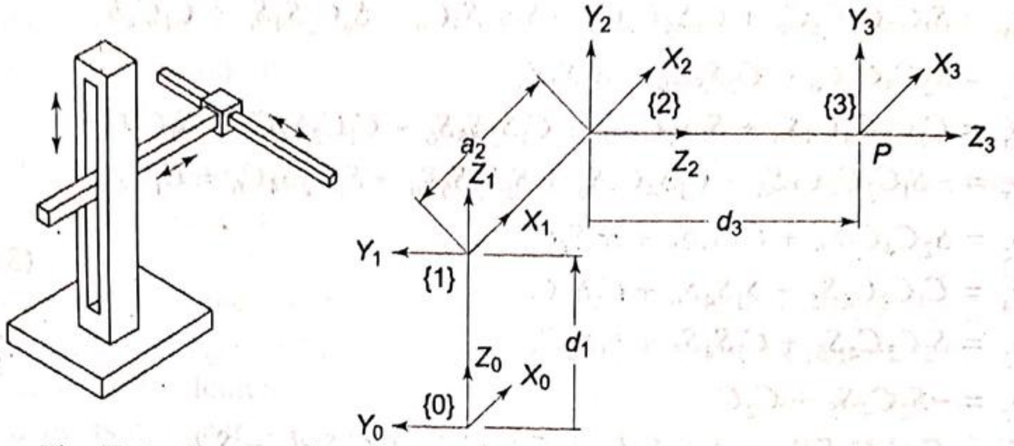

Fig. E3.2 *Frame assignment for a 3-DOF Cartesian configuration arm*

3.3 A 3-DOF cylindrical configuration arm of a manipulator has two prismatic joints and one revolute joint. A typical cylindrical arm with joint offset is shown in Fig. E3.3. Using the Algorithm 3.1 carry out frame assignments and tabulate the joint-link parameters.

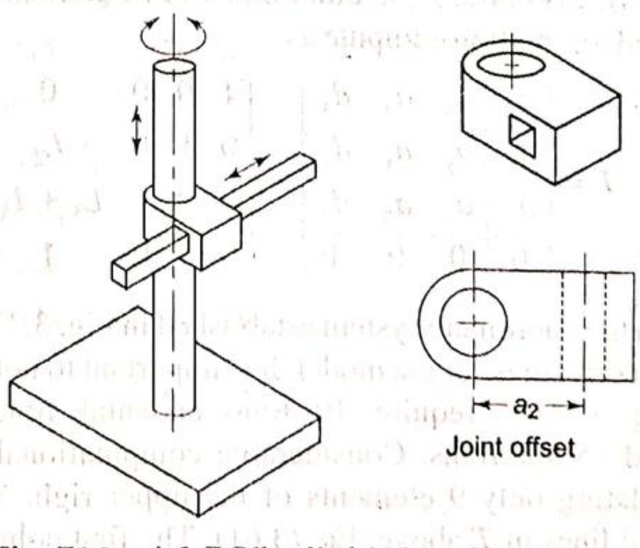

Fig. E3.3 *A 3-DOF cylindrical configuration arm*

3.4 For the cylindrical manipulator arm in Exercise 3.3, obtain the individual link transformation matrices and the overall arm transformation matrix. Verify your answer for the home position.

3.5 The 3R wrist in Example 3.8 is an Euler wrist. Obtain the wrist transformation matrix for the Euler wrist, see Example 3.4.

3.6 For the 3-DOF-manipulator arm shown in Fig. E3.6, assign frames and obtain the joint-link parameters. Also, determine the position of the tool tip with respect to the base frame {0}. Compare this kinematic model with Exercise 3.3.

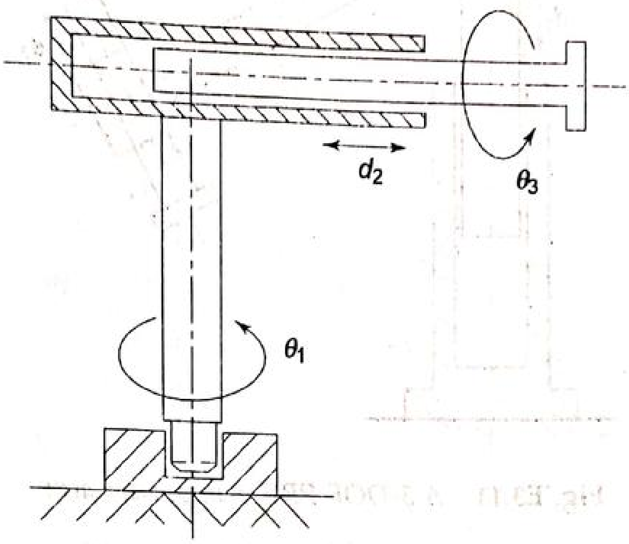

Fig. E3.6 *A 3-DOF RPR-configuration manipulator*

3.7 For the manipulator discussed in Exercise 3.6, obtain the rotation matrix that describes the orientation of the tool relative to the base. Also, compute the value of this rotation matrix for $q = [60° \ 20 \ 30°]^T$.

3.8 For the manipulator discussed in Exercise 3.6, determine the transformation matrices relating successive links. Also, determine its forward kinematic model.

3.9 Obtain the tool transformation matrix for the 3-DOF articulated arm, shown in Fig. 3.16, if its home position is shifted to that shown in Fig. 3.17(b). Also, determine the tool position for $q = [0 \ -90° \ 90°]^T$ and show that it is the same as the original home position.

3.10 Obtain the forward kinematic model for the SCARA manipulator of Example 3.6 taking the base frame at the table, that is, base of the column.

3.11 For the 3-DOF robotic manipulator arm shown in Fig. E3.11, assign frames to each of the links and determine the joint-link parameters and, therefrom, obtain the direct kinematic model.

3.12 Given that the position of an object relative to the base frame of manipulator in Fig. E3.11 as ${}^0P = [7.0 \ 10.0 \ 5.0]^T$, determine the position of this object relative to the tool frame.

3.13 For the SCARA robot discussed in Example 3.6, compute the rotation matrix describing the tool relative to the base when the 4×1 joint-space vector is $q = [45° \ 45° \ 5 \ 30°]^T$. Also, find the orientation of the tool in *ZYX*-Euler angle representation for the given joint space vector.

3.14 For a 5-DOF, RRR-RR articulated configuration manipulator shown in Fig. E3.14 obtain the forward kinematic model.

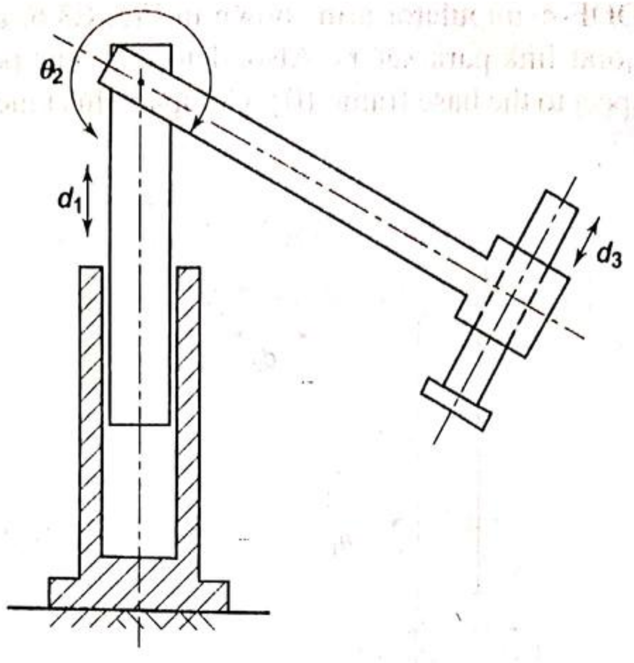

Fig. E3.11 *A 3-DOF PRP manipulator arm*

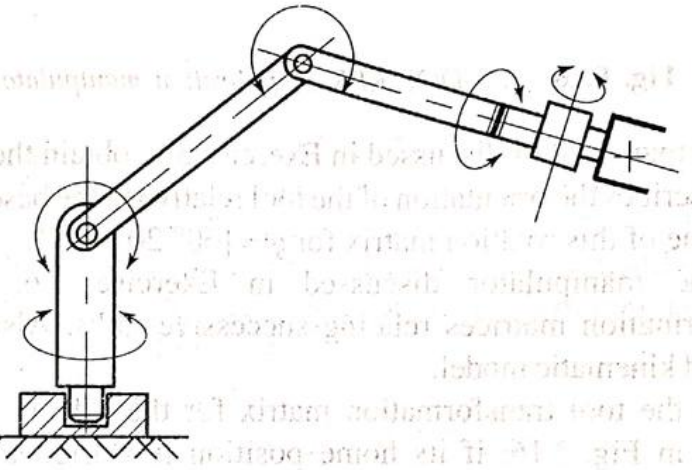

Fig. E3.14 *A 5-DOF articulated manipulator*

3.15 For Exercise 3.14, test the correctness of the forward kinematic model for the home position.

3.16 For the Stanford manipulator in Example 3.8 determine the tool point position for $\boldsymbol{q} = [\pi/2\ -\pi/2\ 100\ \pi\ \pi/2\ -\pi/2]^T$.

3.17 For the manipulator shown in Fig. 3.26 determine the coordinates of the tool point for the joint displacements $\boldsymbol{q} = [30°\ -20°\ 50\ 0°\ -108°\ 34°]^T$.

3.18 Consider the 6-DOF manipulator constructed by attaching an Euler wrist (see Example 3.8) to the faceplate of the 3-DOF articulated arm shown in Fig. 3.15. Attach frames to each link of this manipulator as per Algorithm 3.1 and obtain its forward kinematic model.

3.19 Repeat Exercise 3.18 for the manipulator by fixing a roll-pitch-yaw wrist to the faceplate of manipulator shown in Fig. 3.15.

3.20 A 3-DOF articulated configuration arm of a manipulator has all three revolute joints. In a typical articulated arm, the joint design determines the joint range. The design of joints in Fig. E3.20 gives almost 360° joint range but has joint offsets (the articulated arm discussed in Example 3.3 has no joint offsets). Using the Algorithm 3.1 carry out frame assignments, tabulate the joint-link parameters and obtain the forward kinematic model of the arm.

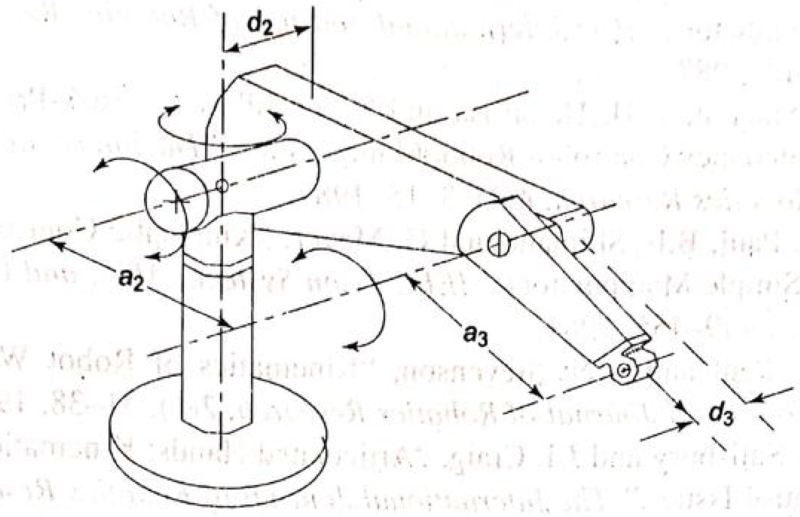

Fig. E3.20 *A 3-DOF articulated arm with joint offsets*

3.21 Why DH convention (Algorithm 3.1) does not give unique frame assignment for a given manipulator? Explain.

3.22 "The forward kinematic model of a manipulator depends on the choice of home position of the manipulator." Comment on this statement.

3.23 Using the DH notation for frame assignment, is it possible to have the a link with zero link length whereas the physical link on the manipulator will have a finite link length?

3.24 What problems will be encountered if the frames are arbitrarily assigned to develop the forward kinematic model of a manipulator?

3.25 Why is it important to choose a frame assignment for an n-DOF manipulator that gives a maximum number of zero joint-link parameters?

3.26 The frame assignment of a manipulator is so carried out that it is found that one of the link's rotation is about y-axis of the frame instead of z-axis. Can the transformation matrix of Eq. (3.3) be used for determining the transformation matrix for the link?

SELECTED BIBLIOGRAPHY

1. J. Denavit and R.S. Hartenberg, "A Kinematic Notation for Lower-Pair Mechanisms Based on Matrices," *ASME. J. of Applied Mechanics*, 215–221, Jun 1955.
2. Colin G. Johnson and Duncan Marsh, "Modeling Robot Manipulators with Multivariate B-Splines," *Robotica*, *17*(3), 239–247, 1999.
3. Wisama Khalil and Denis Creusot, "SYMORO+: A System for the Symbolic Modeling of Robots," *Robotica*, *15*, 153–161, 1997.

4. C.S.G. Lee, "Robot Arm Kinematics, Dynamics and Control," *IEEE Computer*, ***15***(12), 62–80, 1982.
5. J.Y.S. Luh, "An Anatomy of Industrial Robots and their Controls," *IEEE Tr on Automatic Control*, ***28***(2), 133–153, Feb 1983.
6. Y. Nakamura and H. Hanafusa, "Optimal Redundancy Control of Robot Manipulators," *The International Journal of Robotics Research*, ***6***(1), 32–42, 1987.
7. Y. Nakamura, H. Hanafusa and T. Yoshikawa, "Task-Priority Based Redundancy Control of Robot Manipulators," *The International Journal of Robotics Research*, ***6***(2), 3–15, 1987.
8. R.P. Paul, B.E. Shimano and G. Mayer, "Kinematic Control Equations for Simple Manipulators," *IEEE Tr on Systems, Man, and Cybernetics*, ***11***(6), 449–455, 1981.
9. R.P. Paul and C.N. Stevenson, "Kinematics of Robot Wrists," *The International Journal of Robotics Research*, ***2***(1), 31–38, 1983.
10. J.K. Salisbury and J.J. Craig, "Articulated Hands: Kinematic and Force Control Issues," *The International Journal of Robotics Research*, ***1***(1), 4–17, Sep 1982.
11. O.R. Williams, J. Angeles and F. Bulca, "Design Philosophy of an Isotropic Six-Axis Serial Manipulator," *Robotics and Computer-Integrated Manufacturing*, ***10***(4), 275–286, 1993.

4

The Inverse Kinematics

The direct kinematic model discussed in Chapter 3 determines the position and orientation of the end-effector (tool) for given values of joint-link displacements. In other words, it answers the question "Where is the origin of the end-effector?" The direct kinematic model, thus, specifies the end-effector frame, frame $\{n\}$ relative to the base frame $\{0\}$, for the n-DOF manipulator, which is expressed as

$$^0\boldsymbol{T}_n(q_1, q_2, \ldots, q_n) = \prod_{i=1}^{n} {}^{i-1}\boldsymbol{T}_i = \begin{bmatrix} n_x & o_x & a_x & d_x \\ n_y & o_y & a_y & d_y \\ n_z & o_z & a_z & d_z \\ 0 & 0 & 0 & 1 \end{bmatrix} = \boldsymbol{T} \tag{4.1}$$

The joint displacements (q_1, q_2, ..., q_n) that lead the end-effector to a certain position and orientation $\boldsymbol{T}$ can be found by solving the kinematic model equations for unknown joint displacements. Moving each joint by the respective joint displacement, the location (position and orientation) of the end-effector is achieved. This is the inverse kinematic problem already defined in the previous chapter, Section 3.3. It is possible that for the desired end-effector location, multiple or no solutions may exist. A rigorous definition for the inverse kinematic problem is:

"The determination of all possible and feasible sets of joint variables, which would achieve the specified position and orientation of the manipulator's end-effector with respect to the base frame."

In practice, a robot manipulator control requires knowledge of the end-effector position and orientation for the instantaneous location of each joint as well as knowledge of the joint displacements required to place the end-effector in a new location. Therefore, direct and inverse kinematics are the fundamental problems of utmost importance in the robot manipulator's position control. Many industrial applications such as welding and certain types of assembly operations require that a specific path should be negotiated by the end-effector. To achieve this, it is necessary to find corresponding motions of each joint, which will produce the desired tool-tip motion. This is a typical case of inverse kinematic application.

The manipulator transformation matrix $\boldsymbol{T}$ represents the orientation $\boldsymbol{R}$ and position $\boldsymbol{D}$ of the end-effector with respect to the base frame as:

$$\boldsymbol{T} = \left[\begin{array}{ccc:c} & \boldsymbol{R} & & \boldsymbol{D} \\ \hdashline 0 & 0 & 0 & 1 \end{array}\right] \tag{4.2}$$

The position and orientation of the end-effector is collectively referred as *configuration* of the end-effector. The configuration of the end-effector is represented by three position components as displacements along three orthogonal axes of base frame and three rotations about the base frame axes. These six components can be represented by a six dimensional space called *configuration space* or *Cartesian space*. The kinematic description of orientation of the end-effector with respect to the base frame can be according to any of the conventions outlined in Chapter 2. The configuration, or position and orientation, of the end-effector is a function of joint displacement variables $q_1, q_2, \dots q_n$ as shown in Fig. 4.1.

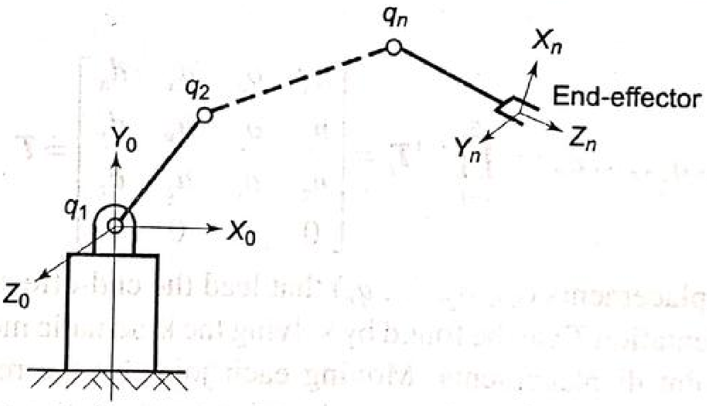

Fig. 4.1 *Configuration of end-effector as a function of joint displacements*

For an n-DOF manipulator the set of n joint displacement variables is represented by a $n \times 1$ vector. The set of all $n \times 1$ joint displacement vectors generates the *joint vector space* or *joint space*. The Cartesian space and joint space representations of a manipulator's end-effector position and orientation are related to each other by mappings shown in Fig. 4.2. The direct kinematic model is the mapping of joint space to Cartesian space, and the mapping from the Cartesian space to the joint space is the inverse problem.

In other words, the inverse kinematics is the determination of the set of positions and orientations in Cartesian space that are reachable by the origin of the end-effector frame as the joint displacements vector $\boldsymbol{q}$ ranges over the joint-space.

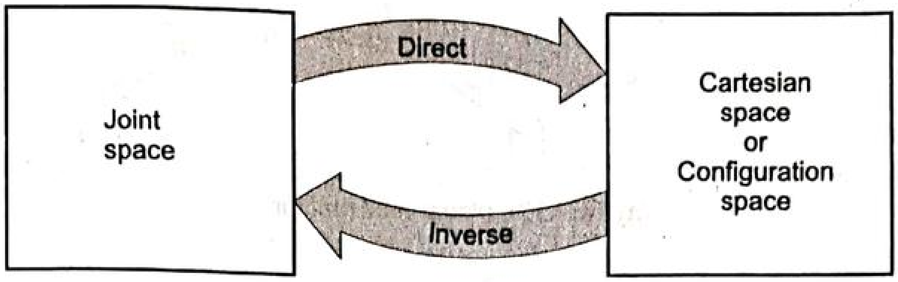

Fig. 4.2 *Mappings between kinematic descriptions*

The inverse kinematic problem is more difficult than the direct problem because no systematic procedures exist for its solution. Inverse problem of every manipulator has to be worked out separately. In this chapter, techniques to solve the inverse problem are presented. First, the concepts of manipulator workspace, solvability of kinematic equations, and existence of multiple solutions are discussed.

4.1 MANIPULATOR WORKSPACE

The workspace of a manipulator is defined as the volume of space in which the manipulator is able to locate its end-effector. The workspace gets specified by the existence or nonexistence of solutions to the inverse problem. The region that can be reached by the origin of the end-effector frame with at least one orientation is called the *reachable workspace* (RWS). If a point in workspace can be reached only in one orientation, the manipulatability of the end-effector is very poor and it is not possible to do any practical work satisfactorily with just one fixed orientation. It is, therefore, necessary to look for the points in workspace, which can be reached in more than one orientation. Some points within the RWS can be reached in more than one orientation. The space where the end-effector can reach every point from all orientations is called *dexterous workspace* (DWS). It is obvious that the dexterous workspace is either smaller (subset) or same as the reachable workspace.

As an example, consider a two-link nontrivial (2-DOF)-planar manipulator having link lengths L_1 and L_2, as shown in Fig. 4.3(a). The RWS for this manipulator is plane annular space with radii $r_1 = L_1 + L_2$ and $r_2 = |L_1 - L_2|$, as shown in Fig. 4.3(b). The DWS for this case is null. Inside the RWS there are two possible orientations of the end-effector for a given position, while on the boundaries of RWS, end-effector has only one possible orientation. For the special case of $L_1 = L_2$, the RWS is a circular area and DWS is a point at the center, as shown in Fig. 4.3(c). It can be shown that for a 3-DOF redundant planar manipulator having link lengths L_1, L_2, and L_3 with $(L_1 + L_2) > L_3$, the RWS is a circle of radius $(L_1 + L_2 + L_3)$, while the DWS is a circle of radius $(L_1 + L_2 - L_3)$.

The reachable workspace of an n-DOF manipulator is the geometric locus of the points that can be achieved by the origin of the end-effector frame as determined by the position vector of direct kinematic model. To locate the tool point or end-effector at an arbitrary position with an arbitrary orientation in 3-D space, a minimum of 6-DOF are required. Thus, for a 6-DOF-manipulator arm,

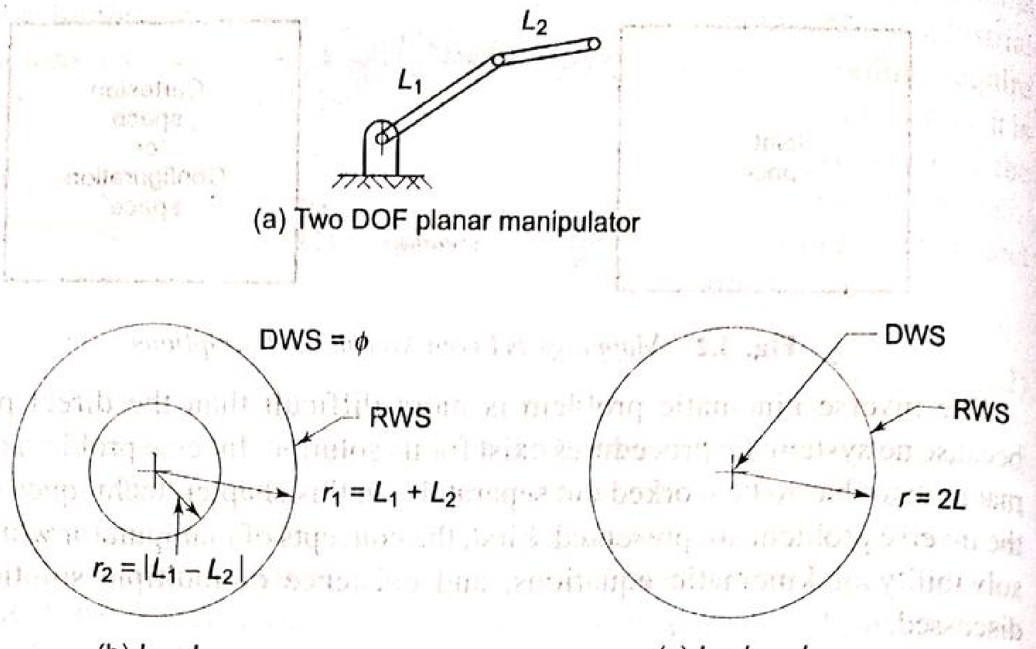

(a) Two DOF planar manipulator

(b) $L_1 \neq L_2$ (c) $L = L_1 = L_2$

Fig. 4.3 *Workspace a of a two-link planar manipulator*

the dexterous workspace may almost approach the reachable workspace. The reachable work envelops of standard manipulator configurations have been discussed in Chapter 1.

The manipulator workspace is characterized by the mechanical joint limits in addition to the configuration and the number of degrees of freedom of the manipulator. It is important to note that in Fig. 4.3, the workspaces are specified assuming a full 360° rotational joint range for each revolute joint. In practice, the joint range of revolute motion is much less than 360° for the revolute joints and is severely limited for prismatic joints, due to mechanical constraints. This limitation greatly reduces the workspace of the manipulator and the shape of workspace may not be similar to the ideal case.

To understand the effect of mechanical joint limits on the workspace, consider the 2-DOF planar manipulator with $L_1 > L_2$ and joint limits on θ_1 and θ_2 as:

$$\begin{aligned} -60^\circ \leq \theta_1 \leq 60^\circ \\ -100^\circ \leq \theta_2 \leq 100^\circ \end{aligned} \tag{4.3}$$

For these joint limits, considering $\theta_1 = \theta_2 = 0$ as home position, the annular workspace in Fig. 4.3(b) gets severely limited. The workspace, obtained geometrically, is not annular any more, rather it has a complex shape and is defined by contour ABCDEFA in Fig. 4.4.

Thus, the factors that decide the workspace of a manipulator apart from the number of degrees of freedom are the manipulator's configuration, link lengths, and the allowed range of joint motions.

4.2 SOLVABILITY OF INVERSE KINEMATIC MODEL

Inverse kinematics is complex because the solution is to be found for nonlinear simultaneous equations, involving transcendental (harmonic sine and cosine)

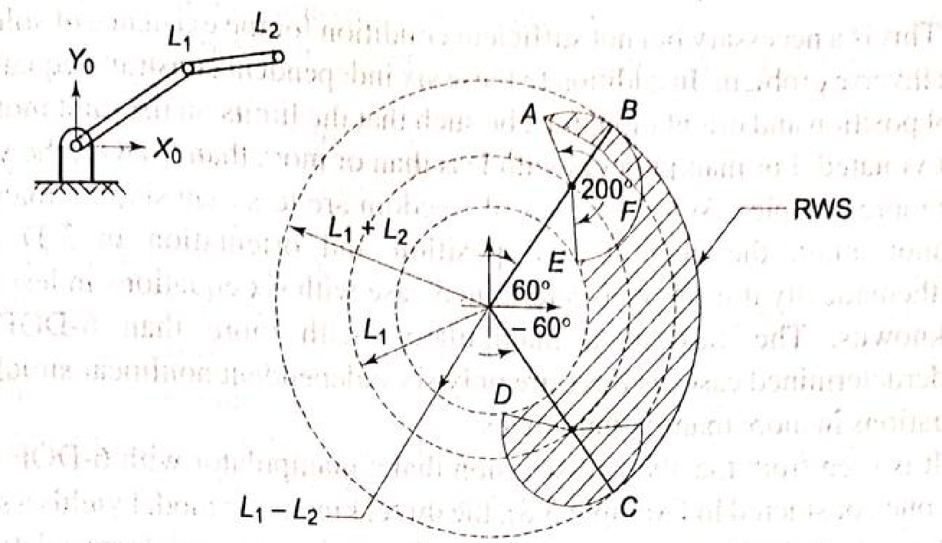

Fig 4.4 *Reachable workspace of a two-link planar manipulator with joint limits*

functions. The number of simultaneous equations is also generally more than the number of unknowns, making some of the equations mutually dependent. These conditions lead to the possibility of multiple solutions or nonexistence of any solution for the given end-effector position and orientation. The existence of solutions, multiple solutions, and methods of solutions are discussed in the following sections.

4.2.1 Existence of Solutions

The conditions for existence of solutions to the inverse kinematic problem are examined first. It is obvious that if the desired point P lies outside the reachable workspace then no solution exists. Even when P is within reachable workspace, not all orientations are realizable, unless P lies within dexterous workspace. If the wrist has fewer than 3-DOF to orient the end-effector, then certain classes of orientations are not realizable. To examine the reasons for this consider Eq. (4.1), the direct kinematic model.

As the last row of the matrix ${}^0\boldsymbol{T}_n$ in Eq. (4.1) is always constant, it can yield a maximum of 12 simultaneous equations, which are nonlinear algebraic equations involving transcendental functions in n unknowns (the joint variables). Out of these, nine equations arise from the rotation matrix (3×3) and three from the displacement vector. The nine equations of the rotation matrix involve only three unknowns corresponding to the orientation of the end-effector expressed by Euler angles or roll-pitch-yaw angles. This means that there are only six (three from orientation and three from displacement) independent constraints in n unknowns. This leads to a very important conclusion. For a manipulator to have all position and orientation solutions, the number of DOF n (equal to the number of unknowns) must at least match the number of independent constraints. That is, for general dexterous manipulation

$$n \geq 6 \tag{4.4}$$

This is a necessary but not sufficient condition for the existence of solutions to the inverse problem. In addition to these six independent constraint equations, the tool position and orientation must be such that the limits on the joint motions are not violated. For manipulators with less than or more than 6-DOF, the solutions are more complex. When degrees of freedom are less than six, the manipulator cannot attain the general goal position and orientation in 3-D space—mathematically it is an over-determined case with six equations in less than six unknowns. The case of a manipulator, with more than 6-DOF, is an underdetermined case, as there are only six independent nonlinear simultaneous equations in more than six unknowns.

It is seen from the above discussion that a manipulator with 6-DOF (such as the one considered in Example 3.8), the direct kinematic model yields a set of six independent equations in six unknowns. These six equations form a determinate set of simultaneous equations, which can be quite difficult to solve. It may be recalled that in direct kinematic model it was emphasized to choose the frames, which make as many of the joint-link parameters as possible, to zero. This leads to less complex kinematic equations and, hence, relatively simpler inverse solutions. For the case of a general mechanism with all nonzero-link parameters, the direct kinematic equations are much more complex and so will be the inverse solutions.

4.2.2 Multiple Solutions

The existence of multiple solutions is a common situation encountered in solving inverse kinematic problem. Multiple solutions pose further problem because the robot system has to have a capability to choose one, probably the best one. Multiple solutions can arise because of different factors. Some common situations, which lead to multiple solutions, are discussed as follows.

Consider the 2-DOF planar arm of Fig. 4.3(a) with a wrist having just one DOF. There are two sets of values of joint displacements (θ_1, θ_2) and (θ'_1, θ'_2), as illustrated in Fig. 4.5, which lead to the same end-effector position and orientation

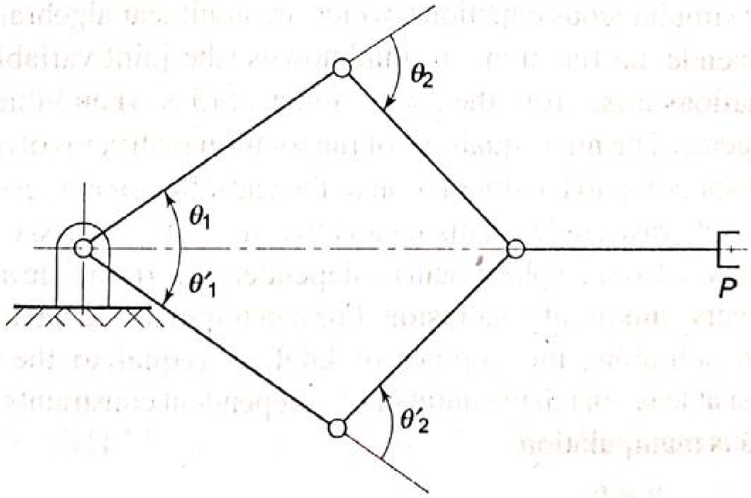

Fig. 4.5 *Multiple solutions due to parallel axes of revolute joints*

for point P. In the configuration space, both solutions are identical as they produce same configuration (position and orientation) of end-effector but are clearly distinct in joint space.

The solution (θ_1, θ_2) is 'elbow-up' position, while solution (θ'_1, θ'_2) is the 'elbow-down' position. Out of these, elbow-up solution may be preferred as in elbow-down solution joint-link may collide with objects lying on the work surface or the work table itself. The two solutions are obtained because the axes of two consecutive revolute joints of the arm are parallel. If more than two joint axes are parallel, the numbers of solutions multiply.

Another cause for multiple solutions is the existence of trigonometric functions in the equations. The harmonic nature of sine and cosine functions gives same magnitude for angles in multiples of π radians. For example, yaw, pitch, and roll motions of the RPY wrist for two sets of joint displacements $(\theta_1, \theta_2, \theta_3)$ and $(\theta'_1, \theta'_2, \theta'_3)$ with $\theta'_1 = 180° + \theta_1$, $\theta'_2 = 180° - \theta_2$ and $\theta'_3 = 180 + \theta_3$ will lead to the same orientation of the wrist. This can be easily verified.

Similarly, if the three motions of the wrist are roll, pitch, and roll; two sets of joint displacements $(\theta_1, \theta_2, \theta_3)$ and $(\theta'_1, \theta'_2, \theta'_3)$ with $\theta'_1 = 180° + \theta_1$, $\theta'_2 = -\theta_2$ and $\theta'_3 = 180° + \theta_3$ will lead to the same orientation of the wrist. With multiple solutions for positioning and orienting the end-effector, the number of solutions may multiply factorially.

The number of solutions also depends on the number of nonzero joint-link parameters and the range of joint motions allowed. In general, the number of ways to reach a certain goal is directly related to the number of nonzero link parameters. For example, for a completely general rotary-jointed, 6-DOF manipulator with all six $a_i \neq 0$, up to sixteen solutions are possible. A manipulator is said to be solvable, if it is possible to find all the solutions to its inverse kinematics problem for a given position and orientation.

Multiple solutions also arise from number of degree of freedom. For example, a manipulator with more than 6-DOF may have infinitely many solutions to the inverse kinematic problem. A manipulator with more degrees of freedom than are necessary is called *kinematically redundant* manipulator. The SCARA configuration is an example of redundant manipulator. It has one redundant degree of freedom in horizontal plane because only two joints (2-DOF) are needed to establish any horizontal position. Redundant manipulators have added flexibility, which can be useful in avoiding obstacles or reaching inaccessible locations, as illustrated in Fig. 4.6.

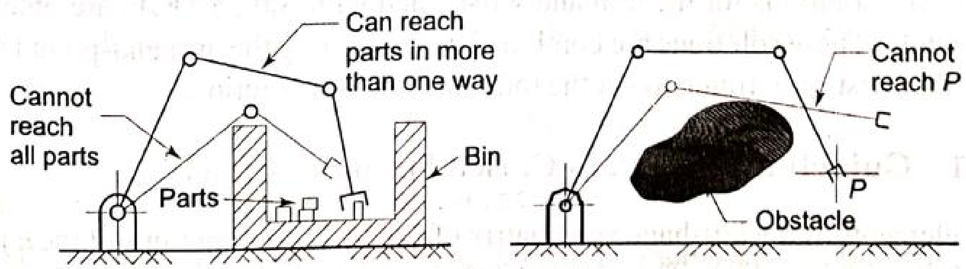

Fig. 4.6 *Use of redundant manipulator to avoid obstacles or reach around them*

4.3 SOLUTION TECHNIQUES

There are two approaches to the solutions to the inverse problem: *closed form solutions* and *numerical solutions*. In the closed form solution, joint displacements are determined as explicit functions of the position and orientation of the end-effector. In numerical methods, iterative algorithms such as the Newton-Raphson method are used. The numerical methods are computationally intensive and by nature slower compared to closed-form methods. Iterative solutions do not guarantee convergence to the correct solution in singular and degenerate cases. Iterative numerical techniques are not discussed in this text.

The "*closed form*" in the present context means a solution method based on analytical algebraic or kinematic approach, giving expressions for solving unknown joint displacements. The closed form solutions may not be possible for all kinds of structures. *A sufficient (but not necessary) condition for a 6-DOF manipulator to possess closed form solutions is that either its three consecutive joint axes intersect or its three consecutive joint axes are parallel.* The kinematic equations under either of these conditions can be reduced to algebraic equations of degree less than or equal to four for which closed form solutions exist. Almost every industrial manipulator manufactured today satisfies one of these conditions so that closed form solutions may be obtained. Manipulator arms with other kinematic structures may be solvable by analytical methods.

4.4 CLOSED FORM SOLUTIONS

Twelve equations, out of which only six are independent, are obtained by equating the elements of the manipulator transformation matrix with end-effector configuration matrix $\boldsymbol{T}$. At the same time, only six of the twelve elements of $\boldsymbol{T}$ specified by the end-effector position and orientation are independent. For a manipulator with less than 6-DOF, the number of independent equations may also be fewer than six. Several approaches such as, inverse transform, screw algebra, and kinematic approach and so on, can be used for solving these equations but none of them is general so as to solve the equations for every manipulator. A composite approach based on direct inspection, algebra, and inverse transform is presented here, which can be used to solve the inverse equations for a class of simple manipulators.

Another useful technique to reduce the complexity is dividing the problem into two smaller parts — the inverse kinematics of arm and the inverse kinematics of wrist. The solutions for the arm and wrist, each with, say, 3-DOF, are obtained separately. These solutions are combined by coinciding the arm end-point frame with the wrist-base frame to get the total manipulator solution.

4.4.1 Guidelines to Obtain Closed Form Solutions

The elements of the left-hand side matrix of Eq. (4.1) are functions of the n joint displacement variables. The elements of the right-hand side matrix $\boldsymbol{T}$ are the desired position and orientation of the end-effector and are either zero or constant. As the matrix equality implies element-by-element equality, 12 equations are obtained. To find the solution for n joint displacement variables from these 12 equations, the following guidelines are helpful.

(a) Look for equations involving only one joint variable. Solve these equations first to get the corresponding joint variable solutions.

(b) Next, look for pairs or set of equations, which could be reduced to one equation in one joint variable by application of algebraic and trigonometric identities.

(c) Use *arc tangent* (Atan2) function instead of *arc cosine* or *arc sine* functions. The two argument $A\tan 2(y, x)$ function returns the accurate angle in the range of $-\pi \leq \theta \leq \pi$ by examining the sign of both y and x and detecting whenever either x or y is zero.

(d) Solutions in terms of the elements of the position vector components of ${}^0\boldsymbol{T}_n$ are more efficient than those in terms of elements of the rotation matrix, as latter may involve solving more complex equations.

(e) In the inverse kinematic model, the right-hand side of Eq. (4.1) is known, while the left-hand side has n unknowns $(q_1, q_2, \ldots, q_n)$. The left-hand side consists of product of n link transformation matrices, that is

$$ {}^0\boldsymbol{T}_n = {}^0\boldsymbol{T}_1\, {}^1\boldsymbol{T}_2\, {}^2\boldsymbol{T}_3 \ldots {}^{n-1}\boldsymbol{T}_n = \boldsymbol{T} \tag{4.5} $$

Recall that each ${}^{i-1}\boldsymbol{T}_i$ is a function of only one unknown q_i. Premultiplying both sides by the inverse of ${}^0\boldsymbol{T}_1$ yields

$$ {}^1\boldsymbol{T}_n = {}^1\boldsymbol{T}_2\, {}^2\boldsymbol{T}_3 \ldots {}^{n-1}\boldsymbol{T}_n = [{}^0\boldsymbol{T}_1]^{-1}\boldsymbol{T} \tag{4.6} $$

The left-hand side of Eq. (4.6) has now $(n-1)$ unknowns $(q_2, q_3, \ldots, q_n)$ and the right-hand side matrix has only one unknown, the q_1. The matrix elements on the right-hand side are zero, constant, or function of the joint variable q_1. A new set of 12 equations is obtained and it may now be possible to determine q_1 from the elements of resulting equations using guideline (a) or (b) above. Similarly, by postmultiplying both sides of Eq. (4.5) by inverse of ${}^{n-1}\boldsymbol{T}_n$, unknown q_n can be determined. This process can be repeated by solving for one unknown at a time, sequentially from q_1 to q_n or q_n to q_1, until all unknowns are found. This is known as *inverse transform* approach.

The closed form solutions for the inverse kinematic model has been using the above guidelines are now illustrated with examples. For some of these examples the direct kinematic models have been obtained in Chapter 3. The multiple solutions and conditions for existence of solutions are also discussed. The first example considered is of the 3-DOF articulated arms solved in Example 3.3.

SOLVED EXAMPLES

Example 4.1 ***Articulated arm inverse kinematics***

For the 3-DOF articulated arm, whose kinematic model has been obtained in Example 3.3, determine the joint displacements for known position and orientation of the end of the arm point.

Solution Let the known position and orientation of the endpoint of arm be given by

$$T = \begin{bmatrix} r_{11} & r_{12} & r_{13} & r_{14} \\ r_{21} & r_{22} & r_{23} & r_{24} \\ r_{31} & r_{32} & r_{33} & r_{34} \\ 0 & 0 & 0 & 1 \end{bmatrix} \tag{4.7}$$

where each r_{ij} has a numeric value.

To obtain the solutions for joint variables (θ_1, θ_2, θ_3), in Eq. (4.7) $\boldsymbol{T}$ is equated to overall transformation matrix for the 3-DOF articulated arm ${}^0\boldsymbol{T}_3$ derived in Example 3.3, that is

$$\begin{bmatrix} C_1C_{23} & -C_1S_{23} & -S_1 & C_1(L_3C_{23}+L_2C_2) \\ S_1C_{23} & -S_1S_{23} & C_1 & S_1(L_3C_{23}+L_2C_2) \\ S_{23} & C_{23} & 0 & L_3S_{23}+L_2S_2 \\ 0 & 0 & 0 & 1 \end{bmatrix} = \begin{bmatrix} r_{11} & r_{12} & r_{13} & r_{14} \\ r_{21} & r_{22} & r_{23} & r_{24} \\ r_{31} & r_{32} & r_{33} & r_{34} \\ 0 & 0 & 0 & 1 \end{bmatrix} \tag{4.8}$$

Equation (4.8) gives 11 nontrivial equations for the three unknown joint variables, θ_1, θ_2, and θ_3 appearing on the left-hand side. The determination of solution for these three joint variables for known r_{ij} is the inverse kinematic problem and is worked out as follows.

Step 1 Applying guideline (a), an inspection of elements of the matrices on both the sides of Eq. (4.8) gives that θ_1 can be obtained from element 3 of row 1. The element (1,3) of left-hand side matrix has a term ($-S_1$) in only one variable θ_1 and a constant r_{13} on right-hand side and, hence, it can give angle θ_1 from $-\sin\theta_1 = r_{13}$. However, according to guideline (c) this is not preferred as correct quadrant of the angle can not be found. Alternatively, applying guideline (b), θ_1 can be isolated by dividing element (2, 1) by (1, 1) or (2, 2) by (1, 2) or (1, 3) by (2, 3) or (2, 4) by (1, 4). Out of these, the last one is preferred as per guideline (d). Thus, equating element (1, 4) and (2, 4), on both sides of the matrix two equations are obtained as

$$C_1(L_1C_{23}+L_2C_2) = r_{14} \tag{4.9}$$

$$S_1(L_3C_{23}+L_2C_2) = r_{24} \tag{4.10}$$

Dividing Eq. (4.10) by Eq. (4.9) gives

$$\frac{S_1}{C_1} = \frac{r_{24}}{r_{14}} \tag{4.11}$$

Therefore, according to guidline (c),

$$\theta_1 = \text{Atan2}(r_{24}, r_{14}) \tag{4.12}$$

Step 2 The other two unknowns, θ_2 and θ_3 cannot be obtained directly. To get a solution for θ_2 and θ_3, inverse transform approach, guideline (e), is used. To isolate θ_3, both sides of Eq. (4.8) are postmultiplied by $({}^2\boldsymbol{T}_3)^{-1}$. This will give

$${}^0\boldsymbol{T}_1\ {}^1\boldsymbol{T}_2 = \boldsymbol{T}[{}^2\boldsymbol{T}_3]^{-1} \tag{4.13}$$

From Eq. (3.21), ${}^2\boldsymbol{T}_3$ is

$$ {}^2\boldsymbol{T}_3 = \begin{bmatrix} C_3 & -S_3 & 0 & L_3C_3 \\ S_3 & C_3 & 0 & L_3S_3 \\ 0 & 0 & 1 & 0 \\ 0 & 0 & 0 & 1 \end{bmatrix} \tag{4.14} $$

The inverse of ${}^2\boldsymbol{T}_3$ is obtained using Eq. (2.53) as

$$ [{}^2\boldsymbol{T}_3]^{-1} = \left[\begin{array}{ccc:c} & {}^2\boldsymbol{R}_3^T & & -{}^2\boldsymbol{R}_3^{T\,2}\boldsymbol{D}_3 \\ \hdashline 0 & 0 & 0 & 1 \end{array}\right] = \begin{bmatrix} C_3 & S_3 & 0 & -L_3 \\ -S_3 & C_3 & 0 & 0 \\ 0 & 0 & 1 & 0 \\ 0 & 0 & 0 & 1 \end{bmatrix} \tag{4.15} $$

Substituting ${}^0\boldsymbol{T}_1$ and ${}^1\boldsymbol{T}_2$ from Eqs. (3.19) and (3.20), Example 3.3, $\boldsymbol{T}$ from Eq. (4.7) and $[{}^2\boldsymbol{T}_3]^{-1}$ from Eq. (4.15), in Eq. (4.13) gives

$$ \begin{bmatrix} C_1C_2 & -C_1S_2 & S_1 & L_2C_1C_2 \\ S_1C_2 & -S_1S_2 & -C_1 & L_2S_1C_2 \\ S_2 & C_2 & 0 & L_2S_2 \\ 0 & 0 & 0 & 1 \end{bmatrix} = \begin{bmatrix} C_3r_{11} - S_3r_{12} & S_3r_{11} + C_3r_{12} & r_{13} & -L_3r_{11} + r_{14} \\ C_3r_{21} - S_3r_{22} & S_3r_{21} - S_3r_{22} & r_{23} & -L_3r_{21} + r_{24} \\ C_3r_{31} - S_3r_{32} & S_3r_{31} - S_3r_{32} & r_{32} & -L_3r_{31} + r_{34} \\ 0 & 0 & 0 & 1 \end{bmatrix} \tag{4.16} $$

Note that the left-hand side of Eq. (4.16) has only θ_1 and θ_2 terms and the right-hand side has only θ_3 terms. A close examination of both sides reveals that equations obtained from elements (1, 4), (2, 4), and (3, 4) are only function of θ_1 and θ_2. Thus, with use of some algebra and trigonometric identities, θ_1 can be eliminated and solution for θ_2 is obtained. Equating the elements (1, 4), (2, 4), and (3, 4) of the two matrices, three equations obtained are

$$ L_2C_1C_2 = -L_3r_{11} + r_{14} \tag{4.17} $$

$$ L_2S_1C_2 = -L_3r_{21} + r_{24} \tag{4.18} $$

$$ L_2S_2 = -L_3r_{31} + r_{34} \tag{4.19} $$

By squaring Eqs. (4.17) and (4.18), and adding gives,

$$ L_2^2C_2^2(C_1^2 + S_1^2) = (-L_3r_{11} + r_{14})^2 + (-L_3r_{21} + r_{24})^2 $$

From this θ_1 is eliminated because $C_1^2 + S_1^2 = 1$, thus

$$ L_2C_2 = \pm\sqrt{(-L_3r_{11} + r_{14})^2 + (-L_3r_{21} + r_{24})^2} \tag{4.20} $$

Dividing Eq. (4.19) by Eq. (4.20), gives

$$ \frac{S_2}{C_2} = \frac{-L_3r_{31} + r_{34}}{\pm\sqrt{(-L_3r_{11} + r_{14})^2 + (-L_3r_{21} + r_{24})^2}} \tag{4.21} $$

Hence,

$$ \theta_2 = \mathrm{Atan2}\left((-L_3r_{31} + r_{34}), \pm\sqrt{(-L_3r_{11} + r_{14})^2 + (-L_3r_{21} + r_{24})^2}\right) \tag{4.22} $$

Step 3 The solution for θ_3 is obtained by first solving for $(\theta_2 + \theta_3)$. Dividing element (3,1) of Eq. (4.8) by element (3,2) gives

$$\frac{S_{23}}{C_{23}} = \frac{r_{31}}{r_{32}} \tag{4.23}$$

or

$$\theta_2 + \theta_3 = \text{Atan2}(r_{31}, r_{32}) \tag{4.24}$$

Thus,

$$\theta_3 = \text{Atan2}\ (r_{31}, r_{32}) - \theta_2 \tag{4.25}$$

Equations (4.12), (4.22), and (4.25) give the complete solution for the 3-DOF articulated arm as expressions for the joint displacements θ_1, θ_2, and θ_3 in terms of known arm end-point position and orientation. Note that the above solution is one of the possible sets of expressions. Alternate expressions for θ_1, θ_2, and θ_3 would be obtained if instead of equating the chosen elements of the matrices, other elements are used, or instead of isolating θ_3, θ_1 is isolated by premultiplying both sides with $({}^0\boldsymbol{T}_1)^{-1}$. It is also possible to find solution without use of the inverse matrix approach and instead of using algebra and trigonometry. For instance, after solving for θ_1, $(\theta_2 + \theta_3)$ can be obtained from elements (3, 1) and (3, 2) and through trigonometric manipulation, θ_2 and θ_3 are obtained.

Example 4.2 *Inverse kinematics of RPY wrist*

For the 3-DOF RPY wrist kinematic model was obtained in Example 3.4, Eq. (3.27), as

$${}^0\boldsymbol{T}_3 = \begin{bmatrix} -C_1S_2C_3 + S_1S_3 & C_1S_2S_3 + S_1C_3 & C_1C_2 & 0 \\ -S_1S_2C_3 - C_1S_3 & S_1S_2S_3 - C_1C_3 & S_1C_2 & 0 \\ C_2C_3 & -C_2S_3 & S_2 & 0 \\ 0 & 0 & 0 & 1 \end{bmatrix} \tag{4.26}$$

Determine the solution for the three joint variables for a given end-effector orientation matrix $\boldsymbol{T}_E$.

$$\boldsymbol{T}_E = \begin{bmatrix} n_x & o_x & a_x & 0 \\ n_y & o_y & a_y & 0 \\ n_z & o_z & a_z & 0 \\ 0 & 0 & 0 & 1 \end{bmatrix} \tag{4.27}$$

Solution The overall transformation matrix ${}^0\boldsymbol{T}_3$ and end-effector matrix $\boldsymbol{T}_E$ represent the same transformations. Thus, equating Eqs. (4.26) and (4.27) gives

$$\begin{bmatrix} n_x & o_x & a_x & 0 \\ n_y & o_y & a_y & 0 \\ n_z & o_z & a_z & 0 \\ 0 & 0 & 0 & 1 \end{bmatrix} = \begin{bmatrix} -C_1S_2C_3 + S_1S_3 & C_1S_2S_3 + S_1C_3 & C_1C_2 & 0 \\ -S_1S_2C_3 - C_1S_3 & S_1S_2S_3 - C_1C_3 & S_1C_2 & 0 \\ C_2C_3 & -C_2S_3 & S_2 & 0 \\ 0 & 0 & 0 & 1 \end{bmatrix} \tag{4.28}$$

The elements of the matrix on left-hand side of matrix equation are known (given), while, the elements of matrix on right-hand side have three unknown joint variables θ_1, θ_2 and θ_3. To get the solution for these joint variables, the more consistent analytical approach (guideline (e)) is used here.

Guideline (e) suggests premultiplying the matrix equation, Eq. (4.28) by inverse of transformation matrix ${}^0\boldsymbol{T}_1$ involving the unknown θ_1 and from the elements of the resultant matrix equation determine the unknown. Recall that the right-hand side of Eq. (4.28) is the product of three transformation matrices ${}^0\boldsymbol{T}_1$, ${}^1\boldsymbol{T}_2$ and ${}^2\boldsymbol{T}_3$ each involving one unknown θ_1, θ_2 and θ_3, respectively.

This process is continued successively, that is, moving one unknown (by its inverse transform) from right-hand side of the matrix equation to the left-hand side of the matrix equation and solving it, then moving the next unknown to the left-hand side, until all unknown are solved.

To solve for θ_1, both sides of Eq. (4.28) are premultiplied by ${}^0\boldsymbol{T}_1^{-1}$. From Eqs. (3.24) – (3.26)

$$\begin{bmatrix} C_1 & S_1 & 0 & 0 \\ 0 & 0 & 1 & 0 \\ S_1 & -C_1 & 0 & 0 \\ 0 & 0 & 0 & 1 \end{bmatrix}\begin{bmatrix} n_x & o_x & a_x & 0 \\ n_y & o_y & a_y & 0 \\ n_z & o_z & a_z & 0 \\ 0 & 0 & 0 & 1 \end{bmatrix} = \begin{bmatrix} -S_2 & 0 & C_2 & 0 \\ C_2 & 0 & S_2 & 0 \\ 0 & 1 & 0 & 0 \\ 0 & 0 & 0 & 1 \end{bmatrix}\begin{bmatrix} C_3 & -S_3 & 0 & 0 \\ S_3 & C_3 & 0 & 0 \\ 0 & 0 & 1 & 0 \\ 0 & 0 & 0 & 1 \end{bmatrix}.$$

or

$$\begin{bmatrix} C_1 n_x + S_1 n_y & C_1 o_x + S_1 o_y & C_1 a_x + S_1 a_y & 0 \\ n_z & o_z & a_z & 0 \\ S_1 n_x - C_1 n_y & S_1 o_x - C_1 o_y & S_1 a_x - C_1 a_y & 0 \\ 0 & 0 & 0 & 1 \end{bmatrix} = \begin{bmatrix} -S_2 C_3 & S_2 S_3 & C_2 & 0 \\ C_2 C_3 & -C_2 S_3 & S_2 & 0 \\ S_3 & C_3 & 0 & 0 \\ 0 & 0 & 0 & 1 \end{bmatrix} \tag{4.29}$$

The left-hand side of Eq. (4.29) has one unknown (θ_1) and the right-hand side has two unknown (θ_2 and θ_3). Scanning the elements of both the matrices in Eq. (4.29), the equation in one unknown (θ_1) is obtained by equating elements (3, 3). That is,

$$S_1 a_x - C_1 a_y = 0 \tag{4.30}$$

or

$$\frac{S_1}{C_1} = \tan\theta_1 = \frac{a_y}{a_x}$$

which gives

$$\theta_1 = \text{Atan2}(a_y, a_x) \tag{4.31}$$

The process of further premultiplication is not necessary because the solutions for the remaining two unknowns (θ_2 and θ_3) can be obtained from Eq. (4.29). Equating (1, 3) and (2, 3) elements on both sides in Eq. (4.29) gives

$$\begin{aligned} C_2 &= C_1 a_x + S_1 a_y \\ S_2 &= a_z \end{aligned} \tag{4.32}$$

From these two equations the solution for θ_2 is obtained as

$$\theta_2 = \text{Atan2}(a_z,\ C_1a_x + S_1a_y) \tag{4.33}$$

Equating elements (3,1) and (3, 2) of Eq. (4.29) gives

$$S_3 = S_1n_x - C_1n_y$$

$$C_3 = S_1o_x - C_1o_y \tag{4.34}$$

Which lead to the solution for θ_3 as

$$\theta_3 = \text{Atan2}(S_1n_x - C_1n_y,\ S_1o_x - C_1o_y) \tag{4.35}$$

The inverse transform technique is to move one unknown to the left-hand side at a time and solve it. Therefore, it is also possible to achieve this by postmultiplying instead of premultiplying by the inverse transform matrix involving an unknown. This is illustrated here.

To solve for θ_3, that is, to move it to the left-hand side, postmultiplying both sides of matrix equation Eq. (4.28) by ${}^2T_3^{-1}$ gives

$$\begin{bmatrix} n_x & o_x & a_x & 0 \\ n_y & o_y & a_y & 0 \\ n_z & o_z & a_z & 0 \\ 0 & 0 & 0 & 1 \end{bmatrix}\begin{bmatrix} C_3 & S_3 & 0 & 0 \\ -S_3 & C_3 & 0 & 0 \\ 0 & 0 & 1 & 0 \\ 0 & 0 & 0 & 1 \end{bmatrix} = \begin{bmatrix} C_1 & 0 & S_1 & 0 \\ S_1 & 0 & -C_1 & 0 \\ 0 & 1 & 0 & 0 \\ 0 & 0 & 0 & 1 \end{bmatrix}\begin{bmatrix} -S_2 & 0 & C_2 & 0 \\ C_2 & 0 & S_2 & 0 \\ 0 & 1 & 0 & 0 \\ 0 & 0 & 0 & 1 \end{bmatrix}$$

or

$$\begin{bmatrix} C_3n_x - S_3o_x & S_3n_x + C_3o_x & a_x & 0 \\ C_3n_y - S_3o_y & S_3n_y + C_3o_y & a_y & 0 \\ C_3n_z - S_3o_z & S_3n_z + C_3o_z & a_z & 0 \\ 0 & 0 & 0 & 1 \end{bmatrix} = \begin{bmatrix} -C_1S_2 & S_1 & C_1C_2 & 0 \\ -S_1S_2 & -C_1 & S_1C_2 & 0 \\ C_2 & 0 & S_2 & 0 \\ 0 & 0 & 0 & 1 \end{bmatrix} \tag{4.36}$$

Comparing elements of the matrices on both sides, the elements (3, 2) gives

$$S_3n_z + C_3o_z = 0$$

and, thus, the solution for θ_3 is

$$\theta_3 = \text{Atan2}\ (-o_z,\ n_y) \tag{4.37}$$

Similarly, from the elements (3,1) and (3, 3), θ_2 is obtained as

$$\theta_2 = \text{Atan2}\ (a_z,\ C_3n_z - S_3o_z) \tag{4.38}$$

and from the elements (1, 2) and (2, 2), θ_1 is obtained as

$$\theta_1 = \text{Atan2}(S_3\,n_x + C_3o_x,\ -S_3\,n_y - C_3o_y) \tag{4.39}$$

In this example, premulitplying or postmultiplying gives solution of similar complexity but this may not be always the case. The decision to premultiply or postmultiply is left to the discretion of the reader.

Example 4.3 *SCARA manipulator inverse kinematics*

Analytically solve the inverse kinematic problem for the 4-DOF SCARA configuration manipulator given in Fig. 3.22, Example 3.6. Discuss the conditions for existence and multiplicity of solutions.

Solution For the SCARA manipulator of Example 3.6, equating ${}^0T_4$ from Eq. (3.40) with T in Eq. (4.7) gives

$$\begin{bmatrix} C_{124} & S_{124} & 0 & L_2C_{12}+L_{11}C_1 \\ S_{124} & -C_{124} & 0 & L_2S_{12}+L_{11}S_1 \\ 0 & 0 & 1 & L_{12}+d_3-L_4 \\ 0 & 0 & 0 & 1 \end{bmatrix} = \begin{bmatrix} r_{11} & r_{12} & r_{13} & r_{14} \\ r_{21} & r_{22} & r_{23} & r_{24} \\ r_{31} & r_{32} & r_{33} & r_{34} \\ 0 & 0 & 0 & 1 \end{bmatrix} \tag{4.40}$$

The solution for joint displacement d_3 is directly obtained by equating the elements (3, 4) on both sides of Eq. (4.40),

$$L_{12} + d_3 - L_4 = r_{34}$$

or

$$d_3 = r_{34} + L_4 - L_{12} \tag{4.41}$$

Next, to solve for θ_1 elements (1, 4) and (2, 4) are compared. This gives

$$L_2C_{12} + L_{11}C_1 = r_{14} \tag{4.42}$$

$$L_2S_{12} + L_{11}S_1 = r_{24} \tag{4.43}$$

Squaring Eqs. (4.42) and (4.43), adding and simplifying using the trigonometric identity $\cos(\alpha+\beta) = \cos\alpha\cos\beta - \sin\alpha\sin\beta$, gives

$$L_{11}^2 + L_2^2 + 2L_{11}L_2C_2 = r_{14}^2 + r_{24}^2 \tag{4.44}$$

$$C_2 = \frac{r_{14}^2 + r_{24}^2 - L_{11}^2 - L_2^2}{2L_{11}L_2} \tag{4.45}$$

Since

$$S_2 = \pm\sqrt{1-C_2^2} \tag{4.46}$$

the solution for θ_2 is obtained from Eqs. (4.45) and (4.46) as

$$\theta_2 = \text{Atan2}(S_2, C_2) \tag{4.47}$$

Now that θ_2 being known, Eqs. (4.42) and (4.43) can be used to compute θ_1. These equations are written as

$$L_2(C_1C_2 - S_1S_2) + L_{11}C_1 = r_{14} \tag{4.48}$$

$$L_2(S_1C_2 + C_1S_2) + L_{11}S_1 = r_{24} \tag{4.49}$$

or

$$(L_{11} + L_2C_2)C_1 - (L_2S_2)S_1 = r_{14} \tag{4.50}$$

$$(L_{11} + L_2C_2)S_1 + (L_2S_2)C_1 = r_{24} \tag{4.51}$$

Let

$$(L_{11} + L_2C_2) = r\cos\phi \text{ and } (L_2S_2) = r\sin\phi \tag{4.52}$$

with

$$r = \sqrt{(L_{11} + L_2C_2)^2 + (L_2S_2)^2} \tag{4.53}$$

and

$$\phi = \text{Atan2}\left(\frac{L_2S_2}{r}, \frac{L_{11} + L_2C_2}{r}\right) \tag{4.54}$$

Eqs. (4.50) and (4.51) reduce to

$$r\cos(\theta_1 + \phi) = r_{14} \tag{4.55}$$

$$r\sin(\theta_1 + \phi) = r_{24} \tag{4.56}$$

From Eqs. (4.55) and (4.56), θ_1 is obtained as

$$\theta_1 = \text{Atan2}\left(\frac{r_{24}}{r}, \frac{r_{14}}{r}\right) - \phi \tag{4.57}$$

$$\theta_1 = \text{Atan2}\left(\frac{r_{24}}{r}, \frac{r_{14}}{r}\right) - \text{Atan2}\left(\frac{L_2 S_2}{r}, \frac{L_{11} + L_2 C_2}{r}\right) \tag{4.58}$$

With θ_1, θ_2 and d_3 determined, only one variable, θ_4 is unknown. From elements (1,1) and (2,1), the equations are

$$C_{124} = r_{11} \tag{4.59}$$

$$S_{124} = r_{21} \tag{4.60}$$

Equations (4.59) and (4.60) give θ_4 as

$$\theta_1 + \theta_2 - \theta_4 = \text{Atan2}(r_{21}, r_{11})$$

or

$$\theta_4 = \theta_2 + \theta_1 - \text{Atan2}\,(r_{21}, r_{11}) \tag{4.61}$$

The complete closed form solution for the joint displacements θ_1, θ_2, d_3 and θ_4, of SCARA manipulator, is given by Eqs. (4.58), (4.47), (4.41) and (4.61), respectively, as explicit functions of the manipulator's tool position and orientation.

Existence of Solutions

Solutions to the inverse kinematic problem of a given arm exist, that is, the given Cartesian position and orientation of the tool is within the manipulator's workspace if the following condition is satisfied:

"Since *sin* and *cos* functions take values in the range [–1,1], right-hand side of the Eq. (4.45) must lie in the range [–1,1]."

Again, these solutions are for full 360 degrees of rotation for the revolute joints and limitless translation for the prismatic joint. The mechanical constraints, however, will permit only such solutions for which the joint variables take a value that lies in the range of motions allowed.

Multiplicity of Solutions

Due to the presence of the square root in Eq. (4.46), there are two solutions for θ_2 for a given position and orientation of the tool with respect to the base. From Eqs. (4.57) and (4.61), observe that there is one set of solution for θ_1 and θ_4 corresponding to each value of θ_2. Thus, the number of solutions to the inverse kinematics problem of the given SCARA arm is two. Note that multiple solutions exist due to the fact that revolute joint axes 1 and 2 are parallel.

Example 4.4 ***Numerical solutions for a 3-DOF manipulator***

For the 3-DOF (RRP) configuration manipulator, shown in Fig. 4.7, the position and orientation of point P in Cartesian space is given by

$$T = \begin{bmatrix} 0.354 & 0.866 & 0.354 & 0.106 \\ -0.612 & 0.500 & -0.612 & -0.184 \\ 0.707 & 0 & 0.707 & 0.212 \\ 0 & 0 & 0 & 1 \end{bmatrix} \tag{4.62}$$

Determine all values of all joint variables, that is, all solutions to the inverse kinematic problem. The joint displacements allowed (joint limits) for three joints are: $-100° < \theta_1 < 100°$, $-30° < \theta_2 < 70°$ and $0.05\text{m} < d_3 < 0.5$ m. Identify the feasible solutions.

Solution A manipulator with this configuration is another common structure widely used in industrial robots, as it is very effective in material handling and other applications, and gives a spherical workspace. The first two joints are revolute joints and provide motion in two perpendicular planes. Their sweep generates a constant radius sphere. The third prismatic joint provides the reach to the arm point where the wrist is attached. The three joint axes intersect at a point.

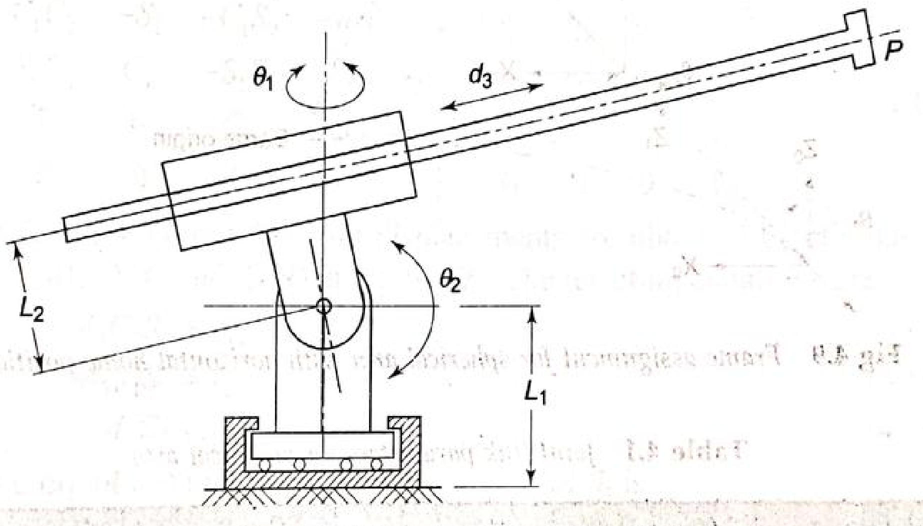

Fig. 4.7 *A 3-DOF spherical configuration arm*

The forward kinematic model is obtained first. For the forward kinematic model, the frame assignment for the home position is carried out first. While assigning frames it is observed that the link dimension L_1 can be eliminated from the kinematic model by choosing the origin of frame {0} to coincide with origin of frame {1} at joint 2 (see Example 3.3). The link dimension L_2 can be made zero by modifying the design slightly as shown in Fig. 4.8 such that the axis of prismatic link passes through the origin of frame {1}.

The final frame assignment with the origin of three frames, frame {0}, frame {1} and frame {2} at the same point is shown in Fig. 4.9. This minimizes the number of non-zero parameters as well as satisfies the necessary condition for existence of closed form solutions.

The joint-link parameters are tabulated in Table 4.1

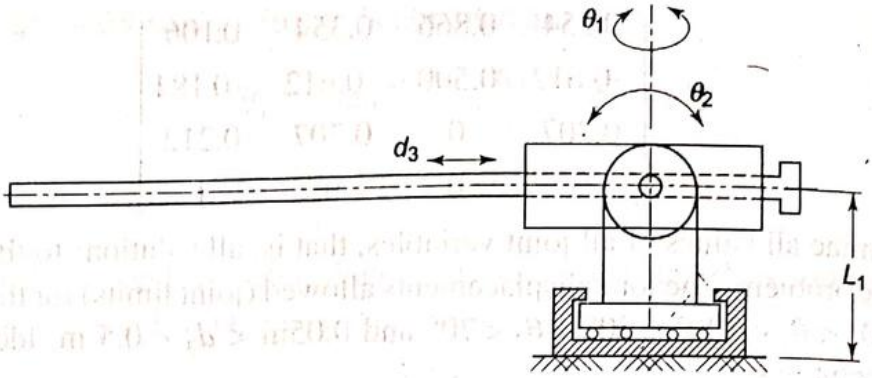

Fig. 4.8 *3-DOF spherical arm in home position:* $\theta_1 = \theta_2 = 0$ and $d_3 = 0.05$

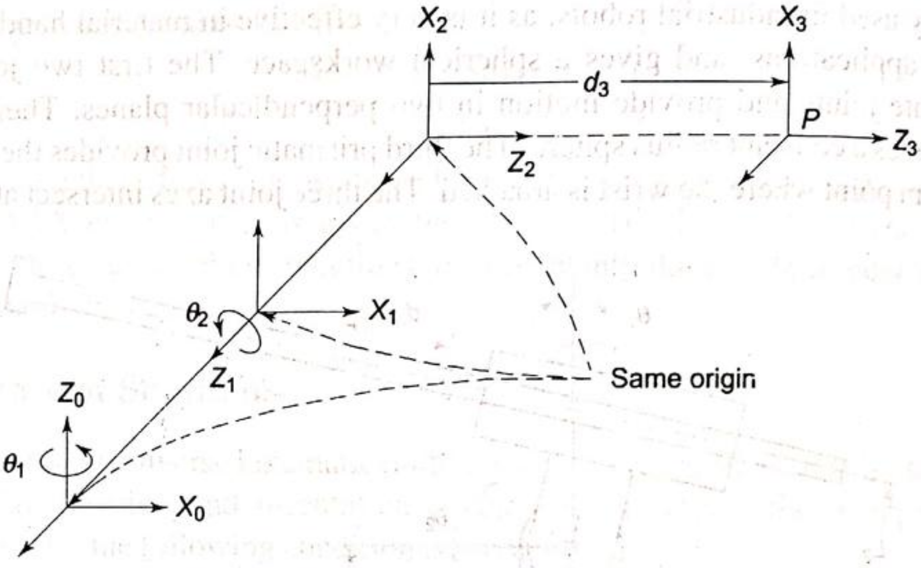

Fig 4.9 *Frame assignment for spherical arm with horizontal home position*

Table 4.1 *Joint-link parameters for spherical arm*

Link i	a_i	α_i	d_i	θ_i	q_i	$C\theta_i$	$S\theta_i$	$C\alpha_i$	$S\alpha_i$
1	0	90°	0	θ_1	θ_1	C_1	S_1	0	1
2	0	−90°	0	θ_2	θ_2	C_2	S_2	0	1
3	0	0	d_3	0	d_3	1	0	1	0

The three link transformation matrices ${}^0T_1$, ${}^1T_2$, ${}^2T_3$ and the overall arm transformation matrix ${}^0T_3$ are obtained as

$$
{}^0T_1(\theta_1) = \begin{bmatrix} C_1 & 0 & S_1 & 0 \\ S_1 & 0 & -C_1 & 0 \\ 0 & 1 & 0 & 0 \\ 0 & 0 & 0 & 1 \end{bmatrix} \tag{4.63}
$$

$$
{}^1T_2(\theta_2) = \begin{bmatrix} C_2 & 0 & -S_2 & 0 \\ S_2 & 0 & C_2 & 0 \\ 0 & -1 & 0 & 0 \\ 0 & 0 & 0 & 1 \end{bmatrix} \tag{4.64}
$$

$$
{}^2T_3(d_3) = \begin{bmatrix} 1 & 0 & 0 & 0 \\ 0 & 1 & 0 & 0 \\ 0 & 0 & 1 & d_3 \\ 0 & 0 & 0 & 1 \end{bmatrix} \tag{4.65}
$$

and, thus,

$$
{}^0T_3 = {}^0T_1\,{}^1T_2\,{}^2T_3 = \begin{bmatrix} C_1C_2 & -S_1 & -C_1S_2 & -d_3C_1S_2 \\ S_1C_2 & C_1 & -S_1S_2 & -d_3S_1S_2 \\ S_2 & 0 & C_2 & d_3C_2 \\ 0 & 0 & 0 & 1 \end{bmatrix} \tag{4.66}
$$

First, a generalized solution is worked out, as in previous examples and then the values from Eq. (4.62) will be substituted to get specific solutions. Let the arm point position and orientation be specified as in Eq. (4.7).

The kinematic model equations are thus, obtained by equating Eq. (4.66) and Eq. (4.7) giving

$$
\begin{bmatrix} C_1C_2 & -S_1 & -C_1S_2 & -d_3C_1S_2 \\ S_1C_2 & C_1 & -S_1S_2 & -d_3S_1S_2 \\ S_2 & 0 & C_2 & d_3C_2 \\ 0 & 0 & 0 & 1 \end{bmatrix} = \begin{bmatrix} r_{11} & r_{12} & r_{13} & r_{14} \\ r_{21} & r_{22} & r_{23} & r_{24} \\ r_{31} & r_{32} & r_{33} & r_{34} \\ 0 & 0 & 0 & 1 \end{bmatrix}, \tag{4.67}
$$

The preferred solutions for joint displacements are obtained by comparing elements (1, 4), (2, 4) and (3, 4) in Eq. (4.67). The resulting equations are

$$-d_3C_1S_2 = r_{14} \tag{4.68}$$

$$-d_3S_1S_2 = r_{24} \tag{4.69}$$

$$d_3C_2 = r_{34} \tag{4.70}$$

Dividing Eq. (4.69) by Eq. (4.68) the solution for θ_1 is

$$\theta_1 = \text{Atan2}(-r_{24}, -r_{14}) \tag{4.71}$$

Squaring and adding Eq. (4.68) and Eq. (4.69) gives

$$d_3^2\, S_2^2\,(C_1^2 + S_1^2) = r_{14}^2 + r_{24}^2$$

or

$$d_3S_2 = \pm\sqrt{r_{14}^2 + r_{24}^2} \tag{4.72}$$

Dividing Eq. (4.72) by Eq. (4.70) gives solution of θ_2 as

$$\theta_2 = \text{Atan2}\left(\pm\sqrt{r_{14}^2 + r_{24}^2}\,,\, r_{34}\right) \tag{4.73}$$

The joint displacement d_3 for joint 3 is obtained by squaring and adding Eqs. (4.68), (4.69) and (4.70). Since the displacement d_3 cannot be negative, only positive sign is used. Thus,

$$d_3 = +\sqrt{r_{14}^2 + r_{24}^2 + r_{34}^2} \tag{4.74}$$

The numerical values for joint displacements are obtained by substituting the values from given arm point position and orientation matrix, Eq. (4.62), in to Eqs. (4.71), (4.73) and (4.74). The specific solutions are:

$$\theta_1 = \text{Atan2}\ (0.184, -0.106) = -\ 60°$$

$$\theta_2 = \text{Atan2}\left(\pm\sqrt{(0.106)^2 + (-0.184)^2},\ 0.212\right) = \pm\ 45° \tag{4.75}$$

$$\theta_3 = \text{Atan2}\ \sqrt{(0.106)^2 + (-0.184)^2 + (0.212)^2} = 0.30$$

The two possible solutions are tabulated in Table 4.2.

Table 4.2 *Two possible solutions for the specified arm point*

Solution No.	θ_1	θ_2	d_3
1	–60°	–45°	0.30
2	–60°	45°	0.30

The joint range specified for joint 2 is: $-30° < \theta_2 < 70°$. The solution 1 specifies angle θ_2 as $\theta_2 = -45°$. This violates the joint range constraint and, hence, solution 1 is not feasible.

Example 4.5 *Inverse Kinematics of 5-DOF Manipulator*

For the 5-DOF industrial manipulator discussed in Example 3.7, obtain the analytical solutions of joint variables.

Solution Let the end-effector tool point transformation matrix be given by

$$\boldsymbol{T}_E = \begin{bmatrix} n_x & o_x & a_x & d_x \\ n_y & o_y & a_y & d_y \\ n_z & o_z & a_z & d_z \\ 0 & 0 & 0 & 1 \end{bmatrix} \tag{4.76}$$

From the kinematic model obtained in Example 3.7, the overall transformation matrix for the end-effector tool point is (Eq. (3.48))

$${}^0\boldsymbol{T}_5 = \begin{bmatrix} C_1S_{234}C_5 + S_1S_5 & -C_1S_{234}S_5 + S_1C_5 & C_1C_{234} & C_1(L_2C_2 + L_3C_{23} + L_5C_{234}) \\ S_1C_{234}C_5 - C_1S_5 & -S_1S_{234}S_5 - C_1C_5 & S_1C_{234} & S_1(L_2C_2 + L_3C_{23} + L_5C_{234}) \\ -C_{234}C_5 & C_{234}S_5 & -S_{234} & L_1 - L_2S_2 - L_3S_{23} - L_5S_{234} \\ 0 & 0 & 0 & 1 \end{bmatrix} \tag{4.77}$$

A close examination of Eqs.(4.76) and (4.77) clearly shows that no direct solution can be found for any of the joint-variables. Hence, the inverse matrix approach of guideline (e) is used here,

In order to solve for first joint variable θ_1, both matrices, Eq. (4.76) and Eq. (4.77) are premultiplied by inverse of ${}^0\boldsymbol{T}_1$ (that is ${}^0\boldsymbol{T}_1^{-1}$. This given left-hand side matrix of equation as

$$
{}^0T_1^{-1}\,{}^1T_E = \begin{bmatrix} C_1n_x + S_1n_y & C_1o_x + S_1o_y & C_1a_x + S_1a_y & C_1d_x + S_1d_y \\ -n_z & -o_z & -a_z & -d_z + L_1 \\ -S_1n_x + C_1n_y & -S_1o_x + C_1o_y & -S_1a_x + C_1a_y & -S_1d_x + C_1d_y \\ 0 & 0 & 0 & 1 \end{bmatrix} \tag{4.78}
$$

and the right-hand side of matrix equation is

$$
{}^1T_5 = {}^1T_2\,{}^2T_3\,{}^3T_4\,{}^4T_5 = \begin{bmatrix} S_{234}C_5 & S_{234}S_5 & C_{234} & L_5C_{234} + L_3C_{23} + L_2C_2 \\ -C_{234}C_5 & C_{234}S_5 & S_{234} & L_5S_{234} + L_3S_{23} + L_2S_2 \\ -S_5 & -C_5 & 0 & 0 \\ 0 & 0 & 0 & 1 \end{bmatrix} \tag{4.79}
$$

or

$$
\begin{bmatrix} C_1n_x + S_1n_y & C_1o_x + S_1o_y & C_1a_x + S_1a_y & C_1d_x + S_1d_y \\ -n_z & -o_z & -a_z & -d_z + L_1 \\ -S_1n_x + C_1n_y & -S_1o_x + C_1o_y & -S_1a_x + C_1a_y & -S_1d_x + C_1d_y \\ 0 & 0 & 0 & 1 \end{bmatrix}
$$

$$
= \begin{bmatrix} S_{234}C_5 & S_{234}S_5 & C_{234} & L_5C_{234} + L_3C_{23} + L_2C_2 \\ -C_{234}C_5 & C_{234}S_5 & S_{234} & L_5S_{234} + L_3S_{23} + L_2S_2 \\ -S_5 & -C_5 & 0 & 0 \\ 0 & 0 & 0 & 1 \end{bmatrix} \tag{4.80}
$$

Comparing elements of Eq. (4.80), the single variable equations in θ_1 are obtained from elements (3, 3) and (3, 4) as:

$$
\begin{aligned} -S_1a_x + C_1a_y &= 0 \\ -S_1d_x + C_1d_y &= 0 \end{aligned} \tag{4.81}
$$

Using the later, the solution for θ_1 is

$$
\theta_1 = A\tan2(d_y,\ d_x) \tag{4.82}
$$

From ratio of elements (3, 1) and (3, 2), solution for θ_5 is obtained as

$$
\begin{aligned} -S_5 &= -S_1n_x + C_1n_y \\ -C_5 &= -S_1o_x + C_1o_y \end{aligned} \tag{4.83}
$$

or
$$
\theta_5 = A\tan2(-S_1n_x + C_1n_y, -S_1o_x + C_1o_y) \tag{4.84}
$$

The solution for remaining three variables θ_2, θ_3 and θ_4 is obtained by first solving for $\theta_2 + \theta_3 + \theta_4$. Equating elements (1, 3) and (2, 3) gives

$$
\begin{aligned} C_{234} &= C_1a_x + S_1a_y \\ S_{234} &= -a_z \end{aligned} \tag{4.85}
$$

which leads to

$$\theta_{234} = \theta_2 + \theta_3 + \theta_4 = A\tan2(-a_z,\ C_1 a_x + S_1 a_y) \tag{4.86}$$

Premultiplying both sides of Eq. (4.80) by $({}^1\boldsymbol{T}_2)^{-1}$, gives

$$({}^1\boldsymbol{T}_2)^{-1}({}^0\boldsymbol{T}_1)^{-1}\boldsymbol{T}_E = {}^2\boldsymbol{T}_3\,{}^3\boldsymbol{T}_4\,{}^4\boldsymbol{T}_5 \tag{4.87}$$

$$\begin{bmatrix} C_2(C_1 n_x + S_1 n_y) - S_2 n_z & C_2(C_1 o_x + S_1 o_y) - S_2 o_z & C_2(C_1 a_x + S_1 a_y) - S_2 a_z & C_2(C_1 d_x + S_1 d_y) - S_2(d_z - L_1) - L_2 \\ -S_2(C_1 n_x + S_1 n_y) - C_2 n_z & -S_2(C_1 o_x + S_1 o_y) - C_2 o_z & -S_2(C_1 a_x + S_1 a_y) - C_2 a_z & -S_2(C_1 d_x + S_1 d_y) - C_2(d_z + L_1) \\ -S_1 n_x + C_1 n_y & -S_1 o_x + C_1 o_y & -S_1 a_x + C_1 a_y & -S_1 d_x + C_1 d_y \\ 0 & 0 & 0 & 1 \end{bmatrix}$$

$$= \begin{bmatrix} S_{34}C_5 & -S_{34}S_5 & C_{34} & L_5 C_{34} + L_3 C_3 \\ -C_{34}C_5 & C_{34}S_5 & S_{34} & L_5 S_{34} + L_3 C_3 \\ -S_5 & -C_5 & 0 & 0 \\ 0 & 0 & 0 & 1 \end{bmatrix} \tag{4.88}$$

From elements (1, 1) and (1, 2), two equations are obtained:

$$C_2\left(C_1 n_x + S_1 n_y\right) - S_2 n_z = S_{34} C_5 \tag{4.89}$$

$$C_2\left(C_1 o_x + S_1 o_y\right) - S_2 o_z = -S_{34} S_5 \tag{4.90}$$

Dividing Eq. (4.90) by Eq. (4.89) and rearranging gives

$$-(C_1 o_x + S_1 o_y)C_2 + S_2 o_z = \tan\theta_5\left[\left(C_1 n_x + S_1 n_y\right)C_2 - S_2 n_z\right] \tag{4.91}$$

or

$$\frac{S_2}{C_2} = \frac{\tan\theta_5\left(C_1 n_x + S_1 n_y\right) + (C_1 o_x + S_1 o_y)}{n_z \tan\theta_5 + o_z}$$

or

$$\theta_2 = A\tan2\left[\tan\theta_5\left(C_1 n_x + S_1 n_y\right) + C_1 o_x + S_1 o_y,\ n_z \tan\theta_5 + o_z\right] \tag{4.92}$$

Similarly from elements (1, 4) and (2, 4) of Eq. (4.88), two equations are obtained after rearrangements as

$$\begin{aligned} L_5 C_{34} + L_3 C_3 &= C_1 C_2 d_x + S_1 C_2 d_y - S_2(d_z - L_1) - L_2 \\ L_5 S_{34} + L_3 S_3 &= -C_1 S_2 d_x + S_1 S_2 d_y - C_2(d_z + L_1) \end{aligned} \tag{4.93}$$

Substituting for C_{34} and S_{34} from elements (1, 3) and (2, 3), respectively form the left-hand matrix of Eq. (4.88) and simplifying gives

$$\begin{aligned} L_3 C_3 &= C_1 C_2 d_x + S_1 C_2 d_y - S_2(d_z - L_1) - L_2 - L_5(C_1 C_2 a_x + S_1 C_2 a_y - S_2 a_z) \\ L_3 S_3 &= -C_1 S_2 d_x - S_1 S_2 d_y - C_2(d_z + L_1) + L_5(C_1 S_2 a_x + S_1 S_2 a_y + C_2 a_z) \end{aligned} \tag{4.94}$$

Form Eq. (4.94) θ_3 is obtained as

$$\theta_3 = A\tan2\begin{pmatrix} L_3S_3 = -C_1S_2d_x - S_1S_2d_y - C_2(d_z + L_1) + L_5(C_1S_2a_x + S_1S_2a_y + C_2a_z), \\ L_3C_3 = C_1C_2d_x + S_1C_2d_y - S_2(d_z - L_1) - L_2 - L_5(C_1C_2a_x + S_1C_2a_y - S_2a_z) \end{pmatrix} \tag{4.95}$$

The last unknown joint variable θ_4 is computed from Eq. (4.86).

$$\theta_4 = \theta_{234} - \theta_2 - \theta_3 \tag{4.96}$$

Example 4.6 *Inverse kinematics for 6-DOF Stanford manipulator*

Obtain all the joint displacements as explicit functions of the position and orientation of the end-effector for the 6-DOF manipulator of Example 3.8 by analytical method. Also, discuss the existence and multiplicity of solutions.

Solution The given 6-DOF-manipulator arm has a wrist whose joint axes 4, 5 and 6 intersect at a point. This satisfies the necessary condition for existence of closed form solutions. Hence, it is possible to solve the inverse problem in closed form.

Let the given position and orientation of the end-effector with respect to the base in Cartesian space be

$$T = \begin{bmatrix} n_x & o_x & a_x & d_x \\ n_y & o_y & a_y & d_y \\ n_z & o_z & a_z & d_z \\ 0 & 0 & 0 & 1 \end{bmatrix} \tag{4.97}$$

From Example 3.8, the manipulator transformation matrix (the forward kinematic model) for the given manipulator is given by Eq. (3.58) that is

$$^0T_6 = \begin{bmatrix} \begin{matrix} C_1C_2C_4C_5C_6 \\ -S_1S_4C_5C_6 \\ -C_1S_2S_5C_6 \\ -C_1C_2S_4S_6 \\ -S_1C_4S_6 \end{matrix} & \begin{matrix} C_1C_2C_4C_5S_6 \\ +S_1S_4C_5S_6 \\ +C_1S_2S_5S_6 \\ -C_1C_2S_4C_6 \\ -S_1C_4C_6 \end{matrix} & \begin{matrix} C_1C_2C_4S_5 \\ -S_1S_4S_5 \\ +C_1S_2C_5 \end{matrix} & \begin{matrix} C_1C_2C_4S_5L_6 \\ -S_1S_4S_5L_6 \\ +C_1S_2C_5L_6 \\ +C_1S_2d_3 - S_1L_2 \end{matrix} \\ \begin{matrix} S_1C_2C_4C_5C_6 \\ +C_1S_4C_5C_6 \\ -S_1S_2S_5C_6 \\ -S_1C_2S_4S_6 \\ +C_1C_4S_6 \end{matrix} & \begin{matrix} -S_1C_2C_4C_5S_6 \\ -C_1S_4C_5S_6 \\ +S_1S_2S_5S_6 \\ -S_1C_2S_4C_6 \\ +C_1C_4C_6 \end{matrix} & \begin{matrix} S_1C_2C_4S_5 \\ +C_1S_4S_5 \\ +S_1S_2C_5 \end{matrix} & \begin{matrix} S_1C_2C_4S_5L_6 \\ +C_1S_4S_5L_6 \\ +S_1S_2C_5L_6 \\ +S_1S_2d_3 + C_1L_2 \end{matrix} \\ \begin{matrix} S_2C_4C_5C_6 \\ -C_2S_5C_6 \\ +S_2S_4S_6 \end{matrix} & \begin{matrix} S_2C_4C_5S_6 \\ +C_2S_5S_6 \\ +S_2S_4C_6 \end{matrix} & \begin{matrix} -S_2C_4S_5 \\ +C_2C_5 \end{matrix} & \begin{matrix} -S_2C_4S_5L_6 \\ +C_2C_5L_6 + C_2d_3 \end{matrix} \\ 0 & 0 & 0 & 1 \end{bmatrix} \tag{4.98}$$

Observe that in Eq. (4.98) neither single variable terms are present nor simple algebra (like division of two elements) will give single variable isolation. Hence, to find a solution two alternatives are: (i) matrix premultiplication or postmultiplication to isolate one variable at a time, as was done in Example 4.1, and (ii) use more involved algebra and trigonometry. In this example latter is used.

Equating elements (1, 3), (1, 4), (2, 3), (2, 4), (3, 3) and (3, 4) in Eqs. (4.97) and (4.98), six equations are obtained.

$$C_1C_2C_4S_5 - S_1S_4S_5 + C_1S_2C_5 = a_x \tag{4.99}$$

$$L_6(C_1C_2C_4S_5 - S_1S_4S_5 + C_1S_2C_5) + C_1S_2d_3 - S_1L_2 = d_x \tag{4.100}$$

$$S_1C_2C_4S_5 + C_1S_4S_5 + S_1S_2C_5 = a_y \tag{4.101}$$

$$L_6(S_1C_2C_4S_5 + C_1S_4S_5 + S_1S_2C_5) + S_1S_2d_3 + C_1L_2 = d_y \tag{4.102}$$

$$-S_2C_4S_5 + C_2C_5 = a_z \tag{4.103}$$

$$L_6(-S_2C_4S_5 + C_2C_5) + C_2d_3 = d_z \tag{4.104}$$

Substituting Eq. (4.99) into Eq. (4.100) gives

$$L_6a_x + C_1S_2d_3 - S_1L_2 = d_x$$

or

$$C_1S_2d_3 - S_1L_2 = d_x - L_6a_x \tag{4.105}$$

Similarly, substituting Eq. (4.101) into Eq. (4.102) gives

$$L_6a_y + S_1S_2d_3 + C_1L_2 = d_y$$

or

$$S_1S_2d_3 + C_1L_2 = d_y - L_6a_y \tag{4.106}$$

Squaring Eqs. (4.105) and (4.106), adding and simplifying gives

$$S_2^2d_3^2 + L_2^2 = (d_x - L_6a_x)^2 + (d_y - L_6a_y)^2$$

or

$$S_2^2d_3^2 = (d_x - L_6a_x)^2 + (d_y - L_6a_y)^2 - L_2^2 \tag{4.107}$$

Also, combining Eqs. (4.103) and (4.104), rearranging and squaring gives

$$C_2d_3 = d_z - L_6a_z \tag{4.108}$$

or

$$C_2^2d_3^2 = (d_z - L_6a_z)^2 \tag{4.109}$$

Equations (4.107) and (4.109) are solved for d_3

$$d_3 = \pm\sqrt{(d_x - L_6a_x)^2 + (d_y - L_6a_y)^2 + (d_z - L_6a_z)^2 - L_2^2}$$

The displacement of prismatic joint d_3 is always positive; therefore, the negative solution is not valid. Thus

$$d_3 = \sqrt{(d_x - L_6a_x)^2 + (d_y - L_6a_y)^2 + (d_z - L_6a_z)^2 - L_2^2} \tag{4.110}$$

Thus, solution for the joint variable d_3, which gives the joint displacement for the prismatic joint, is found. Next, solve for joint displacement θ_2. From Eq. (4.107),

$$S_2 d_3 = \pm\sqrt{(d_x - L_6 a_x)^2 + (d_y - L_6 a_y)^2 - L_2^2} \tag{4.111}$$

Dividing Eq. (4.111) by Eq. (4.108), solution of joint variable θ_2 is obtained as

$$\theta_2 = \text{Atan2}\left(\pm\sqrt{(d_x - L_6 a_x)^2 + (d_y - L_6 d_y)^2 - L_2^2}, (d_z - L_6 a_z)\right) \tag{4.112}$$

Next, to solve for θ_1, Eqs. (4.105) and (4.106) can be used as they have only θ_1 as unknown. First, let the constants K_1 and K_2 be defined as

$$K_1 = S_2 d_3 \quad \text{and} \quad K_2 = L_2$$

Substituting these constants in Eqs. (4.105) and (4.106):

$$K_1 C_1 - K_2 S_1 = d_x - L_6 a_x \tag{4.113}$$

$$K_1 S_1 + K_2 C_1 = d_y - L_6 a_y \tag{4.114}$$

The equations of this form can be solved by making trigonometric substitutions

$$K_1 = r \sin\phi \quad \text{and} \quad K_2 = r\cos\phi \tag{4.115}$$

where
$$r = +\sqrt{K_1^2 + K_2^2}$$

$$\phi = \text{Atan2}\left(\frac{K_1}{r}, \frac{K_2}{r}\right) \tag{4.116}$$

Substituting K_1 and K_2 from Eq. (4.115) in Eqs. (4.113) and (4.114)

$$\sin(\phi - \theta_1) = \frac{d_x - L_6 a_x}{r} \tag{4.117}$$

$$\cos(\phi - \theta_1) = \frac{d_y - L_6 a_y}{r} \tag{4.118}$$

From Eqs. (4.117) and (4.118),

$$\phi - \theta_1 = \text{Atan2}\left(\frac{d_x - L_6 a_x}{r}, \frac{d_y - L_6 a_y}{r}\right) \tag{4.119}$$

Substituting for ϕ, r, K_1, and K_2 and solving for θ_1 gives

$$\theta_1 = \text{Atan2}\left(\frac{S_2 d_3}{\sqrt{S_2^2 d_3^2 + L_2^2}}, \frac{L_2}{\sqrt{S_2^2 d_3^2 + L_2^2}}\right)$$

$$- \text{Atan2}\left(\frac{d_x - L_6 d_x}{\sqrt{S_2^2 d_3^2 + L_2^2}}, \frac{d_y - L_6 a_y}{\sqrt{S_2^2 d_3^2 + L_2^2}}\right) \tag{4.120}$$

Thus, Eqs. (4.110), (4.112) and (4.120) give solutions for the first three joint displacements θ_1, θ_2, and d_3, respectively.

To obtain the solutions for the remaining three joint displacements θ_4, θ_5, and θ_6, another approach will be used. It is possible to view the description of tool frame, frame {6}, with respect to frame {3}, the arm endpoint frame, along two different paths.

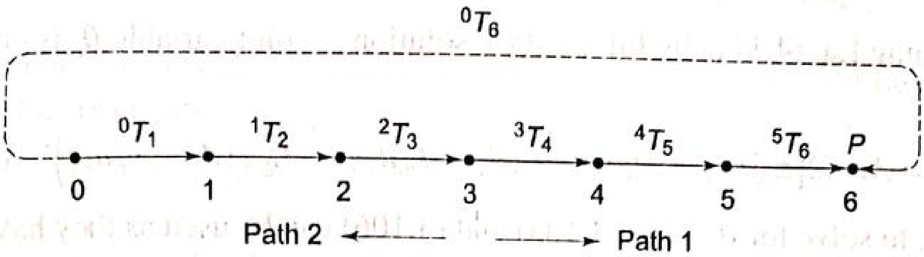

Fig. 4.10 *The transform graph for the manipulator*

The manipulator transformation matrix $^0T_6$ is equal to the product of six link transformation matrices

$$^0T_6 = {}^0T_1\,{}^1T_2\,{}^2T_3\,{}^3T_4\,{}^4T_5\,{}^5T_6 \tag{4.121}$$

This can be represented graphically as shown in Fig. 4.10 with nodes representing frames and edges representing the transform. From the graph in Fig. 4.10 observe that there are two paths to traverse from frame {3} to frame {6}, one is via frame {4} and {5} in the forward direction and other is via frame {0}, the base, in the reverse direction. The use of these two paths to get the solutions is discussed below.

Path 1 frame {3} → frame {4} → frame {5} → frame {6}

Along this path the transformation $^3T_6$ can be obtained as

$$^3T_6 = {}^3T_4\,{}^4T_5\,{}^5T_6 \tag{4.122}$$

In Example 3.8, the transformation matrices $^3T_4$, $^4T_5$, and $^5T_6$ were obtained in terms of θ_4, θ_5, and θ_6 respectively. On multiplying these matrices,

$$^3T_6 = \begin{bmatrix} C_4C_5C_6 - S_4S_6 & -C_4C_5S_6 - S_4C_6 & -C_4S_5 & -L_6C_4S_5 \\ S_4C_5C_6 + C_4S_6 & -S_4C_5S_6 - C_4C_6 & -S_4S_5 & -L_6S_4S_5 \\ S_5C_6 & -S_5S_6 & C_5 & L_6C_5 + L_4 \\ 0 & 0 & 0 & 1 \end{bmatrix} \tag{4.123}$$

Path 2 frame {3} → frame {2} → frame {1} → frame {0} → frame {6}

This is a path via the base. The tool frame is defined with respect to the base and hence, it can be reached from frame {3} traversing the links of the arm. Thus,

$$^3T_6 = {}^3T_2\,{}^2T_1\,{}^1T_0\,{}^0T_6$$

It is known that $^{i-1}T_i = ({}^iT_{i-1})^{-1}$ and $^0T_6 = T$ hence

$$^3T_6 = \left({}^2T_3\right)^{-1}\left({}^1T_2\right)^{-1}\left({}^0T_1\right)^{-1}\,T \tag{4.124}$$

Since θ_1, θ_2, and d_3 are known, the matrices $^2T_3$, $^1T_2$ and $^0T_1$ and their inverse can be computed. Substituting these values and multiplying the matrices, $^3T_6$ can be computed. Let it be denoted as

$$ {}^3T_6 = \begin{bmatrix} r_{11} & r_{12} & r_{13} & r_{14} \\ r_{21} & r_{22} & r_{23} & r_{24} \\ r_{31} & r_{32} & r_{33} & r_{34} \\ 0 & 0 & 0 & 1 \end{bmatrix} \tag{4.125} $$

Since matrices in Eq. (4.123) and (4.125) represent the same point, the arm point, θ_4, θ_5, θ_6 can be found by equating the corresponding elements of matrices. First, for θ_5, the elements in row 3 are equated to give three equations as:

$$ S_5C_6 = r_{31} \tag{4.126} $$

$$ -S_5S_6 = r_{32} \tag{4.127} $$

$$ C_5 = r_{33} \tag{4.128} $$

Squaring Eqs. (4.126) and (4.127), adding and dividing the result by Eq. (4.128) gives solution for θ_5 as

$$ \theta_5 = \text{Atan2}(\pm\sqrt{(r_{31}^2 + r_{32}^2)},\, r_{33}) \tag{4.129} $$

Next, joint angle θ_4 is obtained by equating the elements (2, 4) and (1, 4) as

$$ -L_6S_4S_5 = r_{24} \tag{4.130} $$

$$ -L_6S_4S_5 = r_{14} \tag{4.131} $$

Solving for θ_4 from Eqs. (4.130) and (4.131) gives

$$ \theta_4 = \text{Atan2}\left(\frac{r_{24}}{S_5}, \frac{r_{14}}{S_5}\right) \tag{4.132} $$

Note that since S_5 is a variable and may have more than one value, it is going to influence solution of θ_4. Finally, to solve for θ_6, Eqs. (4.127) is divided by Eq. (4.126) to give

$$ \theta_6 = \text{Atan2}\left(-\frac{r_{32}}{S_5}, \frac{r_{31}}{S_5}\right) \tag{4.133} $$

Thus, expressions for all the six joint displacements of 6-DOF manipulator are obtained as explicit functions of the desired position and orientation of end-effector. The values of joint displacements can be determined from these functions for the desired end-effector location data. Note that the inverse kinematics solutions could have been obtained by following alternate approaches. The issues of existence and multiplicity of solutions are discussed next.

Existence of Solutions

A close examination of the expressions of the joint variables reveals that the solutions to the inverse kinematics problem of the given 6-DOF arm exist only if the following conditions are satisfied:

(i) The term under the square root in Eq. (4.110) is non-negative, that is,

$$ [(d_x - L_6a_x)^2 + (d_y - L_6a_y)^2 + (d_z - L_6a_z)^2 - L_2^2] \geq 0 \tag{4.134} $$

(ii) Similarly, the term under the square root in Eq. (4.111), is nonnegative, that is,

$$[(d_x - L_6 a_x)^2 + (d_y - L_6 a_y)^2 - L_2^2] \geq 0 \tag{4.135}$$

The above conditions are clearly geometric constraints on the dimensions of the links of the manipulator.

There are two ways to look at these. One, for given link dimensions (L_2 and L_6) the end-effector will not be able to attain the desired position (d_x, d_y, d_z) and orientation (a_x, a_y, a_z) if the above conditions are not satisfied, and second, the conditions can be used to design link dimensions L_2 and L_6 for the desired workspace.

Note that, if condition (ii) is satisfied, condition (i) is automatically satisfied. Also, note that here it is assumed that full 360° of rotation for all revolute joints and limitless translations of the prismatic joint are possible. But, due to mechanical constraints, joint motions are restricted and solutions exist only if, in addition to satisfying the conditions given above, each of the joint variables takes a value that lies within the range of motion allowed for that joint.

Multiplicity of Solutions

Equation (4.112) gives two solutions of θ_2 due to the presence of the square root. Since θ_1 depends on θ_2 (Eq. (4.120)), there is one value of θ_1 for each value of θ_2. Similarly, from Eq. (4.129), there are two solutions for θ_5 and hence, it gives one set of solutions for θ_4 and θ_6 for each value of θ_5.

Thus, the number of solutions to the inverse kinematics problem of the given 6-DOF-manipulator arm is four.

Example 4.7 ***Determination of joint variables for a 4-DOF RPPR manipulator***

For a 4-DOF, RPPR manipulator, the joint-link transformation matrices, with joint variables θ_1, d_2, d_3 and θ_4 are

$${}^0\boldsymbol{T}_1(\theta_1) = \begin{bmatrix} C_1 & -S_1 & 0 & 0 \\ S_1 & C_1 & 0 & 0 \\ 0 & 0 & 1 & 0 \\ 0 & 0 & 0 & 1 \end{bmatrix} \tag{4.136}$$

$${}^1\boldsymbol{T}_2(\theta_2) = \begin{bmatrix} 1 & 0 & 0 & 0 \\ 0 & 0 & 1 & 0 \\ 0 & -1 & 0 & d_2 \\ 0 & 0 & 0 & 1 \end{bmatrix} \tag{4.137}$$

$${}^2\boldsymbol{T}_3(d_3) = \begin{bmatrix} 1 & 0 & 0 & 5 \\ 0 & 1 & 0 & 0 \\ 0 & 0 & 1 & d_3 \\ 0 & 0 & 0 & 1 \end{bmatrix} \tag{4.138}$$

$$^3T_4(\theta_4) = \begin{bmatrix} C_4 & -S_4 & 0 & 0 \\ S_4 & C_4 & 0 & 0 \\ 0 & 0 & 1 & 0 \\ 0 & 0 & 0 & 1 \end{bmatrix} \tag{4.139}$$

If the tool configuration matrix at a given instant is as given below, obtain the magnitude of each joint variable.

$$T_E = \begin{bmatrix} -0.250 & 0.433 & -0.866 & -89.10 \\ 0.433 & -0.750 & -0.500 & -45.67 \\ -0.866 & -0.500 & 0.000 & 50.00 \\ 0 & 0 & 0 & 1 \end{bmatrix} \tag{4.140}$$

Solution The kinematic model of the manipulator will be

$$^0T_1\,{}^1T_2\,{}^2T_3\,{}^3T_4 = T_E \tag{4.141}$$

Substituting from Eqs. (4.136) – (4.140) gives

$$\begin{bmatrix} C_1 & -S_1 & 0 & 0 \\ S_1 & C_1 & 0 & 0 \\ 0 & 0 & 1 & 0 \\ 0 & 0 & 0 & 1 \end{bmatrix} \begin{bmatrix} 1 & 0 & 0 & 0 \\ 0 & 0 & 1 & 0 \\ 0 & -1 & 0 & d_2 \\ 0 & 0 & 0 & 1 \end{bmatrix} \begin{bmatrix} 1 & 0 & 0 & 5 \\ 0 & 1 & 0 & 0 \\ 0 & 0 & 1 & d_3 \\ 0 & 0 & 0 & 1 \end{bmatrix} \begin{bmatrix} C_4 & -S_4 & 0 & 0 \\ S_4 & C_4 & 1 & 0 \\ 0 & 0 & 1 & 0 \\ 0 & 0 & 0 & 1 \end{bmatrix} = T_E \tag{4.142}$$

or

$$\begin{bmatrix} C_1C_4 & -C_1S_4 & -S_1 & -d_3S_1 + 5C_1 \\ S_1C_4 & -S_1S_4 & C_1 & d_3C_1 + 5S_1 \\ -S_4 & -C_4 & 0 & d_2 \\ 0 & 0 & 0 & 1 \end{bmatrix} = \begin{bmatrix} -0.250 & 0.433 & -0.866 & -89.10 \\ 0.433 & -0.750 & -0.500 & -45.67 \\ -0.866 & -0.500 & 0.000 & 50.00 \\ 0 & 0 & 0 & 1 \end{bmatrix} \tag{4.143}$$

The solutions for joint-variables are found by using the direct approach, guideline (a)–(d). The solution for first joint variable θ_1 is obtained by comparing elements (1, 3) and (2, 3)

$$-S_1 = -\sin\theta_1 = -0.866 \tag{4.144}$$

$$C_1 = \cos\theta_1 = -0.5$$

or $\theta_1 = \text{Atan2}(0.866, -0.5) = -60°$ (that is: $\theta_1 = \text{Atan2}(-a_x, a_y)$) (4.145)

The solution for second variable d_2 is obtained from element (3, 4) as:

$$d_2 = 50 \text{ (that is : } d_2 = d_z) \tag{4.146}$$

Similarly, the third joint variable d_3 is obtained from elements (1, 4) and elements (2, 4) by squaring, adding and simplifying

$$d_3 = \pm\sqrt{d_x^2 + d_y^2 - 25} \tag{4.147}$$

or $$d_3 = 100 \tag{4.148}$$

Note that d_3 can not be negative. The fourth joint variable θ_4 is computed from elements (3, 1) and (3, 2) as

$$\theta_4 = \text{Atan2}(0.866, 0.5) = 60^\circ \text{ (that is: } \theta_4 = \text{Atan2}(-n_z, -o_z)) \tag{4.149}$$

The given end-effector position and orientation, T_E will be achieved by setting the joint variable vector to

$$q = \begin{bmatrix} -60^\circ & 50 & 100 & 60^\circ \end{bmatrix} \tag{4.150}$$

EXERCISES

4.1 For the two link planar manipulator in Fig. 4.3(a) the first link as is twice as long as the second link ($L_1 = 2L_2$). Sketch the reachable workspace of the manipulator if the joint range limits are

$$\begin{aligned} 0 < \theta_1 &< 170^\circ, \\ -90^\circ < \theta_2 &< 110^\circ. \end{aligned} \tag{4.151}$$

4.2 Sketch the approximate reachable workspace of the tip of a two-link planar arm with revolute joints. For this arm the first link is thrice as long as the second link, that is, $L_1 = 3L_2$ and the joint limits are $30^\circ < \theta_1 < 180^\circ$ and $-100^\circ < \theta_2 < 160^\circ$.

4.3 Sketch the approximate reachable workspace and the dexterous workspace of the 3-DOF planar manipulator shown in Fig. 4.5.

4.4 Show that for a 3R planar manipulator having link lengths as L_1, L_2 and L_3 with $(L_1 + L_2) > L_3$, the RWS is a circle with radius $r_{\text{RWS}} = (L_1 + L_2 + L_3)$ and DWS is a circle with radius $r_{\text{DWS}} = (L_1 + L_2 - L_3)$.

4.5 Explain why closed form analytical solutions are preferred over numerical iterative solutions.

4.6 Discuss the existence of multiple solutions for Example 4.1.

4.7 For a three-link planar manipulator (2-DOF for position and 1-DOF for orientation) two solutions are possible for a given position and orientation, as discussed in Section 4.3.2. If one more degree of freedom is added such that the manipulator is still planar, how many solutions will be possible for a given position and orientation when the added joint is
(a) revolute.
(b) prismatic.

4.8 How many solutions are possible, assuming no joint range limits for the following 3-DOF arm configuration?
(a) PPP manipulator shown in Fig. E4.8.
(b) RPP manipulator shown in Fig. 3.13.
(c) RRP manipulator shown in Fig. 4.7.
(d) RRR manipulator shown in Fig. 3.15.

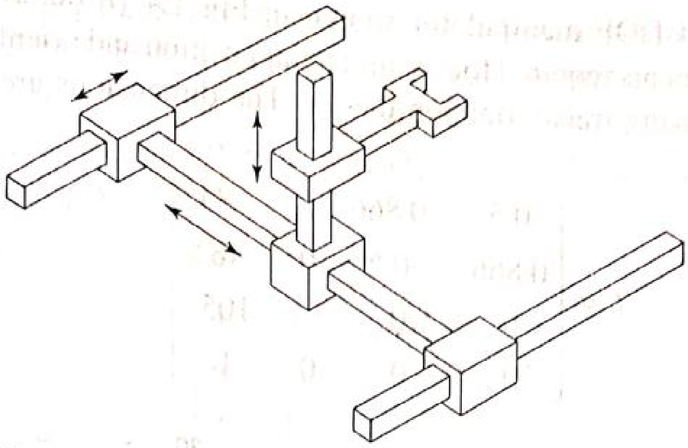

Fig. E4.8 *A three degree of freedom PPP configuration*

4.9 For the two degree of freedom planar RP configuration arm discussed in Example 3.1, how many solutions can be found for a given position and orientation. What will be the number of solutions if following alterations are made in the manipulator configuration?
   (a) Add one revolute joint after the prismatic joint.
   (b) Add one revolute joint before the prismatic joint.
   (c) Add one degree of freedom (1R) wrist.
   In each case, the manipulator remains planar.

4.10 For the 2-DOF manipulator shown in Fig. 3.11 determine the solution for all joint displacements $\boldsymbol{q}$ for a given tool point position and orientation.

4.11 Obtain the inverse kinematics solution for the 3-DOF planar manipulator shown in Fig. 4.5.

4.12 Workout Example 4.1 without using inverse transform approach.

4.13 Obtain the closed form solutions for the joint displacements of the cylindrical configuration arm described in Exercise 3.2.

4.14 For the manipulator arm consisting of 3-DOF described in Exercise 3.6, obtain the inverse kinematics solutions.

4.15 Obtain the inverse kinematics model for the 3-DOF articulated arm discussed in Example 3.3.

4.16 For the 3-DOF-RPY wrist shown in Fig. 3.18, obtain the conditions of singularities.

4.17 For the 3-DOF arm shown in Fig. E4.17, determine the forward kinematic model and, there from, obtain the general solution for inverse dinematics.

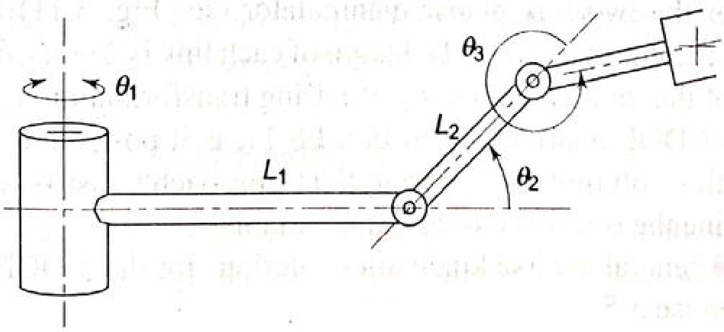

Fig. E4.17 *A three degree of freedom manipulator arm*

4.18 For the 4-DOF manipulator shown in Fig. E4.18 determine the joint displacements required for the tool point position and orientation given by the following transformation matrix. The dimensions are shown in the figure.

$$T = \begin{bmatrix} 0.5 & -0.866 & 0 & -84 \\ 0.866 & -0.5 & 0 & -48.5 \\ 0 & 0 & -1 & 105 \\ 0 & 0 & 0 & 1 \end{bmatrix} \tag{4.152}$$

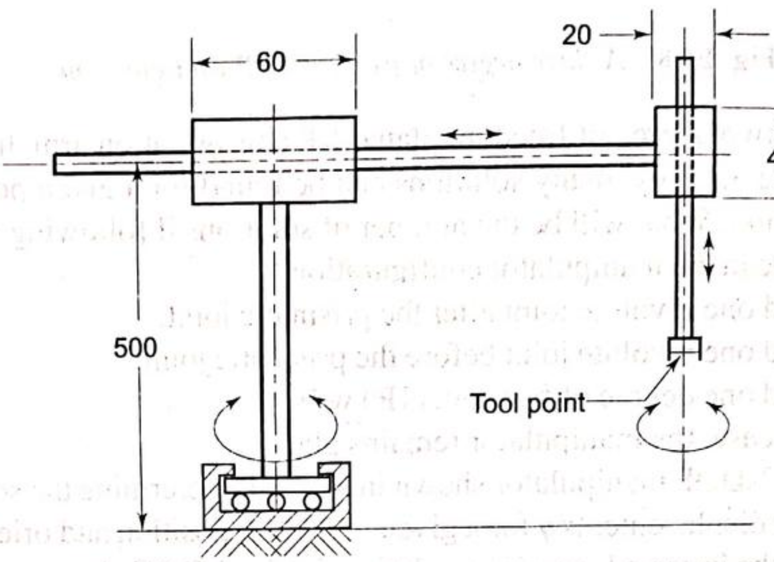

Fig. E4.18 *A 4-DOF manipulator*

4.19 For a 5-DOF, RRR-RR articulated configuration manipulator shown in Fig. E3.14 obtain the inverse kinematics model.

4.20 Consider the 6-DOF manipulator in Exercise 3.18; find solutions for all the joint variables in terms of end-effector position and orientation by analytical method and inverse transform method.

4.21 For the SCARA robot discussed in Example 3.6, end-effector configuration (orientation and position) has been calculated in Exercise 3.13. Taking this as the desired end-effector configuration compute the joint displacement vector.

4.22 Consider the two-link planar manipulator (see Fig. 3.11) with its end-effector located at (4, 0). If the length of each link is 2 units, determine the values of the joint variables (θ_1, θ_2) using transformation matrices.

4.23 For the 3-DOF manipulator in Fig. E3.11, is it possible to find inverse kinematics solutions using analytical approach? Justify your answer. Determine the solutions for all joint variables.

4.24 Find the general inverse kinematics solutions for the 3-DOF Euler wrist, see Exercise 3.5.

4.25 The joint-link parameters of a 6-DOF freedom manipulator are described in Table E4.17. Find the inverse kinematics solutions for all the joint angles $q = [\theta_1 \quad \theta_2 \quad \theta_3 \quad \theta_4 \quad \theta_5 \quad \theta_6]^T$. Assume that the position and orientation of the end-effector with respect to the base coordinates ${}^0T_6$ is known and is given by

$$T = \begin{bmatrix} n_x & o_x & a_x & d_x \\ n_y & o_y & a_y & d_y \\ n_z & o_z & a_z & d_z \\ 0 & 0 & 0 & 1 \end{bmatrix} \tag{4.153}$$

Table E4.17 *Joint-link parameters for a 6-DOF manipulator*

Link i	a_i	α_i	d_i	θ_i	q_i
1	0	–90°	d_1	θ_1	θ_1
2	a_2	0	0	θ_2	θ_2
3	a_3	0	0	θ_3	θ_3
4	a_4	–90°	0	θ_4	θ_4
5	0	90°	d_5	θ_5	θ_5
6	0	0	d_6	θ_6	θ_6

4.26 Describe the workspace of a manipulator. Make a list of factors on which the workspace, the dexterous and reachable workspace, of a given manipulator depends.

4.27 Solutions to inverse kinematics problem are generally difficult. Explain why.

4.28 Explain the factors on which the number of solutions to given inverse kinematics model depend.

4.29 How are the feasible solutions determined? What parameters have control on the number of feasible solutions to the given inverse kinematics problem?

4.30 Is it always possible to find analytical solutions to the inverse kinematics problem? Give a situation when the analytical solution to inverse kinematics problem cannot be found.

4.31 What are closed form solutions to inverse kinematics problem? Explain the methods for obtaining closed form solutions.

4.32 Why closed form solutions are preferred over numerical, iterative or other forms of solutions to the inverse kinematics problem?

SELECTED BIBLIOGRAPHY

1. D. Baker and C. Wampler, "On the Inverse Kinematics of Redundant Manipulators," *The International Journal of Robotics Research*, *7*(2), 1988.

2. A. A.Goldenberg, B.Benhabib and R. G. Fenton, "A complete generalized solution to the inverse kinematics of robots," *IEEE Journal of Robotics and Automation*, ***1***(1), 14–20, 1985.
3. A. A. Goldenberg, and D. L. Lawrence, "A generalized solution to the inverse kinematics of robotic manipulator," *Journal of Dynamic Systems, Measurement, and Control*, ***107***, 103–107, 1985.
4. K.C. Gupta and B. Roth, "Design Consideration for Manipulators Workspace," *J of Mechanical Design*, ***104***, 704–711, Oct 1992.
5. Wisama Khalil and Denis Creusot, "SYMORO+: A System for the Symbolic Modeling of Robots," *Robotica*, ***15***, 153–161, 1997.
6. C.L. Lai and C.H. Meng, "The Dexterous Workspace of Simple Manipulators," *IEEE Journal of Robotics and Automation*, ***107***, 99–103, Jun. 1988.
7. C.S.G. Lee, "A Geometric Approach in Solving Inverse Kinematics of PUMA Robots," *IEEE Tr on Aerospace and Electronic Systems*, ***20***(6), 696–706, Nov. 1984.
8. D. Manocha, and J. F. Canny, "Efficient inverse kinematics for general 6r manipulators," *IEEE Transactions on Robotics and Automation*, ***10***(5), 648–657, 1994.
9. Y. Nakamura and H. Hanafusa, "Inverse Kinematic Solutions with Singularity Robustness for Robot Manipulator Control," *Tr of ASME Journal of Dynamic Systems, Measurement, and Control*, ***108***, 163–171, 1986.
10. F.C. Park and R.W. Brockett, "Kinematic Dexterity of Robotic Mechanisms," *The International Journal of Robotics Research*, ***13***(1), 1–15, Feb. 1994.
11. R.P. Paul, B. Shimano, and G. Mayer, "Kinematic Control Equations for Simple Manipulator," *IEEE Tr on Systems, Man, and Cybernetics*, ***11***(6), 449–455, 1981.
12. R.P. Paul and H. Zhang, "Computationally Efficient Kinematics for Manipulators with Spherical Wrists Based on the Homogeneous Transformation Representation," *The International Journal of Robotics Research*, ***5***(2), 32–44, 1986.
13. R.G. Roberts, "The Dexterity and Singularities of an Under Actuated Robot," *J of Robotic Systems*, ***18***(4), 160–169, April 2001.
14. L. Sciavicco and B. Siciliano, "A Solution Algorithm to the Inverse Kinematic Problem for Redundant Manipulators," *IEEE Journal of Robotics and Automation*, ***4***, 403–410, 1988.
15. C.W. Wampler, "Manipulator Inverse Kinematic Solutions Based on Damped Least-Squares Solutions," *IEEE Tr on Systems, Man, and Cybernetics*, ***16***, 93–101, 1986.
16. T. Yoshikawa, "Manipulability of Robotic Manipulators," *The International Journal of Robotics Research*, ***4***, 3–9, 1985.